A link between NMDA receptor hypofunction and GABAergic inhibition in the modulation of cognition: a comparison of neural and cognitive changes in rat models of NMDA receptor hypofunction and of prefrontal and hippocampal neural disinhibition

Charlotte Jane Latham Taylor

Thesis submitted to the University of Nottingham for the degree of Doctor of Philosophy

September 2023

Abstract

NMDA receptor (NMDAR) hypofunction and impaired GABAergic inhibition, so-called neural disinhibition, in the hippocampus and prefrontal cortex, have both been implicated in the pathophysiology of schizophrenia. Moreover, it has been suggested that NMDAR hypofunction and neural disinhibition are mechanistically linked and may converge on a common pathological hub. NMDAR hypofunction in rodents has been reported to mimic certain aspects of cognitive deficits associated with schizophrenia, alongside pathological reductions in hippocampal and prefrontal GABAergic markers. Given the importance of GABAergic inhibition in the hippocampus and prefrontal cortex for a range of cognitive functions, hippocampal and prefrontal neural disinhibition may underlie some of the cognitive deficits found in rodent models of NMDAR hypofunction. Here, we examined the overarching hypothesis that NMDAR hypofunction impairs cognition by causing neural disinhibition in the hippocampus and prefrontal cortex. In chapter 1, we reviewed the current evidence for this hypothesis, which demonstrated a compelling case for neural disinhibition in acute and neurodevelopmental models of NMDAR hypofunction. However, importantly, studies investigating the impact of sub-chronic NMDAR hypofunction on GABAergic function were equivocal in support of the hypothesis, and the role of these processes in mediating cognition on the watermaze delayed-matching-to-place (DMP) and novel object recognition (NOR) task, respectively, had not been investigated. In subsequent chapters, we aimed to address the hypothesis experimentally, by comparing and examining the cognitive and neural changes in rat models of sub-chronic NMDAR hypofunction and regional neural disinhibition.

In chapter 2, we examined the impact of NMDAR hypofunction, caused by sub-chronic treatment with phencyclidine (scPCP), in rats on the watermaze DMP task. Sub-chronic PCP treatment did not disrupt hippocampal rapid place learning performance. This contrasts with the marked impairments observed following acute pharmacological hippocampal disinhibition and suggests that hippocampal disinhibition is not a pronounced feature of the scPCP model. In chapter 3, we used high throughput simple western analysis to determine the protein levels of key GABAergic biomarkers, GAD67 and parvalbumin, in the brains of the scPCP treated rats used for behavioural studies in chapter 2. No changes in GAD67 or parvalbumin protein expression were found in the prefrontal cortex or dorsal region of the hippocampus. In the intermediate to ventral hippocampus, GAD67 was found to be reduced in female, but not male, rats, suggesting that scPCP treatment may have sex-specific neuropathological effects. Importantly, however, in the scPCP treated rats which underwent watermaze DMP testing, parvalbumin was found to be increased in the intermediate to ventral hippocampus. Overall,

our investigations into GABAergic protein expression changes following NMDAR hypofunction revealed limited evidence for neural disinhibition in the prefrontal cortex and hippocampus. In chapter 4, we investigated whether scPCP treatment results in functional alterations to hippocampal neural activity. Using evoked in vivo recordings under urethane anaesthesia, we applied low frequency train stimulation to the subiculum or CA3 region, with the aim of examining instances of reverberatory responses as a measure of the overall excitability of hippocampal circuits. This study revealed evidence of reverberation in both treatment groups, indicating intact fibre pathways in scPCP treated rats. However, a preliminary analysis did not indicate clear-cut changes in hippocampal excitability following scPCP treatment. Finally, in chapter 5, we investigated whether neural disinhibition in the medial prefrontal cortex, dorsal or ventral hippocampus may account for the NOR deficits reported widely in the scPCP model. Neural disinhibition or functional inhibition was induced in rats via local infusion of picrotoxin or muscimol, respectively, and NOR performance compared using a within-subjects design. We found that hippocampal, but not prefrontal, GABAergic inhibition was required for intact NOR. This finding suggests that hippocampal GABAergic deficits may contribute, in part, to NOR deficits found in NMDAR hypofunction models.

Thus, the experiments reported in chapters 2-5 provide limited evidence for a link between NMDAR hypofunction and neural disinhibition in the hippocampus and prefrontal cortex in the modulation of cognition. The finding that hippocampal, but not prefrontal, GABAergic inhibition is required for intact NOR performance suggests that hippocampal GABAergic impairments could contribute to scPCP-induced NOR deficits. However, the lack of a watermaze DMP impairment in scPCP treated rats, combined with weak post-mortem evidence for reduced GABAergic markers, does not support a marked impairment of hippocampal GABA function in scPCP treated rats. Overall, our findings do not support that scPCP treatment leads to pronounced hippocampal disinhibition or that neural disinhibition in the prefrontal cortex or hippocampus plays a major role in cognitive deficits caused by sub-chronic NMDAR hypofunction.

Acknowledgements

The work presented in this thesis was funded by a UKRI-BBSRC Industrial CASE studentship at the University of Nottingham, with industrial placement undertaken at b-neuro, University of Manchester.

Firstly, I would like to wholeheartedly thank my primary supervisor, Tobias Bast, who has provided exceptional guidance and support throughout my PhD. I am incredibly grateful for the time you have given to reading through my work, helping me with studies or simply being available for a chat. I am in no doubt that my PhD would not have been half as enjoyable had I not been lucky enough to have you as a supervisor! I would also like to thank my second supervisor, Paula Moran, for her input and guidance on creating a well-rounded and enjoyable project.

Thanks also go to all generations of Bast lab members. First, to Miriam, Stu and Sara who warmly welcomed me into the lab and provided invaluable training and advice. Second, to Jacco and Joanna, who, through many a minor lab-based catastrophe and the *slight* inconveniences caused by a global pandemic, were always there to help; it has been a pleasure to start and finish this journey with you both. Third, to Rachel, who I can always count on to put the world to rights with me, or send me adorable pictures of dogs, and Jacob, who I can always count on to make me laugh.

I would also like to thank Michael Harte and John Gigg, my b-neuro supervisors, who made me feel very welcome in Manchester and were always willing to help me realise my thesis aims, even if it meant that I may have stuck around a bit too long! Thanks also go to other Manchester lab members: Ben Grayson, Georgie, Inés and Lauren, to name a few. Special thanks must go to omniscient Jen, who provided endless advice on, well, anything and everything! Also, to Chloe, who patiently trained me for the electrophysiology study and was great company during those *long* recording days.

Finally, I would like to acknowledge my family: Mum, Josie, Freddie and Toby, whose love and support kept me sane amidst many a moment of self-doubt. Also, to Ben, who endured countless late-night phone calls (way past your bedtime), weekend working and stressed out monologues; thank you for helping me to keep going when I felt like I was running on empty. Lastly, I would like to thank my Dad, who instilled in me a love of science, and whom I miss every single day, and hope would have been proud to see what I have achieved.

Contents

List of tables

List of figures

Chapter 1: Introduction

Maintaining the balance between excitatory and inhibitory neurotransmission in the brain is crucial for the modulation of cognition (Ferguson & Gao, 2018). Cortical and hippocampal inhibitory gamma-aminobutyric acid (GABA) neurotransmission plays a key role in shaping neuronal activity and has been linked to mechanisms suggested to be important for cognitive processing, such as the regulation of burst firing and generation of neural oscillations (Bast et al., 2017; Buzsáki & Wang, 2012; Isaacson & Scanziani, 2011; Izhikevich et al., 2003; McGarrity et al., 2017; Pezze et al., 2014; Sohal et al., 2009). Substantial evidence suggests that GABAergic inhibitory neurotransmission is disrupted in schizophrenia (Dienel & Lewis, 2019; Heckers & Konradi, 2015; Lisman et al., 2008). A reduction in GABAergic markers in post-mortem prefrontal and hippocampal samples is amongst the most consistent neuropathological findings in schizophrenia (de Jonge et al., 2017; Gonzalez-Burgos et al., 2010; Heckers & Konradi, 2015), and has been suggested to reflect functional impairments in GABAergic interneurons (Lewis et al., 2012; Lisman et al., 2008). In addition, imaging studies in patients with schizophrenia have demonstrated increased hippocampal and cortical neural activity, consistent with loss of inhibitory neurotransmission (Anticevic et al., 2015; Heckers & Konradi, 2015). Given the role of GABAergic interneurons in facilitating cognitive processes, it has been suggested that impaired GABAergic inhibition may contribute to the cognitive deficits associated with schizophrenia (Dienel & Lewis, 2019; Tregellas et al., 2014). Indeed, reduced GABAergic inhibition, or neural disinhibition, in the hippocampus or prefrontal cortex (PFC) of rats, induced by local microinfusion of the GABA-A receptor antagonist picrotoxin, has been shown to mimic some of the cognitive impairments associated with schizophrenia (Bast et al., 2017; McGarrity et al., 2017; Pezze et al., 2014; Tse et al., 2015). However, the mechanisms which may induce neural disinhibition in schizophrenia have not yet been established. One prominent idea is that neural disinhibition may be mechanistically linked with N-methyl-D-aspartate receptor (NMDAR) hypofunction (Cohen et al., 2015; Hardingham & Do, 2016; Lisman et al., 2008).

NMDAR hypofunction has been implicated in the aetiology of schizophrenia based on early observations that administration of NMDAR antagonists in healthy humans mimic some of the core symptoms of schizophrenia, including deficits in cognition (Javitt & Zukin, 1991; Luby et al., 1959; Umbricht et al., 2000). NMDAR antagonists have also been found to induce cortical neural hyperactivity in humans, similar to that observed in early-stage schizophrenia (Anticevic et al., 2015; Braun et al., 2016; Rowland et al., 2005b, 2010). In addition, NMDAR subunit expression is reported to be altered in patients with schizophrenia (Akbarian et al., 1995;

Bygrave et al., 2019; Catts et al., 2016), further implicating a role for altered NMDAR signalling in the disease. Moreover, NMDAR hypofunction in rodent models has been shown to mimic certain aspects of cognitive deficits associated with schizophrenia (Cadinu et al., 2018; Neill et al., 2010). While the effects of acute NMDAR antagonism are noteworthy, repeated administration of non-competitive NMDAR antagonists, such as phencyclidine (PCP), in rodents causes enduring cognitive deficits which persist long after cessation of treatment (Meltzer et al., 2013; Reynolds & Neill, 2016). Furthermore, NMDAR hypofunction models have been reported to exhibit deficits in GABAergic markers (Abdul-Monim et al., 2007; Gigg et al., 2020; Jenkins et al., 2010), as well as prefrontal and hippocampal neural hyperactivity consistent with neural disinhibition (Homayoun & Moghaddam, 2007; Jackson et al., 2004; Schobel et al., 2013).

This thesis will examine the overarching hypothesis that NMDAR hypofunction impairs cognition by causing neural disinhibition in the hippocampus and medial PFC (mPFC). In this introduction, we briefly discuss the different NMDAR antagonist models (section 1.1) and outline possible mechanisms that may underlie GABAergic changes reported in these models (section 1.2). We then review post-mortem histological (section 1.3) and electrophysiological (section 1.4) evidence for impaired GABAergic function in NMDAR hypofunction models. In addition, we compare the effects of NMDAR hypofunction and impaired GABAergic function on cognitive performance in two rodent memory assays: the watermaze task and novel object recognition (NOR) task (section 1.5), both of which have been suggested to be relevant to the cognitive impairments associated with schizophrenia (Young et al., 2009) and will be used for cognitive testing in this thesis. Finally, the introduction closes with an outline of the thesis aims.

1.1 Acute and sub-chronic pharmacological models of NMDAR hypofunction

In human studies, acute administration of non-competitive NMDAR antagonists, such as PCP and ketamine, has been reported to induce cognitive deficits in healthy volunteers, including impaired performance on the Wisconsin Card Sorting Test and deficits in free recall, recognition memory and verbal fluency (Curran & Monaghan, 2001; Krystal et al., 1994; Luby et al., 1959; Malhotra et al., 1996). In rodents, acute NMDAR antagonism has also been shown to induce deficits in reversal learning, NOR, and perceptual attentional set-shifting tasks, which are suggested to be comparable to some of the cognitive deficits reported in schizophrenia (Egerton et al., 2005; Grayson & Neill, 2004; Idris et al., 2006). However, although acute studies may be able to mimic some schizophrenia-like cognitive deficits, rodent models using repeated

treatment with NMDAR antagonists have been suggested to be of greater face validity, given that NMDAR hypofunction in schizophrenia is likely to be in a persistent state (Jentsch & Roth, 1999). Moreover, testing after acute NMDAR blockade may be insufficient to capture the potential effects of downstream signalling cascades, and other homeostatic or compensatory mechanisms which may occur following long-lasting NMDAR antagonism (Speers & Bilkey, 2021).

Repeated treatment with NMDAR antagonists, followed by withdrawal or cessation of treatment (referred hereafter as sub-chronic treatment), is reported to induce more pronounced and long-lasting schizophrenia-like neural and cognitive changes in rodents, compared to acute administration (Jentsch & Roth, 1999; Lee & Zhou, 2019). Interestingly, sub-chronic NMDAR hypofunction can cause opposite neural changes to acute NMDAR hypofunction. For example, acute administration of PCP in rats has been shown to increase dopamine release in the PFC (Hertel et al., 1995; Jentsch et al., 1997a), whereas a sub-chronic PCP (scPCP) dosing regimen reduced prefrontal dopamine release (Jentsch et al., 1997b). In addition, acute ketamine treatment resulted in an increase in the power of cortical and hippocampal gamma oscillations, whereas repeated treatment was associated with reduced gamma power (Ahnaou et al., 2017; Kittelberger et al., 2012). Furthermore, sub-chronic dosing is suggested to elicit a more selective cognitive deficit profile, which may be more relevant to schizophrenia than the deficits induced by acute models (Jentsch & Roth, 1999).

Cognitive deficits following sub-chronic NMDAR antagonism have been found to persist long after cessation of treatment, indicating long-lasting neuropathological changes in these models. The scPCP model, for example, is reported to result in cognitive deficits which persist for at least 6 months following cessation of PCP treatment (Neill et al., 2016). In addition, in humans, a study assessing the effects of acute ketamine in frequent and infrequent ketamine users found that acute ketamine resulted in learning and memory impairments in both groups (Curran & Monaghan, 2001). However, interestingly, the frequent ketamine users were also reported to exhibit learning and memory impairments 3 days after the acute dose, whereas infrequent users were not impaired. This suggests that frequent ketamine use in humans may result in long-lasting cognitive deficits or may induce hypersensitivity to NMDAR hypofunction-induced behavioural deficits (Curran & Monaghan, 2001; Gilmour et al., 2012). Indeed, rats treated with scPCP show increased locomotor sensitivity towards acute PCP administration (Pyndt Jørgensen et al., 2015). A further advantage of sub-chronic dosing is that it is free from gross sensorimotor and motivational disruptions which may confound interpretation of cognitive impairments in acute NMDAR antagonist studies (Smith et al., 2011). It also allows

for potential schizophrenia treatments to be tested without the confounding effects of a potential drug-PCP pharmacological interaction (Young et al., 2009). For these reasons, the scPCP model of NMDAR hypofunction will be used in these thesis investigations.

1.2 Potential mechanisms mediating GABA dysfunction following NMDAR hypofunction

Given that NMDARs mediate excitatory transmission throughout the brain (Regan et al., 2015; Traynelis et al., 2010), it seems paradoxical that NMDAR hypofunction would result in increased neural activity. Electrophysiological findings suggest that GABAergic interneurons are more sensitive to NMDAR antagonists than pyramidal neurons, leading to the idea that NMDAR blockade may preferentially decrease the excitatory drive on GABAergic interneurons, thereby reducing GABAergic inhibition of pyramidal cells and resulting in neural disinhibition (Grunze et al., 1996; Homayoun & Moghaddam, 2007; Lisman et al., 2008). The mechanisms which may lead to this preferential blockade are not fully understood. Fast spiking GABAergic interneurons have been shown to be more efficiently recruited by excitatory inputs, suggesting that NMDARs exert greater regulatory control over the firing of interneurons, compared with pyramidal neurons (Homayoun & Moghaddam, 2007; Povysheva et al., 2006). The different NMDAR subunit composition expressed in excitatory and inhibitory neurons may also render GABAergic interneurons more sensitive to NMDAR antagonism (Grunze et al., 1996; Wang & Gao, 2009; Xi et al., 2009; Zhang et al., 2012). In addition to this hypothesis of preferential blockade, it has been suggested that NMDAR hypofunction may lead to neural disinhibition due to NMDARs on interneurons acting as sensors for pyramidal cell activity (Lisman et al., 2008). More specifically, when NMDARs are blocked, this may be falsely 'interpreted' as pyramidal cell inactivity, leading interneurons to compensate for the apparent loss of activity by reducing GABAergic output via downregulation of GABAergic protein expression, and this maladaptive compensatory mechanism is thought to cause neural disinhibition (Lisman et al., 2008). It is possible that the hypotheses outlined here may all contribute to NMDAR hypofunction induced neural disinhibition or may differentially contribute depending on the extent of NMDAR hypofunction. Acute and sub-chronic NMDAR antagonism are suggested to cause changes in neural activity via two different mechanisms; acute antagonism may involve the preferential disruption of NMDARs on GABAergic interneurons, whereas sub-chronic antagonism may involve the down regulation of key proteins related to the function of GABAergic inhibitory neurons (Lisman et al., 2008; Zhang et al., 2008). However, the hypothesis of a preferential NMDAR blockade on interneurons has been questioned given that inhibitory parvalbumin (PV) basket cells, a main GABAergic interneuron subtype suggested to be altered in schizophrenia (Lewis et al., 2012), display modest NMDAR-mediated excitatory

drive and are, therefore, unlikely to participate in NMDAR antagonist-mediated disinhibition (Pafundo et al., 2018; Rotaru et al., 2011).

More recent studies have proposed alternative mechanisms as to how NMDAR hypofunction may lead to neural disinhibition, which does not rely on a preferential role of NMDARs in modulating GABAergic interneuron activity. First, presynaptic NMDAR antagonism may induce neural disinhibition by reducing GABA release at PV basket cell-to-pyramidal cell synapses (Pafundo et al., 2018). In the mouse PFC, Pafundo et al. (2018) reported an NMDA-induced increase in PV basket cell-pyramidal cell synaptic current, which was present alongside postsynaptic NMDAR blockade, and was itself attenuated by presynaptic NMDAR blockade. This, therefore, demonstrates a role for presynaptic NMDARs in enhancing GABA release at inhibitory PV basket cell-pyramidal cell synapses, and this role may be disrupted by NMDAR hypofunction, leading to reduced GABAergic inhibition of pyramidal cells.

Second, a mechanism involving oxidative stress, which has been separately linked to schizophrenia pathogenesis, has also been proposed to contribute to neural disinhibition resulting from NMDAR hypofunction (Hardingham & Do, 2016). Fast spiking PV interneurons are particularly vulnerable to oxidative stress due to their high metabolic demands (Hardingham & Do, 2016). In addition, networks of extracellular matrix, known as perineuronal nets (PNNs), which provide an antioxidant defence system around PV interneurons, are also vulnerable to damage by oxidative stress (Cabungcal et al., 2013; Steullet et al., 2017). PNNs have been demonstrated to play a critical role in facilitating GABAergic inhibitory transmission (Fawcett et al., 2019; Wingert & Sorg, 2021). Moreover, abnormal PNNs have been found in post-mortem schizophrenia studies and, thus, may underlie the vulnerability of GABAergic interneurons to functional impairments (Enwright et al., 2016; Mauney et al., 2013; Pantazopoulos et al., 2010). A reciprocal relationship between NMDAR function and oxidative stress is reported, whereby NMDAR hypofunction leads to oxidative stress, due to a downregulation of key antioxidant pathways, however, due to the presence of redox-sensitive cysteine residues on obligatory NMDAR subunits, NMDARs are themselves also vulnerable to oxidative insults (Hardingham & Do, 2016). This aberrant feedback loop thereby increases oxidative stress, which impairs the function of PV-interneurons and, in turn, results in neural disinhibition. Consistent with this, markers of oxidative stress have been reported in rodents following both repeated (Behrens et al., 2007; Wesseling et al., 2015) and acute (He et al., 2018) NMDAR antagonism. Furthermore, oxidative stress induced in rodents by NMDAR antagonism has been linked to the loss of GABAergic protein expression in these models,

suggesting that NMDAR antagonist induced GABAergic deficits may be downstream of oxidative stress (Behrens et al., 2007, 2008; Phensy et al., 2020; Zhang et al., 2016).

1.3 Post-mortem histological evidence for reduced GABA markers following NMDAR hypofunction

The neuropathological hallmarks of schizophrenia strongly implicate GABAergic dysfunction in the disease, with a reduction in GABAergic markers found in the hippocampus and PFC of patients with schizophrenia (de Jonge et al., 2017; Dienel & Lewis, 2019; Gonzalez-Burgos et al., 2010; Heckers & Konradi, 2015). In particular, a sub-type of GABAergic interneuron expressing the calcium binding protein PV was reported to be reduced (Beasley et al., 2002; Zhang & Reynolds, 2002). Subsequent studies have revealed that this reduction in PV may represent decreased expression of PV per neuron, rather than a decreased density of PV interneurons (Hashimoto et al., 2003). Nevertheless, this loss of PV expression has been suggested to decrease inhibitory output from PV interneurons, due to disruptions in calcium homeostasis (Lisman et al., 2008). In addition to reduced PV expression, levels of glutamic acid decarboxylase 67 (GAD67), the rate-limiting enzyme in GABA synthesis, have also been reported to be reduced in post-mortem brain analyses of patients with schizophrenia (Benes et al., 2007; Lewis et al., 2012; Tao et al., 2018; Woo et al., 2004), with around half of prefrontal PV interneurons lacking detectable GAD67 mRNA (Curley et al., 2011; Hashimoto et al., 2003). A reduction in GAD67 is consistent with the idea that levels of presynaptic GABA, and therefore inhibitory transmission, are reduced in schizophrenia (Dienel & Lewis, 2019).

Substantial experimental evidence supports that NMDAR hypofunction also leads to a reduction in GABAergic markers. The rodent NMDAR hypofunction studies examined here were identified, first, by referring to key review papers and, second, by searching the following terms in web of science: NMDA receptor and (PCP or ketamine or MK-801) and (GABA* or GAD67 or parvalbumin) and (immuno* or western or PCR). Any relevant papers cited within the studies identified from this search were also examined. A summary of the findings from these studies is presented in table 1.1.

In PV-immunoreactive (PV+) neuronal cultures, ketamine application induced a time and dose-dependent decrease in PV and GAD67 expression (Kinney et al., 2006). Reductions in hippocampal and prefrontal PV+ cells are also reported in rodent models following NMDAR antagonist administration (Abdul-Monim et al., 2007; Hauser et al., 2017; Jenkins et al., 2010; Keilhoff et al., 2004), as well as decreased GAD67 and PV protein expression (Amitai et al., 2012; Behrens et al., 2007; Gigg et al., 2020; Li et al., 2016; Pérez et al., 2019; Zhang et al.,

2008). There is some controversy as to whether NMDAR antagonism leads to a reduction in the number of PV expressing neurons, or whether this simply reflects a decrease in the average PV expression per cell (Benneyworth et al., 2011; Gandal et al., 2012). Previous studies have reported that repeated ketamine treatment in rodents led to a reduction in PV and GAD67 expression, without a loss of PV+ interneurons (Behrens et al., 2007; Zhang et al., 2008). In line with this, studies investigating GABAergic marker changes following NMDAR antagonism in neurodevelopmental models, also suggest that PV+ cell deficits represent a decrease in PV protein expression, rather than cell death. In adolescent rats treated with the NMDAR antagonist MK-801, Li et al. (2016) reported a decrease in PV+ cells, whereas levels of apoptotic factors were unaffected, indicating no neuronal death. Furthermore, studies administering NMDAR antagonists during postnatal development have reported reductions in PV protein, without concomitant cell loss (Kaalund et al., 2013; Powell et al., 2012).

It is important to note that there are some inconsistencies in the literature, with some studies reporting PV+ cell deficits specific to the hippocampus, with no changes in the PFC (Braun et al., 2007) and vice versa (Cochran et al., 2003; Pérez et al., 2019; Thomsen et al., 2010). These inconsistencies may be due to the variation in dosing regimens or subjects used in these studies (see table 1.1 for details), although it is difficult to identify one, or several, factors that may clearly account for the discrepant findings. In addition, Riordan et al. (2018) reported that scPCP treatment induced a loss of GAD67 protein expression, alongside cognitive impairments, without changes to PV expression. The presence of cognitive deficits induced by scPCP treatment, without a significant loss in PV expression, may suggest that PV deficits are not causal to the cognitive deficits reported in these models, but may have an additive effect alongside other systems affected by NMDAR hypofunction (Bygrave et al., 2019). Furthermore, there are some studies which did not report any changes to PV or GAD67 expression following NMDAR antagonist treatment (Benneyworth et al., 2011; Featherstone et al., 2012; Neugebauer et al., 2018). Of these studies, only Featherstone et al. (2012) also confirmed the presence of behavioural deficits in the rats used for GABA marker anlasyes. The washout period used in these studies may also have influenced the presentation of PV deficits. Featherstone et al. (2012) performed analyses 6 months post treatment; it is possible that this relatively long washout period allowed for a functional recovery of PV levels. Alternatively, Cadinu et al. (2018) reported that, in the scPCP model, PV deficits are most pronounced at 6 weeks post treatment, since Benneyworth et al. (2011) and Neugebauer et al. (2018) performed analyses sooner than 6 weeks, it may be that a PV deficit was missed.

Analysing brain markers of GABA function provides insight into the neurochemical brain changes which may underlie, or contribute, to cognitive deficits found in individual studies. The expression of calbindin and somatostatin interneurons are often overlooked in these studies which, given that these types of interneurons have also been suggested to play a role in the aetiology of schizophrenia (Alherz et al., 2017; Lewis, 2014; Reynolds et al., 2001), should be further explored. Li et al. (2016) reported a reduction in the expression of both calbindin and PV interneurons in adolescent rats following sub-chronic MK-801 treatment, followed by a 24 h or 7 d washout. In addition, following the 24 h washout, changes in somatostatin expression were also found in the cingulate cortex. It is reasonable to consider that deficits in these other GABAergic interneurons, as well as PV, may contribute to cognitive deficits in NMDAR antagonist models, however, more studies are required to determine this.

Overall, reports of reduced PV+ interneurons in rodent NMDAR hypofunction models offer support for impaired GABAergic inhibitory transmission in these models; although, it has been questioned whether this is a true reflection of reduced PV interneuron number, or simply a reduction in PV expression per cell (Benneyworth et al., 2011; Gandal et al., 2012). Furthermore, it is currently unclear as to whether reductions in PV and GAD67 are driving neural disinhibition in these models, or whether they may represent a (maladaptive) compensatory response. In cultured neurons, exposure to the GABA-A receptor agonist muscimol prevented the ketamine-mediated decrease in PV and GAD67 expression found in PV interneurons (Behrens et al., 2007). This suggests that a loss of PV and GAD67 expression in PV interneurons may occur secondary to a loss of inhibitory input to excitatory neurons (Behrens et al., 2007). In addition, PV knockout in mice was reported to enhance calcium dependent GABA release (Vreugdenhil et al., 2003). It seems likely that, as suggested elsewhere (Gonzalez-Burgos & Lewis, 2008; Lewis et al., 2005; Rotaru et al., 2012), NMDAR hypofunction may result in neural disinhibition by causing a reduction in GAD67 levels and, given the evidence that decreased levels of PV enhances GABA release (Vreugdenhil et al., 2003), the downregulation of PV may reflect a compensatory response to these changes.

Table 1.1: ***Summary of studies investigating GABAergic biomarker expression in the hippocampus and prefrontal cortex of NMDAR antagonist rodent models.***

Species	Dosing regime	Method	Hippocampus	Prefrontal Cortex	Reference
Sub-chronic models					
♂ LH rats	PCP (5 mg/kg) for 5 d, 24-h washout	IHC	↓PV+ cells CA3 (n.c. DG)		Schroeder et al., 2000
	PCP (2 mg/kg) bi-daily for 7 d, 6-week washout	IHC	↓PV+ cells CA1, DG (n.c. CA2/3)		Jenkins et al., 2008
		IHC		↓PV+ cells PL (n.c. IL, Cg)	McKibben et al., 2010
	PCP (2 or 5 mg/kg) bi-daily for 7 d, 6-week washout	IHC	↓PV+ cells CA1-3 (n.c. DG)		Jenkins et al., 2010
	PCP (5 mg/kg) bi-daily for 7 d, 9 or 10-d washout	IHC		↓PV+ cells	Redrobe et al., 2012
♁ LH rats	PCP (2 mg/kg) bi-daily for 7 d, 6-week washout	IHC	↓PV+ cells DG, CA2/3 (n.c. CA1)	FCx ↓PV+ cells M1 ↑PV+ cells M2, Cg	Abdul-Monim et al., 2007
	PCP (2 mg/kg) bi-daily for 7 d, 9-week washout	IHC	↓PV+ cells CA3, DG	↓PV+ cells IL	Leger et al., 2015
	PCP (2 mg/kg) bi-daily for 7 d, 12-week washout	IHC		↓PV+ cells	Fletcher et al., 2023
		WB		↑PV	
		qPCR		↑PV mRNA	
	PCP (2 mg/kg) bi-daily for 7 d, 14-week washout	IHC		↓PV+ cells	Landreth et al., 2021
♂ W rats	PCP (2 mg/kg) for 2 d, 24-h or 10-d washout PCP (2 mg/kg) for 2 d + 10 d washout + 5 d PCP (2 mg/kg), 24-h washout	IF		↓PV fluor. ↓GAD67 fluor. in PV+ cells	Amitai et al., 2012
	PCP (5 mg/kg) for 5 d, 72-h washout	ISH	n.c. PV mRNA CA1	↓PV mRNA	Thomsen et al., 2010
♂ LE rats	PCP (2.58 mg/kg) daily on days 1-5, 8, 10, 12, 15, 17, 19, 22, 24, 26, 72-h washout	ISH	n.c. PV mRNA DG, CA1-3	↓PV mRNA PL	Cochran et al., 2003
♁ LE rats	PCP (2 mg/kg) bi-daily for 7 d, 7-d washout	qPCR	n.c. GAD67 mRNA n.c. PV mRNA n.c. SST mRNA	n.c. GAD67 mRNA n.c. PV mRNA n.c. SST mRNA	Neugebauer et al., 2018
Ovari-ectomized ♁ SD rats	PCP (2 mg/kg) bi-daily for 7 d, 3-week washout	IHC	n.c. PV+ cells DH	n.c. PV+ cells PL	Riordan et al., 2018
		WB	↓GAD67 DH	n.c. GAD67 PL	
♁ C57BL/6 mice	PCP (10 mg/kg) for 10 d, 15-week washout	WB	↓PV DH, VH n.c. GAD67 DH, VH	FCx ↓PV n.c. GAD67	Gigg et al., 2020
♂ C57BL/6J mice	PCP (10 mg/kg) for 10 d (days 1-5, 8-12), 72-h washout	ISH		n.c. PV mRNA	Thomsen et al., 2009
	PCP (10 mg/kg) for 14 d, 3-week washout	IF		↓PV+ cells	Tsivion-Visbord et al., 2020
	PCP (6 mg/kg) or KET (30 mg/kg) for 5 d, 72-h washout	IHC	n.c. PV+ cells CA1-3, DG	n.c. PV+ cells IL, PL	Benneyworth et al., 2011
		WB	n.c. PV	FCx n.c. PV	
♂ SD rats	KET (30 mg/kg) for 5 d, 72-h washout	IHC	n.c. PV+ cells CA1-3, DG	n.c. PV+ cells IL, PL	
		WB	n.c. PV	FCx n.c. PV	

♂ SD rats	KET (30 mg/kg) for 5 d, 2-week washout	IHC	↓PV+ cells		Keilhoff et al., 2004
	KET (30 mg/kg) for 5 d, 2-4-week washout	IHC	↓PV+ cells CA1, CA3		Kittelberger et al., 2012
	KET (8 mg/kg) for 18 d, no washout	IF	↑PV+ cells CA3		Sabbagh et al., 2013
	KET (30 mg/kg) for 14 d, 24-h washout	IHC	n.c. PV+ cells CA1, CA3, DG		Honeycutt & Chrobak, 2018
	KET (30 mg/kg) for 14 d, 10-d washout	IHC	↑PV+ cells DG (n.c. CA1, CA3)		
♂ LE rats	KET (30 mg/kg) for 2 d, 24-h washout	IF		n.c. PV+ cells ↓PV fluor. ↓GAD67 fluor. in PV+ cells	Zhang et al., 2008
♂ C57BL/6 mice	KET (30 mg/kg) for 2 d, 24 h, 3 or 10-d washout	IF		↓PV fluor. ↓GAD67 fluor. in PV+ cells	Behrens et al., 2007, 2008
	KET (16 mg/kg) 3 times a week for 4 weeks, 48-h washout	IHC	↓PV+ cells		Schobel et al., 2013
♂ C57BL6/N mice	KET (30 mg/kg) for 14 d, 48-h washout	IHC	↓PV+ cells DH	↓PV+ cells	Hauser et al., 2017
♂ C3H/ HeHsd mice	KET (20 mg/kg) for 14 d, 6-month washout	qPCR	n.c. PV mRNA		Featherstone et al., 2012
♂ SD rats	MK-801 (0.5 mg/kg) bi-daily for 7 d, 7-d washout (during which isoflurane anaesthesia was administered for 5 d)	IF		↓PV+ cells Cg (n.c. PL, IL) ↓CB+ cells Cg (n.c. PL, IL)	Tsai et al., 2022
		WB	↓PV ↓CB n.c. GAD67	n.c. PV n.c. CB n.c. GAD67	
♂ LE rats	MK-801 (0.02 mg/kg) for 21 d, 24-h washout	IHC	↓PV+ cells DG, CA1 n.c. CR+ cells	n.c. PV+ cells n.c. CR+ cells	Braun et al., 2007
♂ W Hannover rats	MK-801 (0.2 mg/kg) bi-daily for 7 d, 18-d washout	IHC	↓PV+ cells DG, CA3 (n.c. CA1) ↓GAD65/67+ cells DG (n.c. CA1, CA3)		Unal et al., 2021
Neurodevelopmental models					
Adolescent ♂ (PD 30) W rats	PCP (5 mg/kg) for 5 d, 72-h washout	ISH	n.c. PV mRNA CA1	↓PV mRNA	Thomsen et al., 2010
Adolescent (1 month) ♂ SD rats	KET (30 mg/kg) for 14 d, 24-h washout	IHC	↓PV+ cells CA1, CA3, DG		Honeycutt & Chrobak, 2018
Adolescent (1 month) ♂ SD rats	KET (30 mg/kg) for 14 d, 10-d washout	IHC	↓PV+ cells CA1, CA3, DG		
Adolescent (PD 28) ♂ C57BL/6 mice	KET (16 mg/kg) 3 times a week for 4 weeks, 3-5-month washout	IHC	↓PV+ cells CA1 (n.c. CA3, DG)	n.c. PV+ cells mPFC (PL, IL)	Koh et al., 2016
Adolescent (PD 45) ♂ SD rats	KET (30 mg/kg) for 7 d, 15-d washout MK-801 (0.1 mg/kg) for 7 d, 15-d washout	IF	CA1 VH n.c. PV+ cells n.c. GAD67+ cells n.c. PV fluor. n.c. GAD67 fluor.	mPFC PL layer II/III ↓PV+ cells ↓GAD67+ cells ↓PV fluor. ↓GAD67 fluor.	Pérez et al., 2019

Adolescent (PD 29) ♂ SD rats	MK-801 (0.2 mg/kg) for 14 d, 24-h washout	IHC		↓PV+ cells Cg (n.c. PL or IL) ↓CB+ cells Cg (n.c. PL or IL) n.c. CR+ cells n.c. GAD65/67+ cells	Li et al., 2016
		IF		↓CB+ cells Cg ↓CB+/SST+ cells Cg ↓SST+ cells Cg deep layers (n.c. Cg superficial)	
		WB		↓PV ↓CB n.c. CR n.c. GAD65/67	
	MK-801 (0.2 mg/kg) for 14 d, 7-d washout	IHC		↓PV+ cells Cg (n.c. PL or IL) ↓CB+ cells Cg (n.c. PL or IL) n.c. CR+ cells	
	MK-801 (0.2 mg/kg) for 14 d, 24 h-, 7-, 14- or 28-d washout	IHC	CA1, CA3, DG n.c. PV+ cells n.c. CB+ cells ↓CR+ cells (14-d washout)		Ma et al., 2020
Adolescent (PD 32-40) ♂ LE rats	MK-801 (0.02 mg/kg) for 14 d, 24-h washout	IHC	n.c. PV+ cells n.c. CR+ cells ↓PV:CR+ cells		Rujescu et al., 2006
Neonatal ♂ Crlj:CD1 (ICR) mice	PCP (10 mg/kg) for 3 d on PD 7, 9, 11, 8-week washout	IHC	↓PV CA1		Nakatani-Pawlak et al., 2009
Neonatal ♂ SD rats	KET (75 mg/kg) for 3 d on PD 6-8, 1-d or 7-week washout	WB	↓PV ↓GAD67	↓PV ↓GAD67	Zhang et al., 2016
Neonatal ♂ CB6-TgG42 mice	KET (30 mg/kg) for 3 d on PD 7, 9, 11. Tissue taken in adulthood	IHC		↓PV+ cells	Jeevakumar et al., 2015
Neonatal ♂ C57BL/6 mice	KET (30 mg/kg) for 3 d on PD 7, 9, 11, 6-week washout	IHC		FCx ↓PV+ cells M2, S1, PL	Powell et al., 2012
Neonatal ♂ ♁ C57BL/6 mice	KET (30 mg/kg) for 3 d on PD 7, 9, 11, 15-week washout	IHC	↓PV+ cells DG (n.c. CA1-3)	↓PV+ cells	Martínez-Pinteño et al., 2020

Abbreviations: ♂ = male, ♁ = female, LH = Lister Hooded, W = Wistar, LE = Long Evans, SD = Sprague-Dawley, PD = postnatal day, PCP = phencyclidine, KET = ketamine, IHC = immunohistochemistry (interneuron cell density), + cells = immunoreactive neurons, IF = immunofluorescence (mean fluorescence/cell), fluor. = fluorescence, ISH = in situ hybridisation, WB = western blot, qPCR = quantitative PCR, n.c. = no changes, ↓ = decrease, ↑ = increase, PV = parvalbumin, CB = calbindin, CR = calretinin, SST = somatostatin, DH = dorsal hippocampus, VH = ventral hippocampus, CA1-3 = cornu ammonis region 1-3, DG = dentate gyrus, mPFC = medial prefrontal cortex, FCx = frontal cortex, PL = prelimbic cortex, IL = infralimbic cortex Cg = cingulate cortex, S1 = somatosensory cortex, M1 = primary motor cortex, M2 = secondary motor cortex.

1.4 Neural activity in NMDAR hypofunction models

Consistent with the hypothesis that NMDAR hypofunction impairs GABAergic inhibition, ketamine administration in human volunteers increases cortical excitation, with widespread elevations in regional cerebral blood flow found using PET imaging, particularly in the orbital frontal and cingulate regions (Breier et al., 1997; Holcomb et al., 2005; Rowland, Bustillo, et al., 2005; Rowland et al., 2010; Vollenweider et al., 1997). In this section, we review the evidence for altered neural activity in rodent models following acute, sub-chronic and neurodevelopmental NMDAR antagonism. The studies examined here were identified by searching the following terms in web of science: NMDA receptor and (PCP or ketamine or MK-801) and ((electrophys* or whole-cell or unit or LFP) near recording). Any relevant papers cited within the studies identified from this search were also examined. A summary of the identified studies which investigated the impact of NMDAR hypofunction specifically on inhibitory neurotransmission is presented in table 1.2.

1.4.1 Neural activity in acute NMDAR hypofunction models

Evidence of impaired GABAergic inhibition following acute NMDAR antagonist administration has been reported in the PFC of awake rats treated with MK-801 (Homayoun & Moghaddam, 2007). Spontaneous neural recordings revealed that acute MK-801 treatment predominantly decreased the firing rate of putative GABAergic interneurons and, at a delayed rate, increased the firing rate of putative pyramidal neurons, resulting in a state of cortical neural disinhibition (Homayoun & Moghaddam, 2007). This led to the suggestion that NMDAR antagonists may induce a disinhibited state via a selective disruption of NMDARs which modulate local circuit inhibition. In agreement with this, NMDAR antagonist exposure in cortical and hippocampal slice preparations has been reported to result in reduced inhibitory neurotransmission (Grunze et al., 1996; Li et al., 2002).

In addition to impairments in inhibitory transmission within the PFC, many studies have demonstrated a role for disinhibition of excitatory inputs from distal brain regions in eliciting cortical excitation. One study reported that systemic acute PCP administration in freely moving rats induced a two-fold increase in the spontaneous discharge rate of pyramidal neurons in the mPFC, whereas microiontophoretic application of PCP to the mPFC had little influence on the firing activity of mPFC neurons (Suzuki et al., 2002). This finding suggests that the acute PCP-induced activation of cortical neurons is mediated by excitatory inputs from brain regions outside the mPFC. In line with this, Jodo et al. (2005) found that local application of PCP and MK-801 to the ventral hippocampus resulted in an increase in the spontaneous firing rate of

mPFC neurons, indicating that disinhibited inputs from the ventral hippocampus may contribute to cortical excitation in these models. Studies also report an increase in hippocampal neural activity following systemic NMDAR antagonism. In freely moving rats, Zhang et al. (2012) found that acute systemic ketamine treatment resulted in a significant increase in the firing rate of pyramidal cells in the CA1 region of the dorsal hippocampus, and this increase was significantly reduced, but not eliminated, by muscimol injection into the nucleus reuniens of the thalamus. This suggests that acute ketamine-induced hippocampal activation may be driven, in part, by disinhibited excitatory input from the thalamus (Zhang et al., 2012). Interestingly, other studies have also demonstrated a role of reduced GABAergic activity in the thalamus in mediating an increase in cortical activity following acute NMDAR antagonism (Amat-Foraster et al., 2019; Kargieman et al., 2007; Santana et al., 2011; Troyano-Rodriguez et al., 2014). These studies, therefore, highlight the role of disinhibition in distal sites in producing local increases in hippocampal and prefrontal neural activity in rodent NMDA receptor hypofunction models.

Acute NMDAR antagonist administration has also been reported to induce a temporal disorganization of pyramidal firing, with more irregular spike activity and a reduction in the synchronisation of spike firing (Jackson et al., 2004; Kargieman et al., 2007; Molina et al., 2014). Given the important role of GABAergic interneurons in regulating burst firing (Bast et al., 2017; Isaacson & Scanziani, 2011; Izhikevich et al., 2003), this may reflect changes in GABAergic interneuron-mediated temporal regulation of pyramidal neuron firing, resulting in a disorganisation of spike train activity.

1.4.2 Neural activity in sub-chronic NMDAR hypofunction models

In contrast to findings of increased cortical activity following acute NMDAR antagonism, scPCP treatment in rats was not reported to alter the firing rate of mPFC neurons during spontaneous single-unit recordings in freely moving rats performing the NOR task (Asif-Malik et al., 2017). However, this study did report reduced average spike synchronisation between the mPFC and nucleus accumbens shell, which supports previous findings of disorganised neural activity following acute NMDAR antagonism (Jackson et al., 2004; Kargieman et al., 2007; Molina et al., 2014). Studies in PFC slice preparations from scPCP treated rats have reported a marked increase in the response of pyramidal cells to NMDA, which may be due, in part, to an upregulation of NMDARs (Arvanov & Wang, 1999; Ninan et al., 2003). Recordings in dorsal lateral septal nucleus slice preparations from rats treated with scPCP have also demonstrated an increase in NMDAR mediated transmission, alongside findings of decreased GABA-A

receptor-mediated inhibitory transmission and increased synthesis of NR1 and NR2A subunits (Yu et al., 2002). This study, therefore, indicates a role for both functional NMDAR hyperactivity and disinhibition in sub-chronic NMDAR antagonist induced changes in neural activity (Yu et al., 2002). Impaired inhibitory neurotransmission has also been reported in PFC slice preparations from rats treated with ketamine (2 days, 24 h washout) (Zhang et al., 2008), supporting the hypothesis that NMDAR hypofunction leads to prefrontal disinhibition.

Changes in synaptic plasticity phenomena measured by evoked field potential recordings have also been reported following sub-chronic NMDAR antagonism. Sub-chronic MK-801 treatment in rats enhanced hippocampal CA3-CA1 long term potentiation (LTP) in response to high frequency stimulation under anaesthesia (Ashby et al., 2010). It was suggested that this potentiation may be caused by an upregulation in function or number of NMDARs on pyramidal neurons, or by a disinhibition of pyramidal cells due to decreased GABAergic interneuron activity (Ashby et al., 2010). In contrast, in vitro studies in scPCP treated rodents have reported impaired CA3-CA1 LTP (Nomura et al., 2016; Pollard et al., 2012), or unchanged CA3-CA1 LTP (Tanqueiro et al., 2021). The contrasting findings of these studies may reflect the different NMDAR antagonist used (MK-801 versus PCP) or, perhaps more likely, the use of slice preparation versus in vivo recordings. Slice preparations lack input from other brain regions, such as the thalamus (Kargieman et al., 2007; Yu et al., 2002), which may be involved in driving a disinhibited hippocampal state. In addition to impaired CA3-CA1 LTP, Nomura et al. (2016) reported evidence of increased hippocampal GABAergic activity, with an increased frequency of spontaneous inhibitory post-synaptic current (IPSCs) recorded in pyramidal neurons, and an increase in the amplitude of stimulation evoked IPSCs. These findings of increased GABAergic inhibitory transmission reported in the CA1 hippocampal region following scPCP treatment (Nomura et al., 2016) do not offer support for the hypothesis that NMDAR hypofunction causes impairments in inhibitory transmission. However, it remains to be seen how increased inhibition in this localised synaptic pathway may translate to regional or brain wide changes in neural activity.

1.4.3 Neural activity in neurodevelopmental NMDAR hypofunction models

The hypothesis that NMDAR hypofunction results in neural disinhibition due to a preferential blockade of NMDARs on GABAergic interneurons has been questioned given that NMDARs are not present on GABAergic interneurons in high numbers (Rotaru et al., 2011, 2012). However, in early stages of development, the number of GABAergic NMDARs is reported to be increased (Rotaru et al., 2011), and thus may present a window of developmental GABAergic

vulnerability to NMDAR antagonism. In vitro recordings in hippocampal CA1 brain slices from rats repeatedly treated with MK-801 in adolescence (postnatal day 32-40) show impaired inhibitory transmission, with a significant reduction in the amplitude of evoked IPSPs (Rujescu et al., 2006). In the PFC, repeated MK-801 treatment during adolescence has also been shown to produce enduring deficits in inhibitory transmission which persist into adulthood, whereas such impairments were not found when the same treatment was given in adulthood (Flores-Barrera et al., 2020; Thomases et al., 2013). In contrast, Zhang et al. (2008) reported GABAergic deficits and enhanced pyramidal cell excitability in the PFC following repeated ketamine treatment in adult, but not adolescent, rats.

In addition to treatment in adolescence, evidence of impaired GABAergic transmission is also reported in the PFC of rodents treated with NMDAR antagonists in the neonatal period (Shojaei et al., 2017; Wang et al., 2021). In vitro recordings in PFC brain slices from mice treated with MK-801 showed a decreased frequency of spontaneous IPSCs in pyramidal neurons, and decreased putative PV interneuron excitability, indicating a reduction in GABAergic inhibitory input to pyramidal neurons (Wang et al, 2021). This reduction in inhibitory neurotransmission caused by neonatal NMDAR antagonism has also been shown to cause lasting changes in GABA function which persist into adulthood (Jeevakumar & Kroener, 2016; Kjaerby et al., 2014; Okamoto et al., 2012).

1.4.4 Summary of neural activity changes following NMDAR antagonism

Overall, substantial evidence suggests that acute NMDAR antagonism induces neural disinhibition in the PFC and hippocampus. This is supported by findings of increased cortical and hippocampal pyramidal neuron activity and by direct findings of reduced inhibitory transmission (see table 1.2 for a summary of studies demonstrating evidence of altered inhibitory neurotransmission). Neurodevelopmental NMDAR hypofunction models also demonstrate evidence of reduced GABAergic inhibitory transmission. However, crucially, there are a lack of studies investigating neural changes following sub-chronic NMDAR antagonism, especially in vivo studies which would allow for brain wide circuit functional interactions to be investigated. Nevertheless, an in vivo study in awake rats performing the NOR task found no changes in mPFC spontaneous single-unit activity following scPCP treatment. Furthermore, studies in slice preparations from sub-chronic NMDAR antagonist treated rodents have produced mixed evidence for impaired inhibitory transmission. Thus, evidence for impaired inhibitory transmission in sub-chronic NMDAR hypofunction models is limited.

Table 1.2: ***Summary of evidence for altered inhibitory neurotransmission in NMDAR antagonist rodent models.***

Subject	Dosing regimen	Recording type and brain region	Findings	Reference
Acute models				
♂ SD rats	MK-801 (0.1 mg/kg) during recording	In vivo, awake mPFC	↓ firing rate of ~69% of putative inhibitory neurons ↑ firing rate of 86% of putative pyramidal neurons	Homayoun & Moghaddam, 2007
♂ W rats	PCP (0.25-5 mg/kg) during recording	In vivo, ANA RtN and PFC	↓ firing rate of GABAergic interneurons in RtN	Troyano-Rodriguez et al., 2014
Sub-chronic models				
♂ SD rats	PCP (10 mg/kg) for 5 d, 3-5-d washout	In vitro DLSN	↓ GABA-A receptor-mediated inhibitory response	Yu et al., 2002
Mice C57Bl/6	PCP (10 mg/kg) bi-daily for 7 d, > 7-d washout	In vitro HPC (CA3-CA1)	↑ amplitude of evoked IPSC ↑ sIPSC frequency ↑mIPSC mean amplitude	Nomura et al., 2016
♂ SD rats	MK-801 (0.1 mg/kg) for 5 d, 25-d washout	In vitro PFC (layer V)	n.c.	Flores-Barrera et al., 2020
♂ LE rats	KET (30 mg/kg) for 2 d, 24-h washout	In vitro PFC (layer V)	↓ frequency and amplitude of mIPSCs	Zhang et al., 2008
Neurodevelopmental models				
Adolescent (PD35) ♂ SD rats	MK-801 (0.1 mg/kg) for 5 d, 25-d washout	In vitro PFC (layer V)	↓ frequency of mIPSC and sIPSC ↓ frequency of GABA-A receptor sensitive postsynaptic currents ↓ frequency of EPSC in fast spiking interneurons	Flores-Barrera et al., 2020
Adolescent (PD 32–40) ♂ LE rats	MK-801 (0.02 mg/kg) for 14 d, 24-h washout	In vitro HPC CA1	↓ IPSP amplitude	Rujescu et al., 2006
Adolescent (1 month) ♂ LE rats	KET (30 mg/kg) for 2 d, 24-h washout	In vitro PFC (layer V)	n.c.	Zhang et al., 2008
Neonatal ♂ C57BL/6J mice	MK-801 (0.5 mg/kg) twice on PD 10, 20-d washout	In vitro PFC (layer II/III)	PC: ↓ frequency of sIPSCs PV-I: ↓ firing frequency with increasing current	Wang et al., 2021
Neonatal ♂ G42 mice	KET 30 mg/kg on PD 7, 9, 11, > 60-d washout	In vitro mPFC (layer II/III or V)	↓ frequency of mIPSCs in layers II/III, but not V ↑ frequency of sEPSCs in PV-I	Jeevakumar & Kroener, 2016
Neonatal ♂ and ♁ W rats	MK-801 (1 mg/kg) on PD 6–10, 11-d (PD21) or 18-d (PD28) washout	In vitro PFC (layer II/III)	PD21: ↑ frequency of mIPSCs PD28: ↓ amplitude of mIPSCs	Shojaei et al., 2017
Neonatal LH rats	PCP (20 mg/kg) on PD 7, 9, 11, 55-69-d washout	In vitro PFC (layer II/III or V)	↓ frequency of mIPSCs in layer II/III, but not V ↓ extrasynaptic GABA-A receptor mediated current	Kjaerby et al., 2014
	22-25-d washout		↑ in extrasynaptic GABA-receptor mediated current	
Neonatal ♂ ddY mice	PCP (15 mg/kg) on PD 7, 9, 11, 55-d washout	In vivo, AEP HPC CA3	↓ proportion of narrow spike neurons (putative inhibitory neurons)	Okamoto et al., 2012

Abbreviations: ♂ = male, ♁ = female, LH = Lister Hooded, LE = Long Evans, SD = Sprague Dawley, W = Wistar, PD = postnatal day, PCP = phencyclidine, KET = ketamine, ANA = under anaesthesia, AEP = auditory evoked paradigm, ↓ = decreased, ↑ = increased, n.c. = no changes, IPSP = inhibitory postsynaptic potential, mIPSC = miniature inhibitory postsynaptic current, sIPSC = spontaneous inhibitory postsynaptic current, sEPSC = spontaneous excitatory postsynaptic current, PC = pyramidal cells, PV-I = PV interneurons, mPFC = medial prefrontal cortex, HPC = hippocampus, RtN = reticular nucleus of the thalamus, DLSN = dorsal lateral septal nucleus, CA1-3 = cornu ammonis region 1-3.

1.5 Cognitive deficits in NMDAR hypofunction and neural disinhibition models

NMDAR hypofunction models show deficits in multiple domains of cognition suggested to be relevant to schizophrenia, including task deficits in NOR, reversal learning and attentional set shifting (see Cadinu et al., 2018 and Neill et al., 2010 for review). As outlined above, NMDAR antagonism has been suggested to result in impaired GABA function. However, it is unclear whether GABAergic deficits may contribute to the cognitive deficits reported in these models. Here, we will compare the cognitive deficits induced in by NMDAR antagonism with those produced by prefrontal or hippocampal disinhibition (Enomoto et al., 2011; McGarrity et al., 2017; Murray et al., 2011; Paine et al., 2011; Pezze et al., 2014). As there is only a partial overlap between the cognitive assays used in NMDAR hypofunction and disinhibition models, we focused on two key behavioural assays of memory in rodents: the watermaze and NOR task, which have been used in a substantial number of studies in both models. In addition, the watermaze and NOR tasks have both been suggested to be a useful preclinical tool for assessing cognitive deficits implicated in schizophrenia (Nuechterlein et al., 2004; Young et al., 2009). Relevant studies were identified by referring to key review papers and by searching key terms in web of science. NMDAR hypofunction studies were identified using the search words: NMDA receptor and (PCP or ketamine or MK-801), followed by either (watermaze or water maze), or (novel object recognition or NOR). Neural disinhibition studies were identified using the search words: GABA near (antagonis* or inhibit* or *function), followed by either (watermaze or water maze), or (novel object recognition or NOR). Any relevant papers cited within the studies identified from this search were also examined.

1.5.1 Place learning and memory in watermaze tasks

Watermaze tasks of place learning and memory require rodents to find the location of a hidden platform in a pool of water (Morris, 1981, 2008). In the original and still most common task variant, rodents incrementally learn the position of the hidden platform, which remains in the same position over multiple trials and days of training. The starting position in the watermaze is changed between trials so that the rodent must use allocentric place memory (based on the relations between visuo-spatial cues provided in the room), rather than egocentric search strategies (based on right or left turns), to find the platform. A reduction in the latency or path length to the platform following the training days is often used to measure incremental long-term place memory. Alternatively, changing the platform location after training can provide a measure of reversal learning. In addition, many studies introduce a probe trial, during which the escape platform is unavailable, which makes it possible to measure the rodents' search preference for goal locations.

Performance on watermaze assays of place learning and memory in rodents is impaired by hippocampal lesions (Logue et al., 1997; Morris et al., 1982; Sutherland et al., 1983). Importantly, the degree of task impairment following hippocampal lesions depends on the watermaze task procedure used. In studies using a long-term incremental learning procedure, where rats are trained to find the same platform location over many days, hippocampal lesioned rats can come to show relatively intact performance, albeit at a much slower rate than sham lesioned rats (Bast et al., 2009; Morris et al., 1990b; Whishaw & Jarrard, 1996). In contrast, hippocampal lesioned rats show pronounced task impairment when using a delayed-matching-to-place (DMP) paradigm, where the platform location changes daily, suggesting that this task is more sensitive to hippocampal dysfunction (Bast et al., 2009; Morris et al., 1990b; Steele & Morris, 1999).

Neural disinhibition and watermaze task performance

Performance on the watermaze DMP task is impaired by acute microinfusion of the GABA-A receptor antagonist picrotoxin in the ventral hippocampus, as demonstrated by a marked reduction in search preference for the correct platform location (McGarrity et al., 2017). This study implicates hippocampal neural disinhibition in one-trial learning deficits and, moreover, suggests that impaired hippocampal GABAergic function may contribute to the virtual watermaze deficits reported in patients with schizophrenia (Fajnerová et al., 2014; Hanlon et al., 2006). In support of the role of hippocampal GABA in watermaze task performance, optogenetic inhibition of GABAergic interneurons in the dentate gyrus (DG) region of the hippocampus in mice was reported to impair spatial learning and memory retrieval in the watermaze test (Andrews-Zwilling et al., 2012). In addition, blocking PV neuron synaptic output in the hippocampal CA1 region was reported to result in strong deficits in spatial short-term/working memory, when assessed using a DMP task variant in a Y-watermaze (Murray et al., 2011). This impairment was suggested to reflect one-trial-specific deficits in information processing caused by reduced GABA function, whereas incremental spatial reference memory remained intact (Murray et al., 2011). Similarly, an investigation into chronic immunotoxin induced (SAVAs; Antonucci et al., 2012) GABAergic cell loss in the dorsal hippocampus found that long term depletion of GABAergic neurons (> 14 days) completely abolished spatial learning capabilities on a modified watermaze task (water cross maze; Kleinknecht et al., 2012) (Reichel et al., 2015). Short-term GABAergic depletion (< 14 days) in the dorsal hippocampus also resulted in spatial memory impairments, but this was specific to the acquisition of new spatial memory, with recall memory intact when GABA depletion was induced after training (Reichel et al., 2015). In contrast, mice with genetic ablation of NMDARs in PV interneurons

showed intact watermaze performance, despite exhibiting aberrant gamma activity and deficits in other learning domains (Carlen et al., 2012). However, in this study an incremental learning procedure was used which, as indicated above, may not be as sensitive to hippocampal dysfunction, including GABA dysfunction, as the DMP variant (Bast et al., 2009; Buckley & Bast, 2018). It is also important to note that hippocampal neural disinhibition may, in some circumstances, be beneficial for hippocampal memory performance (Bast et al., 2017; Donato et al., 2013). Spatio-temporally specific reductions in GABAergic function, which are mediated by endogenous plasticity, enhanced performance on the Morris watermaze task, whereas activation of GABAergic interneurons suppressed watermaze learning (Donato et al., 2013). This suggests that spatio-temporally regulated reductions in GABAergic function can have beneficial effects on cognition (Letzkus et al., 2015).

Overall, the watermaze task is highly dependent on hippocampal function, and the studies above illustrate a critical role of GABAergic interneurons in mediating this performance, particularly when rapid place learning or working memory is required. If NMDAR hypofunction results in pronounced GABAergic deficits in the hippocampus, it is reasonable to expect that watermaze performance would also be impaired in these models.

NMDAR hypofunction and watermaze task performance

The function of hippocampal NMDARs has been shown to be critical for spatial learning and memory (Nakazawa et al., 2004; Tsien et al., 1996). Consistent with this, in humans, acute low-dose ketamine has been reported to induce a deficit in spatial memory performance on a virtual watermaze task (Rowland et al., 2005a). In addition, a study assessing virtual watermaze performance in human ketamine users found that heavy and frequent ketamine use was associated with a specific decline in spatial working memory (Morgan et al., 2014). However, it is necessary to note the limitations in this study as all ketamine users were poly drug users, and so the watermaze deficit cannot be definitively attributed to chronic ketamine use. In rodents, studies in adult rats treated acutely with non-competitive NMDAR antagonists (PCP or MK-801), 15-30 min before each testing day have reported watermaze task deficits, with NMDAR antagonist treated rats showing increased latency and path length to the platform location (Enomoto et al., 2008; Pitkanen et al., 1995; Wass et al., 2006; see table 1.3 for a summary of the effects of NMDAR hypofunction on watermaze performance). However, watermaze task deficits following acute NMDAR blockade have been mainly linked to the role of hippocampal NMDARs in LTP-like hippocampal synaptic plasticity, which has been implicated in hippocampal place learning and memory (Bast et al., 2005; Morris et al., 1986,

1990a; Nakazawa et al., 2004; Tsien et al., 1996; but also see: Bannerman et al., 2014; Morris et al., 2013), whereas deficits following sub-chronic NMDAR antagonism may reflect potential GABAergic changes.

Sub-chronic PCP administration in adult mice (2 mg/kg, 7 days) followed by a 24 h washout period resulted in impaired watermaze performance, with increased latencies in incremental long-term and DMP task variants (Beraki et al., 2009). However, a more recent study in mice failed to replicate the watermaze impairments reported in Beraki et al. (2009) using the same dosing regimen but did report an impairment using a higher dose (10 mg/kg), without any apparent motor deficits (Zain et al., 2018). In addition, sub-chronic MK-801 treatment in adolescent rats (0.2 mg/kg, 14 days, starting at postnatal day 29), followed by a 24 h washout period, resulted in watermaze impairments in reversal learning, with a decreased search preference for the platform location (Li et al., 2016). However, the effects of NMDAR antagonism on watermaze performance in this study may be specific to treatment in adolescence, where PV GABAergic interneurons are suggested to be more vulnerable to NMDAR antagonist induced insults (Rotaru et al., 2011; Solbach & Celio, 1991; Wang et al., 2008). Postnatal NMDAR antagonist administration has also been reported to result in watermaze task deficits in adulthood (Andersen & Pouzet, 2004; Huang et al., 2021; Secher et al., 2009; Sircar, 2003; see table 1.3 for details). In agreement with Li et al. (2016), Anderson & Pouzet (2004) reported watermaze deficits when assessed using reversal learning and DMP measures, but without changes in long-term incremental learning.

Studies utilising a sub-chronic regime with longer washout periods (> 24 h) have yielded mixed results on watermaze performance. In adult mice, a study using scPCP treatment (10 mg/kg, 10 days) followed by a 72 h washout period reported no changes in search preference on a long-term incremental learning variant of the watermaze task (Tanqueiro et al., 2021). Interestingly, however, the authors found a significant increase in path length to the platform location on the first day of testing, suggesting that the initial learning, within the first few trials, was impaired; whereas, after longer incremental training over many trials, performance was intact. Treatment with scPCP (2 or 5 mg/kg, bi-daily for 7 days) in rats, followed by a 7 day washout period, has been shown to induce reductions in PV expression, alongside cognitive deficits in NOR and attentional set-shifting (Cadinu et al., 2018; Horiguchi et al., 2011a; Jenkins et al., 2008). However, this treatment regimen was not reported to result in watermaze task impairments (Janhunen et al., 2015). This study was conducted across three different sites and analysed the effects of scPCP treatment on watermaze task performance in male Lister Hooded rats. At all three sites, investigation into path lengths did not reveal a deficit in either

incremental long-term place memory acquisition, reversal learning or one-trial learning assessed using DMP paradigms (Janhunen et al., 2015). Given that reduced hippocampal GABAergic inhibition markedly impairs watermaze DMP performance (McGarrity et al., 2017), this may suggest that reduced hippocampal GABAergic function is not a pronounced feature of the scPCP model. However, the experimenters focused on path length and did not investigate search preference. Search preference has long been suggested to be a better measure of allocentric place learning and memory than latencies and path length measures, because the latter are strongly influenced by chance, and may be substantially reduced by systematic searching and using single directional cues (da Silva et al., 2014). In line with this, sub-chronic MK-801 treatment (0.2 mg/kg, bi-daily for 7 days, 7 days washout) in rats did not result in watermaze deficits assessed using latency measures but did result in a reduced search preference for the correct platform location (Unal et al., 2021). This may suggest that the watermaze task measures used in the Janhunen et al. (2015) study may not have had the sensitivity to reveal watermaze deficits following sub-chronic NMDAR antagonist treatment.

Summary of watermaze findings in NMDAR hypofunction and hippocampal neural disinhibition models

Overall, changes to hippocampal GABA function have been shown to induce impairments in the watermaze task, especially when using DMP or other working memory task variants. Watermaze testing under acute NMDAR antagonism was reported to result in task deficits, however, this may reflect impairments in NMDAR-mediated synaptic plasticity mechanisms or acute sensorimotor effects, rather than potential lasting changes in GABA function. Postnatal and adolescent NMDAR antagonist administration have also been reported to result in watermaze task deficits, and it is possible that this impairment may reflect the presence of hippocampal neural disinhibition in these models. Sub-chronic NMDAR antagonism, however, seems to yield contradictory results, with less pronounced impairments seemingly correlated with increasing length of washout period. Importantly, one key study (Janhunen et al., 2015) employing scPCP dosing found no deficits in watermaze task performance, which does not offer support for pronounced hippocampal disinhibition in this model.

Table 1.3: ***Watermaze studies of place learning and memory performance in NMDAR antagonist rodent models***

Subject	Dosing regimen	Watermaze task procedure	Findings	Reference
Acute models				
♂ SD rats	PCP (2 mg/kg), 15 min before each testing day	Same platform location over 5 d (probe on trial 1 and 4 of each day)	↑ latency ↑ path length on probe ↑ swim speed	Wass et al., 2006
♂ W rats	MK-801 (0.15 mg/kg), 30 min before each testing day	Same platform location over 5 d	↑ latency/path length Diving behaviour n.c. swim speed	Enomoto et al., 2008
♂ Han:W rats	MK-801 (0.1 mg/kg), 30 min before each testing day	Same platform location over 5 d	↑ latency/path length n.c. swim speed	Pitkanen et al., 1995
Sub-chronic models				
♂ LH rats	PCP (2, 3 or 5 mg/kg) bi-daily for 7 d, 7-d washout	RM: same platform location over 4 d + 1 d probe RL: Platform location changed then kept the same over 4 d + 1 d probe WM: same platform location over 3 d + platform location changed daily over 6 d	n.c.	Janhunen et al., 2015
♂ C57BL/6 mice	PCP (10 mg/kg) for 10 d (days 1-5 and 8-12), testing started on day 10, 72-h washout for probe	Same platform location over 4 d + 1 d probe	↑ path length on trial 1 of testing day 1 n.c. on other trials or testing days	Tanqueiro et al., 2021
♂ C57BL/6 mice	PCP (10 mg/kg) for 7 d, 24-h washout	Same platform location over 5 d + 1 d probe	↑ latency/path length ↑ latency on probe n.c. swim speed	Zain et al., 2018
♂ C57Bl/6J mice	PCP (2 mg/kg) for 7 d, 24-h washout	RM: same platform location over 5 d + probe trial 3 h after final trial WM: platform location changed daily over 6 d	RM: ↑ latency/path length ↑ latency and ↓ platform crossings on probe WM: ↓ savings between trials 1-2 n.c. swim speed	Beraki et al., 2009
♂ W rats	PCP (1.3 mg/kg) for 6 d, started 3-d prior to testing	Same platform location over 3 d	↑ path length ↑ number of 'non-finders' n.c. swim speed	Didriksen et al., 2007
♂ W and LH rats	PCP (1.3, 1.6, 2.0 mg/kg) for 8 d, started 3-d prior to testing	Same platform location over 4 d + 1 d probe	LH rats: ↑ latency ↓ search preference (all doses) W rats: ↑ latency (only 2 mg/kg), neither vehicle nor PCP treated W rats showed significant search preference	Ihalainen et al., 2016
♂ W Hannover rats	MK-801 (0.2 mg/kg) bi-daily for 7 d, 7-d washout	Same platform location over 4 d + 1 d probe	n.c. latency ↓ search preference n.c. swim speed	Unal et al., 2021
Neurodevelopmental models				
Adolescent (PD 29) ♂ SD rats	MK-801 (0.1, 0.2, or 0.4 mg/kg) for 14 d, 24-h washout	RM: Same platform location over 5 d + 1 d probe RL: Platform location changed then kept the same over 4 d + 1 d probe	RM: n.c. RL: ↑ latency on day 1 and 2, ↓ search preference in 0.2 mg/kg group (but not 0.1 or 0.4 mg/kg)	Li et al., 2016

Neonatal ♂ and ♁ SD rats	PCP (1 or 5 mg/kg) on PD 5-15, tested at PD 35 or 60	Same platform location over 5 d	1 mg/kg: n.c. 5 mg/kg: ↑ latency n.c. swim speed	Sircar, 2003
	PCP (8.7 mg/kg) on PD 7, 9, 11, tested at PD 56-77	RM: same platform location over 4 d RL: platform location changed then kept the same over 4 d WM: platform location changed daily over 4 d	RM: n.c. RL: ↑ latency in ♂ rats (n.c. ♁) WM: ↑ latency in ♂ rats (n.c. ♁) ↓ swim speed in both sexes	Andersen & Pouzet, 2004
Neonatal ♂ SD rats	PCP (30 mg/kg) on PD 7, 9, and 11, tested at PD 53	RM: same platform location over 4 d + 1 d probe RL: Platform location changed then kept the same over 4 d + 1 d probe WM: platform location changed daily over 4 d	RM: ↑ latency/path length in trials 2–4, n.c. trial 1, n.c. search preference RL: ↑ latency/path length, n.c. search preference, ↑ swim speed WM: ↓ trial 1-2 savings	Secher et al., 2009
Neonatal ♂ BALB/c mice	PCP (5 or 10 mg/kg) on PD 7, 9, 11, 13, 15, tested at PD 49	Same platform location over 5 d + 1 d probe	↑ latency n.c. platform crossings on probe ↓ swim speed	Huang et al., 2021

Abbreviations: ♂ = male, ♁ = female, LH = Lister Hooded, LE = Long Evans, SD = Sprague Dawley, W = Wistar, Han:W = Hannover Wistar, RM = reference memory, RL = reversal learning, WM = working memory, ac = acute, sc = sub-chronic, PD = postnatal day, NeoN = neonatal ac = acute, sc = sub-chronic, ↓ = decrease, ↑ = increase, n.c. = no changes.

1.5.2 Novel object recognition

The standard NOR task (Ennaceur & Delacour, 1988), which relies on rodents' innate preference for novelty, has been widely used to characterise relevant rodent models of human disorders, with mechanisms of NOR impairments suggested to be relevant to recognition memory impairments in human brain disorders, such as schizophrenia (Grayson et al., 2015; Lyon et al., 2012). In the NOR task, a rodent is allowed to explore two identical objects in an arena for a fixed time period (usually 3-5 mins) then, after a retention delay, the rodent is placed back into the arena with an identical copy of one of the objects used in the acquisition trial and a novel object. Naïve rodents typically spend more time exploring the novel object over the familiar, which was suggested to reflect object recognition memory (Ennaceur & Delacour, 1988). Given that the task does not require any extensive training or reinforcements, it has become a quick and effective way of providing a measure of object recognition memory, which avoids potential confounding effects of stress or motivational differences caused by using reinforcements (Lyon et al., 2012).

The mPFC does not seem to be required for the standard NOR task which involves single item recognition without object recency or location judgements (Morici et al., 2015; Nelson et al., 2011; Warburton & Brown, 2015). Indeed, intact NOR memory has been reported following mPFC lesions and temporary pharmacological inactivation (Barker et al., 2007; Ennaceur et al., 1997; Neugebauer et al., 2018). In contrast, the perirhinal cortex is reported to be critical for standard NOR task performance (Barker et al., 2007; Dere et al., 2007; Warburton & Brown, 2015; Winters et al., 2008). Given that the mPFC displays anatomical connectivity to the perirhinal cortex (Deacon et al., 1983), it is possible that mPFC neural disinhibition may affect task performance via an aberrant projection drive to the perirhinal cortex, as local neural disinhibition has the potential to disrupt cognitive processing mediated by efferent sites (Bast et al., 2017).

The involvement of the hippocampus in NOR has been controversial (Cohen & Stackman Jr, 2015; Mumby, 2001). The majority of lesion studies have demonstrated intact NOR performance following hippocampal lesions, suggesting that the hippocampus is not necessary for task performance (Warburton & Brown, 2015). However, permanent lesions may not have the same outcome as temporary pharmacological inactivation. It is possible that the results from permanent lesion studies could reflect the recruitment of extrahippocampal brain regions, which may compensate for loss of hippocampal function (Wang et al., 2015). Indeed, temporary hippocampal inactivation experiments have demonstrated impaired NOR (Cohen et al., 2013; de Lima et al., 2006; Dere et al., 2007; Hammond et al., 2004). It is therefore likely that both the hippocampus and perirhinal cortex are critically involved in the NOR task. Interestingly, the length of retention delay used has been suggested to influence the brain region involved in mediating NOR task performance; retention delays of less than 10 min are suggested to recruit the perirhinal cortex, whereas longer retention delays may recruit the hippocampal region (Cohen & Stackman Jr, 2015). However, a recent study using temporary pharmacological inactivation of the ventral hippocampus found NOR impairments over a 1 min retention delay, suggesting that the hippocampus is involved in NOR memory over short delays (Neugebauer et al., 2018). In addition to retention delay, the involvement of the hippocampus is suggested to depend on the amount of time spent exploring objects in the acquisition phase, with a threshold value of approximately 30 s of exploration thought to ‘move’ neural control from the perirhinal cortex to the hippocampus (Cohen & Stackman Jr, 2015).

Table 1.4: ***Studies of NOR task performance in rodent models of neural disinhibition***

Means of neural disinhibition	Subject	Dosing regimen	NOR design	Findings	Reference
Overexpression of GABA transporter	Transgenic mice over-expressing GAT1 (CMV promoter-controlled)		Hab.: 10 min on testing day 6-min trials, 1-h or 24-h ITI	↓ PI	Ma et al., 2001
Overexpression of GABA transporter	Transgenic mice over-expressing GAT1 (NSE promoted)		Hab.: 10 min on testing day 6-min trials, 0-h, 1-h or 24-h ITI	↓ PI	Hu et al., 2004
Bilateral intra-DH infusions of GABA-A receptor antagonist	♂ SD rats	Bicuculline (0.5 µl/side of 1 mg/mL), immediately after T1	Hab.: 5 min on day before testing 5-min trials, 24-h ITI	↓ PI ↓ DI	Kim et al., 2014
			Hab.: 5 min/day for 5 d before testing 5-min trials, 24-h ITI	n.c. PI n.c. DI	
Bilateral intra-VH infusions of GABA-A receptor antagonist	♁ LE rats	Bicuculline (67 µg/ 0.5 µl/side), 5 min before T1	Hab.: 1 h/day for 3 d prior to testing Re-acc.: 3 min 3-min trials, 1 min ITI	n.c. DI	Neugebauer et al., 2018
Bilateral intra-DH infusions of GABA-A receptor antagonist	Ovariectomized ♁ SD rats	Bicuculline (250 ng/0.5 µl/side), 20–25 min before T1	Hab.: 20 min/day for 2 d + 5 min/day for 2 d Re-acc.: 3 min. 3-min trials, 1-min ITI	× NOR ↓ DI	Riordan et al., 2018
Bilateral intra-DH infusions of glutamate decarboxylase inhibitor		L-allylglycine (20 µg/0.5 µl/side), 20–25 min before T1		× NOR ↓ DI	
Oral administration of an extrasynaptic α5 subunit selective GABA-A receptor antagonist	♂ albino NMRI mice	S44819 (p.o. 0.3 mg/kg) 2 h before T1	Hab.: 2.5 min on day before testing T1: 5 min, or after 10 s exploration per object ITI: 24 h T2: 4 min	↑DI	Gacsályi et al., 2017
	♂ SD rats	S44819 (p.o. 0.1, 0.3, 1 mg/kg) 2 h before T1		↑DI	Etherington et al., 2017

Abbreviations: ♂ = male, ♁ = female, SD = Sprague Dawley, LE = Long Evans, CMV = cytomegalovirus, NSE = Neuron-specific enolase, GAT1 = GABA transporter 1, DH = dorsal hippocampus, VH = ventral hippocampus, p.o. = oral administration, T1 = trial 1/acquisition trial, ITI = inter-trial interval/retention delay, T2 = trial 2/retention trial, Hab. = habituation, Re-acc. = re-acclimatisation DI = discrimination index [(time spent exploring novel object – time spent exploring familiar object)/total object exploration time], PI = preference index (time spent exploring novel object/total object exploration time), × NOR = impaired novel object recognition (non-significant difference between familiar and novel object exploration time), ✓ NOR = intact novel object recognition (significant difference between familiar and novel object exploration time), n.c. = no changes, ↓ = decreased, ↑ = increased.

Neural disinhibition and NOR task performance

The requirement of GABAergic inhibition in NOR performance has not been extensively studied (see table 1.4 for a summary of studies investigating the effect of neural disinhibition on NOR performance). Studies in rats and mice orally administered with S44819, an α5 subunit selective GABA-A receptor antagonist, have reported enhanced NOR (Etherington et al., 2017; Gacsályi et al., 2017). This may reflect potential enhancing effects of finely and dynamically regulated neural disinhibition on learning and memory performance (Bast et al., 2017; Donato et al., 2013). In contrast, studies in transgenic mice overexpressing the neuronal GABA transporter type 1, which results in reduced GABA activity due to increased clearance of GABA from the synaptic cleft, have reported impairments in NOR at retention delays of 1 h and 24 h (Hu et al., 2004; Ma et al., 2001). In addition, brain-wide reductions of AMPA-mediated excitatory input to PV GABAergic interneurons, via genetic ablation of AMPA receptor subunits, in mice led to impaired NOR performance (Fuchs et al., 2007). Similarly, genetic ablation of NMDARs exclusively on PV GABAergic interneurons resulted in NOR deficits, alongside changes to hippocampal gamma and theta activity (Korotkova et al., 2010). This suggests that impaired PV GABAergic interneuron function may be sufficient to drive NOR impairments, possibly by disrupting neural oscillations which have been suggested to be integral to cognitive processing (Fell & Axmacher, 2011).

However, given that NMDAR hypofunction has been reported to alter levels of GABAergic markers in the PFC and hippocampus (see section 1.3), it is of interest to determine the specific role of regional, rather than systemic, GABA changes on NOR. To our knowledge, the effect of neural disinhibition in the mPFC on NOR task performance has not been studied. Thus, it remains to be examined whether prefrontal GABAergic inhibition is required for NOR task performance. In the hippocampus, a study in ovariectomised female rats found that infusion of the GABA-A receptor antagonist bicuculline in the dorsal hippocampus resulted in impaired NOR (1 min retention delay), which was comparable to that following scPCP administration (Riordan et al., 2018). Furthermore, in male rats, dorsal hippocampal microinfusion of bicuculline after the acquisition phase impaired NOR performance using a 24 h retention delay, suggesting that hippocampal neural disinhibition may disrupt NOR memory consolidation (Kim et al., 2014). However, this study also reported that no significant effect on NOR was found following a prolonged habituation period. This highlights the sensitivity of the task to changes in procedure and suggests that hippocampal disinhibition does not affect task performance when the environment is familiar to the rats. In line with this, ventral hippocampal bicuculline infusions had no effect on NOR over a 1 min retention delay (Neugebauer et al., 2018).

NMDAR hypofunction and NOR task performance

NMDAR antagonism produces robust deficits in NOR (see table 1.5 for a summary of the effects of NMDAR antagonism on NOR performance). Sub-chronic PCP treatment, in particular, has been demonstrated to induce reliable impairments in object recognition memory, which has been translated across different sites, species, strains and sexes (see Cadinu et al., 2018; Neill et al., 2010; Rajagopal et al., 2014 for review). NOR deficits have also been reported in rodent models using acute NMDAR antagonist application (de Lima et al., 2006; Grayson & Neill, 2004; King et al., 2004; Pitsikas et al., 2008). The neuropathological changes which may be driving this NOR impairment following NMDAR antagonism has been investigated in some studies. In acute NMDAR antagonist models, hippocampal oxidative stress has been linked to the NOR task deficit observed 24 h following PCP administration, with higher levels of hippocampal nitrotyrosine, a protein marker of oxidative stress, found in PCP treated rats (He et al., 2018). In this study, higher levels of hippocampal nitrotyrosine in the PCP treated rats was correlated with a decrease in exploratory preference in the retention trial of the NOR task, suggesting that increased oxidative stress may be driving the NOR impairment (He et al., 2018). In addition, oxidative stress has also been linked to NOR deficits induced in neurodevelopmental NMDAR antagonist models; genetic deletion of a mitochondrial matrix protein CyclophilinD, which promotes reactive oxygen species production, was found to prevent PV interneuron dysfunction and NOR deficits in mice treated with perinatal ketamine (Phensy et al., 2020).

In the scPCP model, in vivo electrophysiological recordings found that scPCP treatment prevented an increase in mPFC neural activity which was found during novel object exploration by vehicle treated rats (Asif-Malik et al., 2017). In line with this, an in vivo microdialysis study found that scPCP treatment prevented an increase in PFC dopamine levels observed in vehicle treated rats during the retention phase (McLean et al., 2017). These findings were suggested to indicate that mPFC neural activity is important for NOR memory, although lesion and inactivation studies suggest that the mPFC is not required (Morici et al., 2015; Nelson et al., 2011; Warburton & Brown, 2015). Interestingly, scPCP treated rats which are left undisturbed in the NOR test arena for a 1 min retention delay are still able to perform the task, suggesting that scPCP treatment may not affect the memory encoding stage of NOR (Grayson et al., 2014; Landreth et al., 2021). Investigations into brain volume reductions in scPCP treated rats have also revealed a potential role of impaired perirhinal cortex function in the NOR deficit, with a positive correlation between perirhinal cortex volume reduction and time spent exploring the novel object reported (Doostdar et al., 2019). Given the critical role of the perirhinal cortex for

NOR performance (Dere et al., 2007; Warburton & Brown, 2015), it is likely that these brain changes may contribute to the scPCP-induced NOR deficit.

In addition, there are studies which have investigated the impact of GABA antagonism or agonism on scPCP-induced NOR deficits, and these studies may shed light on the role of GABAergic function in the NOR deficits found in NMDAR hypofunction models. Damgaard et al. (2011) reported that the scPCP-induced NOR deficit was reversed following dose dependent treatment with gaboxadol, a functionally selective extrasynaptic GABA-A receptor agonist, and with AA29504, a positive modulator of extrasynaptic GABA-A receptors. Similarly, Rajagopal et al. (2018) reported that TPA-023, a GABA-A receptor positive allosteric modulator, reversed scPCP-induced NOR task deficits in mice. In addition to these studies using systemic administration, a study in ovariectomised rats found that the scPCP-induced NOR deficit was reversed by dorsal hippocampal infusions of the GABA-A receptor agonist muscimol (Riordan et al., 2018). These results align with the hypothesis that cognitive deficits observed in the scPCP model are caused by deficient GABA transmission, given that activating GABA-A receptors in these models resulted in an attenuation of the NOR deficit. In contrast, there are studies which report an amelioration of NOR deficits following administration of drugs which block GABA activity. Redrobe et al. (2012) reported that the scPCP-induced NOR deficit was attenuated following treatment with RO4938581, a negative modulator of GABA-A α5 receptors. It is possible that the contradictory results in these studies may be due to GABA-A receptor subunit specific roles in regulating neural activity, and may reflect the cognitive enhancing effects found in naïve rats following α5 subunit selective GABA-A receptor antagonism (Etherington et al., 2017; Gacsályi et al., 2017). However, microinfusions of the non-specific GABA-A receptor antagonist bicuculline into the ventral hippocampus was also reported to reverse the scPCP-induced NOR deficit (Neugebauer et al., 2018). Although, it should be noted that the mean exploration times reported in this study were relatively low (< 15 s). Indeed, in the Redrobe et al. (2012) study, rodents which did not reach 15 s of object exploration were excluded from analysis. Given that exploration times are suggested to influence the likelihood of memory recall in NOR (Cohen & Stackman Jr, 2015), these relatively low exploration times may have influenced the results.

Summary of NOR findings in NMDAR hypofunction and neural disinhibition models

Overall, NMDAR antagonism appears to consistently result in NOR deficits, whereas the contribution of GABA function to NOR memory is less clear. Studies which report an attenuation of scPCP-induced NOR deficits following GABA-A receptor agonism support a role for neural disinhibition. However, other studies have reported that GABA-A receptor antagonism results in reversal of scPCP-induced NOR deficits. Therefore, it is important to examine the contribution of GABAergic inhibition to NOR task performance. In the hippocampus, there is mixed evidence that neural disinhibition impairs NOR task performance. The discrepancies between findings may reflect the sensitivity of the NOR task to procedural changes, with length of habituation, sample exploration and retention delay suggested to critically influence NOR task performance (Cohen & Stackman Jr, 2015; Janhunen et al., 2015; Kim et al., 2014). Importantly, the effect of neural disinhibition in the PFC on NOR remains to be investigated.

Table 1.5: ***Studies of NOR task performance in sub-chronic NMDAR antagonist rodent models***

Species	Dosing regimen	NOR design	Findings	Reference
♁ LH rats	PCP (2 mg/kg) bi-daily for 7 d, 7-d washout	Hab.: 1 h/day for 3 d Re-acc.: 3 min on testing day, 3-min trials, 1-min ITI	Exp. 1 and 3: x NOR ↓ DI Exp. 2: x NOR n.c. DI	Grayson et al., 2007
		Hab.: 20 min/day for 3 d Re-acc.: 3 min on testing day; 3-min trials, 1-min ITI	x NOR ↓ DI	Arnt et al., 2010; Grayson et al., 2014; Idris et al., 2010; McLean et al., 2009, 2011; Sood et al., 2011
		Hab.: 20 min/day for 3 d Re-acc.: 7 min on testing day; 3-min trials, 1-min ITI	Exp. 1: x NOR ↓ DI Exp. 2: ✓ NOR ↓ DI	Damgaard et al., 2010
			Exp. 1: x NOR ↓ DI Exp. 2 and 3: x NOR n.c. DI	Damgaard et al., 2011
		Hab.: 1 h day before testing Re-acc.: 3 min on testing day, 3-min trials, 1-min ITI	x NOR ↓ DI	Snigdha et al., 2011a
		Hab.: 15 min day before testing, 3-min trials, 1-min ITI	x NOR ↓ DI	Landreth et al., 2021
	1-, 2- or 9-week washout		x NOR	Mitsadali et al., 2020
♁ LE rats	PCP (2 mg/kg) bi-daily for 7 d, 7-d washout	Hab.: 1 h/day for 3 d Re-acc.: 3 min on testing day, 3-min trials, 1-min ITI	x NOR ↓ DI	Horiguchi et al., 2011a, 2011b, 2012; Horiguchi & Meltzer, 2013; Neugebauer et al., 2018
			Exp. 1,3,4: x NOR ↓ DI Exp. 2: x NOR n.c. DI	Horiguchi et al., 2013
♂ LH rats	PCP (5 mg/kg) bi-daily for 7 d, 7-d washout	Hab.: 2 x 10 min day before testing, 3-min trials, 1-h ITI	x NOR ↓ DI	Maeda et al., 2014; Pyndt Jørgensen et al., 2015; Redrobe et al., 2010, 2012
♂ SD rats	PCP (5 mg/kg) bi-daily for 7 d, 7-d washout	15 min trials, 24-h ITI T1: 2 non-identical objects T2: 1 object replaced with novel object	↓ PI	Shirayama et al., 2007
Ovari-ectomized ♁ SD rats	PCP (2 mg/kg) bi-daily for 7 d, 7-d washout	Hab.: 20 min/day for 2 d + 5 min/day for 2 d Re-acc.: 3 min on testing day, 3-min trials, 1-min ITI	x NOR ↓ DI	Riordan et al., 2018; Roseman et al., 2012
♂ C57BL/6J mice	PCP (10 mg/kg) bi-daily for 7 d, 7-d washout	Hab.: 1 h/day for 3 d T1: 10 min, T2: 15 min, 1-h or 24-h ITI	↓ DI	Rajagopal et al., 2018
♂ W rats	MK-801 (5 mg/kg) for 7 d	Hab.: 3 x 5 min on testing day, 3-min trials, 4-h ITI	x NOR	Wiescholleck & Manahan-Vaughan, 2012
♂ W Hannover rats	MK-801 (0.2 mg/kg) bi-daily for 7 d, 7-d washout	Hab.: 1 h day before testing 3-min trials, 1-h ITI	x NOR ↓ DI	Unal et al., 2021

Abbreviations: ♂ = male, ♁ = female, LH = Lister Hooded, LE = Long Evans, SD = Sprague Dawley, W = Wistar, T1 = trial 1/acquisition trial, ITI = inter-trial interval/retention delay, T2 = trial 2/retention trial, Hab. = habituation, Re-acc. = re-acclimatisation, Exp. = experiment, DI = discrimination index [(time spent exploring novel object - time spent exploring familiar object)/total object exploration time], PI = preference index (time spent exploring novel object/total object exploration time), x NOR = impaired NOR (non-significant difference between familiar and novel object exploration time), ✓ NOR = intact NOR , ↓ = decreased, n.c. = no changes.

1.6 Conclusions

Findings of reduced PV+ cells and GAD67 expression in the PFC and hippocampus of NMDAR antagonist treated rodents strongly implicates a link between NMDAR hypofunction and altered GABAergic inhibition. Electrophysiological evidence of increased cortical and hippocampal neural activity following acute NMDAR antagonism, along with direct evidence of impaired inhibitory transmission, also provides strong support for a link between NMDAR hypofunction and neural disinhibition. Similarly, NMDAR antagonism in early development has demonstrated compelling evidence for impaired GABAergic function in these models. However, crucially, more studies investigating the effect of sub-chronic NMDAR antagonism on inhibitory transmission are needed, with conflicting results reported.

The contribution of altered GABAergic transmission to the cognitive deficits found in NMDAR hypofunction models is also unclear, with some results from studies investigating the effect of NMDAR hypofunction and neural disinhibition on performance in watermaze and NOR tasks difficult to reconcile. Watermaze DMP performance has been shown to be impaired following hippocampal neural disinhibition, whereas results from NMDAR hypofunction studies appear to depend on the specific NMDAR hypofunction model used. NMDAR antagonism in early development results in watermaze task deficits and, given the pathological and electrophysiological evidence for impaired inhibitory transmission in these models, hippocampal neural disinhibition may contribute to these deficits. In contrast, sub-chronic NMDAR antagonist treatment in adulthood does not appear to result in watermaze task deficits. However, importantly, the impact of scPCP treatment on the watermaze DMP task measured using search preference has not been investigated. Moreover, NMDAR hypofunction consistently impairs NOR performance, whereas there are conflicting findings for the role of hippocampal disinhibition, and the role of prefrontal GABAergic inhibition has not been investigated.

It is important to note that there are, of course, limitations of comparing an acute model of regional neural disinhibition with a sub-chronic and systemic model of NMDAR hypofunction. In addition, comparisons between these models may be limited by the substantial evidence for a specific role of PV GABAergic interneuron reductions in NMDAR hypofunction models, whereas pharmacological neural disinhibition models do not often target a specific GABAergic cell type. Nevertheless, the scPCP model, which has been shown to result in lasting neurochemical, pathological and cognitive changes of relevance to schizophrenia, presents a useful tool for analysing the effect of NMDAR hypofunction on GABA markers and cognition.

1.7 Thesis aims

This thesis aims to examine the overarching hypothesis that NMDAR hypofunction impairs cognition by causing hippocampal and prefrontal neural disinhibition. In order to address this hypothesis, the following objectives were pursued:

Aim 1: Investigate whether NMDAR hypofunction, induced by scPCP treatment, impairs everyday-type rapid place learning on the watermaze DMP test

The watermaze DMP test has been shown to require hippocampal GABA function, with hippocampal disinhibition markedly reducing search preference for the correct platform location (McGarrity et al., 2017). In chapter 2, we aimed to investigate watermaze DMP task performance in scPCP treated rats, using search preference as our main measure of one-trial place memory. If NMDAR hypofunction causes hippocampal neural disinhibition, we would expect to see similar impairments on watermaze DMP performance to those produced by ventral hippocampal disinhibition.

Aim 2: Characterise the effect of scPCP treatment on the expression of GABA markers in the PFC and hippocampus

In chapter 3, using high-throughput simple western analysis, we aimed to examine the effect of scPCP treatment on PV and GAD67 protein expression in the PFC and hippocampus. Given previous findings of reduced GABAergic markers in rodent models of NMDAR hypofunction (see table 1.1 for a summary), we hypothesised that we would find a reduction in PV and GAD67 protein levels.

Aim 3: Investigate the effect of scPCP treatment on the synaptic excitability of hippocampal circuits

NMDAR hypofunction in rodent models has been suggested to cause impairments in hippocampal GABAergic inhibition. However, whether these impairments may result in functional alterations to in vivo hippocampal neural activity is unclear. In chapter 4, using evoked potential in vivo electrophysiological recordings, we aimed to examine the synaptic excitability of hippocampal circuits in scPCP treated rats. We hypothesised that, due to impaired hippocampal GABAergic inhibition, synaptic excitability would be increased in scPCP treated rats.

Aim 4: Investigate whether neural disinhibition in the prefrontal cortex or hippocampus impairs NOR

Sub-chronic PCP treatment in rats consistently impairs NOR at 1 min retention delays, and such impairments have been suggested to reflect reduced prefrontal and hippocampal GABA function. However, the contribution of GABAergic inhibition in the mPFC and hippocampus to NOR task performance has not been established. In chapter 5, we aimed to investigate NOR performance following neural disinhibition or functional inhibition of the mPFC, dorsal hippocampus or ventral hippocampus.

Chapter 2: Sub-chronic PCP treatment in rats does not impair hippocampal rapid place learning on the watermaze delayed-matching-to-place task

Declaration: Jacco Renstrom and Joanna Loayza assisted with drug dosing and NOR testing.

Abstract

NMDA receptor hypofunction in rodents, caused by scPCP treatment, has been reported to cause impairments in GABAergic interneurons, including in the hippocampus. However, it is unclear how this impairment may contribute to cognitive deficits in the scPCP rodent model. The watermaze DMP task requires hippocampal GABAergic inhibition, with hippocampal neural disinhibition markedly impairing task performance in rats. Therefore, we investigated whether scPCP treatment in rats would cause watermaze DMP deficits, similar to those produced by hippocampal neural disinhibition.

Young adult male and female Lister Hooded rats were tested on the watermaze DMP task at 1, 3 and 5 weeks following scPCP treatment (males: 5 mg/kg; females: 2 mg/kg, bi-daily for 7 days). Rats also underwent testing of NOR, locomotor activity (LMA), startle reactivity and prepulse inhibition (PPI).

Sub-chronic PCP did not impair watermaze DMP performance. In addition, sensorimotor processes measured using LMA, startle and PPI were unaffected by scPCP treatment. NOR testing at week 1 revealed a deficit in the scPCP treatment group, which was not significant at later time points. The scPCP-induced NOR deficit is consistent with previous studies, although many previous studies reported long-lasting impairments. We hypothesised that handling and/or exercise during watermaze testing may have rescued later NOR deficits, as both handling and exercise have been reported to improve scPCP-induced NOR impairments. To test this hypothesis, we repeated the study in a different cohort of rats, but with only NOR testing and with handling kept to a minimum. In this study, the NOR deficit persisted at all testing time points.

Overall, scPCP treatment did not disrupt hippocampal rapid place learning performance. This contrasts with the marked impairments observed following acute pharmacological hippocampal disinhibition. Our findings also support that the scPCP-induced NOR deficit is sensitive to disruption caused either by handling and/or aerobic exercise.

2.1 Introduction

NMDAR hypofunction has been implicated in the aetiology of schizophrenia since the observation that administration of the NMDAR antagonist PCP induces a psychotomimetic state in humans that closely resembles symptoms of schizophrenia (Javitt & Zukin, 1991; Luby et al., 1959). The scPCP rodent model of NMDAR hypofunction shows behavioural changes relevant to negative symptoms and cognitive deficits in schizophrenia, which are suggested to be more overt and longer lasting than deficits reported in acute NMDAR hypofunction models (Jentsch & Roth, 1999; Lee & Zhou, 2019). Deficits in multiple domains of cognition are evident in scPCP rodent models, including in NOR, reversal learning and attentional set shifting (Cadinu et al., 2018). Furthermore, scPCP treatment in rodents has been reported to produce pathological changes to GABAergic interneurons, with reduced expression of PV+ cells found in the PFC and hippocampus (Abdul-Monim et al., 2007; Gigg et al., 2020; Jenkins et al., 2010), which appear to mirror findings in schizophrenia post-mortem brain tissue (Beasley et al., 2002; Benes et al., 2007; Zhang & Reynolds, 2002). It has been hypothesised that scPCP treatment may impair cognition by causing a regional reduction in GABAergic activity, or neural disinhibition, including in the hippocampus (Cadinu et al., 2018). Here, we examined the impact of scPCP treatment in rats on rapid place learning in the watermaze DMP task, which is highly sensitive to hippocampal dysfunction (Bast et al., 2009; Buckley & Bast, 2018; Pezze & Bast, 2012; Steele & Morris, 1999), including hippocampal neural disinhibition (McGarrity et al., 2017).

The watermaze DMP task requires a rodent to find the location of a hidden platform, which changes daily, in order to escape from a pool of water (Morris, 1981; Steele & Morris, 1999). The location of the new platform must be learned rapidly within the first trial of the day, with one-trial place learning measured by latency/path length reductions between trial 1 and 2, and/or search preference for the correct platform location when trial 2 is run as a probe (Gonçalves et al., 2023; McGarrity et al., 2017). The watermaze DMP task has been reverse translated into a human virtual DMP test, making it a highly translational preclinical tool (Bauer et al., 2021; Buckley & Bast, 2018). Furthermore, patients with schizophrenia have shown impairments on a similar virtual analogue of the watermaze task (Fajnerová et al., 2014; Folley et al., 2010; Hanlon et al., 2006). Hippocampal neural disinhibition, caused by microinfusion of the GABA-A receptor antagonist picrotoxin in the ventral hippocampus, impairs performance on the watermaze DMP task in rats, as demonstrated by a marked reduction in search preference for the correct platform location (McGarrity et al., 2017).

Here, we investigated whether scPCP treatment would result in deficits in watermaze DMP performance, similar to those produced by hippocampal neural disinhibition (study 1). To our knowledge, only one previous study has investigated the effects of scPCP treatment on watermaze DMP performance in rats (Janhunen et al., 2015). This study reported no deficits in one-trial place learning when assessed using latency and path length measures. However, latency and path length measures have been shown to be much less sensitive to hippocampal dysfunction than search preference measures (Bast et al., 2009; da Silva et al., 2014; McGarrity et al., 2017). Indeed, one-trial place learning impairment caused by hippocampal neural disinhibition was clearly revealed by reduced search preference, whereas path length reductions from trial 1 to 2 were not unequivocally impaired (although path lengths were significantly increased across trials) (McGarrity et al., 2017). Thus, it remains to be tested whether scPCP treatment induces watermaze DMP task deficits using search preference measures. NOR testing was also included in study 1 as a positive control, as scPCP treatment is reported to produce robust impairments in object recognition (Cadinu et al., 2018; Neill et al., 2010; Rajagopal et al., 2014). In addition, study 1 also assessed selected sensorimotor functions (acoustic startle response and its prepulse inhibition (PPI); open field locomotor activity (LMA)) to ensure any watermaze DMP deficits could be attributed to changes in cognition, rather than sensorimotor disruptions. Results from study 1 NOR testing revealed a significant NOR impairment in scPCP treated rats at 1 week, but not 3 or 5 weeks, post treatment. We hypothesised that handling and/or exercise during watermaze testing in study 1 may have influenced NOR performance, as both handling and exercise were reported to improve scPCP-induced NOR impairments (Landreth et al., 2023; Mitsadali et al., 2020). To examine this hypothesis, we ran another study (study 2) in a second cohort of rats, which only included NOR testing (performed at the same post treatment time points as in study 1), and limited handling throughout the study.

2.2 Materials and methods

2.2.1 Rats

Both studies included male and female rats, in line with the US National Institutes of Health and UK Research Councils expecting that sex is considered as a biological variable in research design (Miller et al., 2017). In addition, as the scPCP model has been widely developed in female rats (Abdul-Monim et al., 2007; Damgaard et al., 2010, 2011; Grayson et al., 2014; Landreth et al., 2021; Mitsadali et al., 2020), whereas the neural disinhibition experiments have been performed in male rats (Gwilt et al., 2020; McGarrity et al., 2017; Pezze et al., 2014;

Williams et al., 2022), using both sexes allowed for more direct comparisons across previous studies. Two different cohorts of Lister Hooded rats (each n = 32, 16 males and 16 females; Charles River, UK) were used for the two studies (for sample size justification see section 2.2.10 Experimental design). In study 1, rats underwent testing on watermaze DMP, sensorimotor, and NOR tasks, and were aged between 8-9 weeks old (weighing 260-330 g (males); 170-220 g (females)) at the beginning of baseline measurements and 10-11 weeks old (weighing 300-400 g (males); 190-250 g (females)) at the start of scPCP/saline treatment. In study 2, rats underwent testing only in NOR and were aged between 10-11 weeks old (weighing 300-350 g (males); 190-250 g (females)) at the start of scPCP/saline treatment. Rats were housed in groups of four in individually ventilated 'double decker' cages (462 mm x 403 mm x 404 mm; Techniplast, UK) under temperature (21 ± 1.5 °C) and humidity (50 ± 8 %) controlled conditions, on an alternating 12 h light-dark cycle (lights on at 07:00 h) (Bio-Support Unit, University of Nottingham). Rats had *ad libitum* access to food and water throughout the study. All procedures were carried out during the light phase and in accordance with the UK Animals (Scientific Procedures) Act 1986.

2.2.2 Sub-chronic phencyclidine treatment

In each cohort of rats, PCP hydrochloride (Bio-Techne, UK) was administered to half of the male rats (n = 8) at a dose of 5 mg/kg (Le Cozannet et al., 2010; Pyndt Jørgensen et al., 2015; Redrobe et al., 2012) and half of the female rats (n = 8) at a dose of 2 mg/kg (Abdul-Monim et al., 2007; Grayson et al., 2014). The remaining rats received vehicle solution (0.9% saline; n = 16, 8 males and 8 females). Rats received injections (1 ml/kg, intraperitoneal (i.p.)) twice daily (at approximately 09:00 h and 15:00 h) for 7 consecutive days, followed by a 7 day washout period before behavioural testing began. This treatment schedule has been well validated elsewhere and is reported to consistently produce robust and persistent deficits in behaviours relevant to schizophrenia (Barnes et al., 2015; Cadinu et al., 2018; Grayson et al., 2014; Neill et al., 2016). The rats' behaviour was closely monitored for 30 mins following injection and any changes recorded as qualitative observations.

2.2.3 Weight monitoring

In study 1, the rats' body weights were recorded daily from the first PCP/saline injection until the end of the study. In study 2, the rats were not weighed daily in order to reduce handling, instead, the rat's body weights were recorded on day 1, 4 and 7 of PCP/saline injections, and then once weekly. The body weights were normalised to the weight recorded on the morning of the first PCP/saline injection day, in order to compare weights across treatment groups.

2.2.4 Handling

Study 1 rats were handled daily (for about 10 min per cage of 4 rats) during the initial acclimatisation period. After the acclimatisation period, rats were handled for at least 30 s every day for the duration of the study during daily weight monitoring and health checks. This was in addition to the handling required for the watermaze DMP, sensorimotor and NOR testing. In study 2, we reduced handling as much as possible. During the initial acclimatisation week, study 2 rats were only handled on two occasions, with less than 1 min of handling per rat. Following scPCP dosing, where rats were handled briefly twice a day for 7 days for injections, study 2 rats were only handled when necessary, i.e., for fortnightly NOR testing, weekly weight monitoring or cage changes.

2.2.5 Watermaze DMP testing

The watermaze DMP task assesses rapid place learning in rodents and is highly sensitive to hippocampal dysfunction (Bast et al., 2009; Buckley & Bast, 2018; McGarrity et al., 2017; Pezze & Bast, 2012; Steele & Morris, 1999). The watermaze DMP task used here consisted of four trials per day, where the rat must find the location of a hidden platform, which changes daily, in order to escape a pool of water. One-trial place learning may be assessed by a reduction in path length/latency to platform between trial 1 and 2, or by search preference for the correct platform location when trial 2 is run as a probe (i.e., with the platform inaccessible to the rat).

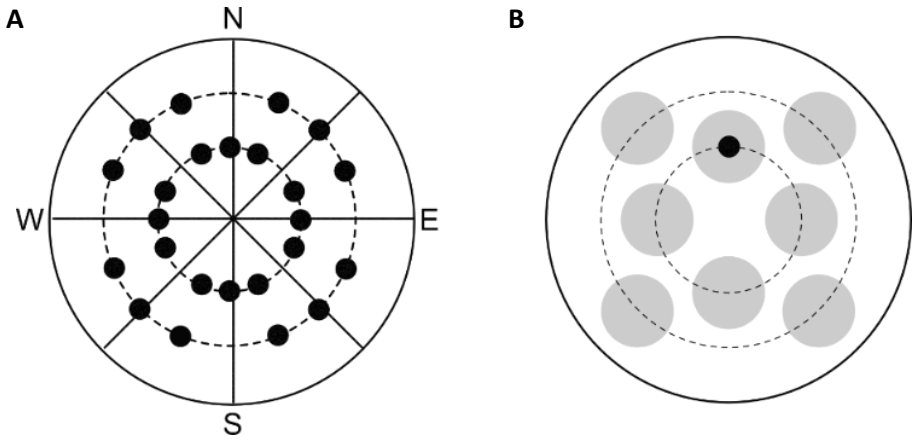

Fig. 2.1. ***Watermaze DMP platform locations and zone analysis*****. A.** Possible locations of the hidden platform (12 cm diameter, black dots). The chosen platform position remained in place for trials 1-4 of each testing day. Rats were released from a different arbitrarily defined starting point (north (N), east (E), south (S) or west (W)) at each trial and had a maximum trial length of 120 s to reach the platform location. **B.** Zone analysis of search preference: eight 40 cm diameter zones (grey circles) were defined, including the correct zone which was concentric with the platform location (black dot). The zones are symmetrically arranged, evenly spaced and non-overlapping.

2.2.5.1 Watermaze apparatus

The watermaze consisted of a circular pool (2 m diameter, 60 cm height), filled with water (25 ± 1 °C) to a depth of 40 cm. The pool was positioned in the centre of a well-lit (200 lux) room, which contained prominent extra-maze visual cues visible from the water surface to aid spatial navigation. The platform (Spooner et al., 1994) was placed 1-3 cm below the water surface at predetermined locations (Fig. 2.1A) and was the rats' only means of escape from the pool. The platform could be lowered and held at > 20 cm below the water surface using a computer-controlled electromagnet (Med Associates Inc., US). This allowed probe trials to be run, where the rats' search preference for the correct zone could be measured in the absence of an accessible platform. After 60 s the platform would return to its normal position, allowing the rat to escape from the pool.

The watermaze pool contained 24 possible platform locations (Fig. 2.1A) which were spread evenly, with half the locations on an inner concentric ring (0.8 m diameter) and half on an outer concentric ring (1.4 m diameter). In order to ensure that performance on any given day was not biased by the platform location, two different sequences of platform locations were used throughout the study, which were counterbalanced between the two treatment groups. This meant that on each testing day, half of the male and female rats were tested on one platform location and the other half tested on a different location. Four release points were arbitrarily defined at equidistant points around the pool circumference (north, east, south and west). The rat was released from a different point at each trial, with the sequence of release points allocated randomly and changing each day, in order to discourage egocentric search strategies.

An overhead camera recorded each trial and live tracking software (Ethovision software, version XT 7, Noldus Technology, Netherlands) was used to obtain search preference, path length and latency to platform, and swim speed. To enable successful tracking, the pool was made opaque by adding non-toxic water-soluble white children's paint (Artmix, Scolaquip Ltd, UK), which increased the contrast between the rat and water surface of the pool.

2.2.5.2 Watermaze DMP procedure

The DMP version of the watermaze task was used (Bast et al., 2009; Steele & Morris, 1999), where the position of the hidden platform was moved to a novel location each day. The procedure was based on a previously established protocol (Gonçalves et al., 2023; McGarrity et al., 2017). Each testing day consisted of four trials per rat, with the platform location

remaining the same across all four trials. The rat was placed into the pool (facing away from the centre) at one of the four defined release points (north, east, south or west) and was required to find the hidden platform in order to escape. The rat had 120 s to find the platform, after which the rat would be guided to the platform by the experimenter. The rat remained on the platform for 30 s before being removed in order to encourage the formation of place memories using the surrounding visual cues. On non-probe days, the interval between the trials was 10-30 s (as short as required for convenience). On probe days, an interval of 20 min was used between trial 1 and 2, with trial 2 run as a probe (platform inaccessible to the rat for 60 s), as this longer retention delay renders the task sensitive to disruption by hippocampal plasticity mechanisms, including mechanisms mediated by NMDARs, which are not required at shorter intervals (Steele & Morris, 1999). The remaining trials were run with a 10-30 s interval.

Before scPCP/saline treatment, rats were pretrained on the watermaze DMP task for 8 days in order to reach asymptotic performance levels (Bast et al., 2009; Jackson et al., 2011; McGarrity et al., 2017). During pretraining, rats received 4 days of testing with a 10-30 sec interval between trials. On the remaining 4 pretraining days, rats were tested with a 20 min interval between trial 1 and 2, with trial 2 on days 6 and 8 run as a probe. After scPCP/saline treatment, rats were tested on the watermaze DMP task at three separate time points (1 week, 3 weeks and 5 weeks post scPCP treatment), each with four days of testing. Days 1 and 3 were run as non-probe days and days 2 and 4 as probe days. Analysis focused on data from trial 2 of each day, where performance relies on rapid place learning during trial 1. Trials 3-4 were run to reinforce the win-stay rule of the task.

2.2.5.3 Behavioural measures of watermaze DMP task performance

Search preference for correct platform zone and previous day's zone

Analysis of one-trial place memory impairments on the watermaze DMP task focused on search preference data obtained during probe trials, as search preference has been reported to be a more sensitive measure of hippocampal function than latency and path length measures (Bast et al., 2009; da Silva et al., 2014; McGarrity et al., 2017; Pezze & Bast, 2012). To measure search preference, eight 40 cm diameter zones were defined within the watermaze pool, including the 'correct zone' and the previous day's zone, which were concentric with the platform location (Fig. 2.1B). The zones were arranged symmetrically around the pool such that they were evenly spaced and non-overlapping, with four zones on an inner concentric ring and four on an outer concentric ring. Search preference for the correct

zone was calculated during the first 60 s of trial 2 on probe days (the duration where the platform was inaccessible to the rat), as follows: time spent in correct zone/time spent in all eight zones x 100%. Search preference for the previous day's location was also calculated, as follows: time spent in previous day's zone/time spent in all eight zones x 100%. Ethovision software was used to quantify the amount of time the rat spent in each zone. Chance exploration was defined as a search preference of 12.5% (equal time spent in all eight zones), whereas higher values would represent a greater search preference.

Path lengths and latencies

Path lengths and latencies were also used to determine watermaze DMP task performance. Path length (cm) and latency (s) to the platform was measured from the point of release into the pool until the platform was reached (on probe trials, the end point was taken when the rat crossed the location where the platform had previously been). Path lengths were only analysed on probe days, whereas latency measures were analysed for all testing days. Impairments in one-trial place memory would be indicated by a marked reduction in path length/latency savings between trial 1 and 2. Path lengths and latencies often show similar patterns, but path lengths are independent of swim speed.

Swim speed

The swim speed was measured during the 60 s probe trial using Ethovision software.

2.2.6 Open-field locomotor activity

Open-field LMA was measured as in previous studies (McGarrity et al., 2017; Pezze et al., 2014). The LMA chambers consisted of 12 clear Perspex boxes (23.5 x 39.5 x 24.5 cm) with metal grid lids, situated in a dimly up-lit room (40-60 lux in chambers). The chambers were surrounded by a frame containing two levels of photobeams in a 4 x 8 configuration (Photobeam Activity System; San Diego Instruments, US). A locomotor count was generated by two consecutive breaks of adjacent beams within the lower level of photobeams. The rat was placed in the centre of the chamber at the start of each session, which lasted 30 min. The sum of locomotor counts for each 10-min block was calculated.

2.2.7 Startle and prepulse inhibition testing

Startle and PPI was measured as in previous studies (McGarrity et al., 2017; Pezze et al., 2014), using four startle response systems (San Diego Instruments, US). Each system was contained in a ventilated sound attenuated chamber (39 x 38 x 58 cm, interior lighting 15 W), and

comprised a clear Perspex cylinder (8.8 cm diameter x 19.5 cm) on a Perspex base, which was linked to an accelerometer. A speaker positioned centrally above the cylinder presented the background noise and the acoustic pulse, with the noise generator controlled by the SR-Lab System (San Diego Instruments, US). The accelerometer was connected to Reflex Testing Software (San Diego Instruments), which recorded individual whole-body startle responses. The whole-body startle amplitude, in response to an acoustic pulse, was defined as the average of 100 accelerometer readings (1 ms per reading) recorded from pulse onset.

The testing session consisted of a 5-min acclimatisation period in the cylinder, with a continuous background noise (62 dB(A)), followed by three separate testing blocks. The first block consisted of 10 startle pulse-alone trials (120 dB(A) broad band bursts, 40 ms), to habituate the rats to a stable level of startle reactivity. The second block consisted of 50 trials to measure PPI. There were 5 different types of trials used: one startle pulse-alone trial, and four prepulse-plus-pulse trials where a different intensity of prepulse (72, 76, 80 or 84 dB(A), 20 ms) preceded the startle pulse by 100 ms. Each trial was presented 10 times in a pseudorandom order and with a variable interval between trials (10-20 s). The third block consisted of five startle pulse-alone trials. The entire test session lasted 23 min.

Startle amplitude was analysed for the pulse-alone trials in each testing block, providing a measure of startle habituation. The percentage of PPI was calculated from the second testing block as follows: (mean startle amplitude on pulse-alone trials - mean startle amplitude on prepulse-plus-pulse trials)/mean startle amplitude on pulse-alone trials x 100%.

2.2.8 NOR testing

The NOR task is widely used in rodents as an indicator of recognition memory, with the time spent exploring a novel object over a previously encountered (familiar) object used as a measure of intact NOR (Ennaceur & Delacour, 1988; Grayson et al., 2015). The NOR procedure used here was adapted from previous studies (Gonçalves et al., 2023; Grayson et al., 2007; Pezze et al., 2015).

The NOR arena consisted of an opaque rectangular box (38 x 40 x 54 cm) with a Perspex lid. The light level in each arena was between 30-40 lux. An overhead camera (HD Everio, GZ-EX515BEK, JVC) was used to record behaviour for subsequent analyses. The objects used were arranged into sets of two objects (one to be used as the novel and one as the familiar) which consisted of different shapes, colours, sizes and materials. The object used as novel was counterbalanced across each group, as was the position of the novel object in the arena (left

or right). Time spent exploring an object was defined as interacting with the object (e.g., sniffing) and directing the nose at the object at a distance of < 1 cm. Object exploration was not recorded if the rat was in contact with the object but not facing it (e.g., standing/sitting on the object or using it as a prop) (Ennaceur & Delacour, 1988). The arena and objects were cleaned with an alcohol-based solution (20% v/v) before each trial to reduce olfactory cues left by the rats.

Each rat was habituated the empty NOR arena for 1 h on the day before testing and reacclimatised to the arena for 3 min on the testing day. The NOR task consisted a 3 min acquisition and retention phase, which were separated by a 1 min retention delay. In the acquisition phase, the rat was placed in the NOR arena with two identical objects. In the retention phase, the rat was returned to the arena with a copy of the object used in the acquisition trial and a novel object. Behaviour was recorded using an overhead camera and exploration times scored using 'The Novel Object Timer' (created by Jack Rivers-Auty, https://jackrrivers.com/program/; Gigg et al., 2020), with the scorer blind to treatment group and object type (novel or familiar). The discrimination index (DI) ((time spent exploring the novel object - time spent exploring the familiar object)/total time spent exploring both objects) was also calculated and used as a measure of NOR performance, with a higher value indicating greater preference for the novel object (Gigg et al., 2020).

2.2.9 Tissue collection

At 6 weeks post scPCP treatment, rats were killed by carbon dioxide inhalation and cervical dislocation. The brains were removed, flash frozen using dry ice, and stored at -80 °C until subsequent post-mortem analyses using simple western (Wes) (chapter 3).

2.2.10 Experimental design

In both studies, saline and scPCP treatment groups underwent repeated behavioural testing at baseline, i.e. before saline or scPCP treatment, and at several time points after the 7 day washout period (see Fig. 2.2 for timeline of testing in study 1 and 2). A sample size of n = 16 rats was chosen to give us > 80% power to detect treatment group differences at an effect size corresponding to Cohen's d = 1, using pairwise comparisons by independent samples t-tests (two-tailed, $p < 0.05$). Rats were allocated to either saline or scPCP treatment groups, according to a randomised block design, with half of each cage of four rats (and half of the male and female rats) assigned to each treatment group. The experimenter was blinded to treatment group at the start of the study. In study 1, rats underwent baseline testing of NOR

(2 days), LMA and startle/PPI (1 day), and pretraining on the watermaze DMP task (8 days) before drug treatment. The watermaze DMP performance level at pretraining was analysed to confirm that the prospective treatment groups were matched as far as possible. Rats were then dosed with either saline (1 ml/kg, i.p.) or PCP (females: 2 mg/kg; males: 5 mg/kg, i.p.) bi-daily for 7 days followed by a 7 day washout period. At 1, 3 and 5 weeks post scPCP treatment, rats were tested on the following behavioural tasks over consecutive days: NOR (2 days), LMA and startle/PPI (1 day), and watermaze DMP task (4 days) (Fig. 2.2A). In study 1, one rat was excluded from NOR analysis as it knocked over an object during the trial at 5 weeks post scPCP treatment. In study 2, rats were tested only on the NOR task, at 1, 3 and 5 weeks post scPCP treatment (Fig. 2.2B).

2.2.11 Statistical analysis

Graphs and statistical tests were completed using GraphPad Prism (version 9) and JASP (version 0.14.1) software, respectively, with $p < 0.05$ considered to indicate statistical significance. The different performance measures outlined above were analysed using analysis of variance (ANOVA) with treatment group (scPCP or saline) and sex as between-subjects factors, testing time point (1, 3 or 5 weeks post treatment) as a within-subjects factor, and, where appropriate, trial (watermaze data), test block (LMA and startle data), prepulse intensity (PPI data), or object (familiar vs novel, NOR data) were included as within-subjects factors. In addition, watermaze DMP search preference and NOR DI measures were compared to chance using planned one-sample t-tests. Planned pairwise t-tests were also used in NOR analyses to examine familiar versus novel exploration time. Baseline/pretraining data were not included in the post treatment ANOVA analysis but were analysed separately using ANOVA (with prospective treatment group and sex as between-subjects factors, and trial, test block, prepulse intensity, or object as within-subjects factors), to ensure that there were no significant group differences before scPCP treatment (Gonçalves et al., 2023). In addition to the overall ANOVA including all post treatment testing time points, we planned to analyse NOR data separately at each time point to examine the significance of NOR deficits, as previous studies have shown conflicting reports as to whether the scPCP-induced NOR deficit is long-lasting (Pyndt Jørgensen et al., 2015; Rajagopal et al., 2014).

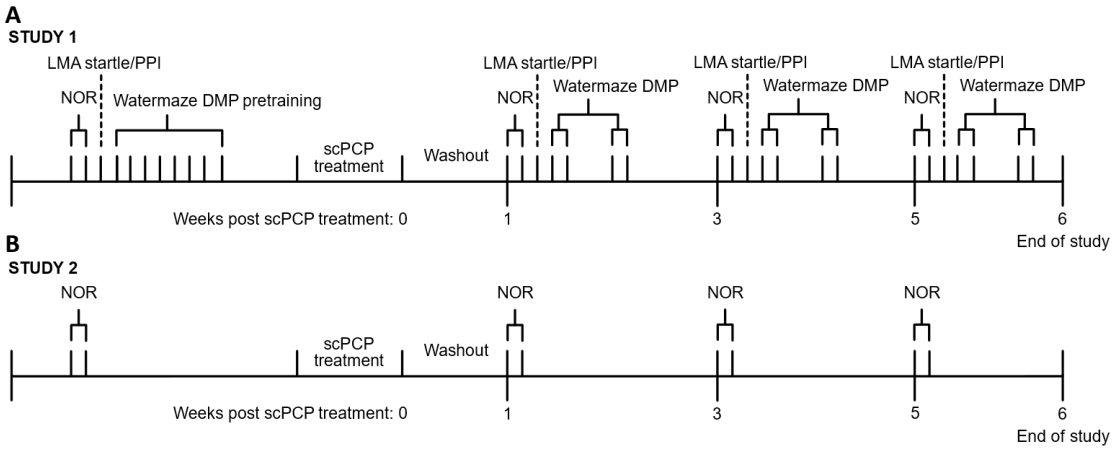

Fig. 2.2. ***Timeline of study 1 and 2.*** **A.** In study 1, rats were tested for baseline performance in novel object recognition (NOR) (2 days), locomotor activity (LMA) and startle reactivity/prepulse inhibition (PPI) (1 day), and pretrained on the watermaze delayed-matching-to-place (DMP) task (8 days). Rats received either PCP or saline (vehicle) injections bi-daily for 7 days, followed by a 7-d washout. Immediately after washout, rats were tested in NOR (2 days), LMA and startle/PPI (1 day) and watermaze DMP task (4 days). This was repeated at 3 and 5 weeks post scPCP treatment until the end of study at 6 weeks post treatment. **B.** In study 2, rats received either PCP or saline (vehicle) injections bi-daily for 7 days, followed by a 7-d washout. Rats then underwent NOR testing at 1, 3 and 5 weeks post scPCP treatment until the end of study at 6 weeks post treatment.

2.3 Results

2.3.1 Visual inspection of acute behavioural changes following PCP dosing

Rats were monitored for at least 30 min following each of the two daily PCP/saline injections and any acute side effects were recorded as qualitative observations (see table 2.1). In the scPCP treated rats, the main side effect observed following dosing was mild ataxia, including a loss of balance (usually noted when the rat would fall backwards during rearing or climbing). This loss of balance was observed across both studies, and in both male and female rats. We also observed rats dragging their rear end while walking around, which may have reflected loss of hind limb muscle coordination. This behaviour appeared to be more prominent in the male rats; in both studies, this behaviour was seen in the females only on the first day of PCP dosing, whereas males continued to show this behaviour at the end of the dosing week. Mild stereotypy in the form of head movements was also observed in some rats following PCP injection. In study 1, head movements were recorded in both males and females, and in different rats. In study 2, this behaviour was exclusively seen in the male rats, and often observed in the same rats, with 4 rats accounting for 15 out of the 17 observed instances. These behavioural effects typically resolved within 2 h. No side effects were observed in the saline rats.

Table 2.1. ***Acute behavioural changes observed in the 30 min following PCP injection for each day during the scPCP dosing week in study 1 and 2.*** Numbers indicate rats where each behaviour was observed in the male PCP (mPCP) or female PCP (fPCP) treated groups, n = 8 rats per group. In study 1, behaviours were recorded cumulatively for the day. In study 2, observations were recorded separately for AM and PM dosing. None of the behaviours listed were observed in saline treated rats.

Study 1															
Observation	**Group**	**PCP/saline dosing day**													
		1		**2**		**3**		**4**		**5**		**6**		**7**	
Loss of balance	mPCP	7		8		7		4		4		4		7	
	fPCP	8		7		6		3		5		6		4	
Head movements	mPCP	1		0		2		1		0		0		0	
	fPCP	1		1		1		0		1		0		0	
Dragging rear end	mPCP	3		1		3		1		1		1		1	
	fPCP	1		0		0		0		0		0		0	
Study 2															
Observation	**Group**	**PCP/saline dosing day**													
		1		**2**		**3**		**4**		**5**		**6**		**7**	
		AM	**PM**	**AM**	**PM**	**AM**	**PM**	**AM**	**PM**	**AM**	**PM**	**AM**	**PM**	**AM**	**PM**
Loss of balance	mPCP	3	1	6	5	5	5	3	6	6	7	7	5	4	7
	fPCP	6	3	5	6	5	4	2	6	4	4	2	4	0	2
Head movements	mPCP	2	4	1	2	2	0	2	3	1	0	0	0	0	0
	fPCP	0	0	0	0	0	0	0	0	0	0	0	0	0	0
Dragging rear end	mPCP	5	6	3	2	1	3	0	0	0	1	1	2	1	1
	fPCP	3	0	0	0	0	0	0	0	0	0	0	0	0	0

2.3.2 Sub-chronic PCP treatment reduced body weight

In study 1, scPCP treated rats showed reduced weight compared to saline treated rats (Fig. 2.3A). Sub-chronic PCP treated rats showed weight loss, compared to their pre-injection weight, during the during the first few days of scPCP dosing. This weight loss peaked at 3 days following the first injection, after which the weight-growth curve converges with that of the saline control group. However, control weight levels were not completely reached in the male scPCP treatment group by the end of the study. This is confirmed by ANOVA which revealed a significant main effect of treatment group across the duration of the study ($F_{(1, 28)} = 7.58$, $p = 0.01$), and a significant interaction between treatment group and day ($F_{(49, 1372)} = 4.46$, $p < 0.001$), reflecting the initial weight loss in the scPCP treatment group followed by a convergence with the saline weight-growth curve. Although body weight reduction in scPCP treated rats was mainly apparent in the males, compared to the females, from around 1-2 weeks following washout, there was no significant interaction or main effect involving sex (sex and treatment interaction: $F_{(1, 28)} = 2.56$, $p = 0.121$; all other $F_{(49, 1372)} < 1$).

In study 2, male rats treated with scPCP showed reduced weight compared to saline treated rats, consistent with our findings in study 1 rats (Fig. 2.3B). However, in contrast to study 1, we did not find a reduction in the weights of female scPCP-treated rats. In addition, the male scPCP treated rats in study 2 reached, and even exceeded, the control weight levels from 5 weeks post-scPCP treatment. This is confirmed by ANOVA which revealed a significant interaction between treatment group and sex ($F_{(1, 28)} = 7.31$, $p = 0.012$), and between treatment group, sex and day ($F_{(8, 224)} = 21.9$, $p < 0.001$) for the duration of the study. Simple main effects analysis of the male body weights revealed a significant main effect of treatment group ($F_{(1, 14)} = 5.22$, $p = 0.038$). In addition, there was a significant interaction between treatment group and day ($F_{(8, 112)} = 28.6$, $p < 0.001$), reflecting the initial weight loss in the scPCP treatment group followed by convergence with the saline weight-growth curve. In contrast, analysis of the female data revealed no main effect of treatment group ($F_{(1, 14)} = 2.14$, $p = 0.166$), however, there was a significant interaction between treatment group and day ($F_{(8, 112)} = 2.04$, $p = 0.047$).

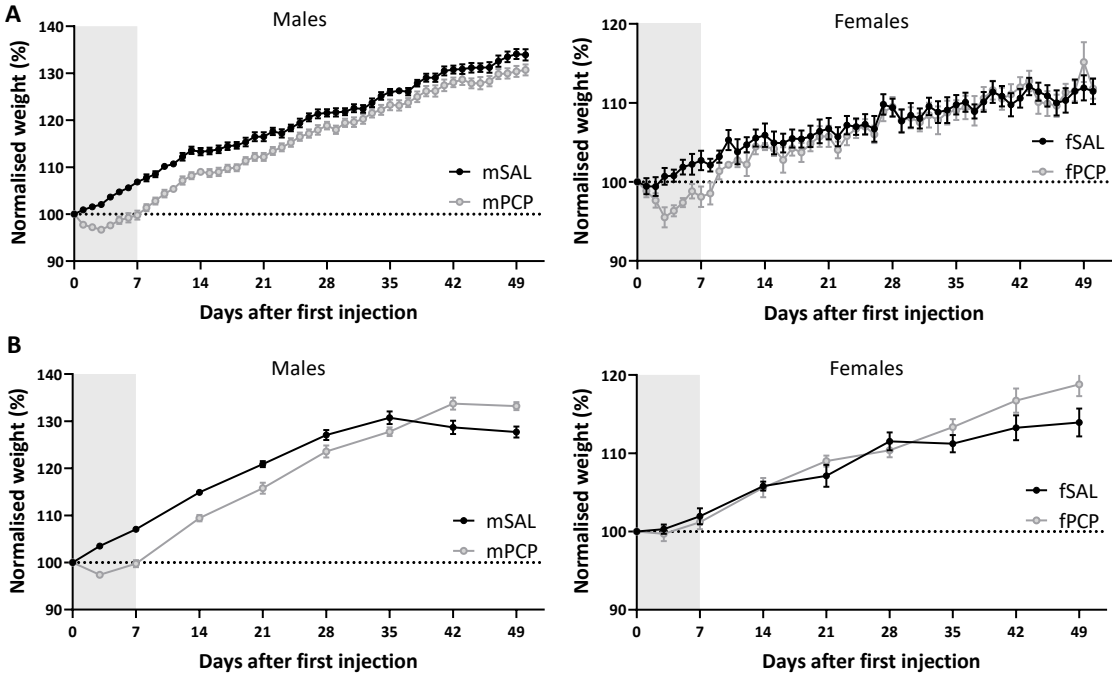

Fig. 2.3. ***Sub-chronic PCP treatment reduced body weight in study 1 rats and in male rats in study 2.*** Normalised weights (mean ± SEM) are shown from the first day of the scPCP/saline dosing week (shaded area) until study completion, for male saline (mSAL), male scPCP (mPCP), female saline (fSAL) and female scPCP (fPCP) treated rats, n = 8 per group. **A.** Study 1: body weight was significantly reduced in scPCP treated rats during the duration of the study. **B.** Study 2: body weight of male scPCP treated rats was significantly reduced.

2.3.3 Study 1: Sub-chronic PCP did not markedly impair watermaze DMP performance, but impaired NOR at 1 week post treatment

2.3.3.1 Behavioural performance at baseline was matched between prospective treatment groups but indicated some sex differences

Male rats tended to show greater search preference than females during watermaze DMP pretraining

Analysis of search preference data on probe days during pretraining (days 6 and 8) showed no differences between performance in the prospective saline versus scPCP treatment groups ($F_{(1.28)} < 1$), with rats in both prospective treatment groups exploring the correct zone significantly above chance ($t_{15} > 4.89$, $p < 0.001$) (Fig. 2.4, pretraining, top left panel). The pretraining search preference data did, however, indicate a sex difference in performance, with a strong trend for males to show greater search preference for the correct platform location than female rats ($F_{(1.28)} = 3.875$, $p = 0.059$). This study is consistent with previous studies on the standard spatial reference memory watermaze task, where male rats tend to perform better (Jonasson, 2005). The human virtual DMP task also showed a male advantage (Buckley & Bast, 2018), supporting the translational validity of the task. Testing at later time points did not, however, reveal any pronounced sex differences (see post treatment results below, section 2.3.3.2), suggesting that female performance on the watermaze DMP task improves with practice. In line with this, the male advantage in previous watermaze studies in rats tended to be larger in studies that did not use pretraining (Jonasson, 2005). In addition, in humans, there is some evidence that regular computer gaming leads to an improved performance on the virtual watermaze DMP test (Buckley & Bast, 2018). Analysis of path lengths to platform location during pretraining revealed no main effect of prospective treatment group ($F_{(1, 28)} < 1$), sex ($F_{(1, 28)} = 1.91$, $p = 0.178$), or an interaction involving these factors ($F_{(1, 34)} < 2.16$, $p > 0.099$) (Fig. 2.6, pretraining, left panels). Analysis of swim speeds during pretraining probe trials (Fig. 2.7, pretraining, left panel) revealed no main effect or interaction involving prospective treatment group ($F_{(1, 28)} < 1.92$, $p > 0.177$), but did reveal a main effect of sex ($F_{(1, 28)} = 7.58$, $p = 0.01$), reflecting increased swim speed in the female rats. This contrasts with previous watermaze studies in rats which found no difference between male and female swim speeds (Beiko et al., 2004; Devan et al., 2016; Hernandez et al., 2020).

Female rats showed increased locomotor activity and reduced startle reactivity compared to males

Baseline testing of open-field LMA revealed no differences between prospective treatment groups (Fig. 2.8, baseline, left panels), with ANOVA revealing no main effect ($F_{(1,28)} < 1$) or interaction involving prospective treatment ($F_{(1,28)} > 1.73$, $p > 0.2$). There was, however, a significant main effect of sex ($F_{(1,28)} = 10.2$, $p = 0.004$), reflecting increased locomotor activity in female rats, compared to the males. There was also a trend for an interaction between sex and test block ($F_{(2,56)} = 2.81$, $p = 0.069$), reflecting that the increased activity in female rats was mainly apparent during the first to second 10-min blocks. This finding of increased locomotor activity in female rats is consistent with previous studies in adult rats (Alstott & Timberlake, 2009; Masur et al., 1980; Valle, 1970).

Startle reactivity was similar across prospective treatment groups during baseline testing, with ANOVA indicating no main effect or interaction involving prospective treatment group ($F < 1$) (Fig. 2.9, baseline, left panels). In addition, female rats showed reduced startle response, compared to the males, indicated by a main effect of sex ($F_{(1,28)} = 16.4$, $p < 0.001$), which was most evident during the first test block (sex and test block interaction: $F_{(2,56)} = 6.05$, $p = 0.004$). This finding of reduced startle reactivity in female rats is consistent with previous studies (Blaszczyk & Tajchert, 1996; Lehmann et al., 1999; Reilly et al., 2009). Prepulse inhibition of the startle response was similar across prospective treatment groups (Fig. 2.10, baseline, left panels), with ANOVA revealing no main effect of prospective treatment group ($F_{(1,28)} < 1$), sex ($F_{(1,28)} < 1$), or an interaction involving these factors ($F < 1.88$, $p > 0.139$).

NOR performance was matched between prospective treatment groups at baseline testing

At baseline NOR testing, during the acquisition phase, rats in both prospective treatment groups showed similar exploration of the left and right objects, with ANOVA revealing no main effect of object ($F_{(1,28)} < 1$), and no main effect or interaction involving prospective treatment group ($F_{(1,28)} < 2.84$, $p > 0.103$) (data not shown). ANOVA indicated no main effect of sex ($F_{(1,28)} = 1.04$, $p = 0.316$), but there was a trend for an interaction between object and sex ($F_{(1,28)} = 3.64$, $p = 0.067$), likely due to the males showing a slight preference for the object located on the right, and the females showing a slight preference for the object located on the left. In the retention phase, rats in both prospective treatment groups spent more time exploring the novel object over the familiar, with ANOVA revealing a main effect of object ($F_{(1,28)} = 44.6$, $p < 0.001$), with no main effect or interaction involving prospective treatment group ($F_{(1,28)} < 1$) (Fig 2.11A, baseline, top left panel). In addition, there was a trend for a main effect of sex ($F_{(1,28)}$

= 2.97, p = 0.096), reflecting a slight reduction in total object exploration in female rats. Planned pairwise t-tests comparing novel object exploration to familiar object exploration indicated that both prospective treatment groups explored the novel object significantly more than the familiar object (t_{15} > 4.29, p < 0.001). ANOVA of the DI revealed no main effect or interaction involving prospective treatment group ($F_{(1,28)}$ < 1), and planned one-sample t-tests also demonstrated significant novel object preference in both prospective treatment groups (t_{15} > 4.59, p < 0.001) (Fig 2.11B, baseline, top right panel). However, female rats tended to show increased DI compared to the males, indicated by a trend for a main effect of sex ($F_{(1,28)}$ = 3.50, p = 0.072). Female rats have been suggested to perform better than male rats on the NOR task (Grayson et al., 2007), however, a previous study reported that this advantage was only apparent at retention delays greater than 30 min (Sutcliffe et al., 2007).

2.3.3.2 Sub-chronic PCP did not affect any behavioural measures of watermaze DMP task performance

Sub-chronic PCP did not markedly affect search preference for the correct platform location

Search preference for the correct platform location assessed during probe trials was not significantly reduced over the three testing time points following scPCP treatment, although there was a weak numerical reduction of search preference in scPCP treated rats compared to saline treated rats across all time points (Fig. 2.4, top right and two bottom panels). ANOVA revealed no main effect of treatment group ($F_{(1,28)}$ = 1.65, p = 0.209), time point ($F_{(2,56)}$ < 1), sex ($F_{(1,28)}$ < 1), or any interaction involving these factors (F < 1). At each time point, rats in both treatment groups explored the correct zone significantly above chance (t_{15} > 4.26, p < 0.001), demonstrating good one-trial place memory.

Search preference for previous day's location was not affected by scPCP treatment

Search preference for the previous day's zone was analysed during the 60 s probe trials run during the three testing time points following scPCP treatment (Fig. 2.5), providing a measure of place memory acquired across the four trials of the previous day (McGarrity et al., 2017; Steele & Morris, 1999). ANOVA of search preference for the previous day's zone revealed no main effect of treatment group ($F_{(1,28)}$ < 1), sex ($F_{(1,28)}$ = 2.54, p = 0.122), or any interaction involving these factors (F < 1), suggesting that scPCP treatment did not affect the expression of place memory from the previous day.

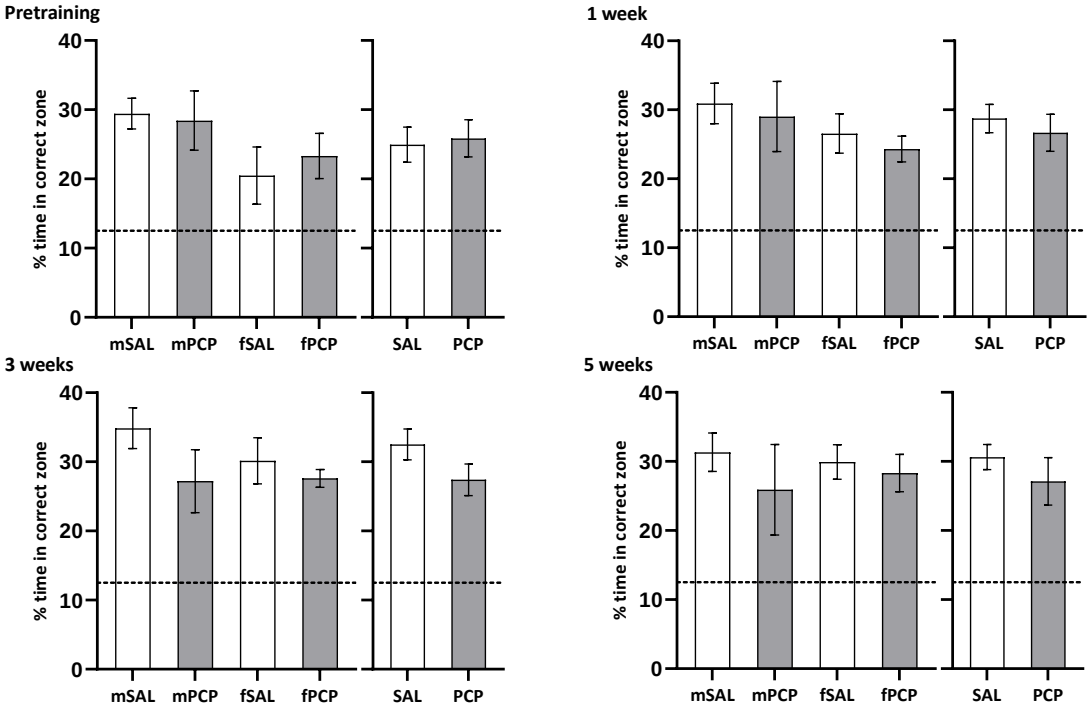

Fig. 2.4. ***Sub-chronic PCP treatment did not impair one-trial place learning on the watermaze DMP task***. Percentage of time spent in the correct zone (mean ± SEM) at pretraining (prior to scPCP treatment), 1 week, 3 weeks and 5 weeks post treatment. Data are presented separately for male (m) and female (f) rats in the saline (SAL) and PCP groups (mSAL, mPCP, fSAL, fPCP; each n = 8 rats), as well as for male and female rats combined (SAL, PCP; n = 16 rats). Both combined scPCP and saline groups explored the correct zone significantly above chance at all time points (12.5%, indicated by dotted line).

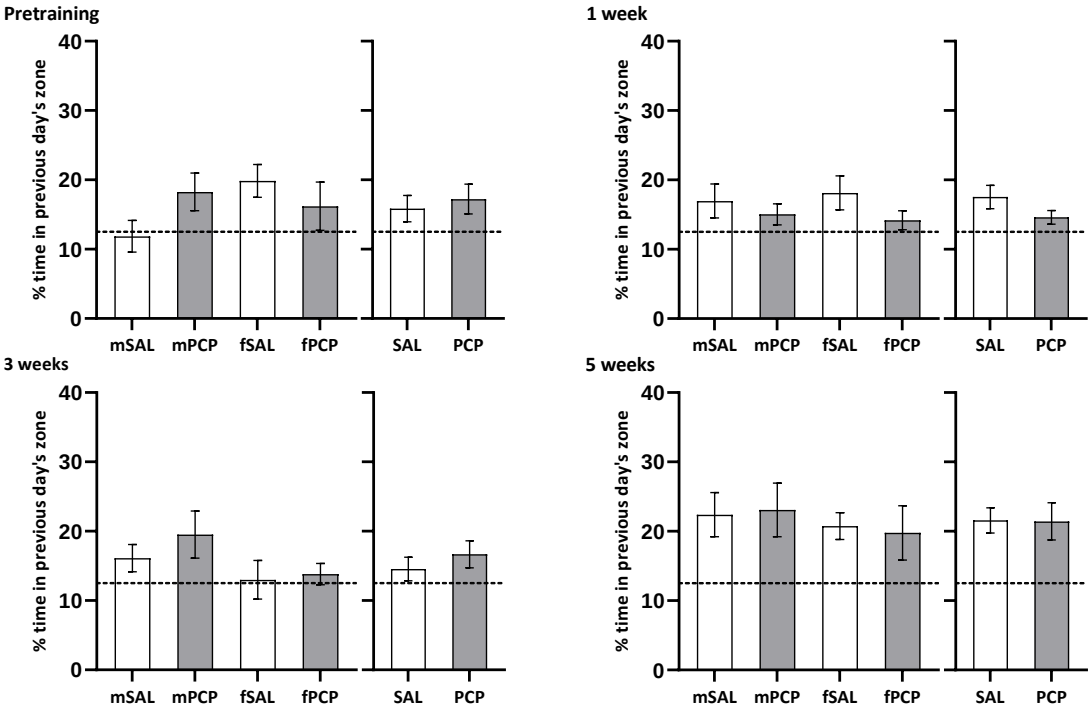

Fig. 2.5. ***Search preference for previous day's location was not affected by scPCP treatment***. Percentage of time spent in the previous day's zone (mean ± SEM) at pretraining (prior to scPCP treatment), 1 week, 3 weeks and 5 weeks post treatment. Data are presented separately for male (m) and female (f) rats in the saline (SAL) and PCP groups (mSAL, mPCP, fSAL, fPCP; each n = 8 rats), as well as for male and female rats combined (SAL, PCP; n = 16 rats). Dotted line indicates chance exploration.

Path lengths and latencies to platform location were not affected by scPCP treatment

Consistent with the search preference measure, path length (Fig. 2.6) and latency measures (data not shown) supported intact rapid one-trial place memory at the three testing time points following scPCP treatment, with pronounced reductions between trial 1 and trial 2. This was confirmed by ANOVA which revealed a significant main effect of trial ($F_{(3,84)} > 151$, $p < 0.001$), with no main effect of treatment group, or interaction involving treatment group ($F < 1.63$, $p > 0.141$). Thus, overall path length and latency measures support intact rapid place learning performance at all testing time points following scPCP treatment.

Swim speed was not affected by scPCP treatment

Sub-chronic PCP treatment had no effect on swim speed, with ANOVA revealing no main effect or interaction involving treatment group ($F < 1$) (Fig. 2.7). Consistent with swim speed during pretraining, ANOVA revealed a significant main effect of sex ($F_{(1, 28)} = 10.3$, $p = 0.003$), reflecting a slight increase in swim speed in female rats.

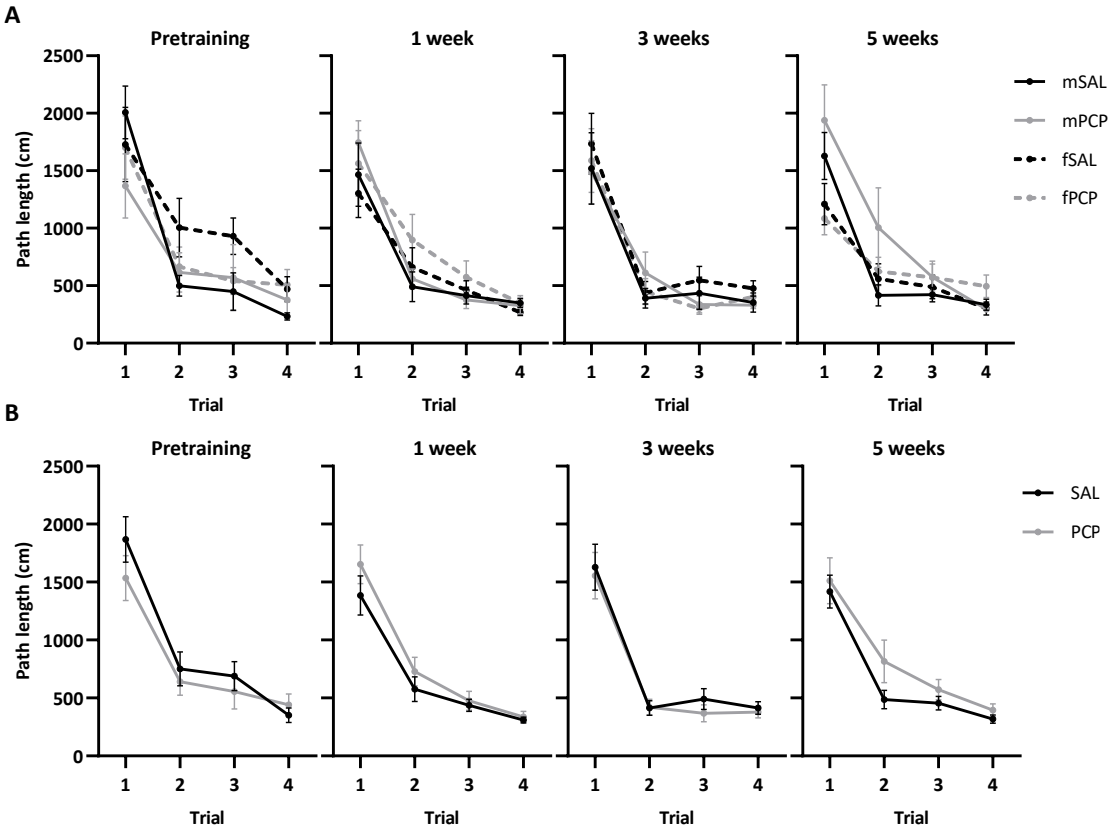

Fig. 2.6. ***Path length to platform location was not affected by scPCP treatment.*** Path length to platform location (mean ± SEM) at baseline (prior to scPCP treatment), 1 week, 3 weeks and 5 weeks post treatment. **A.** Data are presented separately for male (m) and female (f) rats in the saline (SAL) and PCP groups (mSAL, mPCP, fSAL, fPCP; each n = 8 rats), as well as for **B.** male and female rats combined (SAL, PCP; n = 16 rats).

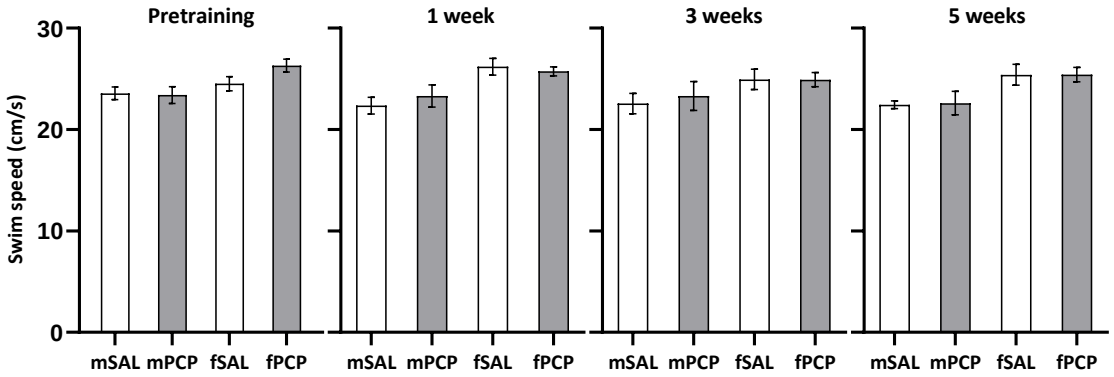

Fig. 2.7. ***Swim speed during the probe trial was not affected by scPCP treatment.*** Swim speed (mean ± SEM) at pretraining (prior to scPCP treatment), 1 week, 3 weeks and 5 weeks post treatment. Data are presented separately for male (m) and female (f) rats in the saline (SAL) and PCP groups (mSAL, mPCP, fSAL, fPCP; each n = 8 rats).

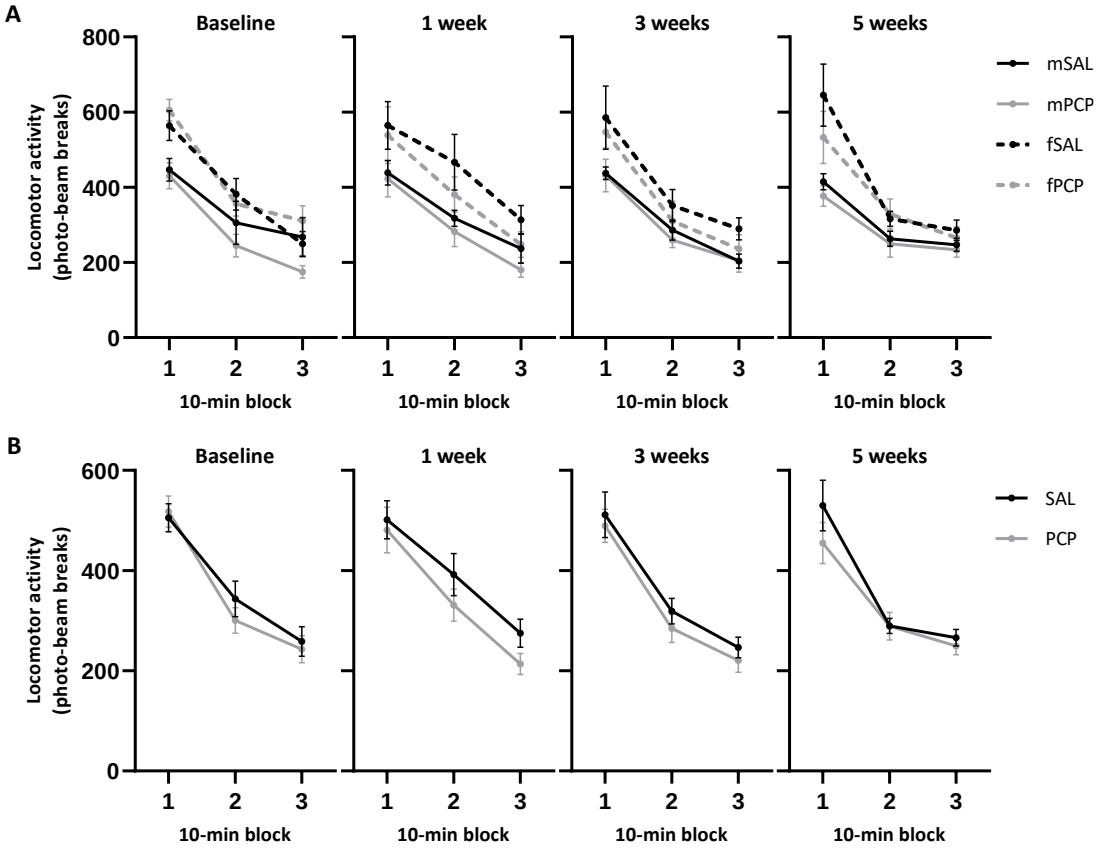

Fig. 2.8. ***Locomotor activity was not affected by scPCP treatment*****.** Locomotor activity (mean ± SEM) at baseline (prior to scPCP treatment), 1 week, 3 weeks and 5 weeks post treatment. **A.** Data are presented separately for male (m) and female (f) rats in the saline (SAL) and PCP groups (mSAL, mPCP, fSAL, fPCP; each n = 8 rats), as well as for **B.** male and female rats combined (SAL, PCP; n = 16 rats).

2.3.3.3 Locomotor activity was not affected by scPCP treatment

Post treatment testing in open field LMA was similar across the scPCP and saline treatment groups (Fig. 2.8), with ANOVA revealing no main effect of treatment ($F_{(1,28)}$ = 1.11, p = 0.301), or an interaction involving treatment (F < 1.96, p > 0.106). All rats showed habituation to the open field, evidenced by a reduction in activity across the testing blocks, and a significant main effect of test block ($F_{(2,56)}$ = 135, p < 0.001). Consistent with baseline testing, female rats showed increased locomotor activity compared to the males (main effect of sex: $F_{(1,28)}$ = 8.12, p = 0.008), which was mainly apparent during the first to second 10-min blocks (sex and test block interaction: $F_{(2,56)}$ = 4.68, p = 0.001).

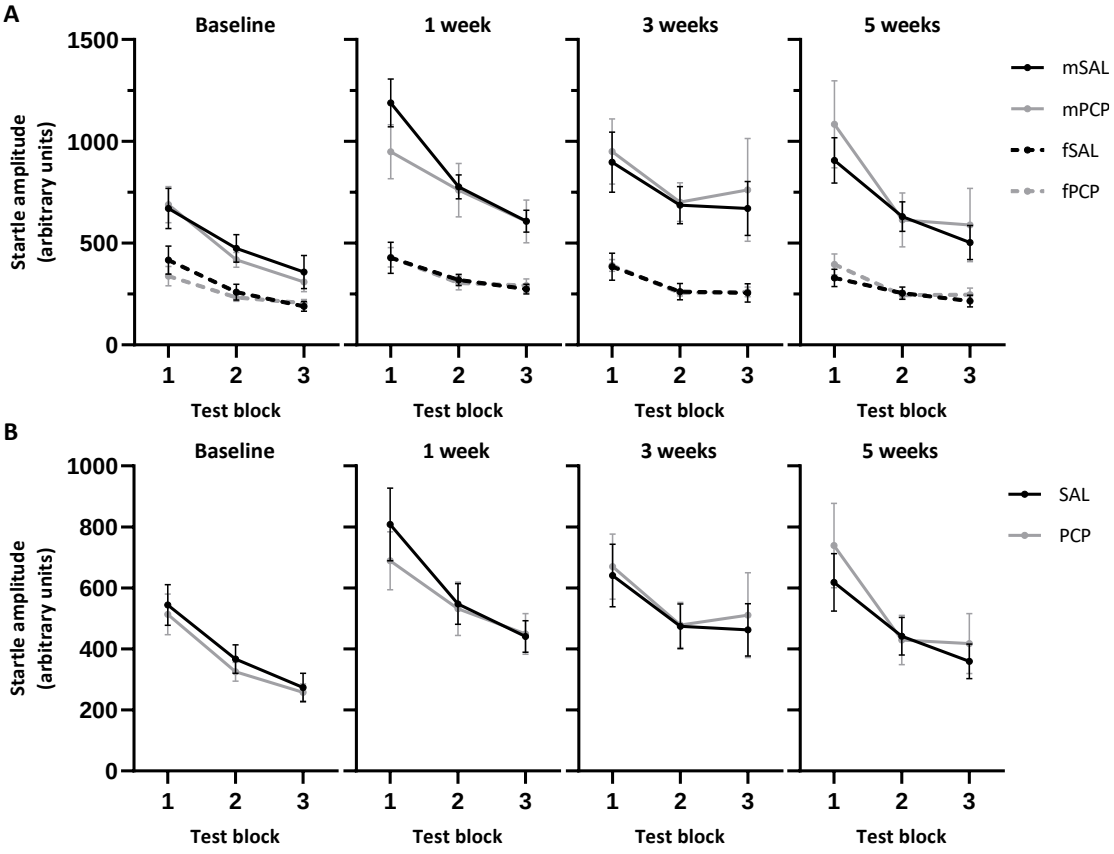

Fig. 2.9. ***Startle was not affected by scPCP treatment*****.** Startle reactivity (mean ± SEM) at baseline (prior to scPCP treatment), 1 week, 3 weeks and 5 weeks post treatment. **A.** Data are presented separately for male (m) and female (f) rats in the saline (SAL) and PCP groups (mSAL, mPCP, fSAL, fPCP; each n = 8 rats), as well as for **B.** male and female rats combined (SAL, PCP; n = 16 rats).

2.3.3.4 Startle and PPI was not affected by scPCP treatment

Sub-chronic PCP and saline treated rats showed similar startle on pulse-alone trials across the three test blocks (Fig. 2.9), with ANOVA revealing no main effect of treatment group ($F_{(1,28)} < 1$), or an interaction involving treatment group ($F < 1.57$, $p > 0.186$). All rats showed habituation to the startle pulse, as reflected by decreased startle amplitude across the three test blocks (main effect of test block: $F_{(2,56)} = 52.1$, $p < 0.001$). Consistent with baseline testing, males showed higher startle response than females (main effect of sex: $F_{(1,28)} = 31.2$, $p < 0.001$), which was most evident during the first test block (significant interaction between sex and test block: $F_{(2,56)} = 10.8$, $p < 0.001$). Prepulse inhibition was similar across the treatment groups, with rats displaying greater inhibition of the startle response with increasing prepulse intensity (Fig. 2.10) (main effect of prepulse intensity: $F_{(3,84)} = 304$, $p < 0.001$), with no main effect of treatment group ($F_{(1,28)} < 1$), sex ($F_{(1,28)} < 1$), or an interaction involving these factors ($F < 1.29$, $p > 0.265$).

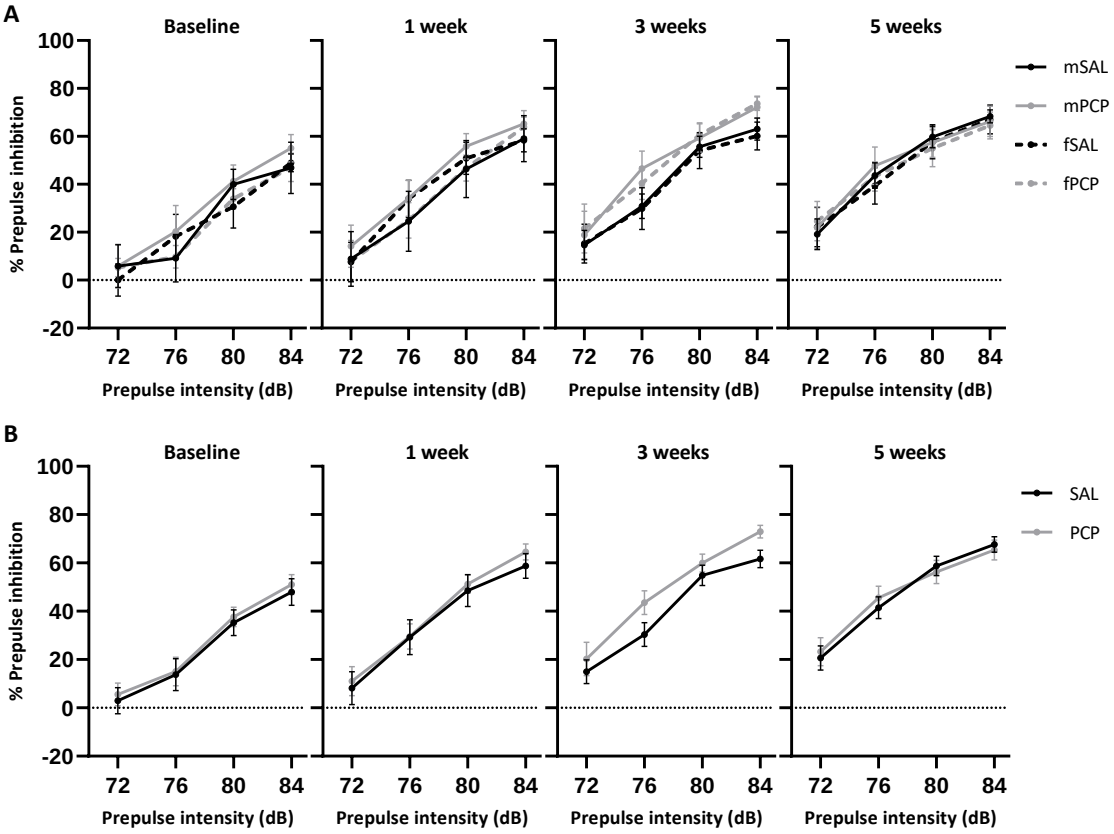

Fig. 2.10. ***Prepulse inhibition was not affected by scPCP treatment*****.** Prepulse inhibition (mean ± SEM) at baseline (prior to scPCP treatment), 1 week, 3 weeks and 5 weeks post treatment. **A.** Data are presented separately for male (m) and female (f) rats in the saline (SAL) and PCP groups (mSAL, mPCP, fSAL, fPCP; each n = 8 rats), as well as for **B.** male and female rats combined (SAL, PCP; n = 16 rats).

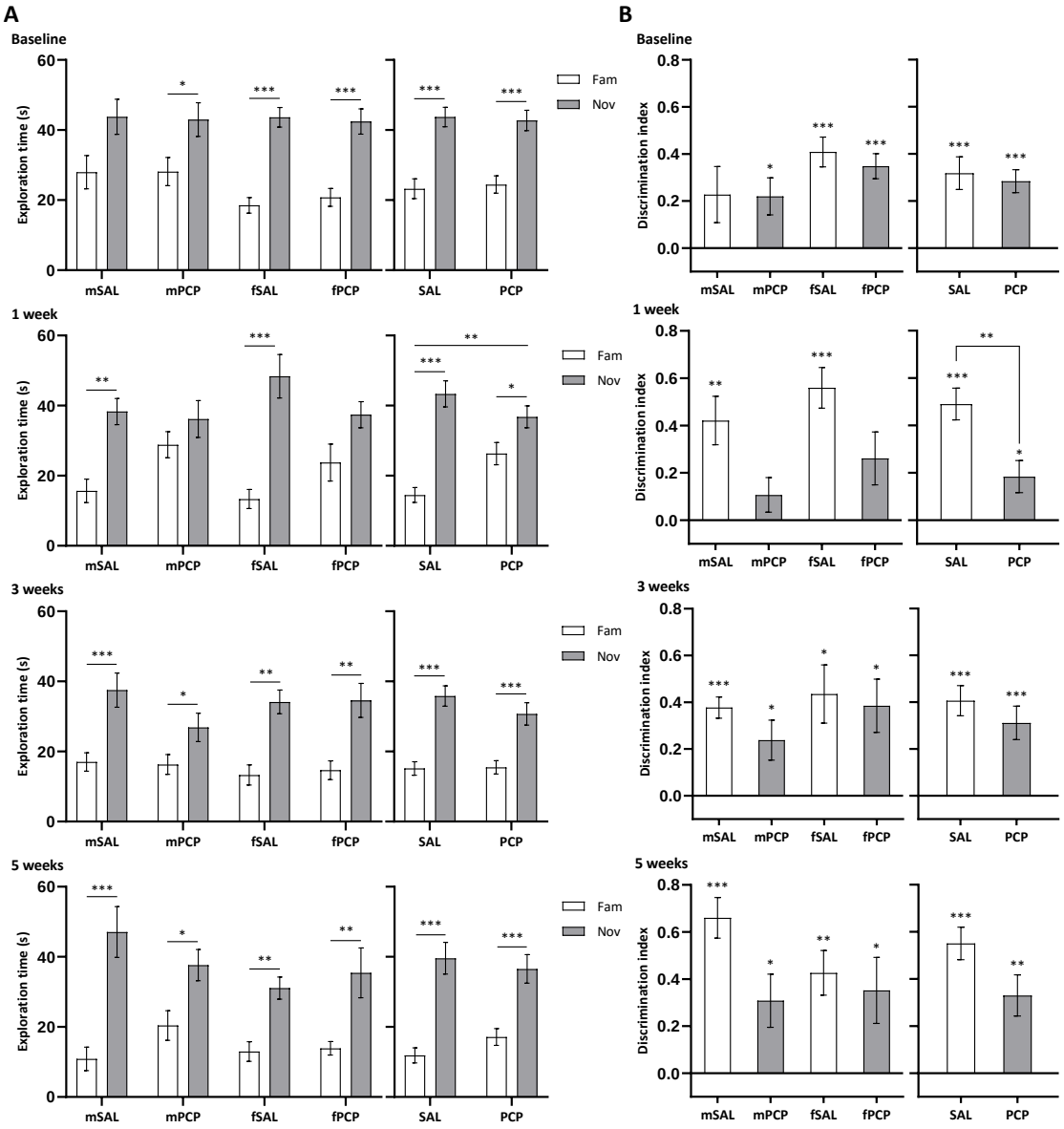

Fig. 2.11. ***Study 1: scPCP treatment significantly impaired NOR at 1 week post treatment***. Data (mean ± SEM) are presented separately for male (m) and female (f) rats in the saline (SAL) and PCP groups (mSAL, mPCP, fSAL, fPCP; each n = 7-8 rats), as well as for male and female rats combined (SAL, PCP; n = 15-16 rats), at baseline (prior to scPCP treatment), 1 week, 3 weeks and 5 weeks post treatment. **A.** Exploration times (s) of the familiar (Fam) and novel (Nov) object during the 3 min retention trial, following a 1 min retention delay. NOR was significantly impaired in scPCP treated rats at 1 week, but not 3 or 5 weeks, post treatment. Asterisks indicate significant differences between novel and familiar object exploration times (planned paired sample t-test, $p < 0.05$) or between treatment groups (ANOVA, $p < 0.05$). **B.** Discrimination index (DI) [(time spent exploring the novel object - time spent exploring the familiar object)/total time spent exploring both objects] confirmed an impairment in scPCP treated rats at 1, but not 3 or 5, week post treatment. Asterisks indicate novel object exploration significantly different to chance (DI = 0) (one-sample t-test, $p < 0.05$) or differences between treatment groups (ANOVA, $p < 0.05$).

2.3.3.5 Sub-chronic PCP treatment impaired NOR at 1, but not 3 and 5, weeks post treatment

At post treatment testing, during the acquisition phase, rats spent a similar amount of time exploring the identical objects (data not shown), with ANOVA showing no main effect of object ($F_{(1,26)} < 1$), treatment group ($F_{(1,26)} = 1.39$, $p = 0.248$), or an interaction involving these factors ($F < 1.48$, $p > 0.235$). There was a strong trend for a main effect of sex ($F_{(1,26)} = 3.93$, $p = 0.058$), and for an interaction between sex and testing time point ($F_{(2,52)} = 2.68$, $p = 0.078$). Simple main effects analysis of time point revealed that this reflects an overall decrease in object exploration in the females rats, compared with the males, at 5 weeks post treatment, as indicated by a main effect of sex ($F_{(1,26)} = 6.62$, $p = 0.016$).

In the retention phase, ANOVA revealed a significant interaction between treatment group and object ($F_{(1,27)} = 6.86$, $p = 0.014$), reflecting reduced novel object preference in the scPCP treatment group, which was most pronounced at 1 week post treatment (Fig. 2.11A). There was a significant main effect of testing time point ($F_{(2,54)} = 3.93$, $p = 0.025$), but no significant interactions involving time point ($F_{(2,54)} < 1.80$, $p > 0.175$), including no interaction between treatment group, object and time point ($F_{(2,54)} = 1.35$, $p = 0.267$). There was also no significant main effect or interaction involving sex ($F_{(2,54)} < 1.80$, $p > 0.175$). ANOVA of DI also revealed a significant main effect of treatment group ($F_{(1,27)} = 11.8$, $p = 0.002$), with no significant interactions involving treatment group and time point ($F_{(2,54)} < 1.20$, $p > 0.308$), reflecting a reduction in the DI of scPCP treated rats which was present across each testing time point (Fig. 2.11B). In addition, ANOVA of DI revealed no main effect or interaction involving sex ($F < 2.27$, $p > 0.143$).

Although ANOVA of retention phase data did not reveal a significant interaction involving treatment group and post-treatment testing time point, we performed exploratory ANOVAs to assess the impact of scPCP treatment on NOR memory separately at each time point, as previous studies have shown conflicting reports as to whether the scPCP induced NOR deficit is long-lasting (Pyndt-Jorgenson et al., 2015; Rajagopal et al., 2014). At 1 week post treatment, scPCP treated rats showed an impairment in NOR, demonstrated by reduced exploration of the novel object versus the familiar (Fig. 2.11A, 1 week), with ANOVA revealing a main effect of object ($F_{(1,28)} = 38.2$, $p < 0.001$) and, importantly, a significant interaction between treatment group and object ($F_{(1,28)} = 8.32$, $p = 0.007$). However, planned pairwise t-tests demonstrated that both treatment groups explored the novel object significantly different to the familiar object ($t_{15} > 2.44$, $p < 0.028$). Analysis of DI also confirmed an NOR deficit in the scPCP treated rats at 1 week post treatment (Fig. 2.11B, 1 week), with ANOVA revealing a main effect of

treatment group ($F_{(1,\ 28)}$ = 10.5, p = 0.003). However, one-sample t-tests demonstrated significant novel object preference in both treatment groups (t_{15} > 2.73, p < 0.016). At 3 and 5 weeks post treatment, there was a weak numerical impairment in NOR, indicated by a reduced DI in the scPCP treatment group, but this was no longer significant (3 weeks: $F_{(1,\ 28)}$ < 1; 5-weeks: $F_{(1,\ 27)}$ = 3.62, p = 0.068), and both treatment groups showed a preference for the novel object which was significantly different to chance ($t_{14\text{-}15}$ > 3.78, p < 0.002). Analysis of object exploration times also demonstrated largely intact NOR in scPCP treated rats at 3 and 5 weeks post treatment, with ANOVA revealing a main effect of object ($F_{(1,\ 27\text{-}28)}$ > 48.2, p < 0.001), but no interaction between treatment group and object ($F_{(1,\ 27\text{-}28)}$ < 1.591, p > 0.218). In addition, at both time points, both treatment groups explored the novel object significantly more than the familiar object ($t_{14\text{-}15}$ > 3.92, p < 0.001). Therefore, separate analysis at individual time points suggests that the scPCP-induced NOR deficit was not long-lasting in study 1.

2.3.4 Study 2: sub-chronic PCP treatment impaired NOR at all three testing time points following treatment

Following the finding in study 1 that impairments in NOR memory were limited to 1 week post treatment, we hypothesised that the amount of handling in the study and/or aerobic exercise during watermaze testing may have rescued later NOR deficits (Landreth et al., 2023; Mitsadali et al., 2020). To investigate this, we ran another study in a second cohort of rats, which only included NOR testing (at the same post treatment time points as in study 1) but included no other testing and limited handling throughout the study.

In study 2, during the acquisition phase, rats spent a similar amount of time exploring the identical objects (data not shown), with ANOVA showing no main effect of object ($F_{(1,27)}$ < 1), treatment group ($F_{(1,27)}$ < 1), or an interaction involving these factors (F < 2.68, p > 0.077). During the retention phase, ANOVA revealed a significant interaction between treatment group and object ($F_{(1,28)}$ = 26.6, p < 0.001), reflecting reduced novel object preference in the scPCP treated group, which was present at all time points (Fig. 2.12A). There was a significant main effect of testing time point ($F_{(2,56)}$ = 6.66, p = 0.003), but no significant interactions involving time point and object ($F_{(2,54)}$ < 1). In addition, there was a significant main effect of sex ($F_{(1,28)}$ = 9.31, p = 0.005) and a significant interaction between time point, treatment group and sex ($F_{(2,56)}$ = 5.25, p = 0.008). Simple main effects analysis of time point indicated that this reflects an overall decrease in exploration time in the female rats, as demonstrated by a significant main effect of sex at 1 and 5 weeks post treatment ($F_{(1,28)}$ > 5.46, p < 0.027), and a trend level effect of sex at 3 weeks post treatment ($F_{(1,28)}$ = 2.94, p = 0.097). In addition, at 1

week post treatment, there was a significant interaction between treatment group and sex ($F_{(1,28)}$ = 4.92, p = 0.035), likely due to a proportionately greater decrease in exploration time in the female saline rats than in the scPCP treated female rats. This decrease in overall object exploration in the female rats, compared to the males, is somewhat consistent with our finding in study 1, where we found a significant reduction in object exploration in the female rats at 5 weeks post treatment during acquisition (data not shown). ANOVA of DI also indicated enduring NOR impairments in the scPCP group, with a significant main effect of treatment group ($F_{(1,28)}$ = 30.2, p < 0.001), and no significant interactions involving treatment group and time point ($F_{(2,56)}$ < 1) (Fig 2.12B). In addition, ANOVA of DI revealed no main effect or interaction involving sex (F < 1). As with study 1 NOR data, we performed exploratory ANOVAs to assess the significance of NOR memory in the scPCP treated rats at each time point.

At all testing time points, ANOVA revealed a significant interaction between treatment group and object ($F_{(1, 28)}$ > 4.25, p < 0.049), demonstrating significant impairments in NOR in the scPCP treatment group. In addition, planned t-tests confirmed that scPCP treated rats did not explore the novel object significantly different to the familiar object at 3 (t_{15} < 1) or 5 weeks post treatment (t_{15} = 1.87, p = 0.081), but did show significant novel object preference at 1 week post treatment (t_{15} = 2.57, p = 0.021), along with the saline treated rats at all time points (t_{15} > 5.10, p < 0.001). ANOVA of DI also demonstrated a long-lasting NOR deficit in the scPCP treated rats, with a significant main effect of treatment group at each time point ($F_{(1, 28)}$ > 6.32, p < 0.018). One-sample t-tests indicated that scPCP treated rats did not explore the novel object significantly different to the familiar object at 3 weeks post treatment (t_{15} < 1), but did show significant novel object preference at 1 and 5 weeks post treatment (t_{15} > 2.21, p < 0.043), along with the saline treated rats at all time points (t_{15} > 5.28, p < 0.001).

Overall, reducing the amount of handling and behavioural testing the rats received did appear to result in a stronger NOR deficit in the scPCP treated rats, which persisted until the end of the study. However, this conclusion is not supported by a combined ANOVA of NOR data from both studies, which did not reveal a significant interaction between treatment group and study ($F_{(1, 55)}$ < 1), or between treatment group, study and object ($F_{(1, 55)}$ = 1.61, p = 0.210). However, an exploratory ANOVA of the simple main effect of study in the scPCP treated rats did reveal a significant main effect of study ($F_{(1, 28)}$ = 10.8, p = 0.003), suggesting that NOR performance differed in the scPCP treated rats between studies.

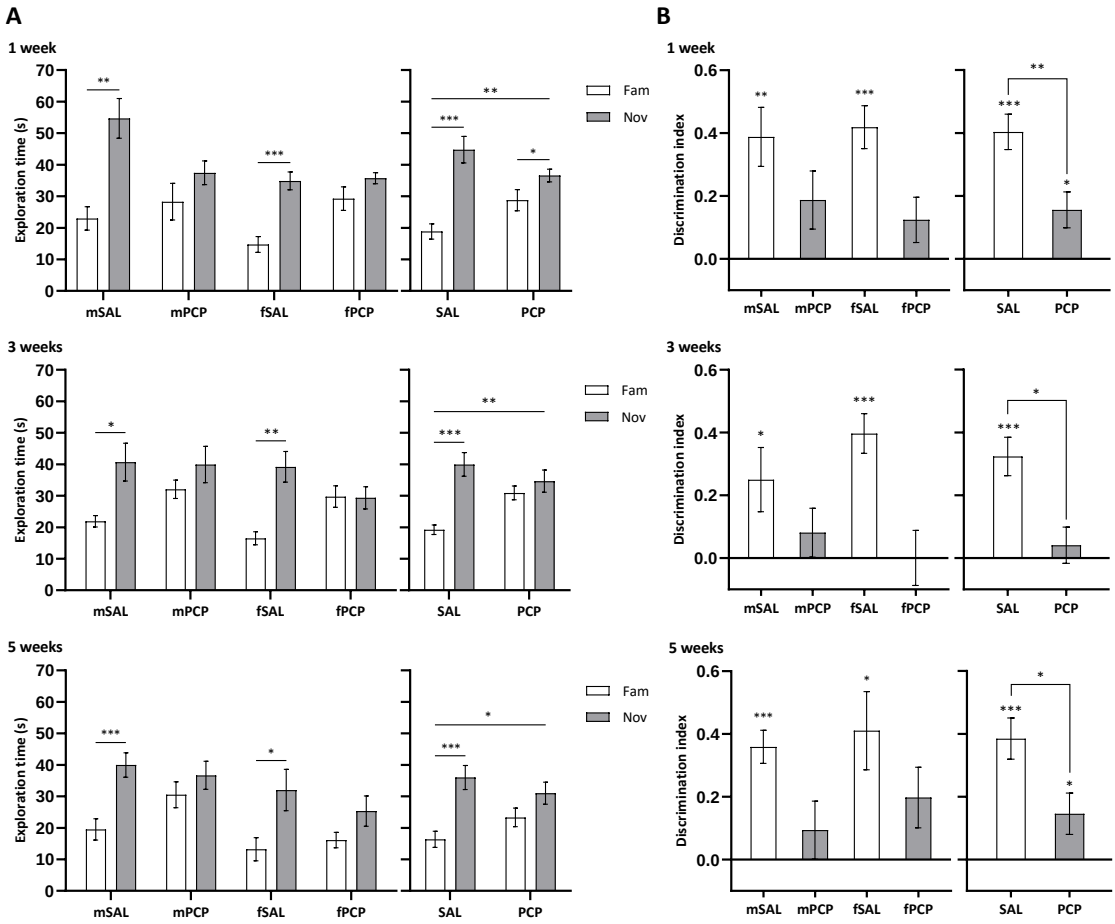

Fig. 2.12. ***Study 2: scPCP treatment markedly impaired NOR at all post treatment testing time points***. Data (mean ± SEM) are presented separately for male (m) and female (f) rats in the saline (SAL) and PCP groups (mSAL, mPCP, fSAL, fPCP; each n = 8 rats), as well as for male and female rats combined (SAL, PCP; n = 16 rats), at 1 week, 3 weeks and 5 weeks post treatment. **A.** Exploration times (s) of a familiar (Fam) and novel (Nov) object during the 3 min retention trial, following a 1 min retention delay. NOR was impaired in scPCP treated rats at all testing time points. Asterisks indicate significant differences between novel and familiar object exploration times (planned paired sample t-test, $p < 0.05$) or between treatment groups (ANOVA, $p < 0.05$). **B.** Discrimination index (DI) [(time spent exploring the novel object - time spent exploring the familiar object)/total time spent exploring both objects] confirmed an impairment in scPCP treated rats at all time points. Asterisks indicate novel object exploration significantly different to chance (DI = 0) (one-sample t-test, $p < 0.05$) or differences between treatment groups (ANOVA, $p < 0.05$).

2.4 Discussion

Sub-chronic PCP treatment did not impair rapid place learning performance on the watermaze DMP task. In addition, scPCP treatment did not affect swim speed, LMA, startle reactivity or PPI. In study 1, scPCP caused a deficit in NOR performance, which was mostly evident at 1 week post treatment, but was no longer significant at the later testing time points. In study 2, where rats only underwent NOR testing, without any other testing and with limited handling, the NOR deficit endured until the end of the study. Furthermore, scPCP treatment resulted in body weight reductions and reduced weight growth in both male and female rats in study 1, and only in male rats in study 2. In addition to assessing the effect of scPCP treatment, the inclusion of both sexes allowed for the main effect of sex to be examined across the different behavioural measures. Here, we report that female rats showed a strong trend for reduced search preference at watermaze pretraining, significantly increased swim speed during the watermaze DMP task, increased LMA, and reduced startle response.

2.4.1 Sub-chronic PCP treatment did not impair one-trial place learning on the watermaze DMP task

The watermaze DMP task, which requires rapid one-trial place memory, is highly sensitive to hippocampal dysfunction. A range of hippocampal manipulations, including small partial hippocampal lesions (Bast et al., 2009) and pharmacological manipulations that interfere with synaptic plasticity mechanisms mediated by NMDARs (Steele & Morris, 1999) and dopamine receptors (Pezze & Bast, 2012), result in pronounced deficits in watermaze DMP performance. Moreover, hippocampal disinhibition, caused by microinfusion of the GABA-A receptor antagonist picrotoxin into the ventral hippocampus, results in impaired watermaze DMP task performance, as evidenced by a marked reduction in search preference for the correct zone (McGarrity et al., 2017). Sub-chronic PCP resulted in a very weak numerical impairment in search preference, which was present at each time point, but was far from significance. The absence of a significant impairment in search preference on the watermaze DMP task does not support that hippocampal function is strongly impaired in scPCP treated rats. Path length and latency measures were also unaffected by scPCP treatment. This is consistent with a study in male scPCP treated Lister Hooded rats, which found no impairment in one-trial learning watermaze performance assessed using path length measures (Janhunen et al., 2015).

In contrast, a study in adult male mice found that 7 days of PCP administration (2 mg/kg, once daily), followed by a 24 h washout period, resulted in impaired watermaze DMP task performance across 6 testing days (Beraki et al., 2009). The discrepancy between this finding

and the current study may be due to the different duration of washouts used, with a period of 11 days between the end of PCP treatment and DMP testing used in the present study, opposed to 24 h in Beraki et al. (2009). It is possible that PCP may still be present in high concentrations in the brain after only 1 day of washout. This may impair watermaze DMP performance due to acute hippocampal NMDAR blockade, which may specifically impair rapid place learning (e.g., by disrupting hippocampal synaptic plasticity), or cause non-specific side effects which disrupt performance. Alternatively, it may be the case that, during the longer washout period used in the present study, potential compensatory mechanisms may have occurred which restore rapid place learning. Nevertheless, given that Beraki et al. (2009) tested performance across 6 days, task performance at the end of this time frame should be comparable to the scPCP model used in the present study. Beraki et al. (2009) do not report whether any changes in performance were seen across days. On the other hand, discrepancies may be due to the different species used.

2.4.2 Sub-chronic PCP treatment did not affect sensorimotor processes

Locomotor activity was not affected by scPCP treatment. This is in line with other studies which reported no changes to LMA following scPCP treatment (Damgaard et al., 2010; Grayson et al., 2007; McLean et al., 2011; Snigdha et al., 2011a). In addition, scPCP treatment did not result in changes to PPI or startle response. Although acute PCP (Geyer et al., 2001) and chronic PCP administration (Schwabe et al., 2005) are reported to result in PPI deficits, PPI recovers to control levels following a washout of 24-48 h (Egerton et al., 2008; Martinez et al., 1999). This suggests that PPI is not sensitive to the neuropathological effects of scPCP exposure. Consistent with the present data, these previous studies also report no changes to startle response following PCP treatment.

2.4.3 Comparison of scPCP effects with those of hippocampal pharmacological disinhibition

The neuropathological hallmarks of schizophrenia strongly implicate GABAergic dysfunction in the disease, with reductions in GABAergic markers found the hippocampus and PFC of schizophrenia patients (Benes et al., 1991; Benes & Berretta, 2001; Gonzalez-Burgos & Lewis, 2012; Torrey et al., 2005). Sub-chronic PCP treatment in rodents also results in functional impairments in GABAergic interneurons, with PV+ cell deficits reported in the PFC and hippocampus (Abdul-Monim et al., 2007; Gigg et al., 2020; Jenkins et al., 2010). These findings suggest that there is some evidence for neural disinhibition in the scPCP model. However, in the present study, scPCP treatment only resulted in a very weak numerical impairment in search preference, which was present at each time point, but was far from significance and in

no way similar to the marked reductions reported following hippocampal neural disinhibition (McGarrity et al., 2017). The absence of a significant impairment in search preference on the watermaze DMP task suggests that hippocampal neural disinhibition is, if it all, much less pronounced than in the pharmacological disinhibition model. Hippocampal neural disinhibition has also been shown to increase LMA and slightly reduce startle reactivity, without affecting PPI (McGarrity et al., 2017). These changes to LMA and startle reactivity were also not observed following scPCP treatment in the present study. The discrepancy between these findings may be due to the limitations of comparing an acute and regionally localised model of neural disinhibition with a sub-chronic and systemic model of NMDAR hypofunction. If neural disinhibition is present in the scPCP model it is likely to be in a chronic state and, therefore, may involve the recruitment of extrahippocampal brain regions which compensate for aberrant hippocampal function (Wang et al., 2015).

2.4.4 Sub-chronic PCP results in NOR deficits

In study 1, NOR was impaired in scPCP treated rats, with significant NOR deficits found at 1 week following cessation of treatment. The presence of an NOR deficit, which is reliably reported in the scPCP model (Cadinu et al., 2018; Rajagopal et al., 2014), validates the treatment regimen used and suggests that the lack of watermaze DMP task impairments cannot be attributed to dosing errors. The NOR deficit observed, however, could be considered somewhat weaker than NOR deficits reported in other studies, where scPCP treated rats fail to show significant novel object discrimination (Arnt et al., 2010; Grayson et al., 2014; Horiguchi et al., 2011a; Redrobe et al., 2012; Snigdha et al., 2011a). However, other studies have also reported instances of residual novel object preference following scPCP treatment, with deficits in object exploration data but non-significant reductions in DI (Damgaard et al., 2011; Grayson et al., 2007; Horiguchi et al., 2013) or vice versa (Damgaard et al., 2010). In addition, in the present study, although ANOVA did not reveal a significant effect of time point, and a numerical NOR impairment persisted throughout the study, a statistically significant NOR deficit was only present at 1 week post treatment. This contrasts with studies where scPCP treated rats showed significant NOR deficits up to 10 weeks following treatment (Mitsadali et al., 2020).

In Lister Hooded rats, aerobic exercise was recently reported to both reverse and prevent scPCP-induced NOR deficits (Mitsadali et al., 2020). In the present study, the 8 days of watermaze pretraining preceding the scPCP dosing week, and the 4 days of watermaze testing following each NOR testing time point, may explain why scPCP-induced NOR deficits were not

significant at later testing time points. However, the exercise regimen employed in the previous study (voluntary wheel running) was considerably more extensive than the 4 trials of swimming per day in the present study. The extensive handling of rats throughout study 1 may also have influenced the presentation of NOR deficits, as handling has been shown to reverse and prevent scPCP-induced NOR deficits in rats (Landreth et al., 2023). In study 1, rats were handled frequently due to daily weight monitoring and repeated testing in four different behavioural tasks, which may have resulted in the rescue of later NOR deficits. Study 2 investigated whether the NOR deficit was longer lasting in rats that underwent no additional testing and only received limited handling. Here, we found NOR deficits which persisted beyond 5 weeks, until the end of the study, suggesting that the less pronounced NOR impairment in study 1 reflected partial rescue due to the additional behavioural testing and handling. A long-lasting NOR deficit is consistent with some (Cadinu et al., 2018; Rajagopal et al., 2014), but not all studies (Pyndt Jørgensen et al., 2015). A study in scPCP treated rats found that the NOR deficit persisted up to 4 weeks after cessation of treatment but was no longer present at 7 weeks (Pyndt Jørgensen et al., 2015), suggesting that the scPCP-induced NOR deficit may diminish over time.

2.4.5 Sub-chronic PCP treatment reduced body weight

Sub-chronic PCP treated male and female rats in study 1, and male scPCP treated rats in study 2, showed a significant body weight reduction following scPCP treatment. A scPCP-induced body weight reduction has previously been reported in male Wistar rats following PCP administration (5 mg/kg, bi-daily for 7 days) (Seillier & Giuffrida, 2009). Interestingly, reduced body weight has also been reported in mice with GABA-A receptor y2 subunit knock-out on PV neurons (Leppä et al., 2011), suggesting that the GABAergic impairments reported in scPCP models, including deficits in PV (Abdul-Monim et al., 2007; Gigg et al., 2020; Jenkins et al., 2010), may contribute to reductions in body weight. In addition, a study in perinatal rats found that PCP treatment (10 mg/kg on perinatal day 7, 9 and 11) resulted in weight loss in both male and female pups, with females, but not males, regaining the lost weight within 24 h (Anastasio & Johnson, 2008). Consistent with Anastasio & Johnson (2008), the present study also demonstrated increased sensitivity to scPCP-induced body weight reductions in male, compared to female, scPCP treated rats. In study 2, female scPCP treated rats did not show significant weight reductions and, in study 1, female scPCP treated rats recovered to control levels at the end of the washout period, whereas male rats showed body weight reductions which persisted until the end of study. The more pronounced scPCP-induced weight reductions in male rats could be due to the different PCP doses used for males and females in the present

study. A higher dose of PCP was used in the male rats as pharmacokinetic data suggest that females are more sensitive to PCP, due to a decreased ability to metabolise the drug (Shelnutt et al., 1999). In addition, the higher dose of 5 mg/kg is widely used in scPCP studies using male rats (Janhunen et al., 2015; Le Cozannet et al., 2010; Pyndt Jørgensen et al., 2015; Redrobe et al., 2010, 2012). Furthermore, a study in male and female Lister Hooded rats found that scPCP treatment using the same dose (2 mg/kg, bi-daily for 7 days), resulted in widespread decreases in expression of brain-derived neurotrophic factor in regions of the female brain, including in the mPFC and hippocampus but, in the male brain, only the orbital cortex and central amygdaloid region was affected (Snigdha et al., 2011b). This suggests that the female brain is more sensitive to PCP-associated neurotoxicity. However, the pronounced decrease in male scPCP rats' weight in the present study suggests that scPCP treatment produces sexually dimorphic effects, whereby male and female rats have different physiological vulnerabilities to scPCP treatment.

2.4.6 Conclusions

The absence of watermaze DMP task impairments following scPCP treatment does not support that hippocampal function is substantially impaired by scPCP treatment. Moreover, key behavioural effects of pharmacological hippocampal disinhibition (locomotor hyperactivity, decreased startle reactivity, impaired watermaze DMP performance; McGarrity et al., 2017) are not observed in the scPCP model. It remains to be investigated whether the NOR deficits found here following scPCP treatment may be a consequence of reduced GABAergic function (chapter 5). Further investigations into the neuropathological effects of scPCP treatment, using simple western analyses of the brains removed in this study, may confirm whether there is any post-mortem evidence of reduced GABA function (chapter 3).

Chapter 3: GABAergic biomarker changes in the medial prefrontal cortex and hippocampus of sub-chronic phencyclidine treated rats

Declaration: Jennifer Fletcher provided consultation on methodology.

Abstract

A reduction in GABA markers is one of the most reliable post-mortem findings in schizophrenia. Sub-chronic treatment with phencyclidine has been reported to reduce GABA markers in the prefrontal cortex and hippocampus, with many studies reporting a reduction in PV-immunoreactive cells using immunohistochemistry. Here, we used high throughput simple western (Wes) analysis to determine the protein levels of GAD67 and PV in the brains of the two cohorts of scPCP treated rats used for the behavioural studies in chapter 2. We did not find any changes in GAD67 or PV protein levels in the prefrontal cortex or dorsal region of the hippocampus. We did, however, find changes in the intermediate to ventral hippocampus. In both cohorts, GAD67 was reduced in the female, but not male, rats, suggesting that scPCP treatment may have sex-specific neuropathological effects. Interestingly, however, in the first cohort of rats we found an increase in PV protein levels in both the male and female scPCP rats, compared to the saline treated rats, but no changes were seen in the second cohort of rats. We propose that this finding may reflect an experience-related decrease of PV expression in control rats and an aberrant regulation of PV circuits in scPCP treated rats. The present findings are discussed in light of previous immunohistochemical findings which indicated a reduction in PV-immunoreactive cells.

3.1 Introduction

GABAergic dysfunction is strongly implicated in schizophrenia, with reductions in GABA markers found in the hippocampus and PFC of patients with schizophrenia (de Jonge et al., 2017; Dienel & Lewis, 2019; Gonzalez-Burgos et al., 2010; Heckers & Konradi, 2015). In particular, reductions in immunoreactivity of the GABAergic calcium binding protein, PV, are widely reported in schizophrenia (Batiuk et al., 2022; Beasley et al., 2002; Beasley & Reynolds, 1997; Bitanihirwe & Woo, 2014; Enwright et al., 2016; Fung et al., 2010; Hashimoto et al., 2003; Volk et al., 2000; Zhang & Reynolds, 2002). There is some uncertainty in the literature as to whether these PV reductions represent fewer GABAergic interneurons, a decrease in mRNA or protein levels per neuron, or both (Enwright et al., 2016; Hashimoto et al., 2003; Kaar et al., 2019; Reynolds, 2022; Sakai et al., 2008). However, a recent study, using a novel multiplex fluorescent in situ hybridisation approach, suggests that PV mRNA deficits in

schizophrenia are attributable to lower levels of transcript per neuron (Dienel et al., 2023). In addition, reductions in the expression GAD67 are reported in post-mortem brain analyses of patients with schizophrenia (Akbarian et al., 1995; Benes et al., 2007; Curley et al., 2011; Guidotti et al., 2000; Hashimoto et al., 2003; Rocco et al., 2016; Volk et al., 2000; Woo et al., 2004). These alterations in GABAergic markers have been suggested to underlie the cognitive deficits associated with schizophrenia (Lewis et al., 2012). The pathological processes which may lead to GABAergic dysfunction in schizophrenia are not fully understood, however, GABAergic dysfunction has been suggested to be a consequence of NMDAR hypofunction (Gonzalez-Burgos & Lewis, 2012; Hardingham & Do, 2016; Lisman et al., 2008; Nakazawa et al., 2012; Steullet et al., 2016).

Reductions in hippocampal and prefrontal PV-immunoreactivity are also reported in rodent models of NMDAR hypofunction (Abdul-Monim et al., 2007; Braun et al., 2007; Hauser et al., 2017; Jenkins et al., 2008, 2010; Keilhoff et al., 2004; Kittelberger et al., 2012; Landreth et al., 2021; McKibben et al., 2010; Redrobe et al., 2012; Schobel et al., 2013; Schroeder et al., 2000; Tsai et al., 2022; Tsivion-Visbord et al., 2020; Unal et al., 2021), supporting the idea that NMDAR hypofunction contributes to GABAergic deficits. Given that the reduced PV-immunoreactivity reported in human schizophrenia studies was suggested to reflect a reduction in protein and/or mRNA per neuron, rather than cell death (Dienel et al., 2023; Enwright et al., 2016; Hashimoto et al., 2003), it is important to also investigate PV protein and mRNA levels in NMDAR antagonist rodent models. Benneyworth et al. (2011) did not find decreases in PV protein levels in the frontal cortex or hippocampus of scPCP and ketamine treated mice. However, the relatively short washout duration (3 days) used in this study may not have been long enough for the detection of GABAergic changes (Cadinu et al., 2018). Nevertheless, decreases in prefrontal, but not hippocampal, PV mRNA levels have been reported following a 3 day washout period in rats receiving repeated PCP administration (Cochran et al., 2003; Thomsen et al., 2010), suggesting that GABAergic changes may occur over a 3 day washout window. However, this may reflect differences in the time course of PV mRNA versus PV protein changes. In addition, decreases in PV protein levels have been reported in the frontal cortex and hippocampus of scPCP treated mice (Gigg et al., 2020) and in the hippocampus, but not PFC, of sub-chronic MK-801 treated rats (Tsai et al., 2022), using washouts of 15 weeks and 7 days, respectively. Thus, studies investigating PV protein or mRNA levels following NMDAR hypofunction have produced varied results, which may be due to methodological differences, including the washout periods and dosing regimens used. Similarly, studies investigating GAD67 protein and mRNA levels in NMDAR antagonist models

have been mixed. GAD67 protein levels were reported to be reduced in the dorsal hippocampus, but not PFC, of scPCP treated rats, whereas other studies have found no changes to GAD67 protein (Beninger et al., 2010; Gigg et al., 2020; Tsai et al., 2022) or mRNA (Neugebauer et al., 2018) levels in the hippocampus or frontal cortex following NMDAR antagonism.

Here, we used simple western (Wes) analysis (Gigg et al., 2020; Harris, 2015; Lück et al., 2021) to investigate the levels of PV and GAD67 protein in the PFC, dorsal hippocampus (DH), and intermediate to ventral hippocampus (I-VH) of the scPCP treated rats used for behavioural testing in chapter 2. We chose to examine these brain regions due to the GABAergic changes previously reported in these regions, in both human schizophrenia and rodent-NMDAR-antagonist studies (Cadinu et al., 2018; Gonzalez-Burgos et al., 2010; Heckers & Konradi, 2015). We hypothesised that PV and GAD67 protein levels would decrease in all regions examined. The results of the brain analyses are discussed in the context of the behavioural studies performed in chapter 2, given that GABAergic changes are suggested to contribute to the cognitive deficits found in NMDAR antagonist models (Cadinu et al., 2018).

3.2 Materials and methods

3.2.1 Rats

Simple Western protein analyses used the brains of the rats from chapter 2 (n = 64). Briefly, this consisted of two cohorts of Lister Hooded rats. In each cohort (n = 32, 16 males and 16 females; Charles River, UK), half of the rats were treated with scPCP (males: 5 mg/kg; females: 2 mg/kg, bi-daily for 7 days) and the other half with vehicle (saline, 0.9%, bi-daily for 7 days). For sample size justifications see chapter 2 (section 2.2.10) . Rats in cohort 1 underwent testing in the watermaze DMP task, sensorimotor activity and NOR, with unrestricted handling. Rats in cohort 2 only underwent testing in NOR and handling was restricted throughout the study (< 1 min per rat during initial acclimatisation week, then to only to where necessary for the remainder of the study; see chapter 2 for details). Across the two cohorts, rats were age matched at the point of scPCP treatment (10-11 weeks old) and brains were taken at 6 weeks post treatment.

3.2.2 Brain tissue preparation

Brain tissue was prepared for Wes analyses similar to previous studies (Gigg et al., 2020). The brains were free hand dissected on ice into approximately 1 mm coronal sections. Using a rat brain atlas (Paxinos & Watson, 2006), the PFC (AP +4.2 to +2.52 mm; Fig. 3.1A), dorsal

hippocampus (DH; AP -1.92 to -4.2 mm; Fig. 3.1B) and intermediate to ventral hippocampus (I-VH; AP -4.36 to -6.3 mm; Fig. 3.1C) were collected into 1 ml labelled Eppendorf tubes, and the tissue was stored at -80 °C until further use.

Homogenisation buffer (10 mM Trizma base, 320 µM sucrose, 2 mM EDTA disodium salt; Sigma-Aldrich, UK) was activated immediately before use with phenylmethanesulfonyl fluoride (0.1 M, 1% v/v; Sigma-Aldrich, UK), sodium orthovanadate (0.1 M, 1% v/v; Sigma-Aldrich, UK) and cOmplete™ protease inhibitor cocktail (1X; Roche, UK). The activated homogenisation buffer was then added to the thawed tissue on ice at a volume (µl) 10-fold the approximate weight of the tissue (mg). The tissue was homogenised in the buffer using micropestles, and the homogenate centrifuged at 800 x *g* for 15 min at 4 °C. The pellet (containing the nuclear fraction) was discarded, and the resulting supernatant (S1) further centrifuged at 11,700 x *g* for 20 min at 4 °C. The resulting supernatant (S2) containing the soluble protein was collected. A small equal volume of S2 was taken for each rat, and combined with samples for each brain region within the same cohort, to create a pool for Wes optimisations (see section 3.2.4). The samples were stored at -20 °C until further use.

3.2.3 Protein concentration assay

The protein concentration of each sample was determined using a Bradford assay. Standards were prepared by diluting bovine serum albumin (Sigma-Aldrich, UK) in homogenisation buffer at known concentrations (1, 0.75, 0.5, 0.2, 0.1 mg/ml). Brain homogenate samples were also diluted using homogenisation buffer (PFC, 1:5; DH and I-VH, 1:10). The standards and blank control (homogenisation buffer) were loaded in triplicate, and the diluted samples loaded in duplicate, into a 96-well plate (Corning, Amsterdam, Netherlands). Samples for each brain region and cohort were kept on the same plate in order to reduce errors caused by potential plate to plate variability. Protein assay dye reagent concentrate (1X; Bio-Rad, California, USA) was added to all wells, and the plate incubated at room temperature for 5 min on a shaker. The plate absorbance was read at a wavelength of 595 nm using the Hidex Sense Microplate Reader and associated software (Hidex, Finland). The triplicate and replicate values for each standard and sample, respectively, were checked for precision by calculating the co-efficient of variation (CV = standard deviation/mean), and then averaged to obtain one value for each standard and sample. The average absorption values for the standards were used to create a standard curve, from which the protein concentration of each sample was interpolated. The final protein concentrations for the samples were calculated by multiplying the interpolated

value by the dilution factor. This final protein concentration was then used to calculate the sample dilutions required for simple western analysis.

3.2.4 Simple western analysis: protein quantification by capillary electrophoresis immunoblotting

The relative protein levels of the GABAergic markers PV and GAD67 were measured using simple western analysis, as in Gigg et al. (2020). Simple western analysis was performed using the Wes instrument (ProteinSimple, San Jose, USA), according to the ProteinSimple protocol (https://www.bio-techne.com/pdf-download-arena-document/product-insert/pl3-0005) (Harris, 2015; Lück et al., 2021). The optimal concentration of primary antibodies and sample protein (Table 3.1) was determined for each brain region using the combined sample pool collected during tissue preparation. Samples were diluted to the optimal concentration using 0.1X Sample Buffer (ProteinSimple, San Jose, USA) and combined with a master mix containing dithiothreitol and a fluorescent standard (ProteinSimple, San Jose, USA). Samples were then heat denatured at 95 °C for 5 min and kept on ice. The primary antibodies (sheep anti-PV, AF5058, R&D Systems, Abingdon, UK, 1:50; mouse anti-GAD67, ab26116, Abcam, Cambridge, UK, 1:50) were diluted to the optimal concentration using antibody diluent (ProteinSimple, San Jose, USA). A biotinylated ladder, the prepared samples, blocking reagent (antibody diluent), primary antibody, horseradish peroxidase (HRP)-conjugated streptavidin, HRP-conjugated secondary antibody, and chemiluminescent substrate (luminol-peroxide) were dispensed into the designated wells on a 384-well assay plate (ProteinSimple, San Jose, USA). The plates were pre-filled with stacking and separation matrices (ProteinSimple, San Jose, USA). The plate was then loaded into the Wes instrument and assays run at room temperature using the instrument default settings. Size-based protein separation by electrophoresis, immobilisation and immunodetection took place in the capillary system and was fully automated. A quantitative measure of the target protein for each sample was assessed by calculating the area under the curve of the detected intensity peaks, using the Compass for SW software (version 6.1.0; ProteinSimple, San Jose, USA). Target protein levels were then normalised to the total protein value of the sample and expressed as percentage of control. The total protein value for each sample was determined using the Total Protein Detection Module and Total Protein assay (ProteinSimple, San Jose, USA), with plates loaded as outlined above for the target protein analyses, but with primary and secondary antibodies replaced with a biotin labelling reagent and Streptavidin-HRP, respectively.

Table. 3.1. ***Optimised sample protein concentrations (mg/ml) used for each brain region (PFC: prefrontal cortex; DH: dorsal hippocampus; I-VH: intermediate to ventral hippocampus) and cohort.*** The optimal concentration of GAD67 and parvalbumin (PV) antibody used for each brain region and cohort was 1:50.

	Sample protein concentration (mg/ml)					
	Cohort 1			**Cohort 2**		
Antibody	**PFC**	**DH**	**I-VH**	**PFC**	**DH**	**I-VH**
GAD67 (1:50)	0.2	0.2	0.1	0.2	0.1	0.2
PV (1:50)	0.4	0.4	0.4	0.8	0.2	0.4

3.2.5 Statistical analysis

The levels of PV and GAD67 were normalised to control in order to compare results across cohorts, as some Wes analyses were performed using different optimised protein concentrations (Table 3.1). The relative protein levels were analysed using ANOVA, with cohort, sex and treatment group as between subjects factors. Any significant interactions were followed up using simple main effects analysis. Graphs and statistical tests were completed using GraphPad Prism (version 9) and SPSS (version 0.14.1) software, respectively, with $p < 0.05$ considered to indicate statistical significance.

3.3 Results

3.3.1 Prefrontal cortex: scPCP treatment did not change levels of PV or GAD67

In the PFC, levels of GAD67 and PV in scPCP-treated rats were not different to control levels (Fig. 3.1D and G). ANOVAs of GAD67 and PV levels revealed no main effect of treatment group, sex or cohort, and no significant interaction involving any of these factors (GAD67: $F_{(1, 56)} < 1.61$, $p > 0.21$; PV: $F_{(1, 56)} < 2.3$, $p > 0.135$).

3.3.2 Dorsal hippocampus: scPCP treatment did not change levels of PV or GAD67

In the DH, levels of GAD67 and PV in scPCP-treated rats were not different to control levels (Fig. 3.1E and H). ANOVAs of GAD67 and PV levels revealed no main effect of treatment group, sex or cohort, and no significant interaction involving any of these factors (GAD67: $F_{(1, 53)} < 1.36$, $p > 0.248$; PV: ($F_{(1, 55)} < 1$).

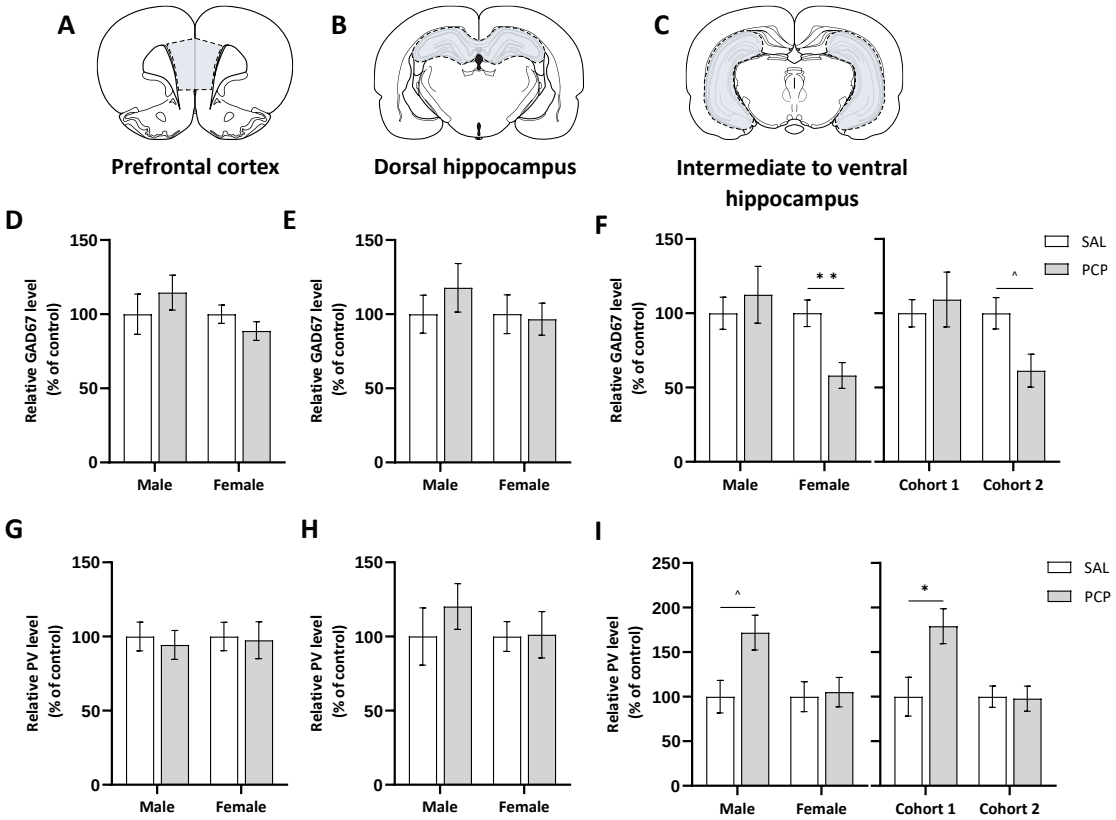

Fig. 3.1. ***Relative protein expression levels for parvalbumin (PV) and GAD67 in the prefrontal cortex, dorsal hippocampus and intermediate to ventral hippocampus of sub-chronic phencyclidine (PCP) and saline (SAL) treated rats.*** Coronal sections showing the brain area dissected (shaded in grey) for the **A.** prefrontal cortex (PFC), **B.** dorsal hippocampus (DH) and **C.** intermediate to ventral hippocampus (I-VH), illustrated using the rat brain atlas (Paxinos & Watson, 2006). **F.** GAD67 levels were significantly reduced in the female scPCP treated rats in the I-VH, with no changes in the **D.** PFC or **E.** DH. **I.** PV levels were significantly increased in cohort 1 scPCP treated rats in the I-VH, with no changes in the **D.** PFC or **E.** DH. Data are shown as mean (± SEM), n = 30-32 per treatment group (SAL or PCP). Asterisks indicate a significant simple main effect of treatment group following a significant ANOVA interaction,*$p < 0.05$, **$p < 0.01$. ^ indicates a significant simple main effect of treatment group following a strong trend for an ANOVA interaction, $p < 0.05$.

3.3.3 Intermediate to ventral hippocampus: scPCP treatment decreased GAD67 levels in female rats but increased PV levels in cohort 1 rats

In the I-VH, levels of GAD67 were significantly reduced in the female rats across both cohorts (Fig. 3.1F). ANOVA of GAD67 protein levels revealed no main effect of treatment group ($F_{(1, 56)}$ = 1.5, p = 0.225), but did reveal a significant interaction between treatment group and sex ($F_{(1, 56)}$ = 5.12, p = 0.027), and a strong trend for an interaction between treatment group and cohort ($F_{(1, 56)}$ = 3.97, p = 0.051), but no interaction between sex, treatment group and cohort ($F_{(1, 56)}$ = 1.17, p = 0.284). Simple main effects analysis of the female GAD67 data across both cohorts revealed a significant main effect of treatment group ($F_{(1, 30)}$ = 11.3, p = 0.002), reflecting a reduction in GAD67 levels in the female scPCP treated rats compared to the female saline

treated rats. Simple main effects analysis of the male GAD67 data across both cohorts revealed no main effect of treatment group ($F_{(1, 30)} < 1$). To follow up the strong trend for an interaction between treatment group and cohort, simple main effects analysis of cohort 1 data across both sexes revealed no significant effect of treatment group ($F_{(1, 30)} < 1$), whereas cohort 2 data revealed a significant main effect of treatment group ($F_{(1, 30)} = 6.69$, $p = 0.017$), reflecting a decrease in GAD67 levels.

ANOVA of the PV data revealed a significant main effect of treatment group ($F_{(1, 56)} = 5.28$, $p = 0.025$), a significant interaction between treatment group and cohort ($F_{(1, 56)} = 5.92$, $p = 0.018$), and a strong trend for an interaction between treatment group and sex ($F_{(1, 56)} = 3.98$, $p = 0.051$), but no interaction between sex, treatment group and cohort ($F_{(1, 56)} < 1$). Simple main effects analysis of cohort 1 data across both sexes revealed a significant main effect of treatment group ($F_{(1, 30)} = 7.34$, $p = 0.011$), reflecting an increase in PV levels in scPCP treated rats compared to saline treated rats in cohort 1. Simple main effects analysis of cohort 2 data revealed no significant main effect of treatment group ($F_{(1, 30)} < 1$). To follow up the strong trend for an interaction between treatment group and sex, simple main effects analysis of the female data revealed no main effect of treatment group ($F_{(1, 30)} < 1$), whereas simple main effects analysis of the male data revealed a significant effect of treatment group ($F_{(1, 30)} = 7.20$, $p = 0.012$), reflecting an increase in PV in the scPCP treated rats.

3.4 Discussion

Sub-chronic PCP treatment resulted in changes in GAD67 and PV protein expression in the intermediate to ventral hippocampus, with no changes in the PFC or dorsal hippocampus. Across both cohorts of rats, GAD67 was reduced in the female rats, but not in the males, suggesting that scPCP treatment may have sex-specific effects. Interestingly, however, in the first cohort of rats, which were used for watermaze testing and received more handling than the rats in cohort 2, we found an increase in PV protein levels in both the male and female scPCP treated rats, compared to saline treated rats, whereas no changes in PV levels were found in the second cohort of rats across both sexes.

3.4.1 Reduced GAD67 in the intermediate to ventral hippocampus in female scPCP treated rats

In the I-VH we found decreases in GAD67 protein levels in the female scPCP treated rats, compared to saline treated female rats, which was present across both cohorts. This finding is in contrast with a study in scPCP treated female mice which, using simple western analysis, found no significant changes to GAD67 in the ventral hippocampus (Gigg et al., 2020).

However, this discrepancy may be due to the different species used. Nonetheless, in agreement with the present study, this study also reported no changes to GAD67 in the DH or PFC of female treated mice (Gigg et al., 2020). Using western blot, a study in scPCP treated female ovariectomised rats found a significant decrease in GAD67 in the dorsal hippocampus, with no changes in the prelimbic region of the PFC (Riordan et al., 2018). Although we found changes in the I-VH opposed to the dorsal region, this study does largely support our findings of reduced hippocampal GAD67 expression in scPCP treated female rats, with no changes in the PFC. However, a recent study in scPCP treated female rats reported reductions in GAD67 expression in the PFC using simple western analysis (Fletcher et al., 2023). Considering that this study used a relatively long (12 weeks) washout period, it is possible that changes to GAD67 in the PFC of females rats emerge at later time stages than examined in the present study and Riordan et al. (2018) study, which had a washout period of 6 weeks and 3 weeks, respectively. Nevertheless, the measurements made in mice were conducted after a 15-week washout and still found no changes in GAD67 expression in the PFC (Gigg et al., 2020), suggesting that length of washout may not have influenced the results.

In contrast to our findings in the female rats, we found no changes in GAD67 protein levels in the males across both cohorts, suggesting that the scPCP treatment may have sex-specific effects in terms of GAD67 protein expression in the I-VH. To our knowledge, only one other study has directly compared the impact of sex on scPCP induced neurochemical changes. This study, investigating regional brain-derived neurotrophic factor expression in male and female scPCP-treated rats, found more widespread decreases in female compared to male rats (Snigdha et al., 2011b), suggesting that females may be more sensitive to neurological changes caused by scPCP treatment. As outlined above, studies investigating GAD67 protein expression in females have yielded mixed results. In males, previous studies of western blot analyses of GAD67 protein expression in rats treated with sub-chronic MK-801 during adulthood or adolescence found no changes in GAD67 in the PFC or hippocampus (Li et al., 2016; Tsai et al., 2022). However, repeated administration of ketamine to male neonatal rats did result in significant reductions in GAD67 protein in the PFC and hippocampus, when measured in adulthood (Zhang et al., 2016). This suggests that male rats may be vulnerable to NMDAR hypofunction induced GAD67 protein alterations when treatment is given early in development.

Nevertheless, studies using immunofluorescence to measure GAD67 protein levels in male rats and mice treated with repeated NMDAR antagonist administration have found reductions in GAD67 in the PFC, albeit using different dosing regimens to the present study (Amitai et al.,

2012; Behrens et al., 2007, 2008; Pérez et al., 2019; Zhang et al., 2008). Importantly, many of these reductions in GAD67 fluorescence were specific to PV-interneurons (Amitai et al., 2012; Behrens et al., 2007, 2008; Zhang et al., 2008). If a reduction in GAD67 protein expression was specific to PV interneurons, this could explain why, in the present study, we found no changes to GAD67 levels in the PFC following Wes analyses. Given that PV interneurons are reported to make up only around 40% of inhibitory interneurons in the rat PFC (Gabbott et al., 1997), it is possible that the Wes analyses were not sensitive enough to detect this cell-specific change, due to unaffected GAD67 levels within other GABAergic interneuron subtypes. In addition to cell specificity, Wes analyses may not have been sensitive enough to detect any subregion-specific changes. For example, adult male rats treated for 7 days with MK-801, followed by a 2-week washout, were reported to have decreased GAD65/67-immunoreactive cells in the DG of the dorsal hippocampus, with no changes in the CA1 or CA3 region (Unal et al., 2021). These subregion-specific changes may, therefore, have been missed in the Wes analyses of the male scPCP treated rats which looked at average expression across the entire DH region. Therefore, overall, although western blot analyses of GAD67 changes in adult male rodents, including the present study, do not support a change in GAD67 protein levels, immunofluorescent and immunohistochemical analyses suggest that NMDAR antagonism may produce subregion- and PV-interneuron-specific changes to GAD67 expression in male rodents. To our knowledge, there are no published studies in females which have used immunohistochemistry or immunofluorescence to investigate GAD67 expression. However, using quantitative PCR, one study in scPCP treated female rats found no changes to GAD67 mRNA levels in the PFC and hippocampus (Neugebauer et al., 2018).

3.4.2 Increased PV in the intermediate to ventral hippocampus in cohort 1 scPCP treated rats

In the present study we found no changes to PV levels in the DH or PFC, and no changes in the I-VH of cohort 2 rats across both sexes. This agrees with a study in scPCP treated mice, which found no changes to PV protein levels in the hippocampus or frontal cortex, albeit using a much shorter washout period (3 days) (Benneyworth et al., 2011). In cohort 1 rats, however, we found increased PV levels in the I-VH compared to saline treated rats. At first glance, this finding seems at odds with the idea that NMDAR hypofunction leads to an impairment in GABAergic function. Our finding also contrasts with a study in scPCP treated mice that, using simple western analysis, reported decreases in PV levels in the ventral hippocampus, DH, as well as the frontal cortex (Gigg et al., 2020). In addition, PV decreases using western blot have been reported in the hippocampus of sub-chronic MK-801 treated rats (Tsai et al., 2022), in

the PFC of adolescent sub-chronic MK-801 treated rats (Li et al., 2016), and in both the hippocampus and PFC of adult rats treated with repeated ketamine in the neonatal period (Zhang et al., 2016). Interestingly, however, there have been other reports of increased PV expression in NMDAR antagonist treated rats (Abdul-Monim et al., 2007; Fletcher et al., 2023; Honeycutt & Chrobak, 2018; Sabbagh et al., 2013). Using simple western analysis, PV levels were found to be increased in the PFC of scPCP treated female rats and, moreover, PV mRNA levels were also found to be increased (Fletcher et al., 2023). Although we found PV increases in the I-VH, with no changes in the PFC, this finding still supports the idea that scPCP treatment can lead to regional increases in PV protein levels. Remarkably, this study also found a decrease in the number of PV+ cells, examined using immunohistochemistry (Fletcher et al., 2023). Thus, it is possible that an increase in PV protein levels may be a compensatory mechanism for a regional loss of PV interneurons. Many other studies have shown decreases in PV+ cells following scPCP treatment (Abdul-Monim et al., 2007; Jenkins et al., 2008, 2010; Landreth et al., 2021; Leger et al., 2015; McKibben et al., 2010; Redrobe et al., 2012; Schroeder et al., 2000), although there are some inconsistencies in the literature with regard to which sub-region this loss occurs in. For example, Jenkins et al. (2008) reported decreases in the CA1 and DG region of the hippocampus, with no changes in CA2 or CA3, whereas Abdul-Monim et al. (2007) found no changes in CA1, but decreases in DG, CA2 and CA3. In contrast, Riordan et al. (2018) and Benneyworth et al. (2011) found no changes in PV+ cells in the PFC or hippocampus, although these findings may have been influenced by the relatively short washout period of 3 weeks and 3 days, respectively.

We did not find any PV changes in the DH or PFC, whereas the literature largely supports a loss of PV+ cell expression in these regions following scPCP treatment. Therefore, it is possible that global PV protein levels remained unchanged in these regions, whereas the number PV+ cells in specific sub-regions may be reduced. However, this idea of PV interneuron cell death following NMDAR antagonist treatment has been contested in previous studies where ketamine treatment (2 days) in rodents led to a reduction in PV and GAD67 expression, without a loss of PV+ cells (Behrens et al., 2007, 2008; Zhang et al., 2008). In line with this, Li et al. (2016) suggested that the decrease in PV+ cells recorded in sub-chronic MK-801-treated adolescent rats was likely due to decreased PV expression, rather than neuronal death, as demonstrated by unaffected levels of apoptotic factors. The present study, however, where we found no changes to PV protein levels in the DH or PFC, does not support this. Furthermore, care should be taken when equating the effects of different NMDAR antagonists (Dix et al., 2010; Gilmour et al., 2009; Hevers et al., 2008; Smith et al., 2011), and where

different antagonists are used in rodents of different developmental ages (Honeycutt & Chrobak, 2018), with different dosing regimens and washout periods.

In contrast to studies reporting a loss of PV+ cells, Sabbagh et al. (2013) reported an increase in PV+ cells in the dorsal hippocampal CA3 region of chronic ketamine treated rats (18 days). Although this study, unlike the present study, did not include a washout period, it may support the idea that, in contrast to GAD67 levels which have only ever been reported to decrease or not change, PV expression changes caused by repeated NMDAR antagonist administration may be more dynamic. Increases in PV+ cells have also been reported in the cingulate cortex and motor area of scPCP treated rats (Abdul-Monim et al., 2007), as well as in the hippocampal DG of sub-chronic ketamine treated rats (Honeycutt & Chrobak, 2018). This may suggest that the relationship between NMDAR hypofunction and PV expression is complex, with discrete brain regions and sub-regions showing different PV protein and PV+ cell expression. In support of this idea of PV being dynamically regulated, PV levels in the rat retina and PFC have been shown to fluctuate throughout the day, whereas levels of prefrontal GAD65/67 do not show such diurnal fluctuation (Gábriel et al., 2004; Harkness et al., 2019). Furthermore, PV protein expression has also been found to be influenced by sex, age, early environment, sleep deprivation, exercise and behaviour (Donato et al., 2013; Ellis & Honeycutt, 2021; Fletcher et al., 2022; Gomes da Silva et al., 2010; Harkness et al., 2019; Honeycutt & Chrobak, 2018; Sampedro-Piquero et al., 2016; Selakovic et al., 2017; Urakawa et al., 2013). Thus, the dynamic nature of PV expression may render PV protein levels an unreliable marker of pathological changes.

3.4.3 GABAergic marker changes and changes in behaviour

The finding of the present study that PV levels were increased in the I-VH of cohort 1 rats, whereas no changes were found in the same region of cohort 2 rats, may suggest a sampling error in cohort 1 rats, given that both cohorts received the same dosing regimen of PCP, were age matched at time of treatment, and had an equal washout period before tissue collection. However, there were differences between the cohorts in terms of the behavioural tasks undertaken. Cohort 1 rats underwent repeated testing on the watermaze DMP task, NOR, LMA, startle and PPI, whereas cohort 2 rats only underwent repeated testing on NOR (see chapter 2 for details). In addition, the amount of handling the rats received was different between the cohorts; cohort 1 rats were handled daily for weight monitoring, whereas handling of cohort 2 rats was restricted to less than 1 min per rat in the initial acclimatisation period and then to only where necessary. It is possible that these differences between cohorts

may have influenced the expression of PV protein. We hypothesised in chapter 2 that frequent handling and/or aerobic exercise on the watermaze may have rescued the scPCP-induced NOR deficits in cohort 1 rats. It is possible that these two factors may also have influenced the expression of PV. For example, exercise has been shown to increase the number of PV+ cells (Fletcher et al., 2022; Gomes da Silva et al., 2010; Selakovic et al., 2017). To our knowledge, there have been no studies evaluating the effect of handling on PV expression, however, environmental enrichment has been shown to increase PV+ cell levels (Sampedro-Piquero et al., 2016; Urakawa et al., 2013).

Alternatively, it is possible that training on the watermaze task itself may have influenced PV expression in cohort 1 rats. Donato et al. (2013) reported that recent experience can modulate the differentiation state of PV interneurons. In the dorsal hippocampal CA3b area, Donato et al. (2013) used PV immunoreactivity to monitor the differentiation state of PV interneurons, with PV interneurons classified as low-PV or high-PV based on threshold intensity signals. The authors reported that training on the Morris watermaze task induced a shift to a low-PV network in the mouse hippocampus, without changes in the total number of PV interneurons (Donato et al., 2013). At the end of watermaze training, the low-PV network was reported to shift to a high-PV state. However, a low-PV network remained when the visual cues used in the task were rearranged, which may have similar effects to the daily changing of the watermaze platform location used in our watermaze DMP task. The low-PV network induced by watermaze training was found to last at least 3 days, but subsided 7 days, after watermaze training (Donato et al., 2013). Given that we sacrificed the cohort 1 rats only 2 days after the end of watermaze DMP testing, it is possible that PV levels may have been influenced by this testing. Indeed, the increase in PV protein levels reported here in scPCP treated rats may, instead, reflect a decrease in PV in the saline treated rats, caused by a watermaze-training induced shift to a low-PV network; whereas, in scPCP treated rats, this ability to regulate PV expression in response to learning requirement may be abolished (although without any significant impact on watermaze DMP performance). If this was the case, we should expect to see differences in the PV levels of saline treated cohort 1 and 2 rats. Supplementary analyses (see section S1) of absolute PV protein levels revealed that PV levels in saline treated rats were in fact lower in cohort 1 (Fig. S1). This supports the idea that scPCP treatment may alter PV regulation by preventing shifts in PV differentiation in response to experience (Donato et al., 2013), and this may contribute to the learning and memory impairments found in the model. Moreover, Donato et al. (2013) suggest that these PV shifts are highly system specific, with watermaze training inducing PV shifts in the hippocampus, but not in the primary motor

cortex, and motor learning tasks inducing shifts in the motor cortex, but not hippocampus. Nevertheless, it is possible that changes in the current study may simply reflect differences due to variability between the Bradford assay and/or Wes plates used in the simple western analyses across the two cohorts.

In addition, although we found increased PV levels in the I-VH of scPCP treated cohort 1 rats, we did not find any differences in watermaze DMP task performance, and NOR impairment was mainly evident at 1, but not 3 or 5 weeks, after scPCP treatment. This suggests that these potential shifts in I-VH PV levels were not sufficient to cause watermaze DMP task impairment or sustained NOR deficits. Similarly, GAD67 reductions found in the I-VH of scPCP treated female rats, which would be expected to reduce GABA synthesis and, thereby, reduce GABA release (Farrant & Nusser, 2005; Zhang et al., 2008), did not lead to watermaze DMP or sustained NOR task impairments in cohort 1. It follows, therefore, that the GAD67 reductions in cohort 2 female scPCP treated rats, where the NOR deficit persisted throughout the study, may not entirely account for the NOR impairment. Therefore, it is likely that other neuropathological changes reported following NMDAR antagonist treatment may contribute to NOR impairments, such as changes in expression of brain-derived neurotrophic factor, perineuronal nets, postsynaptic density 95 protein, vesicular glutamate and/or GABA transporters, or a decrease in global brain volume (Doostdar et al., 2019; Fletcher et al., 2023; Gigg et al., 2020; Klimczak et al., 2021; Ma et al., 2020; Snigdha et al., 2011b).

3.4.4 Conclusions

Overall, the data provides support that NMDAR hypofunction caused by scPCP treatment leads to limited alterations in GABAergic markers. First, GAD67 levels were reduced in the I-VH of female scPCP-treated rats. Second, PV levels were increased in scPCP treated rats compared to saline treated rats in cohort 1. The reductions in GAD67 which were only found in the female scPCP treated rats across both cohorts suggest that scPCP treatment can cause a sex-specific impairment in GABAergic activity. The present study, therefore, highlights the importance of using both sexes in research. Unlike changes in GAD67, PV levels were increased in the I-VH of both male and female scPCP treated rats in cohort 1. However, closer inspection of this change, by comparing absolute PV levels in cohort 1 and 2 saline treated rats, suggests that PV increases in the scPCP treated rats may rather reflect an experience-related decrease of PV in control rats. The study, therefore, highlights potential issues of using PV protein expression as a disease marker; PV appears to be spatially and dynamically regulated, with changes in environment and behaviour potentially influencing protein expression. This is perhaps

problematic when attempting to correlate post-mortem PV changes caused by scPCP treatment with changes in cognition, as certain behavioural tasks may themselves alter PV expression. Nevertheless, the present study may suggest an abnormal regulation of PV in scPCP treated rats, which may impair plasticity and contribute to cognitive deficits reported in the model. However, given the variability within the data and the small sample sizes, it is also possible that the findings presented here reflect sampling errors. Moreover, the disparate findings found here contributes to an already complex pattern of findings reported in previous studies investigating PV and GAD67 protein changes following NMDAR hypofunction.

S1 Supplementary analysis of PV protein levels in the intermediate to ventral hippocampus

Previous findings suggested that the learning of a new place on the watermaze task can induce a shift in dorsal hippocampal CA3b PV-interneurons to a low-PV state, which facilitates new place learning (Donato et al., 2013). Therefore, we investigated whether the increase in PV found in the I-VH of watermaze trained scPCP treated rats, relative to watermaze trained saline treated rats, may have reflected that scPCP-treated rats failed to shift to a low-PV state, rather than an increase in PV per se. If this was the case, we would expect to see a decrease in the PV levels of saline treated rats in cohort 1, which were sacrificed only 2 days following the end of watermaze training, compared to the saline treated rats in cohort 2, which received no watermaze training. To make this comparison, we used the absolute PV data, which was not normalised to control (Fig. S1). This was possible in the I-VH as Wes analyses were performed using the same concentration of protein and antibody (Table 3.1). ANOVA of these absolute PV levels demonstrated a significant interaction between cohort and treatment group ($F_{(1, 56)}$ = 4.94, p = 0.03), with a main effect of cohort at trend level ($F_{(1, 56)}$ = 3.31, p = 0.074). Simple main effects of analysis of the data from scPCP treated rats revealed no main effect of cohort ($F_{(1, 30)} < 1$), indicating that absolute PV levels were similar across both cohorts of scPCP treated rats. However, simple main effects analysis of the data from saline treated rats revealed a main effect of cohort ($F_{(1, 30)}$ = 6.70, p = 0.015), reflecting a decrease in PV protein levels in cohort 1 compared to cohort 2 saline treated rats. Thus, this analysis suggests that the apparent increase in PV levels found in scPCP treated cohort 1 rats, may rather reflect a decrease in PV levels in cohort 1 saline treated rats, possibly due to a watermaze training induced shift to a low-PV state (Donato et al., 2013).

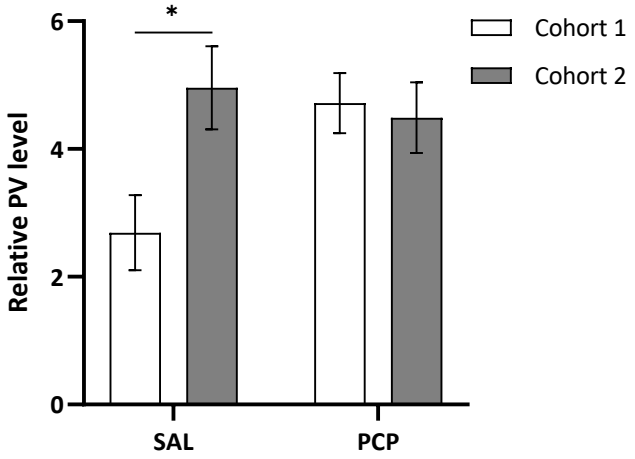

Fig. S1. ***Relative protein expression levels for parvalbumin (PV) not normalised to control in the intermediate to ventral hippocampus of scPCP treated rats.*** PV levels were significantly decreased in saline (SAL) treated rats in cohort 1 compared to saline treated rats in cohort 2. Data are shown as mean (± SEM), n = 32 per treatment group (SAL or PCP), *$p < 0.05$.

Chapter 4: In vivo electrophysiological recordings of evoked reverberatory responses in the hippocampal circuit of sub-chronic phencyclidine treated rats

Declaration: Ningyuan Sun carried out the drug administration and equally contributed to data collection.

Abstract

NMDAR hypofunction in rodent models has been suggested to result in impairments in GABAergic inhibition, including in the hippocampus. However, whether these impairments may result in functional alterations to in vivo hippocampal neural activity is unclear. Here, we used evoked in vivo recordings under urethane anaesthesia to examine the synaptic excitability of hippocampal circuits in scPCP treated rats. We applied low frequency train stimulation to the subiculum or CA3 region with the aim of replicating previous findings of reverberatory responses (or re-entrance) in the hippocampal formation. This re-entrance of hippocampal output back into the hippocampus is considered to mediate information storage and may provide a measure of the overall excitability of hippocampal circuits. We found that a subset of both scPCP and saline treated rats exhibited reverberatory responses in the hippocampal formation following low frequency train stimulation. Current source density analysis indicated a laminar profile of synaptic currents that was similar across treatment groups, for both the initial evoked response and for the longer latency re-entrance, indicating intact fibre pathways in scPCP treated rats. In addition, the normalised slope and amplitude of the evoked dentate gyrus response was similar across treatment groups. However, observations of increased population spiking in the dentate gyrus following subiculum train stimulation in scPCP treated rats may suggest increased hippocampal excitability following NMDAR hypofunction.

4.1 Introduction

Hippocampal hyperactivity is a core feature of schizophrenia (Bast et al., 2017; Heckers & Konradi, 2015; Kätzel et al., 2020; Schobel et al., 2013). Neuroimaging findings of increased hippocampal activity in schizophrenia have been related to cognitive dysfunction and are consistent with post-mortem findings of decreased hippocampal GABA markers (Heckers & Konradi, 2015; Tregellas et al., 2014). Rodent models of sub-chronic NMDAR hypofunction, such as the scPCP model, also exhibit cognitive deficits relevant to schizophrenia, alongside changes in hippocampal GABA markers (Cadinu et al., 2018; Neill et al., 2010). However, it is

unclear whether these GABAergic changes translate to a functional disruption in GABAergic activity, which may be observed as aberrant hippocampal activity. Here, we examined the excitability of synaptic circuits in the hippocampal formation of scPCP treated rats.

The rodent hippocampal formation is comprised of three distinct subregions: the dentate gyrus (DG), the hippocampus proper (which consists of three CA subregions, CA1-3), and the subiculum (van Strien et al., 2009) (Fig. 4.1). Each region is connected via a unidirectional feed-forward route, traditionally known as the trisynaptic pathway (Andersen et al., 1971; van Strien et al., 2009). The first pathway emerges from the neighbouring entorhinal cortex (EC), which relays input from layer II EC cells to the molecular layer of the DG via the perforant path (Andersen et al., 1971). The second pathway emerges from the DG mossy fibres and projects to the CA3 region. Thirdly, CA3 Schaffer collaterals input onto the stratum radiatum of CA1, completing the trisynaptic circuit (Amaral & Witter, 1989). This trisynaptic pathway represents the most prominent hippocampal pathway and the main route of information flow (Fig. 4.1A).

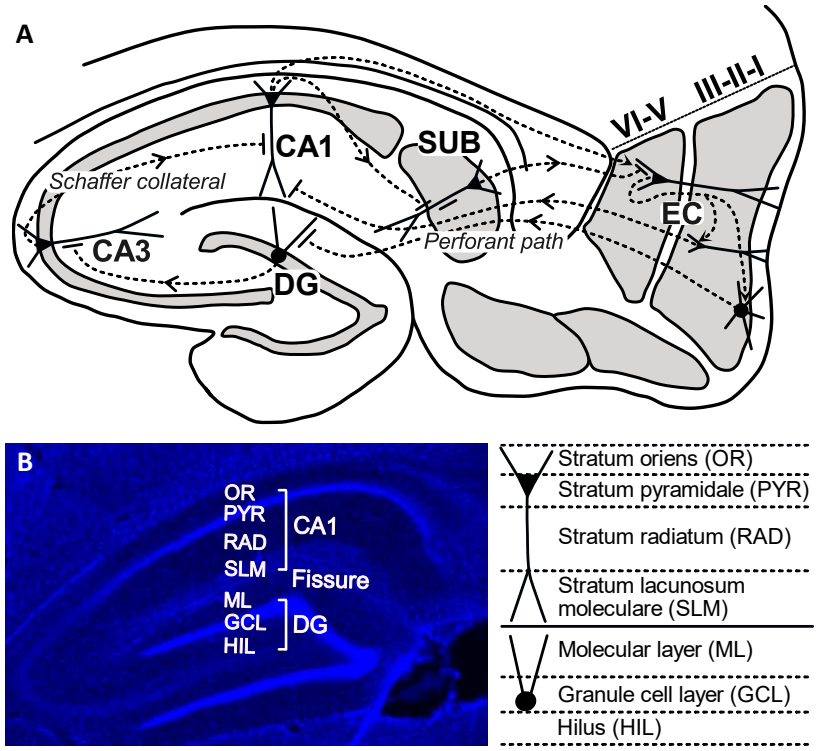

Fig. 4.1. ***Major synaptic pathways and laminar structure of the hippocampal formation.*** **A.** Layer II pyramidal and stellate neurons of the entorhinal cortex (EC) target dendrites of dentate gyrus (DG) granule cells in the molecular layer (ML) via the perforant path, which traverses the subiculum (SUB). Neurons in Layer III of the EC target the CA1 apical dendrites in the stratum lacunosum moleculare (SLM) via the temporoammonic pathway. DG granule cells target the CA3 region via the mossy fibre pathway. CA3 Schaffer collaterals project to CA1 stratum radiatum (RAD). CA1 projects to the SUB and deep layers of the EC. Hippocampal re-entrance occurs via the connection between the deep to superficial layers of the EC. **B.** DAPI stained section of the dorsal hippocampus illustrating the cell layers of the CA1-DG axis. Figures based on Kloosterman et al. (2004) and Davies et al. (2014).

However, many other pathways contribute to the circuits within the hippocampal formation, including several parallel pathways and back-projections (Stepan et al., 2015; van Strien et al., 2009). The complexity of hippocampal circuitry is facilitated by the laminar structure of the DG and CA fields, which enables optimal assembly of neuronal circuits for information processing (Ledda & Paratcha, 2017) (Fig. 4.1B). The cell layers of CA1 consist of the stratum oriens, stratum pyramidale; stratum radiatum (RAD), which contains the majority of CA3-CA1 synapses; and the stratum lacunosum moleculare (SLM), which receives EC input via the temporoammonic pathway. The hippocampal fissure separates CA1 from the DG, which comprises three layers: the molecular layer containing the granule cell dendrites; the granule cell layer containing densely packed granule cell bodies; and the hilus, or polymorphic layer, which consists of interneurons and hilar mossy cells (Sosa et al., 2018; Stepan et al., 2015; van Strien et al., 2009).

Processed information from the hippocampal formation is received in the deep layers of the EC, either directly from CA1, or from the subiculum via the CA1-subiculum connection (Dolorfo & Amaral, 1998a). Here, the hippocampal output may either be relayed to the neocortex and/or re-enter the hippocampus via deep to superficial EC connections which result in activation of the perforant path (Kloosterman et al., 2003, 2004). This 're-entrance' of hippocampal activity has been proposed as one of the mechanisms mediating the temporal storage of information in a neuronal network (Iijima et al., 1996; Kloosterman et al., 2003; Ohara et al., 2018). Furthermore, it has been suggested to enable the EC to act as a comparator, where incoming neocortical input can be compared and/or integrated with hippocampal output (Buzsáki, 1996; Kloosterman et al., 2004; Lőrincz et al., 2002). Thus, given the proposed importance of hippocampal re-entrance in memory formation, it is of interest to determine if and how this re-entrance is affected in NMDAR hypofunction models.

To our knowledge, there have been no previous studies investigating the presence of hippocampal response re-entrance in NMDAR hypofunction models. Previous studies investigating changes in hippocampal neural activity following sub-chronic NMDAR hypofunction have focused on plasticity changes at single synapses and have produced mixed results. Sub-chronic MK-801 treatment was found to enhance CA3-CA1 LTP in vivo (Ashby et al., 2010), whereas in vitro studies in slice preparations have reported either no change (Tanqueiro et al., 2021), or weaker CA3-CA1 LTP following scPCP treatment in rats (Nomura et al., 2016; Pollard et al., 2012). The complex circuitry of the hippocampal formation makes it difficult to discern the effect of single synapse changes on overall hippocampal activity. Here,

we sought to examine the excitability of the hippocampal circuit as a whole, by investigating response reverberation (or re-entrance) of evoked responses.

Using a multi-site electrode array, which spanned the CA1-DG axis, we measured the extracellular field excitatory post-synaptic potentials (fEPSP) evoked in vivo by stimulation of the Schaffer collaterals (SCHAFF) in CA3, or by stimulating the passing fibres of the perforant path in the subiculum (SUB) (Fig. 4.1A). We focused our analysis on the response elicited by low frequency train stimulation, which comprised 5 trains of 20 constant current pulses applied at a frequency of 5 Hz and 10 Hz. Using current source density analysis, the pattern of evoked synaptic sinks and sources was mapped across the CA1-DG axis. As in Kloosterman et al. (2004) and Davis et al. (2014), we expected to see evidence of response re-entrance, with the aim to qualitatively examine any gross differences across treatment groups. We hypothesised that instances of re-entrance would be increased in scPCP treated rats, due to increased hippocampal activity caused by a reduction in local GABAergic inhibition.

4.2 Materials and methods

4.2.1 Rats

The study used adult female Lister Hooded rats (Charles River, UK). An initial cohort of n = 20 rats was used, however, after excluding rats required for the optimisation of the SUB stimulation co-ordinates (see section 4.3.1), n = 5 rats were later added to the study (for final sample sizes and justification, please see section 4.2.3.3, Sample sizes and justification). All rats weighed between 200-250 g at the time of scPCP/saline dosing (PCP hydrochloride, 2 mg/kg, Sigma-Aldrich, UK; or saline, 0.9%; 1 ml/kg, i.p., bi-daily for 7 days; e.g., Abdul-Monim et al., 2007; Damgaard et al., 2010; Horiguchi & Meltzer, 2013), and weighed between 235-342 g at time of electrophysiological recordings, which were taken at 4-15 weeks following the end of scPCP/saline treatment. Rats were housed in groups of five, separated according to treatment group (PCP or saline), in individually ventilated 'double decker' cages (GR1800; 462 x 403 x 404 mm; Techniplast, UK). Temperature (21 ± 2 ˚C) and humidity (50 ± 10%) conditions were controlled and an alternating 12 h light-dark cycle was used (lights on at 07:00 h) (Biological Service Facility, University of Manchester). Rats had *ad libitum* access to food and water throughout the study. All procedures were carried out during the light phase and in accordance with the UK Animals (Scientific Procedures) Act 1986.

4.2.2 Novel object recognition testing

The NOR task is widely used in rodents as an indicator of recognition memory, with task deficits suggested to be relevant to recognition memory impairments in human brain disorders, including schizophrenia (Grayson et al., 2015; Lyon et al., 2012). The initial cohort of rats (n =20) was tested on the NOR task at 1 week post scPCP/saline treatment, in order to verify cognitive impairment in the scPCP treated rats, as reported previously in the literature (Grayson et al., 2007; Neill et al., 2010), and here in chapter 2 (also see references therein).

The NOR testing procedure was performed as outlined in chapter 2 and 5, but different apparatus and objects were used as the study took place in another animal facility. The NOR arena consisted of an open plexiglass box (52 x 52 x 30 cm), with black walls and a white floor demarcated into a 3x3 grid. The object pair used in the NOR task consisted of a Diet Coke can and a brown medicine bottle and had been previously validated for equal baseline preference (Grayson et al., 2007; Landreth et al., 2021). The object used as novel and the location of the novel object (left or right) was counterbalanced across treatment groups.

Each rat was habituated to the empty NOR arena for 1 h on the day before testing and reacclimatised to the arena for 3 min on the testing day. On the NOR testing day, rats were placed into the NOR arena with two identical objects and allowed to explore for 3 min. Rats were then removed from the arena and placed into a holding box (Plexiglas; 24 x 44 cm x 19 cm) for the 1 min retention delay. After the retention delay, rats were placed back into the NOR arena with an identical copy of the previously encountered object (the familiar object) and a novel object, and allowed to explore for 3 min. The arena and objects were cleaned with surface disinfectant (Anistel, Tristel Solutions, UK) before each trial to reduce olfactory cues left by the rats. Behaviour was recorded using an overhead camera and exploration times scored offline using 'The Novel Object Timer' (created by Jack Rivers-Auty, https://jackrrivers.com/program/; Gigg et al., 2020), with the scorer blind to treatment group and object type (novel or familiar). Time spent exploring an object was defined as interacting with the object (e.g., sniffing) and directing the nose at the object at a distance of < 1 cm. Object exploration was not recorded if the rat was in contact with the object but not facing it (e.g., standing/sitting on the object or using it as a prop) (Ennaceur & Delacour, 1988).

As in chapter 2, object exploration time was analysed using ANOVA with treatment group as between-subjects factors and object type (familiar/novel) as a within-subjects factor. Pairwise student t-tests were used for planned comparisons of familiar versus novel exploration time. Discrimination index ((time spent exploring the novel object - time spent exploring the familiar

object)/total time spent exploring both objects) was also used as a measure of NOR performance, with a higher value indicating greater preference for the novel object (Gigg et al., 2020). DI was analysed using ANOVA with treatment group as between-subjects factors, and one-sample t-tests used as planned comparisons to chance exploration (DI = 0).

4.2.3 In vivo electrophysiological recordings of evoked hippocampal responses

4.2.3.1 Surgical implantation of electrodes for acute electrophysiological recordings

Rats were anaesthetised using urethane (30% w/v in 0.9% saline; 1.4 g/kg; i.p.; Sigma-Aldrich, UK) and monitored for areflexia. If required, top-up doses of urethane were administered up to a maximum dose of 1.8 g/kg. Urethane anaesthesia was used as it produces a long-lasting steady surgical plane of anaesthesia, with minimal effects on cardiovascular and autonomic systems, making it suitable for a typical recording day lasting around 8 h (Sorrenti et al., 2021). Once a suitable plane of anaesthesia was established (with rats showing no toe pinch withdrawal reflex), rats were secured in a stereotaxic frame (1430, Kopf, USA) using ear bars coated in signa electrode gel (Parker, USA). A rectal probe and homeothermic heating blanket (Harvard Apparatus, USA) were used to maintain the rats core body temperature at approximately 37 °C. The skin was disinfected using iodine solution and a midline scalp incision was made to expose the skull, with bregma and lambda aligned horizontally. Using a high-speed drill (Foredom, USA), three holes were drilled into the skull on the left hemisphere for the two bipolar stimulating electrodes (twisted 125 µm diameter Teflon-insulated stainless-steel wires; Advent Research Materials, UK) and the recording electrode (A2x16-10mm-100-500-177-A32, 50 µm thickness; NeuroNexus Tech, USA). The recording electrode was a multi-electrode array, consisting of two parallel silicon shanks, separated by 500 µm, each containing 16 linearly aligned electrode contacts spaced 100 µm centre-to-centre. The recording electrode was inserted into mid CA1 (AP: -4.25, ML: -2.6, DV: 2.8-3.0 mm, Fig. 4.2A) and lowered such that it spanned the CA1-DG axis approximately perpendicularly, as in Sun et al. (2022, 2023). A stimulating electrode was aimed at the CA3 region (AP: -1.8, ML: -2.4, 30° angle from vertical, Fig. 4.2A), to stimulate the CA3-CA1 SCHAFF pathway, as in Sun et al. (2022, 2023). Another stimulating electrode was aimed at the dorsal SUB (AP: -6.0, ML: -2.4, 20° angle from vertical, Fig. 4.2B), to stimulate the passing fibres of the EC to DG perforant path (Kloosterman et al., 2003, 2004). Each stimulating electrode was slowly lowered to the target depth by monitoring the fEPSP at each recording electrode contact in response to single pulse stimulation at 110 µA current. In practice, this was an approximate depth of 2.3-2.9 mm for SCHAFF stimulation and 2.2-2.9 mm for SUB stimulation. All electrodes were coated with

fluorescent dye (CM-DiI; Invitrogen, Paisley, UK) prior to insertion to label the electrode location.

4.2.3.2 Stimulation protocol

Electrical stimuli were delivered using a constant current stimulator (DS3, Digitimer, UK), which was triggered using a 1 ms 5V square-wave output from a National Instruments PCI card (PCI-6071E, UK), and controlled using custom written scripts in LabVIEW software (version 19, National Instruments, UK). The stimulus duration was set to 0.2 ms for all protocols.

The fEPSP signals recorded at each electrode contact could be visualised in situ using an oscilloscope (HAMEG instruments GmbH, USA), and this was used to determine the depth of the stimulating electrodes and recording electrode. The stimulating electrode was slowly lowered to the target region by monitoring the fEPSP response to single pulse stimulation at 110 µA. In response to SCHAFF stimulation, we expected to see: (i) negative going potential in the CA1 region and (ii) a positive DG response, possibly due to a back projection of mossy fibres (Gruart et al., 2015; Leung et al., 2008; Scharfman, 2007; Sun et al., 2022, 2023). A typical response profile to SCHAFF stimulation is presented in Figure 4.3 and 4.4 (pulse 1). Following Kloosterman et al. (2003, 2004), we monitored the fEPSP response to single pulse SUB stimulation and expected to see: (i) a large positive potential in the hilus and granule cell layer of DG, which reversed in the molecular layer, reflecting activation of layer II EC perforant path inputs to the dendrites of granule cells; (ii) an antidromic spike in the pyramidal cell layer of CA1; (iii) a long latency negative potential in the RAD of CA1, reflecting activation of the tri-synaptic pathway. In all experiments, SUB stimulation evoked a characteristic large positive-going potential in the hilus of the DG, with a granule cell population spike also visible in most cases under train stimulation. However, as we prioritised recording in the DG region, in many cases the recording electrode was too deep to record the CA1 responses in the stratum pyramidale and RAD. A typical response profile to SUB stimulation is presented in Figure 4.6 and 4.7 (pulse 1). After a characteristic field potential laminar profile was established, an input-output current-voltage response curve was plotted by measuring the amplitude of the voltage response to single pulse stimulation (0.33 Hz) at varying current inputs (25-1000 µA). This curve was used to calculate the current input which resulted in 25%, 50% and 75% of the maximum fEPSP in the DG molecular layer or DG hilar/granule cell layer for SCHAFF and SUB stimulation, respectively. These current values determined the current to be applied during the different stimulation protocols.

We aimed to record three different components of hippocampal synaptic connectivity following SCHAFF or SUB stimulation. Firstly, we measured short term plasticity by applying paired pulses of varying inter-pulse-intervals (50% maximum current; 25, 50, 100, 200, 500 and 1000 ms; 3 s interval between pairs; 20 repeats). Secondly, we examined the effect of low frequency repetitive stimulation on re-entrance into the hippocampal circuit, by applying 5 trains of 20 constant current pulses (25% and 50% maximum current) at a frequency of 5, 10 and 20 Hz, as in Kloosterman et al. (2004) and Davis et al. (2014). These frequencies were chosen as we predicted that they would not result in any long-lasting plasticity (Kloosterman et al., 2004). Finally, we measured LTP and long-term depotentiation by recording the response to single pulse stimulation, as well as the response to paired pulses and trains, at 50% current following high frequency stimulation (HFS; 75% maximum current; 5 repeats of 20 pulses at 200 Hz; 3 s between repeats) and low frequency stimulation (50% maximum current, 900 pulses at 1 Hz), respectively.

Data was acquired using a Recorder64 system (Plexon, USA), with signals amplified at source by a 32-channel AC headstage (x20 fixed gain, Plexon, USA), and further amplified to give a total gain of x500. Local field potentials were low pass filtered at 1 kHz (1-pole Butterworth filter) and sampled at 10 kHz per channel using a 12-bit A/D converter. The LFP signals and event markers for stimulus triggers were recorded in a PLX file format and stored for offline analyses.

4.2.3.3 Data analysis

For the purpose of this thesis, we focused on the effect of low frequency train stimulation on hippocampal circuitry. Due to time constraints, only the pre-HFS data recorded in response to train stimulation at 50% current and at a frequency of 5 Hz and 10 Hz were analysed and reported.

Sample sizes and justification

Based on previous studies in our lab using in vivo electrophysiology to investigate changes in evoked CA1-DG responses (Davis et al., 2014; Sun et al., 2022), we were aiming for n = 8 rats per treatment group. The main focus of this study was to qualitatively examine gross differences across treatment groups using the current source density profiles of the evoked response. We started with n = 10 rats per group, however, four saline-treated rats were excluded during the optimisation of the subiculum stimulating electrode location (see section 4.3.1). An additional three rats were excluded from SUB stimulation data due to the use of a

double wired stimulating electrode, which would limit comparisons across treatment groups due to a larger surface area being stimulated in these rats. Therefore, we included an additional n = 5 saline treated rats to give a final sample size of n = 8 for SUB stimulation and n = 11 for SCHAFF stimulation for the saline treated rats. In the scPCP treatment group, two rats were excluded from SUB stimulation analysis: one rat was excluded as the incorrect current was used for the evoked response, and no data was obtained in another rat as stimulation was mistakenly done on the SCHAFF pathway. This gave a final sample size for the scPCP treatment group of n = 8 for SUB stimulation data and n = 10 for the SCHAFF data.

Current source density analysis

The use of a multi-electrode array allows for the determination of the anatomical location of synaptic sinks and sources produced by applied stimulation or ongoing network activity. The location of excitatory input onto a synapse can be visualised in extracellular recordings as a current sink, which is produced by the movement of positive sodium ions from the extracellular space into the neuron. A current source is also produced where positive sodium ions flow out of the neuron towards the sink. As evoked responses are recorded as voltages, which can reflect volume-conducted far-field effects, it is necessary to determine the current (ion flow) in order to visualise the laminar profile of local synaptic activity. This can be achieved using current source density (CSD) analysis (Davis et al., 2014; Freeman & Nicholson, 1975; Pettersen et al., 2006). CSD is based on the principle of Kirchoff's law, which states that the total current entering a node is equal to the total current exiting that node. At the location of an active synapse, current will leave or enter the extracellular space and, therefore, produce a non-zero CSD.

Train stimulation data were imported into the data analysis software Spike 2 (Version 8.1.4, Cambridge Electronic Design LTD, UK), to extract the voltages for pulse 1, 5, 10, 15 and 20 from the first applied train. The data were rearranged in order of descending electrode contacts and then imported into Matlab to calculate the CSD. Current source density was estimated using the Matlab toolbox (CSDplotter 0.1.1) by Pettersen et al. (2006) which had been incorporated into a single Matlab function (S. Tanni, unpublished data). The step inversed CSD method was used which, unlike traditional CSD methods, produces a continuous CSD estimation across all electrode contacts, without losing data at the outermost electrode locations. This method produces a spatially smoothed CSD by using a Gaussian spatial filter (standard deviation 0.1 mm) which is convolved with the estimated CSD from the unfiltered potentials. In addition, another advantage of this step inversed CSD method is that the

distances between electrode contacts do not need to be constant. This was particularly useful in recordings where one electrode contact was defective. The CSD plots generated arbitrary units and were scaled to the maximum/minimum values of pulse 1-20 in each rat. The 'jet' colour map was used in Matlab to display the CSD, with current sources depicted as reds and yellows, current sinks as blues, and current neutral regions as green. CSD was used to qualitatively examine any changes in hippocampal circuitry across treatment groups. We first ascertained whether re-entrance could be found, consistent with the results reported in Kloosterman et al. (2004) and Davis et al. (2014), and, secondly, whether any qualitative differences could be seen across treatment groups.

Amplitude and slope measures

The amplitude and slope of the evoked response in the DG, following train stimulation of the SUB or SCHAFF pathway, was measured using a custom designed Matlab script (version 2018a, Mathworks, USA). The fEPSP amplitude was measured as the potential difference (mV) between the baseline value immediately before the stimulus artefact and the response peak. The fEPSP slope was measured as the maximum gradient of the initial ascending component of the response (mV/ms). The largest DG response was measured: for SCHAFF stimulation, this was in the molecular layer, and for SUB stimulation this was in the hilus or granule cell layer. Data were normalised to the first pulse of the train to demonstrate any facilitation or depression. The response was measured for pulse 1-20 across each of the 5 trains. Normalised slope and amplitude values were analysed using ANOVA with pulse (1-20) and train (1-5) as within subjects factors and treatment group (saline or PCP) as a between subjects factor. In addition, the number of DG population spikes which occurred during the 5 Hz or 10 Hz train following SUB stimulation was recorded and analysed using ANOVA, with frequency (5 or 10 Hz) as a within subjects factor and treatment group as a between subjects factor.

4.2.3.4 Histology

Upon completion of the electrophysiological recordings, rats were killed by urethane overdose and cervical dislocation. The brain was removed and post-fixed in paraformaldehyde (4% in saline) for histological verification of electrode placement. Histological verification was only performed in a sub-set of rats due to time constraints. Brains were sliced in the sagittal plane using a vibratome at 100 μm thickness and sections mounted with DAPI (Mounting Medium with DAPI, ab104139, Abcam) on microscope slides (Superfrost Plus, Thermo Scientific, UK). Images were acquired on a 3D-Histech Pannoramic-250 microscope slide-scanner using a 20x/0.80 Plan Apochromat objective (Zeiss) and the DAPI and TRITC filter sets.

Snapshots of the slide-scans were taken using the Slide Viewer software (3D-Histech) (Bioimaging Centre, University of Manchester).

4.3 Results

4.3.1 Optimisation of subiculum stimulating electrode placement

The co-ordinates used for SUB electrode placement were initially determined using the rodent stereotaxic atlas (Paxinos & Watson, 2006), with the approximate co-ordinates for the dorsal SUB determined to be -6.3 AP, -2.4 ML, -2.9 DV mm, and the co-ordinates for electrode insertion at a 20˚ angle to target this region determined to be -7.2 AP, -2.4 ML, -2.9 DV mm (Fig. 4.2A). However, stimulation applied at these co-ordinates did not result in a stable, nor characteristic, response along the CA1-DG axis. In addition, although LFP traces were seen in response to stimulation, CSD analyses revealed no sources or sinks, indicating that we were not activating the synaptic sites near the recording electrode. Histological investigation of the electrode locations revealed correct placement of the SCHAFF stimulating electrode and of the recording electrode, but incorrect placement of the SUB electrode, with co-ordinates too posterior and the SUB stimulating electrode instead located in the retrosplenial granular cortex (Fig. 4.2C). A recent study also reported that co-ordinates determined using the atlas by Paxinos and Watson (2013) resulted in more posterior locations in male Lister Hooded rats, whereas target regions were consistent with co-ordinates determined using an in vivo MR Atlas of the male Lister Hooded rat brain (McGarrity et al., 2017; Prior et al., 2021). We, therefore, used the MR Atlas (Prior et al., 2021) to determine new co-ordinates for electrode insertion. In ITK-snap (Yushkevich et al., 2016), using the MR atlas delineations and with reference to landmarks in the Paxinos & Watson (2006) atlas, the new co-ordinates for the dorsal SUB were determined to be -4.95 AP, -2.4 ML, -2.9 DV mm. Using the image annotation mode, the co-ordinates for insertion at an angle of 20˚ to target this region were determined to be -6.0 AP, -2.4 ML, -2.6 DV mm (Fig. 4.2B). These new co-ordinates produced a stable LFP response along the CA1-DG axis, consistent with Kloosterman et al. (2004). In addition, histological investigation in two rats revealed electrode placement located in the SUB region (one shown in Fig. 4.2D), and also correct SCHAFF (Fig. 4.2G) and recording electrode placement (Fig. 4.2E, F). Histological confirmation of electrode placement in all rats is to be completed, however, the LFP response profiles recorded in situ suggested perforant path and SCHAFF activation and, therefore, adequate electrode placement.

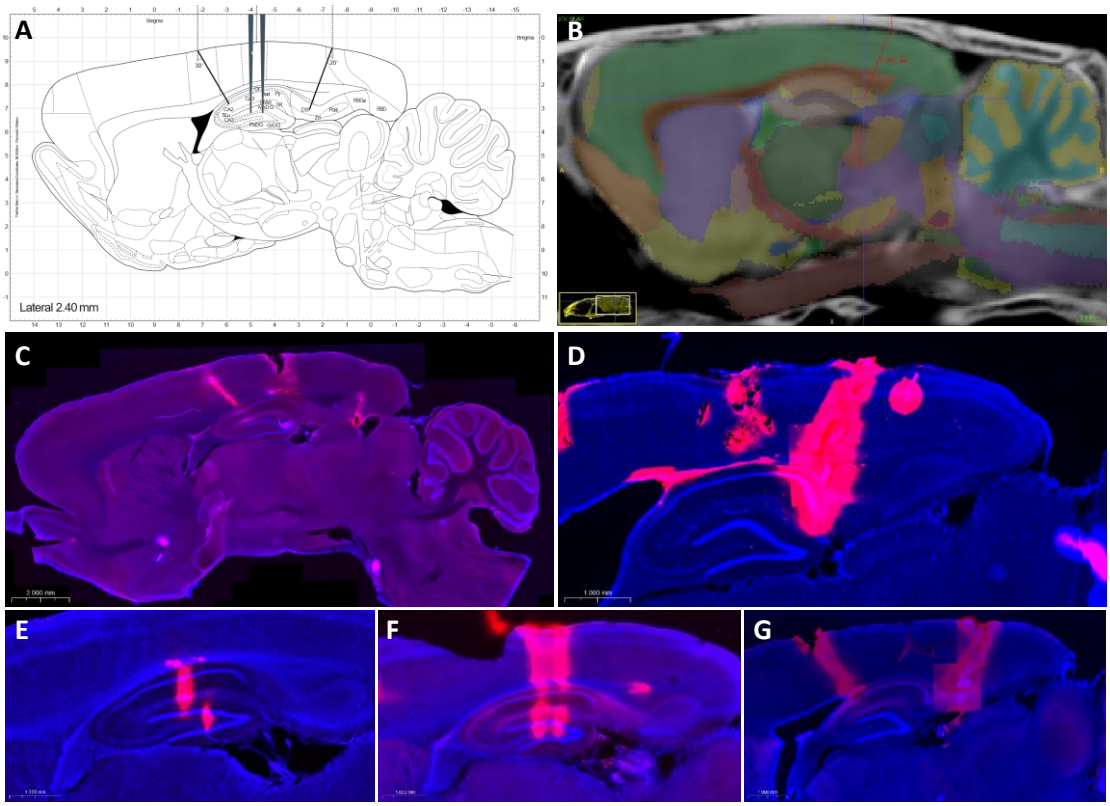

Fig. 4.2. ***Histological determination and optimisation of electrode placement***. **A.** Electrode co-ordinates determined using the atlas by Paxinos & Watson (2006) correlated to a more posterior location in the female Lister Hooded rat, with the stimulating electrode placed outside the subiculum, as shown in **C. B.** New subiculum stimulating coordinates were determined using the in vivo MR atlas of the Lister hooded rat brain (Prior et al., 2021). The cross hairs indicate the location of the dorsal subiculum target region, and the red line indicates the desired electrode placement. **C-G.** DAPI stained sagittal sections with electrode track indicated by a pink fluorescence trace. **D.** Subiculum co-ordinates determined using the MR atlas resulted in correct placement in the target region. **E. F.** Histological verification of recording electrode placement along CA1-DG axis and **G.** CA3 Schaffer collateral stimulating electrode placement.

4.3.2 Responses in CA1 and DG evoked by SCHAFF stimulation

4.3.2.1 CSD and LFP profile

To investigate neuronal reverberation within the hippocampal circuit, we applied low frequency train stimulation to the SCHAFF pathway, in the form of 5 trains of 20 constant current pulses at a frequency of 5, 10 and 20 Hz. CSD was estimated for the first train on pulses 1, 5, 10, 15 and 20 for the 5 Hz and 10 Hz stimulation frequency. The CSD profile of pulse 1 evoked by SCHAFF stimulation was consistent across all rats, with a current sink seen in the CA1 region and a current source in the DG (Fig. 4.3, pulse 1). The voltage plot at pulse 1 also demonstrated a negative potential in the CA1 region, which reversed to a positive going wave in the DG (Fig. 4.4, pulse 1). This is consistent with previous recordings along the CA1-DG axis

following SCHAFF stimulation in our lab (Sun et al., 2022, 2023) and others (Gruart et al., 2015; Leung et al., 2008). The CA1 current sink reflects the excitatory input onto the RAD from the activated CA3 SCHAFF pathway (Ledda & Paratcha, 2017), whereas the current source in DG likely reflects a back projection of the pyramidal cells in CA3 to DG, which has been reported at the hilus, granule cell layer and molecular layer of the DG (Myers & Scharfman, 2011; Scharfman, 2007; van Strien et al., 2009).

Following SCHAFF train stimulation, only one scPCP treated rat (n = 10) and two saline treated rats (n = 11) showed evidence of hippocampal re-entrance. The CSD in the saline treated rat and scPCP treated rat revealed a clear long latency (> 20 ms) response in the DG following train stimulation at a frequency of 10 Hz (Fig. 4.3B and E, respectively), but not 5 Hz (Fig. 4.3A and D, respectively). This long-latency DG response was evident in both rats by pulse 15. At pulse 15 the current sources and sinks can be viewed as follows: (1) Early DG source and (2) CA1 sink (ca. 10 ms) generated by SCHAFF activation, proceeded by a (3) long latency DG granule cell layer/hilus source and (4) concomitant DG molecular layer current sink. In the scPCP treated rat, a long latency current sink can also be seen at the DG inferior blade molecular layer, below the hilus region (Fig. 4.3E, pulse 15 and 20). This re-entrant response was also seen in both rats at pulse 20. This response likely reflects activation of the perforant path, as the response was very similar to the CSD profile observed following SUB stimulation (Fig. 4.3C and F). Re-entrance can also be visualised in the LFP profiles of these rats (Fig. 4.4), where a long latency negative going potential and a positive going potential can be seen in the molecular layer and hilus of DG, respectively, from pulse 15 at 10 Hz. In the two rats, for which data are shown in Figures 4.3 and 4.4, no re-entrance was found following train stimulation at 5 Hz. However, one saline treated rat (data not shown) showed a similar DG long latency response (> 20 ms) following both 5 Hz and 10 Hz stimulation, which was evident from pulse 5 at both frequencies. All other rats showed consistent LFP and CSD profiles across pulses 1-20.

Overall, re-entrance was only seen in a small subset of rats, with 2 out of 11 saline rats and 1 out of 10 scPCP treated rats showing evidence of re-entrance into the hippocampal circuit in the form of a long-latency DG response. No re-entrance was seen in the CA1 region following SCHAFF stimulation at 5 Hz or 10 Hz.

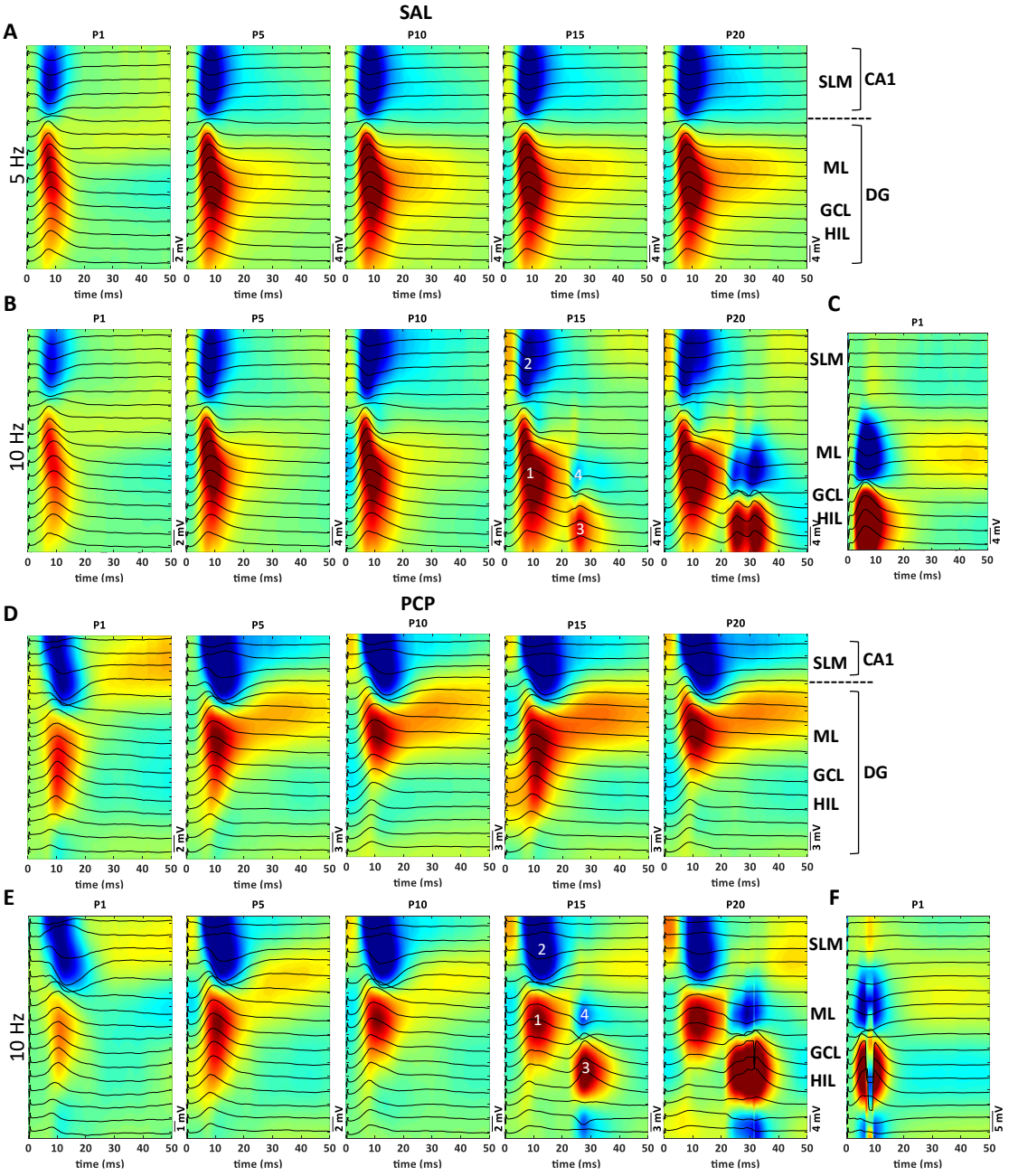

Fig. 4.3. ***Current source density (CSD) of the evoked response along the CA1-DG axis following Schaffer collateral (SCHAFF) train stimulation revealed evidence of long latency DG re-entrance in a subset of rats.*** CSD estimation of the response to pulse (P) 1, 5, 10, 15 and 20 of SCHAFF train stimulation (left to right) is presented with associated voltage traces superimposed. The arbitrary scale indicates current sources (reds and yellows), sinks (blues) and neutral regions (green). Approximate cell layers are labelled as follows; stratum lacunosum moleculare (SLM); DG molecular layer (ML); DG granule cell layer (GCL); and hilus (HIL). **A.** CSD estimation in a saline (SAL) treated rat following train stimulation at 5 Hz and **B**. 10 Hz. **D** CSD estimation in a scPCP treated rat following train stimulation at 5 Hz and **E.** 10 Hz. At 10 Hz stimulation, re-entrance can be seen in both rats by pulse 15. The numbers indicate the following synaptic events: 1. DG ML source; 2. CA1 sink due to SCHAFF activation; 3. long latency current source in DG GCL/HIL; and 4. long latency current sink in DG ML. This long-latency DG response was similar to the CSD profile produced by 10 Hz subiculum stimulation in the same **C.** saline- or **F.** scPCP-treated rat. Note the presence of a DG population spike in **F.** and at pulse 20 in panel **E.** in the scPCP treated rat.

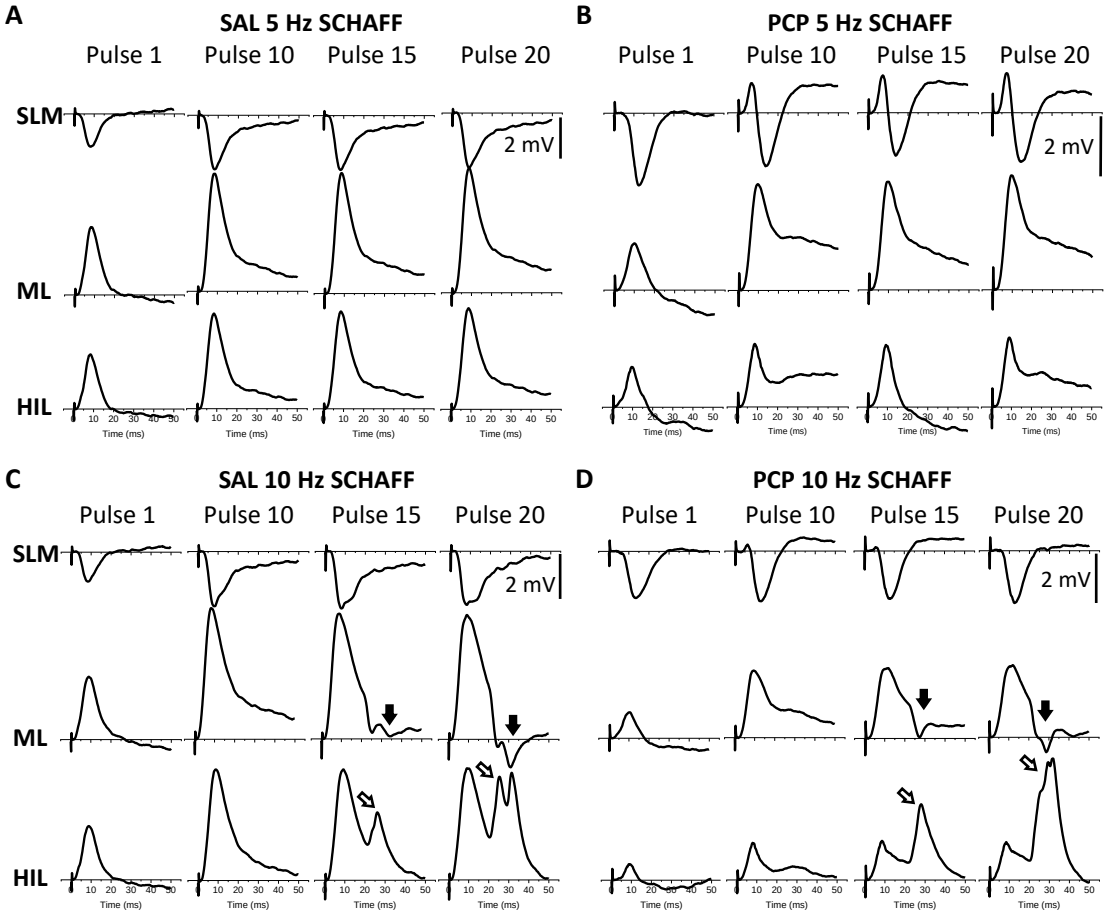

Fig. 4.4. ***Voltage plots of the evoked response in the stratum lacunosum moleculare (SLM), dentate gyrus molecular layer (ML) and dentate gyrus hilus (HIL) following Schaffer collateral (SCHAFF) train stimulation.*** Voltage plots correspond to the CSD profiles in Fig. 4.3. No re-entrance was seen following 5 Hz train stimulation in either the **A.** saline (SAL) or **B.** scPCP treated rat. At 10 Hz, a long latency DG response could be seen in the **C.** saline and **D.** scPCP treated rat by pulse 15. The black solid arrow and open arrow indicate the long latency negative potential in the ML and positive potential in the hilus, respectively.

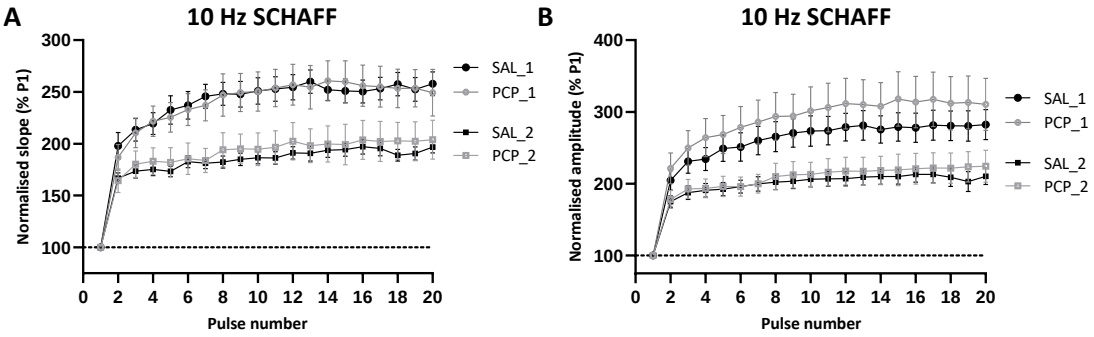

Fig. 4.5. ***Normalised* A. *slope and* B. *amplitude of the evoked response in the dentate gyrus molecular layer following Schaffer collateral (SCHAFF) train stimulation at 10 Hz was similar across treatment groups.*** Data is presented as mean ± SEM for each of the 20 pulses applied during train stimulation in the saline (SAL; n = 11) and scPCP (n = 10) treated rats for train 1 (SAL_1; PCP_1) and train 2 (SAL_2; PCP_2). Both slope and amplitude measures were facilitated with increasing pulse, however, there was a decrease in pulse facilitation at trains 2-5, due to a sustained increase in the response to pulse 1 compared to the first train.

4.3.2.2 Amplitude and slope analysis

To compare excitability within the hippocampal circuit between treatment groups and across trains and pulses, the amplitude and slope of the evoked DG molecular layer response, following SCHAFF train stimulation, was measured for pulse 1-20 for each of the 5 trains, and normalised to the first pulse in each train. Due to time constraints, we focused on train stimulation at 10 Hz. For clarity, only the first two trains are shown in Fig. 4.5, although all 5 trains were included in the analysis. In both treatment groups, the amplitude and slope of the DG response was similarly facilitated with increasing pulse number. ANOVA revealed a main effect of pulse ($F_{(19,\ 361)} > 91.9$, $p < 0.001$), with no main effect or interaction involving treatment group ($F < 1$). There was a significant main effect of train for both the normalised slope and amplitude ($F_{(4,\ 76)} > 23.7$, $p < 0.001$), and a significant interaction between pulse and train ($F_{(76,\ 1444)} > 11.3$, $p < 0.001$). This is likely due to a ceiling effect, whereby there was decreased facilitation following pulse 1 for trains 2-5, due to a sustained facilitation of pulse 1 in trains 2-5 compared to pulse 1 in the first train. Overall, these findings did not indicate any differences in excitability between saline and scPCP treated rats.

4.3.3 Responses in CA1 and DG evoked by SUB stimulation

4.3.3.1 CSD and LFP profile

We also investigated the hippocampal response along the CA1-DG axis in response to perforant path activation, by applying low frequency train stimulation in the SUB. As for SCHAFF train stimulation, CSD was estimated for the first train on pulses 1, 5, 10, 15 and 20 for the 5 Hz and 10 Hz stimulation frequency. The evoked response to pulse 1 in the DG was similar across all rats, with a current sink in the DG molecular layer and a current source in the granule cell layer/hilus, consistent with layer II EC perforant path excitatory inputs to the dendrites of granule cells (van Strien et al., 2009). In some rats we observed an early latency current sink in CA1, possibly due to antidromic activation of the CA1-SUB pathway, or due to activation of the layer III EC-CA1 temporoammonic pathway, which also traverses the SUB (Kloosterman et al., 2003, 2004). However, this was only seen in 2 out of 8 scPCP treated rats and in 4 out of 8 saline treated rats. In addition, in most rats, we observed a CA1 source at pulse 1 which occurred after the peak of the initial perforant path activated DG response, consistent with Davis et al. (2014).

Following SUB train stimulation, 4 out of 8 scPCP treated rats showed re-entrance (2 rats at both 5 Hz and 10 Hz and 2 rats only at 10 Hz) and 2 out of 8 saline treated rats (at both 5 and 10 Hz) showed evidence of hippocampal re-entrance. Figure 4.6 illustrates the CSD of a saline and scPCP treated rat where a long latency (> 20 ms) response can be seen in the DG and CA1 region following both 5 Hz and 10 Hz train stimulation. This response reverberation can be seen in the saline treated rat by pulse 5 at both 5 Hz and 10 Hz stimulation. In the scPCP treated, the long latency response can be seen by pulse 10 at 5 Hz and by pulse 5 at 10 Hz train stimulation. The characteristic perforant path induced response and subsequent long latency re-entrance can be viewed as follows: (1) DG hilus/granule cell layer current source and (2) DG molecular layer sink (ca. 7 ms) generated by stimulation of the perforant path; (3) early CA1 sink possibly due to antidromic activation of the CA1-SUB pathway; (4) CA1 source; (5) long latency current source at DG hilus (> 20 ms); (6) concomitant long latency current sink at DG molecular layer; and (7) long latency CA1 source. In the scPCP treated rat, a rapid current sink can be seen in the SLM region (Fig. 4.6C and D), which may be due to activation of the temporoammonic pathway which synapses in the SLM (van Strien et al., 2009). Re-entrance can also be visualised in the LFP profiles of these rats (Fig. 4.7), where a long latency negative going potential and a positive going potential can be seen in the molecular layer and hilus of DG, respectively, from pulse 5 at both 5 Hz and 10 Hz, as well as a positive going potential in CA1. All other rats showed consistent LFP and CSD profiles across pulses 1-20.

Subiculum stimulation also often resulted in DG population spikes in the granule cell layer/hilus, which can be seen for the scPCP treated rat in Fig. 4.6 and 4.7D (pulse 1). A DG population spike can also be seen in the long-latency re-entrant response following SCHAFF stimulation in the scPCP treated rat presented in Fig. 4.3E (pulse 20) and F. Population spikes in the DG following either 5 Hz or 10 Hz SUB train stimulation was observed in 5/8 scPCP treated rats and 4/8 saline treated rats. However, scPCP rats tended to show DG population spikes on a greater number of occasions during the trains (Fig. 4.8), indicating increased excitability of the hippocampal circuit. However, ANOVA of the number of population spikes revealed no significant main effect of treatment group ($F_{(1,7)} = 1.26$, $p = 0.299$), nor a main effect or interaction involving frequency ($F_{(1,7)} < 1$), although this analysis is limited by the small sample size.

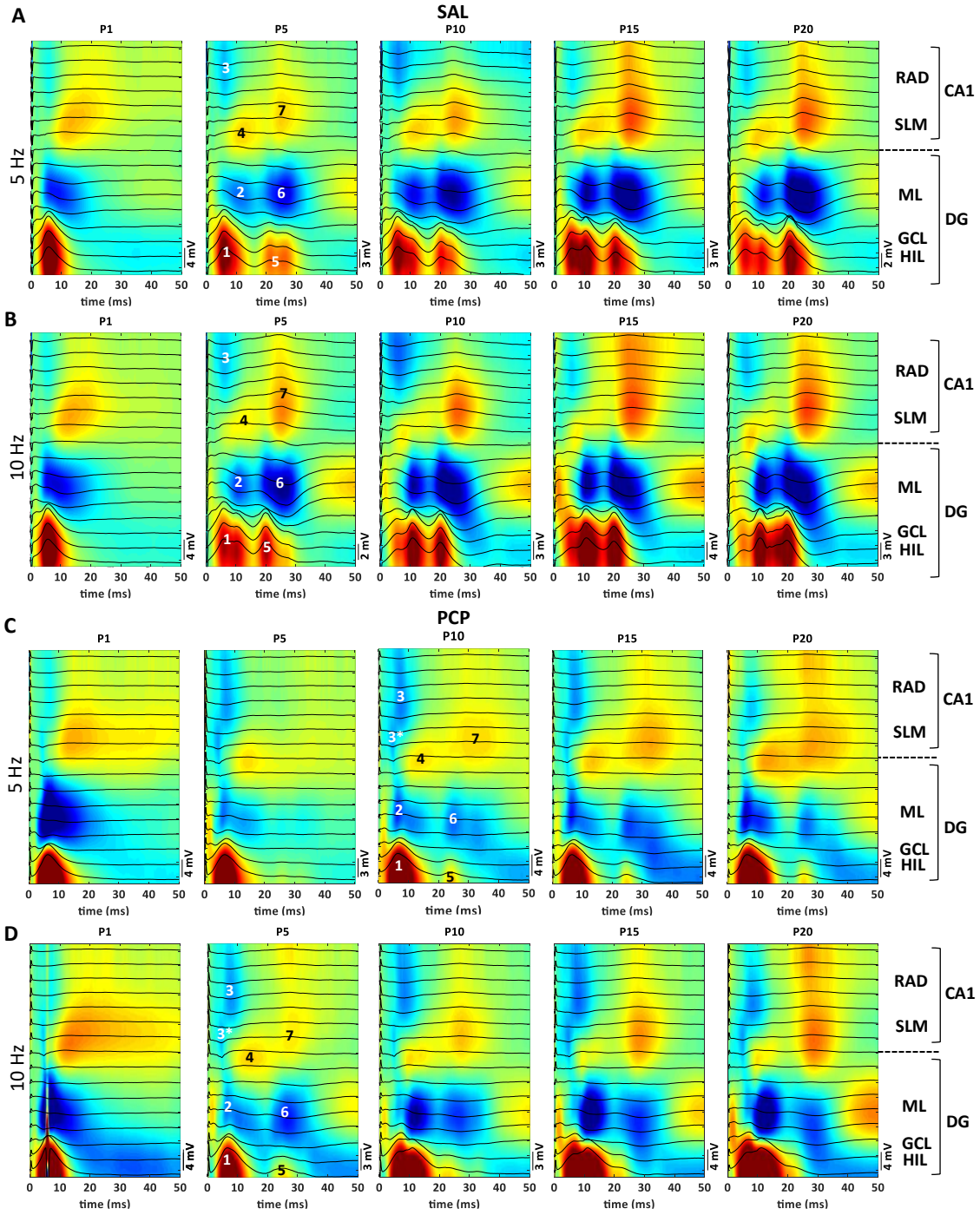

Fig. 4.6. ***Current source density (CSD) of the evoked response along the CA1-DG axis following subiculum (SUB) train stimulation revealed evidence of long latency DG re-entrance in a subset of rats.*** CSD estimation of the response to pulse (P) 1, 5, 10, 15 and 20 of SUB train stimulation (left to right) is presented with associated voltage traces superimposed. The arbitrary scale indicates current sources (reds and yellows), sinks (blues) and neutral regions (green). Approximate cell layers are labelled as follows; stratum radiatum (RAD); stratum lacunosum moleculare (SLM); DG molecular layer (ML); DG granule cell layer (GCL); and hilus (HIL). **A.** CSD estimation of a saline (SAL) treated rat following train stimulation at 5 Hz and **B**. 10 Hz. **C.** CSD estimation of a scPCP treated rat following train stimulation at 5 Hz and **E.** 10 Hz. Re-entrance can be seen in both rats by pulse 10. The numbers indicate the following synaptic events: (1) DG HIL/GCL current source and (2) DG ML sink generated perforant path stimulation; (3) early CA1 sink; (4) CA1 source; (5) long latency HIL/GCL source; (6) concomitant ML long latency sink; and (7) long latency CA1 source. In the scPCP treated rat, a rapid early SLM current sink can also be seen (**C** and **D;** 3*), which may be due to activation of the temporoammonic pathway.

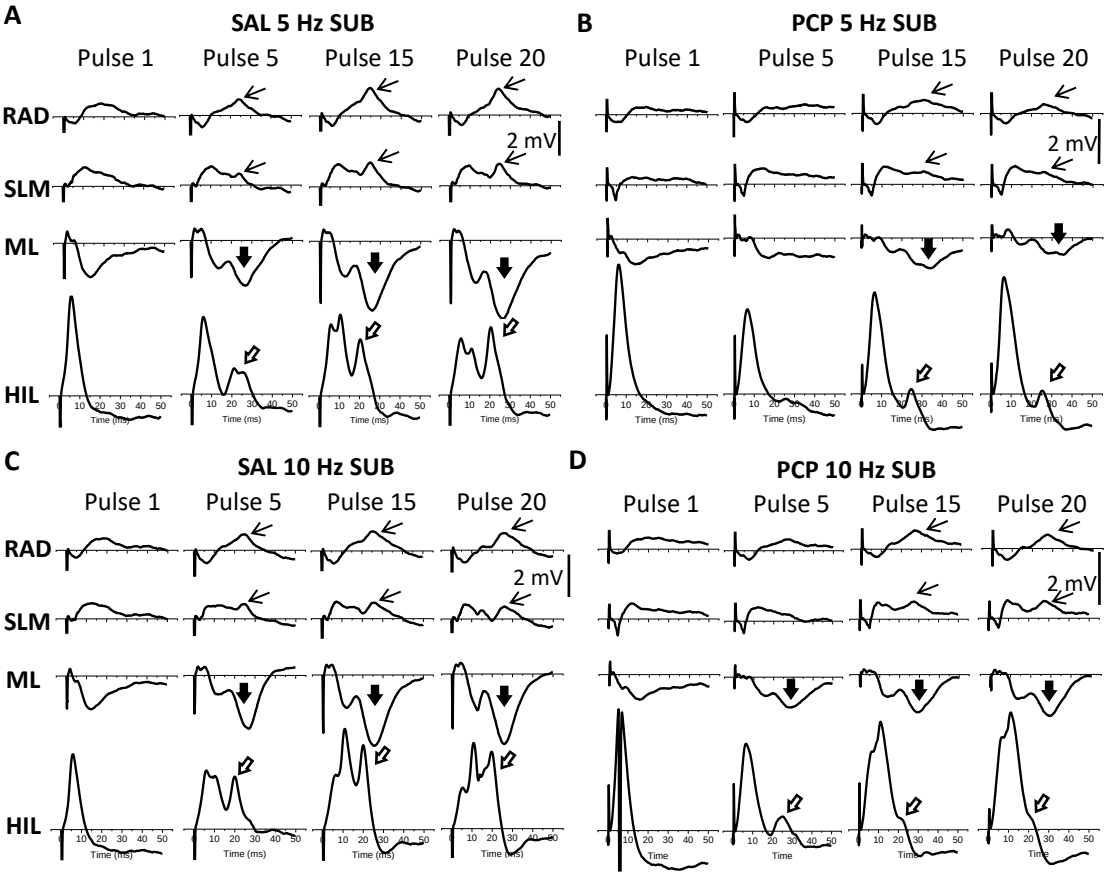

Fig. 4.7. ***Voltage plots of the evoked response in the stratum radiatum (RAD), stratum lacunosum moleculare (SLM), dentate gyrus molecular layer (ML) and dentate gyrus hilus (HIL) following subiculum (SUB) train stimulation.*** Voltage plots correspond to the CSD profiles in Fig. 4.6. Re-entrance can be seen in the saline (SAL) treated rat by pulse 5 at **A.** 5 Hz and **C.** 10 Hz; and in the scPCP treated rat by pulse 15 at **B.** 5 Hz and by pulse 5 at **D.** 10 Hz train stimulation. The thin black arrow indicates the long-latency CA1 positive going potential; the black solid arrow indicates the long latency negative potential in the ML; and the open arrow indicates positive potential in the HIL. Note the DG population spike in **D.** at pulse 1 in response to 10 Hz SUB stimulation in the scPCP treated rat.

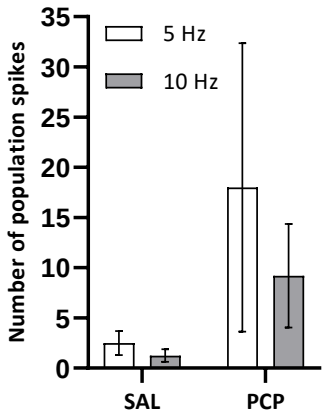

Fig. 4.8. ***Number of population spikes recorded in the dentate gyrus following subiculum (SUB) train stimulation at 5 Hz and 10 Hz appeared to be increased in scPCP treated rats.*** Population spikes were counted across the 5 trains of 20 constant current pulses (100 pulses in total). Data is presented as mean ± SEM for the saline (SAL; n = 4) and scPCP (n = 5) treated rats, which showed at least one dentate gyrus population spike during either the 5 Hz or 10 Hz SUB stimulation train.

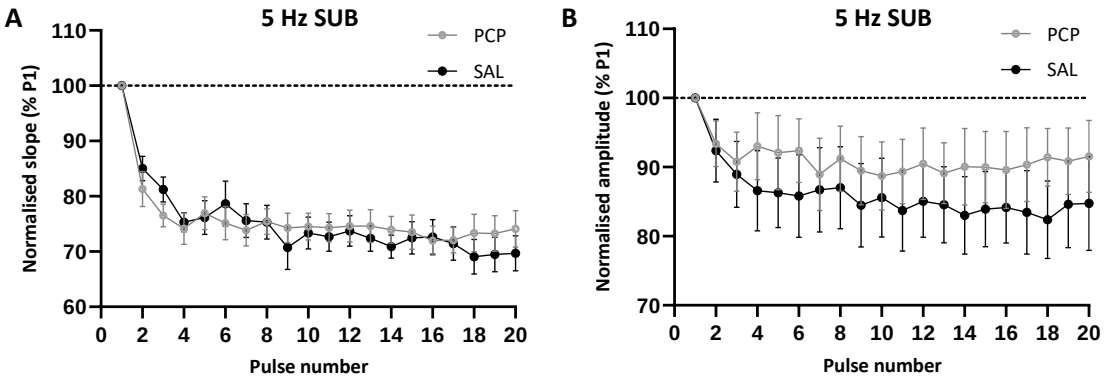

Fig. 4.9. ***Normalised*** **A. s*lope and*** **B. a*mplitude of the evoked response in the dentate gyrus granule cell layer/hilus following subiculum (SUB) train stimulation at 5 Hz was similar across treatment groups.*** Data is presented as mean ± SEM for each of the 20 pulses applied during train stimulation in the saline (SAL; n = 8) and scPCP (n = 8) treated rats for all 5 trains.

4.3.3.2 Amplitude and slope analysis

The amplitude and slope of the DG response in the hilus or granule cell layer was measured for pulses 1-20 over the 5 trains following SUB train stimulation at 5 Hz. The response was normalised to the first pulse of each train. In both treatment groups, the amplitude and slope measures were slightly depressed with increasing pulse number, consistent with Davis et al. (2014). ANOVA revealed a main effect of pulse ($F_{(19, 266)} > 5.38$, $p < 0.001$), and no main effect or interaction involving treatment group ($F < 1.44$, $p > 0.13$). There was no significant main effect or interaction involving trains ($F < 1.28$, $p > 0.061$) (Fig. 4.9 shows the normalised slope and amplitude data averaged across the 5 trains).

4.3.4 NOR

NOR was investigated in the initial cohort of 20 rats (n = 10 per group), at 1 week post scPCP/saline treatment. Sub-chronic PCP treated rats showed impaired NOR (Fig. 4.10). During the retention phase, ANOVA of object exploration times demonstrated a significant interaction between treatment group and object ($F_{(1,18)} = 5.16$, $p = 0.036$), alongside a main effect of object ($F_{(1,18)} = 27.8$, $p < 0.001$), and a strong trend for a main effect of treatment group ($F_{(1,18)} = 4.24$, $p = 0.054$). The latter was due to a decrease in total object exploration in the scPCP treated rats. This was also observed in the acquisition phase, where ANOVA revealed no significant main effect of object, or a significant interaction between object and treatment group ($F < 1$), but did reveal a main effect of treatment group ($F_{(1,18)} = 15.5$, $p < 0.001$) reflecting decreased total exploration time in the scPCP treated rats. In addition, although a significant interaction between object and treatment group during the retention phase suggests impaired NOR, planned pairwise t-tests demonstrated significant NOR in both

treatment groups (t_9 > 3.37, p < 0.008). Moreover, ANOVA of DI revealed an effect of treatment group at trend level ($F_{(1,18)}$ = 3.21, p = 0.09), and planned one-sample t-tests demonstrated novel object preference significantly different to chance in both treatment groups (t_9 > 3.50, p < 0.007).

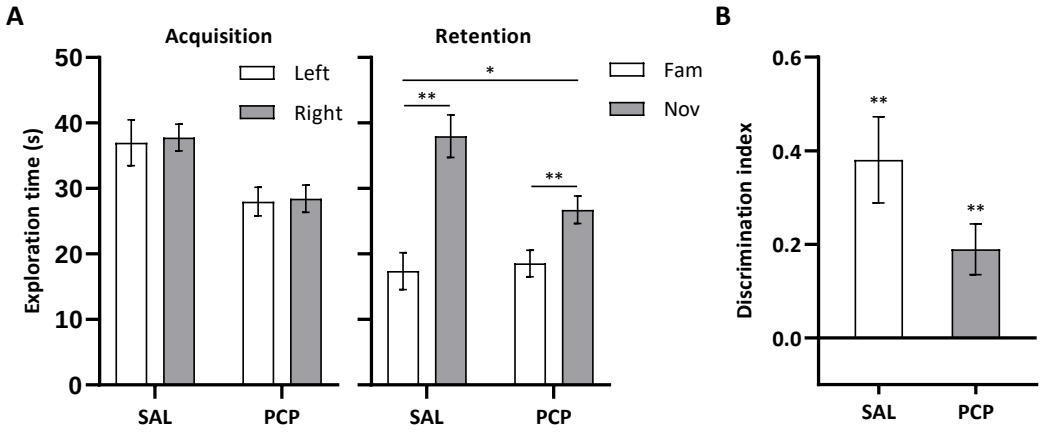

Fig. 4.10. ***NOR was impaired in the scPCP group.*** Data is presented as mean ± SEM, for the saline (SAL) and scPCP treated rats, n = 10. **A.** Exploration times (s) of the identical objects located on the left and right of the NOR arena during the 3 min acquisition phase; and of the familiar (Fam) and novel (Nov) object during the 3 min retention phase, following a 1 min retention delay. **B.** Discrimination index (DI) [(time spent exploring the novel object - time spent exploring the familiar object/total time spent exploring both objects] was reduced in the scPCP treated rats, but only at trend level. Asterisks indicate significant novel object preference (paired sample or one-sample t-tests), or significant differences between treatment groups (*p < 0.05, **p < 0.01).

4.4 Discussion

Qualitative examination of voltage and CSD profiles demonstrated that both scPCP and saline treated rats exhibited reverberatory responses in the hippocampal formation following low frequency train stimulation targeted at the SCHAFF or SUB, although this was only seen in a subset of rats. In addition, CSD analysis indicated a laminar profile of synaptic currents that was similar across treatment groups, for both the initial evoked response and for the longer latency re-entrance, indicating intact fibre pathways in scPCP treated rats. In addition, the normalised slope and amplitude of the DG response elicited by SCHAFF or SUB stimulation was similar across treatment groups. However, DG population spiking activity appeared to be increased in scPCP treated rats, which may indicate increased hippocampal excitability.

4.4.1 Re-entrance following SCHAFF stimulation was observed in both scPCP and saline treated rats

Schaffer collateral stimulation in the CA3 region of scPCP and saline treated rats evoked a characteristic laminar profile of CA1 sinks and DG current sources (Gruart et al., 2015; Leung et al., 2008; Sun et al., 2022, 2023). The presence of a CA1 sink is consistent with CA3 Schaffer collaterals providing excitatory input onto the apical dendrites of CA1 pyramidal neurons in the RAD (van Strien et al., 2009). This connection represents the third excitatory synapse according to the traditional model of the hippocampal trisynaptic circuit (Amaral & Witter, 1989; Andersen et al., 1971). However, in addition to this unidirectional excitatory trisynaptic pathway, the hippocampal formation has been revealed to include complex associational loops, circuits mediating feedforward and/or feedback inhibition and disinhibition processes, as well as multiple back-projections (Stepan et al., 2015; van Strien et al., 2009). The DG current source observed here following SCHAFF stimulation likely represents one of these back-projections, e.g., the axon collaterals of CA3 pyramidal cells which innervate mossy cells, hilar interneurons, granule cells, and the DG molecular layer (Myers & Scharfman, 2011; Penttonen et al., 1997; Scharfman, 2007). In most rats, the CSD profile evoked at pulse 1 remained consistent across the 20 pulses delivered during SCHAFF train stimulation. However, in a small subset of rats, a long-latency DG response was observed from pulse 5. This response occurred after the initial SCHAFF evoked response, at a latency of 20-30 ms, and consisted of a DG molecular layer sink and a DG granule cell/hilus source. One benefit of the current study was the use of both a SCHAFF and SUB electrode in the same rat, which allowed for a direct comparison of the re-entrant response to the response elicited by perforant path activation. Comparing the SCHAFF re-entrant response to the SUB early DG response, strongly suggests

that the late DG response is due to perforant path input to the DG from EC afferents. The latency and synaptic profile of this re-entrant DG response is consistent with other studies reporting re-entrance following SCHAFF stimulation (Canning et al., 2000; Deadwyler et al., 1975; Kloosterman et al., 2004; Wu et al., 1998). These studies also concluded that the late DG response reflects a reverberation in the hippocampus via the perforant path and found that this response was dependent on an intact EC (Deadwyler et al., 1975; Kloosterman et al., 2004; Wu et al., 1998).

At 10 Hz SCHAFF train stimulation, this re-entrant response was seen in one out of ten scPCP treated rats, and in two out of eleven saline treated rats. In addition, one saline treated rat did show a small long latency DG response following train stimulation at 5 Hz, which was evident from pulse 5. Given that we only found evidence of re-entrance in a few rats, and had a slightly larger sample size of saline treated rats, it is difficult to draw conclusions from between treatment group comparisons. However, one could tentatively infer that the SCHAFF pathway is less excitable in the scPCP treated rats, given that we saw one fewer rat exhibiting re-entrance at 10 Hz and no scPCP treated rats exhibiting re-entrance at 5 Hz. The laminar profile, however, of both the early and late responses appeared consistent across treatment groups, suggesting that similar synaptic connections are present. In the rats that exhibited a long latency DG response, presumably due to perforant path activation, we may have expected to also see a response at CA1 (Leung et al., 1995), but this was not observed. However, a CA1 response was often also not observed following SUB stimulation in the current study, as discussed in more detail below. Nevertheless, our results are consistent with Kloosterman et al. (2004), who report only one example (out of n = 7 rats) of a small long-latency CA1 response following SCHAFF activation, which may suggest that the EC layer II-DG pathway is the main re-entrant pathway in the hippocampal formation, or is more readily activated than the EC layer III-CA1 connection.

In addition to investigating the synaptic currents evoked by SCHAFF stimulation, we also measured the slope and amplitude of the DG response to each pulse of the 10 Hz SCHAFF train. This allowed us to investigate any differences in the facilitation of the response. In both treatment groups we a saw a similar level of facilitation with increasing pulse number. This facilitation is consistent with potentiation induced by a train of repetitive stimuli, whereby a short-term increase in synaptic efficiency is elicited due to a build-up of residual intracellular calcium in the pre-synaptic terminal from a previous pulse (Zucker & Regehr, 2002). Thus, the short-term plasticity mechanisms mediating the SCHAFF response to low frequency train stimulation were not affected by scPCP treatment.

4.4.2 Re-entrance following SUB stimulation was observed in both scPCP and saline treated rats

We also examined the response to train stimulation in the SUB, which we expected would result in activation of the traversing fibres of the perforant path. CSD estimations revealed an initial DG response, which was similar across treatment groups, consisting of a current sink in the molecular layer and a current source in the granule cell layer/hilus. This DG response likely reflects perforant path inputs from layer II of the EC, which synapse on the dendrites of granule cells, and is consistent with the DG response reported in previous studies following perforant path activation (Buzsáki & Czeh, 1981; Deadwyler et al., 1975; Douglas & Goddard, 1975; Gruart et al., 2015; Kloosterman et al., 2003, 2004; Leung et al., 1995; McNaughton & Barnes, 1977; Payne et al., 1982; Wu et al., 1998). The perforant path, however, is not the only pathway which may be activated by SUB stimulation. The temporoammonic pathway, from layer III neurons in the EC, also traverses the SUB, forming excitatory contacts with the distal dendrites of CA1 pyramidal neurons in the SLM (Witter, 1993). In addition, a subicular back-projection to CA1 has recently been confirmed, which innervates all layers of CA1 (Sosa et al., 2018; Sun et al., 2014). Therefore, SUB stimulation may also be expected to result in a CA1 response. Finally, the SUB-EC efferent pathway may also be stimulated (Kloosterman et al., 2003). In some rats we found an early latency current sink in the CA1 region, consistent with a CA1 response following SUB stimulation, but in most rats, this was not observed. Compared with the perforant path activated DG response, the CA1 response is reported to be much smaller and to require a higher stimulus intensity (Aksoy-Aksel & Manahan-Vaughan, 2013; Canning et al., 2000; Leung et al., 1995). This may explain why, in most cases, we did not observe an early CA1 sink. It may also be that electrode placement was sub-optimal, with histological verification of stimulating electrode placement still to be completed in all rats. Nevertheless, Kloosterman et al. (2004) also reported that they did not find a mono-synaptically evoked CA1 SLM response after SUB stimulation, and the emergence of a CA1 sink was also reported to be variable following SUB train stimulation in mice (Davis et al., 2014).

Subiculum stimulation has also been reported to produce a longer latency CA1 SLM sink, reflecting activation of the trisynaptic pathway (Kloosterman et al., 2003, 2004), but this was not observed in any rats in the present study. We did, however, often see a small CA1 current source, which was present in most rats from pulse 1, and appeared to peak after the initial DG response. CA1 current sources have been reported following perforant path activation but have been suggested to represent a passive source of a CA1 SLM sink-source pair (Canning et al., 2000; Davis et al., 2014; Kloosterman et al., 2004; Leung et al., 1995). It is possible that the

large DG molecular layer response may be masking a CA1 SLM sink associated with the CA1 source observed. Alternatively, the CA1 source may be due to volume conduction from the DG response. However, the CA1 source appears to peak after the initial DG response, suggesting that they are separate synaptic events. Nevertheless, the CSD profile observed in rats at pulse 1 in response to SUB train stimulation was consistent across both treatment groups, suggesting intact fibre pathways in scPCP treated rats.

As with SCHAFF stimulation, re-entrance following SUB low frequency train stimulation was only found in a subset of rats, although in a larger number of rats. Half of the scPCP treated rats (n = 8) and two saline treated rats (n = 8) showed a long latency response consistent with a re-entrant response into the hippocampal formation. This was most apparent as a DG molecular layer sink, suggesting additional activation of the perforant path. This long latency DG response is consistent with the DG re-entrant response reported in Kloosterman et al. (2004) and appeared to be a repeat of the initial early response, rather than a response elicited via the trisynaptic pathway from CA3 neurons. It is, therefore, likely due to be a result of EC activation, either via: stimulation of the SUB-EC efferent pathway; antidromic activation of the perforant path; and/or, in some rats, stimulation of the subicular back-projection to CA1 or stimulation of the temporoammonic pathway which traverses the SUB, followed by activation of the CA1-EC efferent. Re-entrance back into the hippocampal formation would then be facilitated by the deep to superficial connections in the EC, resulting in a secondary activation of the perforant path (Dolorfo & Amaral, 1998b; Kloosterman et al., 2003, 2004). This deep to superficial connection between the layers of the EC has been more recently confirmed using transsynaptic retrograde tracing, which revealed a tri-synaptic pathway mediating hippocampal re-entrance (Ohara et al., 2018). As previously outlined, it is difficult to make comparisons between treatment groups, however, it appeared that the re-entrant response to SUB stimulation was more readily seen in the scPCP treated rats, as half of these rats exhibited some form of re-entrance compared with a quarter of the saline treated rats. This may suggest that the re-entrance pathway mediated via the SUB is more excitable in the scPCP treated rats.

The slope and amplitude of the DG response to each pulse of the 5 Hz SUB train was also investigated, with both treatment groups demonstrating depression of the response with increasing pulse number, presumably due to increased inhibitory feedback, in line with previous studies (Alger & Teyler, 1976; Davis et al., 2014). This suggests that short term plasticity mechanisms mediating the SUB-DG response are unaffected by scPCP treatment.

One other marker of neural activity we examined was the frequency of population spikes elicited in the DG during SUB train stimulation. Stimulation of the perforant path can activate a population of DG granule cells synchronously and the simultaneous firing of these cells may be recorded extracellularly as a population spike, which consists of a negative-going spike transient superimposed on the DG positive wave (Kloosterman et al., 2003). Granule cells of the DG typically have a low spontaneous firing rate due to high levels of GABAergic inhibitory control from local inhibitory interneurons; GABAergic inhibition appears to regulate the CA3-DG back-projection, and the perforant path input (Penttonen et al., 1997; Scharfman, 2007; Sosa et al., 2018). Such inhibitory influence reduces the efficacy of these major glutamatergic inputs, resulting in relatively quiescent granule cell activity (Scharfman, 2007; Sosa et al., 2018). When this inhibitory cell activity is minimal, perforant path stimulation will evoke a large granule cell population spike. In contrast, if inhibitory circuits are activated e.g., experimentally by stimulating commissural CA3-DG feedforward inhibition, the perforant path evoked population spike will be supressed (Buzsáki, 1984; Buzsáki & Czeh, 1981; Sloviter, 1991). Thus, an increase in DG population spiking may reflect a decrease in GABAergic inhibitory control. Indeed, application of the GABA-A receptor antagonist bicuculline was found to block the commissural mediated suppression of DG perforant path-induced population spikes (Buzsáki, 1984; Douglas et al., 1983). In line with Davis et al. (2014), population spiking following SUB train stimulation was observed in around half of all rats (5/8 scPCP treated rats and 4/8 saline treated rats). In addition, of the rats which exhibited population spiking, two saline and two scPCP treated rats also exhibited evidence of re-entrance, suggesting a general increase in excitability in these rats. Although the number of rats demonstrating at least one population spike following SUB trains at 5 Hz or 10 Hz was similar across treatment groups, scPCP treated rats tended to show greater numbers of DG population spiking during the trains. This may suggest that the GABA mediated local inhibitory input is impaired following scPCP treatment, although this conclusion is limited by the small sample size.

4.4.3 Evidence for changes in hippocampal excitability in sub-chronic NMDAR hypofunction models

The present study suggests limited evidence for increased hippocampal excitability in scPCP treated rats, indicated by increased instances of re-entrance following SUB stimulation and increased frequency of DG population spikes during trains. However, decreased instances of re-entrance following SCHAFF stimulation may suggest that some hippocampal circuits are less excitable. Previous work in our lab group examining SCHAFF evoked CA1 responses has

revealed mixed evidence for impaired inhibition in scPCP treated rats (Sun et al., 2022, 2023). Sub-chronic PCP treated rats demonstrated greater paired pulse facilitation at short inter-pulse-intervals compared with saline treated rats, suggesting reduced inhibitory control. However, scPCP treated rats were also found to have weaker excitatory drive from CA3 to CA1, as revealed by input-output curves, and weaker slope facilitation following high frequency SCHAFF stimulation, suggesting that the CA3-CA1 pathway is not disinhibited in scPCP treated rats. A decrease in CA3-CA1 LTP is consistent with findings of impaired CA3-CA1 LTP in slice preparations of scPCP treated rats (Nomura et al., 2016; Pollard et al., 2012), but inconsistent with findings of enhanced CA3-CA1 LTP in in vivo recordings in sub-chronic MK-801 treated rats (Ashby et al., 2010). Thus, overall, previous data is mixed with regards to evidence for impaired GABAergic inhibition in scPCP treated rats, however, it is unclear how changes at individual pathways affect the complex hippocampal circuitry, and, furthermore, how this may translate to brain wide changes in neural activity.

4.4.3. Limitations of the present study

Apart from the small sample sizes, another caveat of the present study is that recordings were conducted across a relatively long time period: from 4 to 13 weeks post scPCP treatment. In addition, although we made an effort to conduct recording from both treatment groups as concurrently as possible, the inclusion of a second cohort of saline treated rats (due to rats being excluded during electrode optimisation; see section 4.3.1) part way through the study meant that a subset of saline treated rats were tested sooner after scPCP treatment and, presumably, at a younger age. Given that age was found to influence the likelihood of re-entrance following SUB train stimulation in mice, with young but not old mice exhibiting re-entrance (Davis et al., 2014), age may have influenced the data. However, the differences in ages in Davis et al. (2014) were considerably greater (approximately 1 year) than in the present study. Nevertheless, when looking at saline treated rats as separate cohorts, none of the saline rats in the initial older cohort exhibited re-entrance (n = 6, tested 10-13 weeks post-scPCP treatment; 245-300 g), whereas, in the second, younger, cohort, three rats exhibited re-entrance (n = 5, 4-6 weeks post-treatment; 235-277 g). The scPCP treated rats, however, were all tested 12-15 weeks (252-342 g) post treatment. It is possible that, if the treatment groups were more closely matched with regards to age and time post-treatment, we may have seen more differences between groups. In addition, although NOR object exploration data revealed evidence of impairment in the scPCP treatment group, other measures such as the DI and planned t-tests suggested intact NOR. Therefore, electrophysiological changes are not strongly supported by a robust cognitive deficit. However, this may be due to the relatively

smaller sample size, compared to the sample sizes used in chapter 2, making us underpowered to detect significant differences. Nevertheless, to our knowledge, this study is the first to confirm that re-entrance is present in scPCP treated rats, and we tentatively suggest that an increase in the frequency of population spikes may be indicative of impaired GABAergic inhibition in the model.

4.4.4 Conclusions

In summary, we have demonstrated that both scPCP and saline treated rats exhibit similar patterns of synaptic currents following SCHAFF or SUB train stimulation, suggesting intact hippocampal circuitry. Furthermore, a subset of rats in both treatment groups demonstrated hippocampal response reverberation, consistent with re-entrance via the deep to superficial connections in the EC, followed by activation of the perforant path. Therefore, re-entrance, which has been suggested to be important for the temporal storage of information, appears to be unaffected by scPCP treatment. There was limited evidence for increased instances of re-entrance (and perhaps hyperexcitability) in scPCP treated rats following SUB stimulation, whereas SCHAFF stimulation resulted in decreased instances of re-entrance in scPCP treated rats. In addition, an increase in DG population spikes in scPCP treated rats following SUB train stimulation may suggest weaker inhibitory control, in line with post-mortem findings of reduced hippocampal GABA markers. Overall, these findings suggest that some aspects of hippocampal circuitry may be hyperexcitable, but others hypoexcitable, and this may account for the mix of findings reported in previous studies investigating hippocampal neural activity in NMDAR hypofunction models. However, it is important to note that conclusions from this study are limited by the small sample size.

Chapter 5: Too little and too much: balanced hippocampal, but not prefrontal, neural activity is required for intact novel object preference in rats

Declaration: Jacco Renstrom, Joanna Loayza, Stuart Williams and Miriam Gwilt contributed to surgeries and data collection. Rachel Grasmeder Allen contributed to anaesthesia monitoring during surgeries.

Abstract

Impaired GABAergic inhibition, so-called neural disinhibition, in the PFC and hippocampus has been linked to cognitive deficits in schizophrenia. The NOR task has been used widely to study cognitive deficits in rodent models of relevance to schizophrenia, including the scPCP model. Sub-chronic PCP treatment is reported to impair NOR at 1 min retention delays, and such impairments have been suggested to reflect reduced prefrontal and hippocampal GABA function. However, the contribution of GABAergic inhibition in the PFC and hippocampus to NOR task performance has not been established. Here, we investigated NOR performance in male Lister Hooded rats following neural disinhibition or functional inhibition of the mPFC, ventral hippocampus or dorsal hippocampus. The NOR task consisted of a 3 min acquisition and retention phase, separated by a 1 min retention delay. NOR performance was compared using a within-subjects design, following bilateral regional saline, picrotoxin or muscimol infusions made before acquisition. In the mPFC, neither functional inhibition by muscimol nor disinhibition by picrotoxin affected NOR. In both the dorsal and ventral hippocampus, neural disinhibition impaired NOR relative to saline control, mainly by a reduction in novel object exploration. Functional inhibition in the dorsal hippocampus also impaired NOR, whereas ventral hippocampal functional inhibition reduced novel object exploration only at the higher dose. Overall, our data suggest that hippocampal, but not prefrontal, GABAergic inhibition contributes to NOR at a 1 min retention delay. In addition, NOR performance requires balanced neural activity in the dorsal hippocampus, with both too little and too much activity impairing novel object preference.

5.1 Introduction

Neural disinhibition, or reduced GABAergic inhibition, in the PFC and hippocampus has been implicated in several cognitive disorders (Bast et al., 2017). In particular, such disinhibition has emerged as key neuropathological features of schizophrenia, based on post-mortem findings of reduced prefrontal and hippocampal GABA markers (Batiuk et al., 2022; Gonzalez-Burgos et

al., 2010; Heckers & Konradi, 2015). Rodent studies support that prefrontal and hippocampal GABAergic disinhibition contribute to cognitive impairments relevant to schizophrenia (Bast et al., 2017; McGarrity et al., 2017; Tse et al., 2015). One task used widely to study cognitive deficits in rodent models is the NOR task. In the standard NOR task (Ennaceur & Delacour, 1988), a rodent is placed into an open-field arena and allowed to explore two identical objects for the acquisition phase, then, after a retention delay, the rodent is returned to the arena which contains an identical copy of one of the objects used in the acquisition phase (the 'familiar' object) and a novel object (i.e. not previously encountered by the rodent). Due to rodents' innate preference for novelty (Ennaceur & Delacour, 1988), rodents with intact NOR should explore the novel object preferentially over the familiar object. NOR deficits are suggested to be relevant to recognition memory impairments in human brain disorders, including schizophrenia (Grayson et al., 2015; Lyon et al., 2012). Indeed, the NOR task is used widely in NMDAR hypofunction models of relevance to schizophrenia, including in the scPCP model, which results in NOR deficits using retention delays as short as 1 min (see chapter 2 and references therein). NMDAR hypofunction models also report pathological changes to prefrontal and hippocampal GABA markers (Cadinu et al., 2018; Gigg et al., 2020), and such impairments may contribute to the NOR deficits found in this model over 1 min retention delays (Cadinu et al., 2018). However, the contribution of prefrontal and hippocampal GABAergic inhibition to NOR has not been established.

Previous functional inhibition studies suggest that the mPFC is not required for the standard NOR task, which involves single item recognition (see Morici et al., 2015 for review). However, more recent studies have contested this, with deficits reported in NOR memory consolidation and retrieval at 24 h retention delays (de Landeta et al., 2020; Pezze et al., 2017; Tanimizu et al., 2018; Tuscher et al., 2018). The outcomes of lesion and functional inhibition studies on the requirement of the hippocampus for NOR have been mixed (Cohen & Stackman Jr, 2015; Warburton & Brown, 2015). In the dorsal hippocampus, functional inhibition by local infusion of the GABA-A receptor agonist muscimol impaired NOR at long (> 20 min) (Ásgeirsdóttir et al., 2020; Cinalli Jr et al., 2020; Cohen & Stackman Jr, 2015; Stackman Jr et al., 2016), but not short (5 min) retention delays (Ásgeirsdóttir et al., 2020). In contrast, other studies reported no impairment following dorsal hippocampal muscimol infusion, even at long retention delays (Oliveira et al., 2010; Sawangjit et al., 2018). Evidence on the requirement of the ventral hippocampus for NOR is limited, but one study reported impaired NOR at a 1 min retention delay (Neugebauer et al., 2018). The effect of regional neural disinhibition on NOR is less studied and has, to our knowledge, not been investigated in the mPFC. Hippocampal neural

disinhibition induced by infusion of the GABA-A receptor antagonist bicuculline was reported to impair NOR in the dorsal (Kim et al., 2014; Riordan et al., 2018), but not ventral hippocampus (Neugebauer et al., 2018).

Here, we examined the impact of functional inhibition and neural disinhibition, induced by microinfusion of the GABA-A receptor agonist muscimol or antagonist picrotoxin, respectively, in the mPFC (experiment 1), dorsal hippocampus (experiment 2) and ventral hippocampus (experiment 3) on NOR at a 1 min retention delay. Given evidence that the mPFC plays a limited role in NOR (Morici et al., 2015), we hypothesised that prefrontal functional inhibition would not impair NOR. However, because regional neural disinhibition can disrupt cognitive processing mediated by projection sites (Bast et al., 2017), and the mPFC projects to the perirhinal cortex (Deacon et al., 1983), a region reported to be critical for NOR (Warburton & Brown, 2015), we hypothesised that prefrontal neural disinhibition may impair NOR. In addition, we hypothesised that hippocampal neural disinhibition would impair NOR, due to a functional disruption in both the hippocampus and its projection sites (Bast et al., 2017; Williams et al., 2020).

5.2 Materials and methods

5.2.1 Rats

Three cohorts of 16 male Lister Hooded rats (experiment 1: Charles River, UK; experiments 2 and 3: ENVIGO, Harlan, UK) weighing 277-340 g and approximately 8-9 weeks of age at surgery were used. For final sample sizes, sample size justification and exclusion criteria, see section 5.2.7 Experimental design. Rats were housed in groups of four in individually ventilated 'double decker' cages (GR1800; 462 x 403 x 404 mm; Techniplast, UK) under temperature (21 ± 1.5 °C) and humidity (50 ± 8 %) controlled conditions, and on an alternating 12 h light-dark cycle (lights on at 07:00 h) (Bio-Support Unit, University of Nottingham). Rats had *ad libitum* access to food and water throughout the study. All rats were habituated to handling by the experimenter prior to any procedures. All procedures were carried out during the light phase and in accordance with the UK Animals (Scientific Procedures) Act 1986.

5.2.2 Implantation of guide cannulae into mPFC, dorsal or ventral hippocampus

Rats were anaesthetized using isoflurane delivered in medical oxygen (induction: 5%; maintenance: 1–3%; flow rate: 1 L/min) and prepared for surgery by shaving and washing the prospective incision site, and administering a perioperative analgesic (Rimadyl, Small Animal Solution, Zoetis, UK; 5 mg/kg, sub-cutaneous (s.c.) or Metacam, Boehringer Ingelheim; 1

mg/kg, s.c.). During the surgery, rats were secured in a stereotaxic frame. To minimise any discomfort a local anaesthetic (EMLA cream 5%; lidocaine/prilocaine, Aspen) was applied to the ear bars, and a topical ocular lubricant (Lubrithal, Dechra) used to protect the eyes. The scalp was incised to expose the skull, and bregma and lambda were aligned horizontally. Bilateral infusion guide cannulae (stainless steel, 26-gauge, Plastic Ones, Bilaney, UK), with stylets (stainless steel, 33-gauge, Plastics One, Bilaney, UK) inserted to prevent occlusion, were implanted through small holes drilled in the skull. Guide cannulae were aimed at 0.5 mm dorsal to the infusion site, as the injectors protruded 0.5 mm from the tip of the guides. For the mPFC, we used a double guide cannula ("mouse" model C235GS-5-1.2), aimed at: AP +3.0, ML ± 0.6, DV -3.5 mm (from skull), as in Pezze et al. (2014). For the dorsal hippocampus, we also used a double cannula (model C235G-3.0-SPC), aimed at: AP -3.0, ML ± 1.5, DV -3.5 mm (from dura); coordinates were adapted from previous studies in Wistar rats (Zhang et al., 2002a, 2002b, 2014), and based on pilot studies in Lister Hooded rats (T. Bast, unpublished data). For the ventral hippocampus we implanted two single guide cannulae (model C315G/SPC), aimed at: AP -5.2, ML ± 4.8, DV -6.5 mm (from dura), as in Williams et al. (2022) and McGarrity et al. (2017). A pedestal was built around the cannulae using dental acrylic (Simplex Rapid, Kemdent, UK), and anchored by four stainless-steel screws drilled into the skull. The scalp incision was sutured around the pedestal. The rat was injected with saline (1 ml, i.p.) to counter effects of dehydration/blood loss. The breathing rate was monitored throughout the surgery and kept at 40-60 breaths/min by adjusting the depth of anaesthesia accordingly. After surgery, rats were allowed at least 5 d of recovery before testing, during which the rats were checked daily and habituated to the manual restraint necessary for the drug microinfusions. Rats also received daily injections of prophylactic antibiotics (Synulox, Zoetis, UK; 140 mg amoxicillin, 35 mg clavulanic acid/ml; 0.2 ml/kg, s.c.), starting on the day of surgery until the end of the study.

5.2.3 Microinfusion drugs and procedure

The GABA-A receptor agonist muscimol (experiment 1: 62.5 ng/0.5 µl; experiment 2 and 3: 500 ng/0.5 µl) and antagonist picrotoxin (experiment 1: 300 ng/0.5 µl; experiment 2 and 3: 150 ng/0.5 µl) (Sigma-Aldrich, UK) were dissolved in saline. Doses used in experiment 1 were based on previous studies involving prefrontal microinfusions (Pezze et al., 2014). For experiments 2 and 3, the picrotoxin dose was based on previous studies which found that 150 ng/0.5 µl/side picrotoxin infusions into the dorsal or ventral hippocampus resulted in moderate increases in locomotor activity, without inducing seizure-related behavioural or electrophysiological changes (Bast et al., 2001a; McGarrity et al., 2017; S McGarrity & T Bast,

unpublished findings). The muscimol dose (500 ng/0.5 µl) was based on previous studies investigating functional inhibition in the dorsal or ventral hippocampus on various behavioural tasks (Bast et al., 2001b; de Lima et al., 2006; McDonald et al., 2010; Oliveira et al., 2010; Sawangjit et al., 2018; Zhang et al., 2014). In experiment 3, the dose of picrotoxin and muscimol was reduced after the first series of testing to 100 ng/0.5 µl and 250 ng/0.5 µl, respectively, due to adverse behavioural drug effects (see section 5.2.7 and 5.3.3.4). The experimenter was blinded to the drug conditions at the start of testing. However, in practice, blinding was difficult to maintain due to the presence of some behavioural drug effects.

Rats were gently restrained throughout the microinfusion procedure. Stylets were removed from the guide cannulae and replaced with injectors (33 gauge; Plastic Ones, Bilaney, UK), which protruded 0.5 mm below the guides. Each injector was connected to an SGE micro-syringe (5 µL; World Precision Instruments, UK) mounted on a microinfusion pump (SP200IZ syringe pump, World Precision Instruments, UK) by polyethylene tubing (PE50, Bilaney Consultants, Germany). An air bubble was included in the tubing to verify successful infusion of the drug into the brain. A volume of 0.5 µl/side of saline (0.9%), muscimol or picrotoxin was bilaterally infused over 1 min. The injector was kept in place for a further 1 min to allow for tissue absorption of the drug bolus. The injectors were then removed, and the stylets replaced. After the infusion, rats were placed individually into holding boxes for 10-20 min before NOR testing began (see section 5.2.7 for timing details). Rats were visually inspected for any gross behavioural effects of infusion, as we have previously observed some seizure-related effects following ventral hippocampal picrotoxin (150 ng/side) infusions (Williams et al., 2022).

5.2.4 NOR testing

The NOR procedure was adapted from Pezze et al. (2015) and Gonçalves et al. (2023), and was suitable for repeated testing of the same rat, as required for within-subjects testing of the intracerebral infusion effects. Four NOR arenas were used, which consisted of an opaque rectangular box (38 x 40 x 54 cm) with a Perspex lid. The light level in each arena was between 30-40 lux. An overhead camera (HD Everio, GZ-EX515BEK, JVC) was used to record behaviour for subsequent analyses. The objects used were mainly bottles or jars filled with sand and/or water (Fig. 5.1D) and were arranged into sets of two objects (one to be used as the novel and one as the familiar) which consisted of different shapes, colours, sizes and materials. The object used as novel was counterbalanced across each group, as was the position of the novel object in the arena (left or right). Time spent exploring an object was defined as interacting with the object (e.g., sniffing) and directing the nose at the object at an estimated distance of

< 1 cm. Object exploration was not recorded if the rat was in contact with the object but not facing it (e.g., standing/sitting on the object or using it as a prop) (Ennaceur & Delacour, 1988). The arena and objects were cleaned with an alcohol-based solution (20% v/v) before each trial to reduce olfactory cues left by the rats.

On the day before each NOR testing day, rats were placed individually into the empty arena for 1 h for habituation. On the testing day, rats were re-acclimatised to the empty arena for 3 min, before receiving one of three bilateral infusions: saline, picrotoxin or muscimol. After 10-20 min, rats were placed into the arena with two identical objects for the acquisition phase and allowed to explore for 3 min. After a 1 min retention delay, rats were returned to the arena with a copy of the familiar object used in the acquisition phase and a novel object for the 3 min retention phase. Object exploration was scored from the video recordings using 'The Novel Object Timer' (created by Jack Rivers-Auty, https://jackrrivers.com/program/; Gigg et al., 2020), with the scorer blind to the infusion condition and object type (novel or familiar).

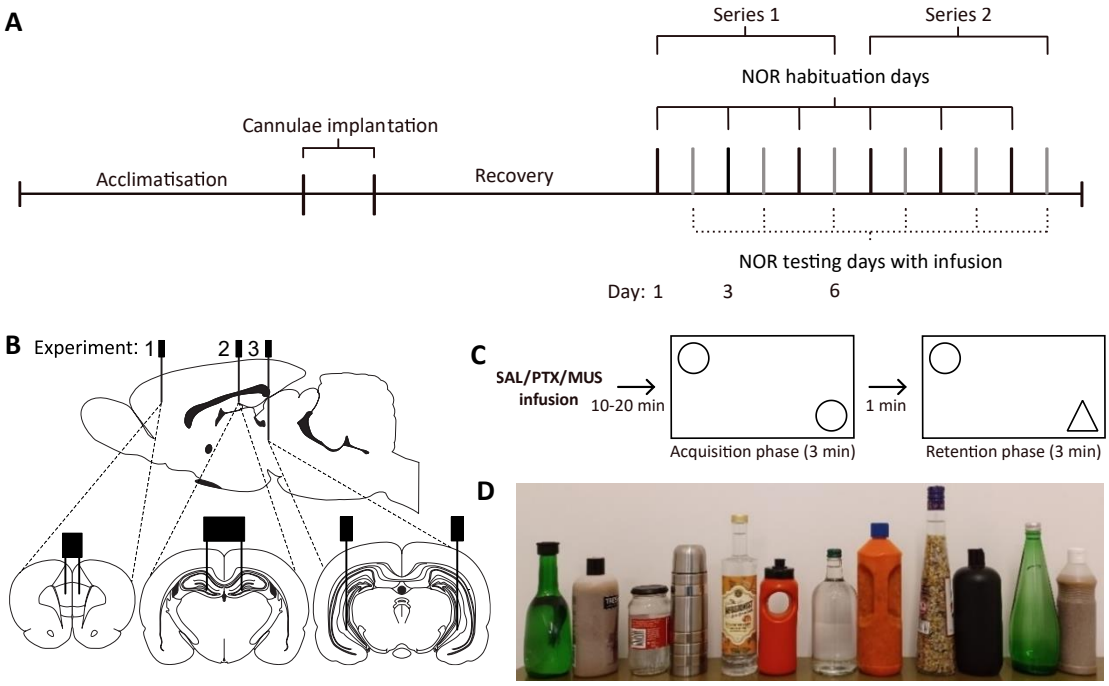

Fig. 5.1. ***Timeline of experiment and NOR paradigm.*** **A.** Following arrival in the facilities, rats were allowed at least 7 d for acclimatisation before surgical implantation of guide cannulae and at least 5 d for recovery. The impact of intracerebral drug infusions on novel object recognition (NOR) performance was tested using a within-subjects design, with two series of testing. Each series consisted of 6 days: NOR habituation (1 h) on days 1, 3 and 5 and infusion (saline, picrotoxin or muscimol) followed by NOR testing on days 2, 4 and 6. The order of infusion conditions was counterbalanced according to a Latin square design. **B.** Illustration of intended cannulae placement in medial prefrontal cortex (experiment 1), dorsal hippocampus (experiment 2), and ventral hippocampus (experiment 3). Adapted from Paxinos & Watson (2006). **C.** NOR testing commenced 10-20 min following intracerebral microinfusions of either saline (SAL), picrotoxin (PTX) or muscimol (MUS), and consisted of a 3 min acquisition and retention phase, separated by a 1 min retention delay. **D.** Image of objects used in NOR testing: objects are arranged in the pairs used as familiar and novel.

5.2.5 Measurement of locomotor activity using line crossings during NOR testing

After completion of experiment 1, the NOR arena floor was demarcated into 12 equal sectors measuring 13 cm x 14 cm, in order to obtain a crude measure of locomotor activity during the NOR trial, with the aim of using this as a positive control for drug effects in experiments 2 and 3. The number of line crossings (or sectors crossed) were manually counted from the video recordings, with the scorer blind to the infusion condition.

5.2.6 Verification of cannulae placements

At the end of the study, rats were overdosed with injectable anaesthetic (i.p., approximately 1 ml; sodium pentobarbital, 200 mg/ml, Dolethal, Vetoquinol, UK) and transcardially perfused with saline (0.9%) followed by paraformaldehyde (4% in saline). Brains were then removed and stored in paraformaldehyde (4% in saline). Brains were sliced using a vibratome at 80 µm thickness and sections containing the relevant brain regions mounted on microscope slides. Injection sites were identified using a light microscope and mapped onto coronal sections of a rat brain atlas (Paxinos & Watson, 1998).

5.2.7 Experimental design

NOR performance following microinfusions was examined using a within-subjects design, with two series of testing for each experiment (see Fig. 5.1A for timeline). Each series was run over 6 d, with habituation (1 h in empty arena) on days 1, 3 and 5, and NOR testing on days 2, 4 and 6. Rats received a different infusion condition (saline, muscimol or picrotoxin) on each testing day in a counterbalanced order, according to a Latin square design. Series 2 of testing began one day after the end of series 1. For convenience, the four rats from the same cage were tested simultaneously on the NOR task. Rats in each cage were infused in batches of two pairs, by two experimenters: one pair of rats were infused, followed by the second pair, and NOR testing started 10 min after the last rat had been infused. In practice, this meant that the delay between infusion completion and the start of NOR testing was 10-20 min. The timings for the start of behavioural testing following infusions are based on previous electrophysiological measurements, where the peak effect of picrotoxin on neuronal firing in the mPFC and ventral hippocampus was recorded between 10-30 min following infusion (McGarrity et al., 2017; Pezze et al., 2014). In experiments 1 (mPFC) and 2 (dorsal hippocampus), the doses of picrotoxin and muscimol used were the same across the two series of testing. In experiment 3 (ventral hippocampus) the second series was run with lower doses of picrotoxin and muscimol, based on non-specific effects observed in series 1 testing (see section 5.3.3.4).

All three experiments started with 16 rats, and we were aiming for a sample size of 12-16 rats for our statistical analysis. This sample size would give a power of > 80% to detect effect sizes of Cohen's d = 1 for differences between infusion conditions (using within-subjects pairwise comparisons, two-tailed, with a significance threshold of $p < 0.05$; G*Power (Faul et al., 2007)). In all experiments, some rats had to be excluded from the analysis of one or both series of NOR testing. Rats were excluded from NOR analysis if: an object was displaced during the trial; they showed convulsive seizures; they did not explore the objects for at least 5 s in both the acquisition and retention phase due to infusion-induced motor impairment; or if histology showed that cannula were not located in the desired brain region. In experiment 1 (mPFC), n = 13 rats were included in the overall analysis: two rats were excluded due to an object falling over during the trial, and one rat was excluded due to the infusion cannula tips being positioned too anterior (see section 5.3.1.1). In experiment 2 (dorsal hippocampus), n = 13 rats were included in the analysis: two rats were excluded as they did not reach at least 5 s of object exploration time due to infusion-induced motor impairments (one following picrotoxin infusion and one following muscimol infusion), and one rat was excluded due to object displacement. In experiment 3 (ventral hippocampus), four rats were excluded from analysis of series 1 and 2. In series 1, two rats were excluded as they showed convulsive seizures following picrotoxin infusion (150 ng/side). Two more rats were excluded as they showed hypoactivity following muscimol infusion (500 ng/side), both of these rats were culled as they did not recover within 3 h. At the end of series 1 testing, one rat was culled due to falling ill. Despite reducing the doses for series 2, one rat had to be excluded from series 2 analysis because it showed a convulsive seizure following picrotoxin (100 ng/side) infusion. Overall, this gave a final sample size of n = 12 for series 1 and 2 of ventral hippocampal drug infusions.

5.2.8 Statistical analysis

In experiments 1 and 2, which used the same doses across the two series of testing, object exploration time was analysed using a three-way repeated measures ANOVA with series (1 or 2), infusion condition (saline, picrotoxin, muscimol) and object (familiar versus novel) as within-subjects factors. In experiment 3, which used two different doses across the two series of testing, the data from each series was analysed separately, using a two-way ANOVA with infusion condition and object as within-subjects factors. Where the ANOVA revealed a significant interaction between condition and object, a simple main effects analysis was performed for the familiar and novel object exploration times. Significant main effects were examined further using Fisher's LSD test. Pairwise student t-tests were used for planned comparisons of familiar versus novel exploration time to test for significant NOR memory in all

conditions. Discrimination index (DI) ((time spent exploring the novel object - time spent exploring the familiar object)/total time spent exploring both objects) was also used as a measure of NOR, with a higher value indicating greater preference for the novel object (Cohen et al., 2013; Kim et al., 2014). The DI was analysed using ANOVA with infusion condition as a within-subjects factor, and any main effects were examined further using Fisher's LSD test. One-sample t-tests were used as planned comparisons to chance exploration (DI = 0).

In experiments 2 and 3, the number of line crossings was used as a measure of locomotor activity. This was analysed using ANOVA with series and infusion condition as within-subjects factors (experiment 2), or infusion condition as a within-subjects factor (experiment 3).

Graphs were completed using GraphPad Prism (version 9) and statistical tests were performed using either JASP (version 0.16.2) or SPSS (version 25) software, with p values of < 0.05 considered to indicate statistical significance.

5.3 Results

5.3.1 Experiment 1: Medial prefrontal cortex

5.3.1.1 Infusion sites in the medial prefrontal cortex

One rat was excluded from the NOR analysis due to the infusion cannula tips being located too anteriorly in the in the medial orbital cortex. All other infusion cannula tips were located in the mPFC, within an area that corresponded to approximately 2.7–4.2 mm anterior to bregma in the atlas by Paxinos and Watson (1998) (Fig. 5.2A and B).

5.3.1.2 Medial prefrontal cortical disinhibition and functional inhibition did not affect NOR

During acquisition, rats in all infusion conditions spent a similar amount of time exploring the two identical objects (left and right) (Fig. 5.2C), with ANOVA revealing no main effect of object, condition or any interaction of these two factors ($F < 1$). In the retention phase, rats across all infusion conditions showed similar NOR, with more time spent exploring the novel object versus the familiar, and no differences between the conditions (Fig. 5.2C). Planned pairwise t-tests confirmed that in all three conditions rats spent more time exploring the novel object ($t_{12} > 4.47$, $p < 0.001$). ANOVA also revealed a main effect of object ($F_{(1, 12)} = 64.7$, $p < 0.001$), with no main effect of condition or an interaction involving condition ($F_{(2, 24)} < 1$). Analysis of the DI confirmed intact NOR, with novel object exploration significantly different from chance in all conditions ($t_{13} > 4.94$, $p < 0.001$) and no main effect of condition ($F_{(2, 24)} < 1$) (Fig. 5.2D).

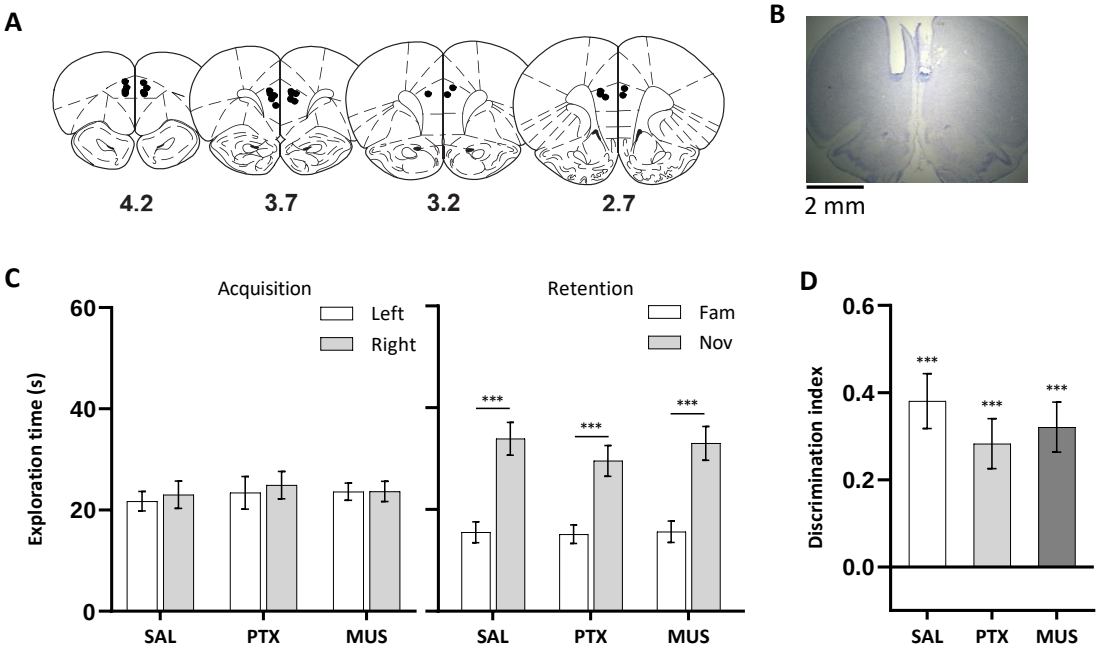

Fig. 5.2. ***Medial prefrontal cortical disinhibition and functional inhibition did not affect NOR performance.*** **A.** Approximate locations of infusion cannula tips (black dots) in the mPFC shown on coronal plates adapted from the atlas by Paxinos & Watson (1998), numbers indicate distance from bregma (mm). **B.** Cresyl violet-stained coronal section showing exemplary infusion site in mPFC. **C.** Exploration time (s) of objects during the acquisition and retention phase following prefrontal disinhibition or functional inhibition, by microinfusion of picrotoxin (PTX, 300 ng/side) or muscimol (MUS, 62.5 ng/side), respectively, or following saline (SAL) control infusions. During the retention phase, rats across all three conditions spent more time exploring the novel compared to the familiar object with no differences between conditions. **D.** Discrimination index confirmed that rats in all infusion conditions showed similar novel object preference. Asterisks indicate significant novel object preference (paired or one-sample t-tests) ($p < 0.001$). Data are shown as mean (± SEM), n = 14, within-subjects design.

5.3.2 Experiment 2: Dorsal hippocampus

5.3.2.1 Infusion sites in the dorsal hippocampus

All infusion cannula tips were located in the dorsal hippocampus, within an area that corresponded to approximately 2.12–3.6 mm posterior to bregma in the atlas by Paxinos and Watson (1998) (Fig. 5.3A and B).

5.3.2.2 Dorsal hippocampal disinhibition and functional inhibition impaired novel object preference

During acquisition, rats in all infusion conditions spent a similar amount of time exploring the two identical objects, with ANOVA revealing no main effect of condition ($F_{(2,24)} < 1$) (Fig. 5.3C). However, ANOVA did reveal a main effect of object ($F_{(1,12)} = 9.5$, $p = 0.01$) alongside a strong trend for an interaction between object and condition ($F_{(1,12)} = 2.83$, $p = 0.079$), likely due to a

slight increase in exploration of objects located on the right in the picrotoxin and muscimol conditions.

In the retention phase, both muscimol and picrotoxin impaired NOR, as reflected by reduced exploration of the novel object versus the familiar (Fig. 5.3C). ANOVA revealed a significant interaction between condition and object ($F_{(2,24)}$ = 6.7, p = 0.005), alongside a main effect of object ($F_{(1,12)}$ = 57.1, p < 0.001). Simple main effects analysis revealed a significant main effect of condition for novel object exploration time ($F_{(2,24)}$ = 5.16, p = 0.014), but not familiar object exploration time ($F_{(2,24)}$ = 1.7, p = 0.204). Post hoc comparisons revealed that both picrotoxin and muscimol infusion reduced novel object exploration time compared to saline (p < 0.047), with no significant difference between the picrotoxin and muscimol condition (p = 0.966). Planned pairwise t-tests indicated that rats in the saline and picrotoxin condition explored the novel object more than the familiar object (t_{12} > 3.73, p < 0.003), whereas rats in the muscimol condition showed a non-significant trend to preferentially explore the novel object (t_{12} = 1.87, p = 0.086).

The DI also demonstrated an NOR impairment in the picrotoxin and muscimol condition (Fig. 5.3D). ANOVA showed a significant main effect of condition ($F_{(2,24)}$ = 5.75, p = 0.009), reflecting a reduced DI in both the picrotoxin and muscimol condition, compared to saline (p < 0.021), with no significant difference between muscimol and picrotoxin (p = 0.843). Planned one-sample t-tests revealed that rats in the saline and picrotoxin condition showed significant novel object preference (t_{12} > 3.36, p < 0.006) and rats in the muscimol condition showed a strong trend for novel object preference (t_{12} = 2.17, p = 0.051). Additionally, in the retention phase, there was a significant interaction between condition and series ($F_{(2,24)}$ = 4.03, p = 0.031), reflecting a significant reduction in overall object exploration time in the saline condition between series 1 and 2 ($F_{(1,12)}$ = 7.15, p = 0.02) (data not shown), with no significant differences between series observed for the picrotoxin or muscimol condition ($F_{(1,12)}$ < 1).

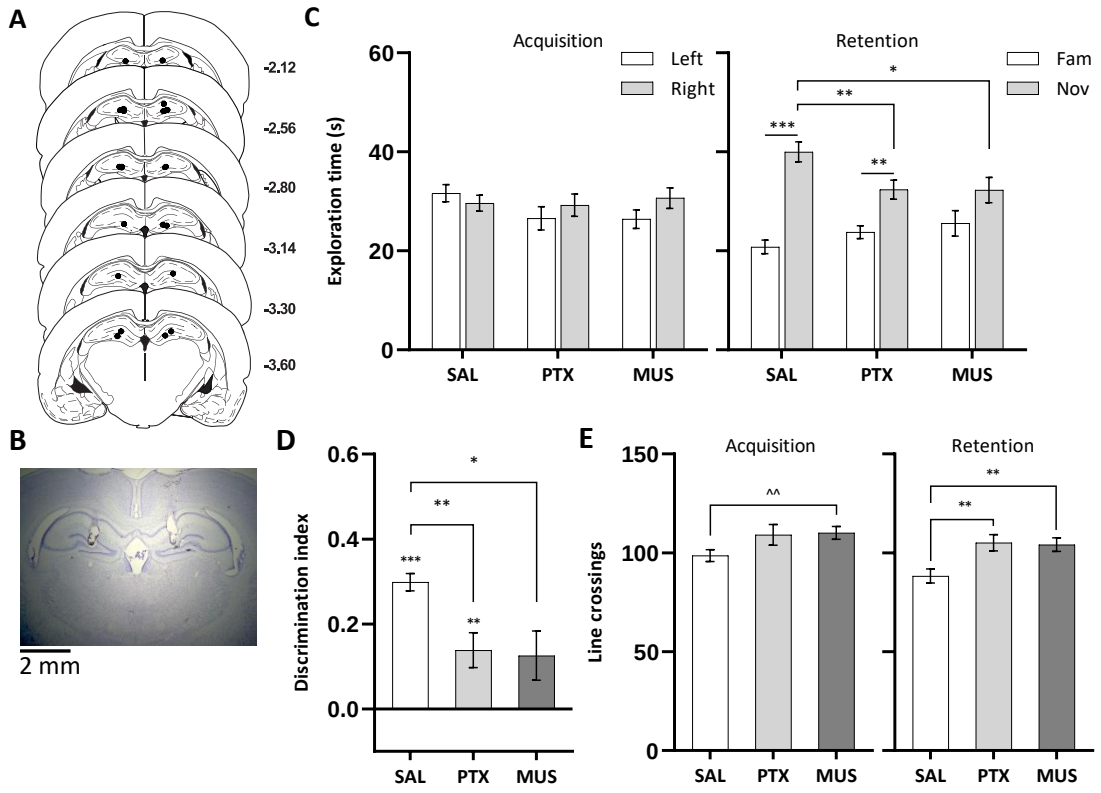

Fig. 5.3. ***Dorsal hippocampal disinhibition and functional inhibition impaired novel object preference.*** **A.** Approximate locations of infusion cannula tips (black dots) in the dorsal hippocampus shown on coronal plates adapted from the atlas by Paxinos & Watson (1998), numbers indicate distance from bregma (mm). **B.** Cresyl violet-stained coronal section showing exemplary infusion site in the dorsal hippocampus. **C.** Exploration time (s) of objects during the acquisition and retention phase following dorsal hippocampal disinhibition or functional inhibition, by microinfusion of picrotoxin (PTX, 150 ng/side) or muscimol (MUS, 500 ng/side), respectively, or following saline (SAL) control infusions. In the retention phase, there was a significant reduction in novel object exploration time in the picrotoxin and muscimol condition. **D.** Discrimination index was significantly reduced in the picrotoxin and muscimol condition. **E.** Number of line crossings increased following picrotoxin and muscimol infusion, compared to saline. Asterisks indicate significant novel object preference ($p < 0.01$, paired or one-sample t-tests); or significant differences between conditions ($p < 0.05$; Fisher's LSD test following a significant main effect of condition). ^^ indicates a statistically significant difference between conditions following a trend towards a main effect of condition ($p < 0.01$; Fisher's LSD test). Data are shown as mean (± SEM), n = 13, within-subjects design.

5.3.2.3 Dorsal hippocampal disinhibition and functional inhibition increased locomotor activity

Dorsal hippocampal picrotoxin and muscimol infusion increased locomotor activity during NOR testing, as indicated by increased number of lines crossing during NOR testing (Fig. 5.3E). In the acquisition phase, picrotoxin and muscimol both tended to increase the number of line crossings, with ANOVA revealing a strong trend for a main effect of condition ($F_{(2,26)} = 3.12$, $p = 0.061$). Post hoc comparisons revealed that muscimol increased ($p = 0.008$) and picrotoxin tended to increase ($p = 0.062$) the number of line crossings compared to saline, with no difference between the muscimol and picrotoxin condition ($p = 0.873$). In the retention phase,

ANOVA revealed a significant main effect of condition ($F_{(2,24)}$ = 6.42, p = 0.006). Subsequent post hoc comparisons revealed that both picrotoxin and muscimol increased the number of line crossings compared to saline (p < 0.007), with no significant difference between the picrotoxin and muscimol condition (p = 0.873). This increase in line crossings is consistent with our previous findings of increased open field locomotor activity following dorsal hippocampal picrotoxin or muscimol infusion (Bast & Feldon, 2003; S. McGarrity & T. Bast, unpublished findings).

5.3.2.4 Gross behavioural effects of dorsal hippocampal picrotoxin and muscimol infusions as revealed by visual inspection

The gross behavioural effects of infusion were recorded for all 16 rats, with 3 rats subsequently removed from the analysis (see section 5.2.7 Experimental design). Dorsal hippocampal infusion of picrotoxin (150 ng/side) caused some seizure-related behaviours in some rats, with wet dog shakes observed in 3 out of 16 rats, with one of those three rats also showing clonic limb movement (this rat was removed from the analysis due to insufficient object exploration), although we did not observe any full motor seizures. One rat also showed pronounced hypoactivity and compulsive chewing and licking behaviours following the first of two dorsal hippocampal muscimol (500 ng/side) infusions, which resolved within 4 h (this rat was also removed from the analysis due to insufficient object exploration).

5.3.3 Experiment 3: Ventral hippocampus

5.3.3.1 Infusion sites in the ventral hippocampus

For all rats included in the NOR analyses, infusion cannula tips were located in the ventral hippocampus, within an area that corresponded to approximately 4.8–6.3 mm posterior to bregma in the atlas by Paxinos and Watson (1998) (Fig. 5.4A and B). However, it should be noted that, in most rats, cannula infusion tips were located in the subiculum region of the ventral hippocampus. Nevertheless, we expect that the infusion drug bolus would diffuse beyond the infusion site. In addition, we expect that diffusion of the drug would be facilitated in the dorsal direction by the cannula tracks, and that the drug would likely remain in the hippocampus due to the surrounding densely packed fibre bundles (Jacobs et al., 2013; Williams et al., 2022). In addition, previous multiunit electrophysiological recordings, using the same co-ordinates as the present study, found that ventral hippocampal picrotoxin infusions resulted in enhanced burst firing in multiple subregions (including CA1, CA3 and DG), with no changes in neural firing recorded outside the medial and lateral boundaries of the ventral hippocampus (McGarrity et al., 2017). Therefore, it is likely that, although many infusion

cannula tips were located in the subiculum region, the results of this study reflect drug effects across several regions of the ventral hippocampus.

5.3.3.2 Ventral hippocampal disinhibition impaired novel object preference in both series of testing

In both series, during acquisition, rats in all infusion conditions spent a similar amount of time exploring the two identical objects (left and right) (Fig. 5.4C), with ANOVA revealing no main effect of object ($F_{(1,11)} < 1.66$, $p > 0.224$). In series 2 there was a trend level interaction between object and condition ($F_{(2,22)} = 3.14$, $p = 0.063$), due to decreased exploration of objects located on the left in the picrotoxin condition compared to saline, and decreased exploration of objects located on the right in the picrotoxin condition compared to muscimol. In addition, in both series, during the acquisition phase ANOVA revealed a main effect of condition ($F_{(2,22)} > 6.41$, $p < 0.006$). Subsequent post hoc comparisons indicated that this was due to a decrease in overall exploration time in the picrotoxin condition compared to the saline and muscimol condition ($p < 0.022$), with no significant difference between saline and muscimol ($p > 0.228$).

During retention in series 1, picrotoxin or muscimol infusion resulted in impairments in NOR performance, demonstrated by reduced exploration of the novel object, compared with the saline condition (Fig. 5.4C, series 1). ANOVA revealed a main effect of object ($F_{(1,11)} = 64.8$, $p < 0.001$) and a strong trend for an interaction between condition and object ($F_{(2,22)} = 3.15$, $p = 0.063$). Simple main effects analysis revealed a significant main effect of condition for novel object exploration time ($F_{(2,22)} = 5.20$, $p = 0.014$), but not familiar object exploration time ($F_{(2,22)} < 1$). Post hoc comparisons revealed that both ventral hippocampal picrotoxin and muscimol infusion reduced novel object exploration time, compared to saline ($p < 0.044$), with no difference between picrotoxin and muscimol ($p = 0.231$). Planned pairwise t-tests indicated that saline and muscimol infused rats explored the novel object significantly more than the familiar object ($t_{11} > 4.21$, $p = 0.001$), and picrotoxin infused rats also tended to show such novel object preference ($t_{11} = 1.90$, $p = 0.085$). In addition, during retention in series 1, ANOVA revealed a main effect of condition ($F_{(2,22)} = 6.85$, $p = 0.005$), with post hoc comparisons indicating a significant reduction in overall exploration time in the picrotoxin and muscimol condition, compared to saline ($p < 0.024$), with no significant difference between picrotoxin and muscimol ($p = 0.163$).

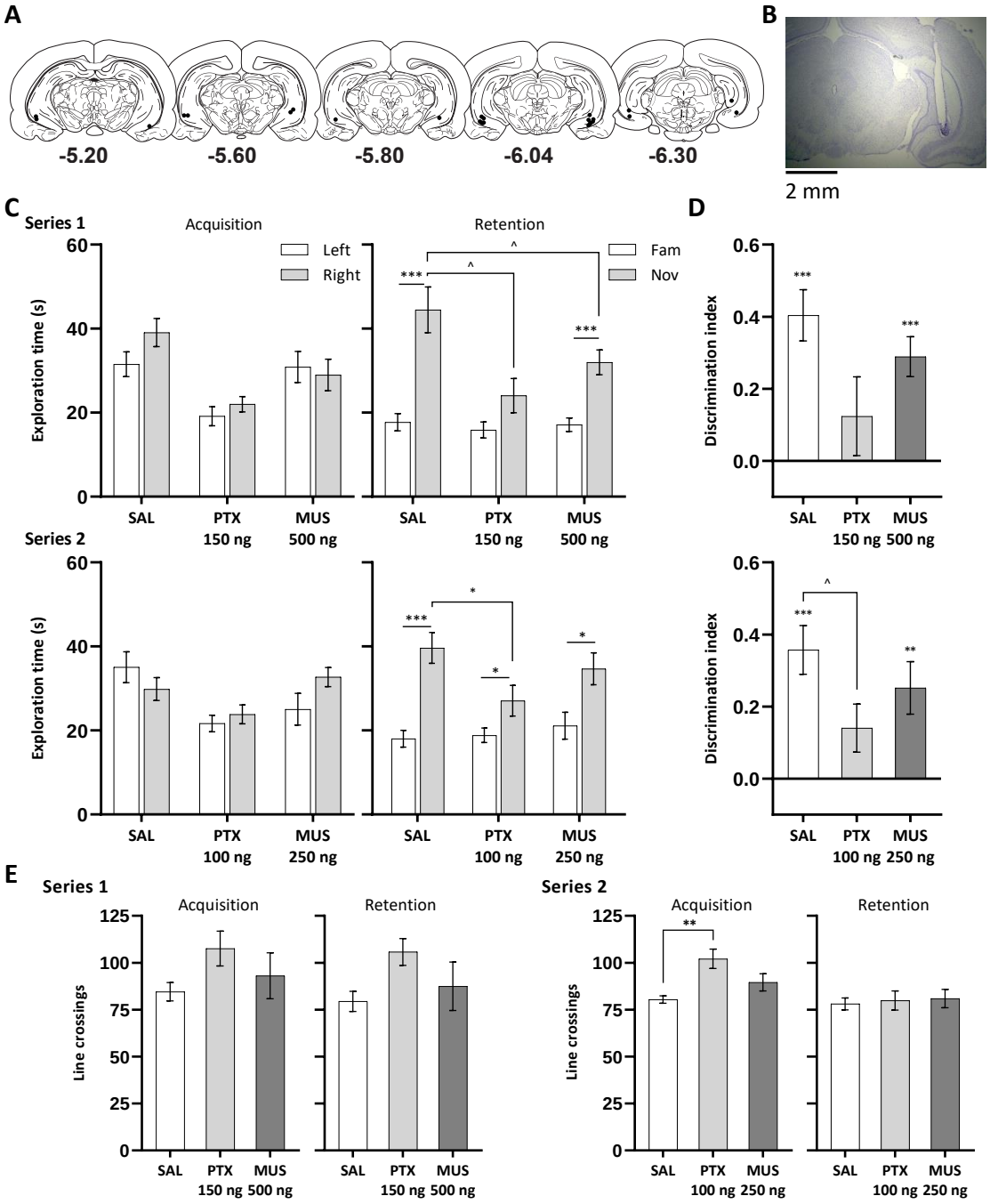

Fig. 5.4. ***Ventral hippocampal neural disinhibition impaired novel object preference.*** **A.** Approximate locations of infusion cannula tips (black dots) in the ventral hippocampus shown on coronal plates adapted from the atlas by Paxinos & Watson (1998), numbers indicate distance from bregma (mm). **B.** Cresyl violet-stained coronal section showing exemplary infusion site in the ventral hippocampus. **C.** Exploration times (s) of objects during the acquisition and retention phase in series 1 and 2. In series 1, novel object exploration was reduced in the picrotoxin (PTX, 150 ng/side) and muscimol (MUS, 500 ng/side) condition, compared to saline (SAL) control. In series 2, novel object exploration was reduced in the PTX (100 ng/side) condition. **D.** Discrimination index was numerically reduced following PTX infusion in series 1 and significantly reduced in series 2. **E.** Number of line crossings increased following PTX infusion in series 1 and 2. Asterisks indicate significant novel object preference ($p < 0.05$, paired or one-sample t-tests); or significant differences between conditions ($p < 0.05$; Fisher's LSD test following a significant main effect of condition). ^ indicates a statistically significant difference between conditions following a trend towards a main effect of condition ($p < 0.01$; Fisher's LSD test). Data are shown as mean (± SEM), n = 12, within-subjects design.

Although the DI was numerically reduced following picrotoxin compared to saline infusion, ANOVA of the DI did not reveal a significant main effect of condition ($F_{(2,22)}$ = 2.29, p = 0.125) (Fig. 5.4D, series 1). Planned one-sample t-tests demonstrated that novel object exploration was significantly different from chance in the muscimol and saline condition (t_{11} > 5.22, p < 0.001), but not in the picrotoxin condition (t_{11} = 1.13, p = 0.281). Overall, series 1 testing in the ventral hippocampus demonstrated reduced novel object exploration in the picrotoxin and muscimol condition, compared with saline, and t-tests of exploration data and DI indicated that rats in the picrotoxin condition did not show significant novel object preference. However, no changes were found in the DI between conditions. In addition, interpretation of these findings may be limited by the reduced overall object exploration time found in the picrotoxin and muscimol condition.

In series 2, ventral hippocampal picrotoxin infusion also reduced novel object exploration, compared to the saline condition, whereas muscimol infusions had little effect (Fig. 5.4C, series 2). ANOVA revealed a significant interaction between condition and object ($F_{(2,22)}$ = 3.74, p = 0.04), alongside a main effect of object ($F_{(1,11)}$ = 22.0, p = 0.001) and no main effect of condition ($F_{(2,22)}$ = 1.99, p = 0.160). Simple main effects analysis revealed a significant main effect of condition for novel object exploration time ($F_{(2,22)}$ = 4.04, p = 0.032), but not familiar object exploration time ($F_{(2,22)}$ < 1). Post hoc comparisons revealed that ventral hippocampal picrotoxin reduced novel object exploration time compared to saline (p = 0.03) and tended to reduce novel exploration time compared to muscimol (p = 0.062), with no difference between muscimol and saline (p = 0.296). Nevertheless, rats in all infusion conditions showed significant novel object preference, with planned pairwise t-tests demonstrating a significant difference between familiar and novel object exploration times in all conditions (t_{11} > 2.30, p < 0.042). Analysis of the DI also supported NOR impairments in the picrotoxin condition (Fig. 5.4D, series 2), with ANOVA showing a trend for a main effect of condition ($F_{(2,22)}$ = 2.93, p = 0.074). Post hoc comparisons revealed that ventral hippocampal picrotoxin reduced the DI compared to saline (p = 0.034), with no significant differences between the other conditions (p > 0.193). Planned one-sample t-tests indicated that rats in the saline and muscimol condition explored the novel object significantly different from chance (t_{11} > 3.45, p < 0.005), and rats in the picrotoxin condition also strongly tended to show novel object preference (t_{11} = 2.1, p = 0.059).

Table 5.1. ***Gross behavioural effects of ventral hippocampal picrotoxin and muscimol infusions as revealed by visual inspection.*** Numbers indicate rats where each behaviour was observed in either series 1 (PTX, 150 ng/0.5 µl/side, n = 15; MUS, 500 ng/0.5 µl/side, n = 16) or series 2 (PTX, 100 ng/0.5 µl/side, n = 13; 250 ng/0.5 µl/side, n = 13). Side effects are reported for all rats which received either picrotoxin or muscimol infusion, regardless of whether they were included in the final analysis. Rats which showed a seizure with loss of postural control or did not reach at least 5 s exploration due to infusion-induced motor impairments, were excluded from the data analysis. No side effects were observed following saline infusion.

Observation	Series 1 (PTX, 150 ng/side)	Series 2 (PTX, 100 ng/side)	Series 1 (MUS, 500 ng/side)	Series 2 (MUS, 250 ng/side)
Facial twitching	1	0	0	0
Wet dog shakes	13	10	0	0
Wild running	2	1	0	0
Clonic limb movement	3	1	0	0
Seizure with loss of postural control	2	1	0	0
Sedation	0	0	3	0
Reversing	0	0	3	0
Oral tendencies	0	0	4	0
Agonistic behaviour in cage	0	0	2	3

5.3.3.3 Ventral hippocampal disinhibition increased the number of line crossings

In series 1, there was a numerical increase in line crossings in the picrotoxin condition, although this was not significant during either phase ($F_{(2,22)} < 2.21$, $p > 0.133$) (Fig. 5.4E, series 1). In series 2, during acquisition, line crossings were increased in the picrotoxin condition, with ANOVA revealing a significant main effect of condition ($F_{(2,22)} = 7.07$, $p = 0.004$) (Fig. 5.4E, series 2). Post hoc comparisons revealed a significant increase in the picrotoxin condition compared to saline ($p = 0.001$), with no significant differences between the other conditions ($p > 0.1$). This increase in line crossings is consistent with our previous findings of increased in open field locomotor activity following ventral hippocampal picrotoxin infusion (Bast et al., 2001a; McGarrity et al., 2017). In the retention phase, rats in all conditions showed a similar number of line crossings, with no main effect of condition ($F_{(2,22)} < 1$).

5.3.3.4 Gross behavioural effects of ventral hippocampal picrotoxin and muscimol infusions as revealed by visual inspection

The gross behavioural effects of ventral hippocampal infusions reported here are for all rats which received either a muscimol or picrotoxin infusion, regardless of whether these rats were included in the final NOR analyses. Following ventral hippocampal picrotoxin infusion, most rats showed wet dog shakes and other seizure-related behaviours, including facial twitching and wild running, which can often be observed before full motor seizures (Lüttjohann et al., 2009; Racine, 1972; Williams et al., 2022). However, only 2 rats out of 15 infused with picrotoxin in series 1 (150 ng/side) and 1 out of 13 rats infused with picrotoxin in series 2 (100

ng/side) showed full seizures with loss of postural control (Table 5.1). These behavioural effects were observed within 5-30 min following picrotoxin infusion. In our earlier studies using ventral hippocampal picrotoxin infusions of up to 150 ng/side, we did not observe seizures or seizure-related effects in Wistar or Lister Hooded rats (Bast et al., 2001a; McGarrity et al., 2017). However, a more recent study using ventral hippocampal picrotoxin (150 ng/side) infusions in rats undergoing testing in fear conditioning did observe seizure-related effects; it was suggested that the stress due to water restriction and fear conditioning contributed to the higher incidence of seizure-related effects (Williams et al., 2022). However, the current study suggests that ventral hippocampal picrotoxin infusions at a dose of 150 ng/side can cause seizures and seizure-related behavioural effects in a substantial number of rats, even without increased stress due to aversive stimuli.

In series 1 of testing, we also observed behavioural side effects following muscimol infusion (500 ng/side) (Table 5.1). In three rats, muscimol infusion resulted in hypoactivity. During the NOR test sessions, these three rats would often move backwards or 'reverse' into the corners of the NOR arena, and showed oral tendencies, such as putting their tail in their mouth and/or licking the arena and objects. Such oral tendencies were also evident in these rats on return to their home cage following task completion. This behaviour was very similar to what was observed in one rat following dorsal hippocampal muscimol infusion. Two out of three of these rats did not show normal behaviour after 3 h and were culled. Inspection of the cannula placement in these rats showed that the infusion cannulae were located more anterior and ventral than placements in the other rats, with tips crossing the fibre bundles into the amygdalohippocampal area, suggesting that these side effects may not be driven by functional inhibition of the ventral hippocampus. In two other rats, agonistic behaviours were observed when the rats were returned to the home cage; the rats would face each other standing on their hind legs, showing their teeth and occasionally hissing. This behaviour was still present 4 h following infusion but subsided within 24 h. The cannula locations in these rats were within the ventral hippocampus (Fig. 5.4D), suggesting that this behaviour is related to functional inhibition of the ventral hippocampus. In series 2, which used a lower muscimol dose of 250 ng/side, we did not observe hypoactivity or unusual behaviour during the NOR sessions, but some agonistic behaviours were still observed in three rats on return to the home cage. In our previous studies, using ventral hippocampal infusions of 500 ng/side and 1 ug/side of muscimol, we observed marked hypoactivity, but not any of the other behaviours (Bast et al., 2001b; Zhang et al., 2014).

5.4 Discussion

Our findings suggest that balanced neural activity within the hippocampus, but not in the mPFC, is important for novel object preference over short (1 min) retention delays. Neural disinhibition in the ventral and dorsal hippocampus impaired NOR relative to saline control, demonstrating a role for hippocampal GABAergic inhibition in NOR. Functional inhibition of the dorsal hippocampus also resulted in impaired novel object preference. In the ventral hippocampus, there was some evidence for impaired NOR following functional inhibition, although this was only observed at the higher dose. In contrast, neither functional inhibition nor disinhibition of the mPFC impaired NOR, suggesting that prefrontal GABAergic inhibition is not required for short term object recognition memory.

5.4.1 Medial prefrontal cortical functional inhibition and disinhibition had no effect on NOR

Prefrontal functional inhibition, caused by microinfusion of muscimol, did not result in an NOR deficit. This is consistent with a study in female Long-Evans rats, where muscimol infusion into the mPFC did not impair NOR over a 1 min retention delay (Neugebauer et al., 2018). Furthermore, this supports the view that the mPFC is not required for standard NOR performance which involves single item recognition (Morici et al., 2015; Warburton & Brown, 2015). However, it should be noted that there are studies which support a role for the PFC in NOR memory consolidation and retrieval over a 24 h retention delay (Akirav & Maroun, 2006; de Landeta et al., 2020; Pezze et al., 2017; Tanimizu et al., 2018; Tuscher et al., 2018).

Neural disinhibition in the mPFC, caused by the microinfusion of picrotoxin, also did not result in an NOR deficit, suggesting that prefrontal GABAergic function is not required for NOR memory over short retention delays. To our knowledge, this is the first study to examine the effects of blocking GABAergic function in the mPFC on NOR. However, in support of the present study, a previous study reported that increased prefrontal neural activity, caused by optogenetic stimulation of mPFC glutamatergic pyramidal neurons, did not impair NOR at a 5 min retention delay (Benn et al., 2016). Given that the mPFC projects to the perirhinal cortex, a region reported to be critically involved in NOR (Warburton & Brown, 2015), we had hypothesised that prefrontal disinhibition would impair NOR due to an aberrant drive of projections to this region (compare Bast et al., 2017). A previous study found that disconnection of the mPFC-perirhinal pathway with crossed lesions did not impair standard NOR performance (Barker et al., 2007), suggesting that the mPFC-perirhinal functional interaction is not necessary for intact NOR. Our finding that prefrontal disinhibition did not affect NOR suggests that an aberrant drive of the mPFC-perirhinal projection also does lead to

NOR impairments. However, although we know that mPFC disinhibition enhances prefrontal burst firing (Pezze et al., 2014), the functional impact on prefrontal projection sites, including the perirhinal cortex, remains to be examined.

5.4.2 Dorsal hippocampal functional inhibition impaired novel object preference

Previous studies have been equivocal in support for a role of the hippocampus in NOR, with temporary pharmacological inactivation studies reporting both impaired (Ásgeirsdóttir et al., 2020; Baker & Kim, 2002; Cinalli Jr et al., 2020; Cohen et al., 2013; de Lima et al., 2006; Haettig et al., 2011; Hammond et al., 2004; Rossato et al., 2007; Stackman Jr et al., 2016) and intact NOR (de Landeta et al., 2020; Oliveira et al., 2010; Sawangjit et al., 2018). Similarly, hippocampal lesion studies have reported impairments in NOR (Ainge et al., 2006; Broadbent et al., 2010; Clark et al., 2000; Gaskin et al., 2010), whereas other lesion studies report no changes in NOR (Albasser et al., 2010, 2012; Barker & Warburton, 2011; Cole et al., 2020; Forwood et al., 2005; Good et al., 2007; Mumby et al., 2005; Winters et al., 2004). The disparate findings in the literature regarding the role of the hippocampus in NOR memory were addressed in a review by Cohen & Stackman Jr et al. (2015), who proposed that the hippocampus is only required for NOR when the retention delay is greater than 10 min, and when a threshold value of approximately 30 s of object exploration is met during the acquisition phase. This hypothesis is supported by two recent studies (Ásgeirsdóttir et al., 2020; Cinalli Jr et al., 2020). Ásgeirsdóttir et al. (2020) reported a delay dependent impairment in NOR following dorsal hippocampal muscimol infusion, with a retention delay of 20 min, but not 5 min, resulting in NOR impairments. A threshold exploration value for hippocampal involvement in NOR is supported by a study using a 24 h retention delay, where muscimol infusion into the dorsal hippocampus impaired NOR when 30 s, but not 10 s, of exploration was reached (Cinalli Jr et al., 2020). However, the results of the present study do not fully support the conclusion proposed by Cohen & Stackman Jr (2015). In experiment 2, there was only one rat which did not reach 30 s of exploration (exploration time was 24 s) and removing this rat did not change the significance of the findings. All other rats reached this exploration threshold, suggesting that the memory was under hippocampal control (Cohen & Stackman Jr, 2015). However, using a 1 min retention delay, we found impaired NOR following dorsal hippocampal muscimol infusion, suggesting that the dorsal hippocampus is involved in NOR at short retention delays. In support of a role of the hippocampus at shorter retention intervals, Gaskin et al. (2010) found NOR impairments in rats with dorsal hippocampal lesions over a 35 s retention delay.

More recent studies investigating the role of the dorsal hippocampus in NOR using chemogenetics have also produced varied results. Chemogenetic hM4Di mediated inhibition of dorsal hippocampal neurons did not impair NOR at a 24 h retention delay (López et al., 2016; Tuscher et al., 2018). In addition, overactivation of dorsal CA1 inhibitory interneurons after the acquisition phase did not impair NOR memory at a 24 h retention delay (Yu et al., 2018). However, Yu et al., (2018) also did not find an effect on locomotor activity, whereas in the present study we found an increase in line crossings consistent with previously reported changes in locomotor activity following dorsal hippocampal muscimol infusion (Bast & Feldon, 2003). This suggests that chemogenetic activation of inhibitory neurons may have a different behavioural profile to pharmacological activation by muscimol. In contrast, however, chemogenetic inhibition of the dorsal hippocampus using KORD mediated DREADDs did impair NOR memory, suggesting that different forms of DREADDs may differentially influence NOR capacity (Tuscher et al., 2018). Moreover, studies using chemo/optogenetics to target specific hippocampal circuits between CA1 and CA3 have also found impairments in NOR memory at 5 min and 24 h retention delays (Lin et al., 2021; Raam et al., 2017).

Nevertheless, our finding that dorsal hippocampal functional inhibition impairs NOR is consistent with the idea that the hippocampus, as part of the medial temporal lobe system, performs a pivotal role in bringing together a range of object features from different sensory modalities derived from neocortical areas into one memory representation (Olsen et al., 2012; Preston & Eichenbaum, 2013; Squire & Zola-Morgan, 1991). In line with this idea, object exploration is associated with increased neural activity in the hippocampal CA1 region (Cohen et al., 2013; Nagelhus et al., 2023), which is suggested to process both spatial and non-spatial object information (Ásgeirsdóttir et al., 2020; Beer et al., 2013). Furthermore, NOR acquisition sessions were reported to result in potentiation of hippocampal CA3-CA1 synapses, although this effect was not evident before 6 h after the session (Clarke et al., 2010).

Thus, overall, studies support a physiological role for the hippocampus in NOR, however, many studies investigating dorsal hippocampal involvement in NOR continue to produce mixed results, and the findings of the present study do little to settle this controversy. Performance on the NOR task is reported be sensitive to task procedure, with length of habituation, sample object exploration, and retention delay all reported to influence performance (Cohen & Stackman Jr, 2015; Oliveira et al., 2010; Stefanko et al., 2009; Waters et al., 2023). This may explain discrepancies between studies and highlights the need for a standardised NOR task procedure which can be used across different sites and research groups.

5.4.3 Limited evidence for ventral hippocampal functional inhibition to impair NOR

Experiment 3 provided weak evidence that ventral hippocampal functional inhibition impaired NOR. In series 1, ventral hippocampal muscimol infusion slightly reduced novel object exploration time, but left the DI largely unaffected and reduced exploration times during the acquisition phase. However, in series 2, when the muscimol dose was reduced, there was no longer evidence for an NOR impairment. Consistent with a limited impact of ventral hippocampal functional inhibition on NOR, optogenetic inhibition of ventral hippocampal excitatory neurons during the NOR retention phase did not impair NOR at a 10 min retention delay (Sun et al., 2020). In contrast, ventral hippocampal infusion of a relatively low dose of muscimol (50 ng/side) before the acquisition phase in female Long Evans rats impaired NOR at a 1 min retention delay (Neugebauer et al., 2018). However, mean exploration times reported in this study were less than 15 s, i.e., low compared to 50-70 s in the present study. Given that exploration times are suggested to influence the likelihood of memory recall in NOR (Cohen & Stackman Jr, 2015), these relatively low exploration times may have influenced the results. Alternatively, the contrasting results may reflect sex differences with respect to hippocampal involvement in NOR memory, or the different doses of muscimol used.

Overall, the results of the present study suggest that NOR may be more sensitive to disruption by dorsal than ventral hippocampal functional inhibition. There is some evidence that dorsal and ventral hippocampal regions may support different aspects of recognition memory, with the dorsal region involved in the encoding of specific objects and their contextual location, whereas the ventral region may be involved with linking events within a context and distinguishing different contexts (Preston & Eichenbaum, 2013). This, therefore, may underlie the different sensitivities of standard NOR to ventral and dorsal hippocampal functional inhibition.

5.4.4 Dorsal and ventral hippocampal disinhibition impaired novel object preference

Neural disinhibition in both the dorsal and ventral hippocampus resulted in NOR impairments. This is in line with findings of impaired NOR following dorsal hippocampal infusion of the GABA-A receptor antagonist bicuculline at a 1 min (Riordan et al., 2018) and 24 h (Kim et al., 2014) retention delay. In contrast, ventral hippocampal bicuculline infusion was reported to have no effect on NOR at a 1 min retention delay (Neugebauer et al., 2018). However, as previously mentioned, the low exploration times in this study may have influenced the results.

In the present study, given that ventral hippocampal disinhibition impaired novel object preference, whereas ventral hippocampal functional inhibition had limited effects, it is possible that the NOR impairments found may be due to an aberrant drive of projections to other brain regions. A recent metabolic imaging study has shown that picrotoxin infusion (150 ng/side) into the ventral hippocampus increased regional cerebral blood flow locally around the infusion site, but decreased regional cerebral blood flow in the dorsal hippocampus (Williams et al., 2020), possibly reflecting ventral hippocampal feedforward inhibition (Sik et al., 1994). This may suggest that the NOR impairments found following ventral hippocampal disinhibition could, partly, be due to an inactivation of the dorsal hippocampus. Alternatively, disinhibition in the ventral or dorsal hippocampus may impair object preference due to an aberrant drive of projections to regions outside the hippocampus which are reported to be involved in recognition memory, such as the perirhinal and entorhinal cortex (Chao et al., 2022).

The reduced total object exploration time during the acquisition phase found here following ventral hippocampal disinhibition may confound the interpretation of impaired novel object preference. However, It is likely that such changes were caused by the effect of picrotoxin infusion on locomotor activity, whereby increased movement through the arena detracts from object exploration. In the present study, the number of line crossings was increased following ventral hippocampal picrotoxin infusion, suggesting that locomotor activity was increased, in line with previous studies (Bast et al., 2001a; McGarrity et al., 2017). Still, it is possible that reduced sample object exploration could result in a weaker memory for the familiar object, thereby impacting the recollection of this object in the retention trial. However, in experiment 3, exploration times in all conditions were above 30 s, suggesting that exploration time was sufficient for ‘strong’ memories to be formed in all conditions (Cohen & Stackman Jr, 2015).

5.4.5 Hippocampal disinhibition and functional inhibition may impair novelty detection

Interestingly, in the present study, NOR impairments following hippocampal disinhibition and dorsal hippocampal inhibition mostly manifested as a marked reduction in novel object exploration, with familiar object exploration time was not significantly affected (although there were some numerical increases). It is unclear whether other studies have also found a novel object specific change in exploration following hippocampal manipulations, as often only the DI, rather than individual object exploration times for both familiar and novel objects, are reported (Ásgeirsdóttir et al., 2020; Cinalli Jr et al., 2020; Cohen et al., 2013; de Lima et al., 2006; Neugebauer et al., 2018; Oliveira et al., 2010; Sawangjit et al., 2018; Stackman Jr et al.,

2016; Tuscher et al., 2018). If object memory is impaired, rats may explore both objects as novel (impaired familiarity detection), due to an inability to recognise the previously encountered object. Alternatively, rats may view both objects as familiar (impaired novelty detection). Consistent with the long-standing idea that the hippocampus is important for novelty detection (Kumaran & Maguire, 2007; Numan, 2015; Olsen et al., 2012; Vinogradova, 2001), it was suggested that novelty and familiarity processing are partly independent and make distinct contributions to object recognition memory (Kafkas & Montaldi, 2018). The authors suggested that the novelty signals computed in the perirhinal and para-hippocampal cortex selectively contribute to the detection and evaluation of relative familiarity, whereas hippocampal processing is important for novelty detection (Kafkas & Montaldi, 2018). It is, therefore, possible that NOR deficits may not be entirely due to a memory impairment, but rather to a deficit in hippocampus dependent processing of novelty, or in the rats' natural propensity for novel object exploration (Mumby, 2001). The impaired novel object exploration could also result from a decrease in perceived salience of the novel object. Indeed, a link between hippocampal activity and salience attribution has been demonstrated in both human and rodent studies (see Kätzel et al., 2020 for review).

5.4.6 A comparison to NMDAR hypofunction induced NOR deficits

The finding of the present study that mPFC neural disinhibition does not impair NOR memory suggests that the NOR deficits reported following NMDAR hypofunction (Cadinu et al., 2018) cannot be directly attributed to reduced GABA function in the mPFC. It follows, that GABAergic marker changes reported in the mPFC of scPCP treated rats (Gigg et al., 2020; McKibben et al., 2010; Redrobe et al., 2012) cannot be exclusively linked to the NOR impairment. In contrast, studies in scPCP treated rats suggest a key role for the mPFC in NOR deficits. In vivo electrophysiology experiments found that scPCP treatment prevented the increase in mPFC neural activity seen during novel object exploration by vehicle treated rats (Asif-Malik et al., 2017). In line with this, an in vivo microdialysis study found that scPCP treatment prevented the increase in prefrontal cortex dopamine levels seen in vehicle treated rats during the retention trial (McLean et al., 2017). These studies also suggest that reduced mPFC activity, rather than hyperactivity induced by disinhibition, may contribute to the scPCP NOR deficit, although the present study does not support this conclusion.

The finding that hippocampal neural disinhibition impairs NOR using a 1 min retention delay may suggest that the NOR deficits reported following NMDAR hypofunction could be attributed to a loss of hippocampal GABAergic function (Cadinu et al., 2018). However, the

pattern of the NOR deficits found in experiment 2 and 3 of the present study, whereby impairments mainly manifested as a reduction in novel object exploration, appear to be different to the scPCP-induced NOR deficits reported, which often show an increase in familiar object exploration (Arnt et al., 2010; Damgaard et al., 2011; Grayson et al., 2007, 2014). Further analysis of the scPCP-induced NOR deficit reported here in chapter 2, revealed that scPCP treatment resulted in a significant increase in familiar object exploration ($F_{(1,28)}$ = 15.5, p < 0.001), as well as a strong trend for a reduction in exploration of the novel object ($F_{(1,28)}$ = 3.63, p = 0.067). In addition, the NOR impairment found in the present study is arguably weaker than the scPCP-induced NOR deficit as, although NOR was impaired relative to saline, t-tests often demonstrated significant or trend level novel object preference following hippocampal muscimol or picrotoxin infusion, whereas this preference is often not significant following scPCP treatment (Arnt et al., 2010; Damgaard et al., 2011; Grayson et al., 2007, 2014). Therefore, it is perhaps more likely that hippocampal GABAergic dysfunction may contribute to the scPCP induced NOR impairments, rather than exclusively drive this deficit. Indeed, some studies have reported an amelioration of scPCP-induced NOR deficits following systemic enhancement of GABA function (Damgaard et al., 2011; Rajagopal et al., 2018). However, in support of a causal link between localised dorsal hippocampal GABAergic dysfunction and scPCP-induced NOR deficits, a study in ovariectomised rats found that the scPCP-induced NOR deficit was reversed by dorsal hippocampal infusions of muscimol (Riordan et al., 2018). In contrast, ventral hippocampal microinfusions of bicuculline was reported to reverse the scPCP-induced NOR deficit (Neugebauer et al., 2018). The discrepancy between these two studies regarding the contribution of hippocampal GABA transmission to scPCP-induced NOR deficits may be due to the region examined; it is possible that ventral and dorsal hippocampus regions may be differentially contributing to the NOR impairments. However, the present study does not support an involvement of enhanced ventral hippocampal GABA activity in producing NOR deficits.

5.4.7 Conclusions

In summary, balanced hippocampal, but not prefrontal, neural activity contributes to novel object preference at a 1 min retention delay. We have outlined evidence for a role of the hippocampus in NOR at short delays; however, it is likely that object recognition is mediated by a complex circuit recruiting multiple brain regions, which may be disrupted by excessive or reduced hippocampal activity. In addition, the present study suggests that ventral and/or dorsal hippocampal GABA deficits may contribute to scPCP-induced NOR impairments, whereas mPFC neural disinhibition is unlikely to be causal to scPCP-induced deficits in NOR.

Chapter 6: General discussion

The work outlined in this thesis examined the link between NMDAR hypofunction and neural disinhibition (i.e., reduced GABAergic inhibition) in the PFC and hippocampus, with a focus on how these processes may mediate cognitive deficits in rat models. GABAergic inhibition has been linked to mechanisms suggested to be important for cognitive processing, such as the regulation of burst firing and generation of neural oscillations (Buzsáki & Wang, 2012; Izhikevich et al., 2003; McGarrity et al., 2017; Pezze et al., 2014; Sohal et al., 2009). Given that impaired GABAergic inhibition in the PFC and hippocampus is a core feature of schizophrenia, neural disinhibition has been suggested to contribute to the cognitive deficits associated with schizophrenia (Bast et al., 2017; Dienel & Lewis, 2019; Tregellas et al., 2014). Such GABAergic deficits have also been suggested to be mechanistically linked with NMDAR hypofunction (Cohen et al., 2015; Hardingham & Do, 2016; Lisman et al., 2008; Steullet et al., 2016). Findings of reduced levels of GABAergic biomarkers in rodent models of NMDAR hypofunction, alongside impairments in cognition, support the hypothesis that these two pathologies may converge on a common pathological hub (Cadinu et al., 2018; Hardingham & Do, 2016; Lisman et al., 2008). In chapter 1, we reviewed the current evidence for this hypothesis and highlighted gaps of knowledge in the literature. In subsequent chapters, we aimed to address this hypothesis experimentally, by comparing and examining the cognitive and neural changes in rat models of NMDAR hypofunction and regional neural disinhibition.

6.1 Overview of main findings

The studies reviewed in chapter 1 demonstrated significant evidence for reduced GABAergic markers following NMDAR hypofunction, however, this was mainly apparent in studies examining PV interneuron density using immunohistochemistry. In addition, previous studies using acute and neurodevelopmental models of NMDAR hypofunction demonstrated compelling electrophysiological evidence for neural disinhibition in these models. However, importantly, studies investigating the impact of sub-chronic NMDAR hypofunction on GABAergic function were equivocal in support of a link between NMDAR hypofunction and neural disinhibition. Moreover, the role of sub-chronic NMDAR hypofunction and regional neural disinhibition in mediating cognition on the watermaze DMP and NOR task, respectively, had not been investigated.

In chapter 2, we examined the behavioural changes induced by scPCP treatment in male and female rats. We hypothesised that, if scPCP treatment resulted in pronounced deficits in hippocampal GABAergic inhibition, scPCP treatment would result in a similar behavioural

profile to that produced by ventral hippocampal microinfusions of the GABA-A receptor antagonist picrotoxin (i.e., impaired watermaze DMP performance, locomotor hyperactivity, decreased startle reactivity; McGarrity et al., 2017). We found that scPCP treatment did not impair watermaze DMP performance, nor did it affect locomotor activity or startle reactivity. This suggests that hippocampal disinhibition is not a pronounced feature of the scPCP model. In this study, we also tested scPCP treated rats in NOR, in order to confirm previous reports of long-lasting impairments over a short 1 min retention delay (Cadinu et al., 2018; Neill et al., 2010; Rajagopal et al., 2014). However, we found that the NOR deficit was only significant at 1 week post scPCP treatment and not significant from 3 weeks post treatment. As previous reports had indicated a long-lasting reduction in NOR caused by scPCP treatment, we hypothesised that frequent handling and/or watermaze training may have influenced the presentation of this deficit. Repeating the study with only NOR testing and limited handling, resulted in an NOR deficit which persisted until the end of study at 6 weeks post-treatment. This highlights the sensitivity of scPCP-induced NOR deficits to potential disruption by changes in environment/behaviour, consistent with recent evidence from other studies (Landreth et al., 2023; Mitsadali et al., 2020).

In chapter 3, we aimed to examine the link between NMDAR hypofunction and regional neural disinhibition more directly by using simple western analysis to investigate the relative protein levels of GAD67 and PV in the PFC, DH and I-VH of the two cohorts of rats used in chapter 2. We aimed to interpret any GABAergic biomarker changes in the context of the behavioural results in chapter 1, i.e., no watermaze DMP impairment but NOR deficits (and amelioration of NOR deficits in cohort 1). We found no changes in GAD67 or PV protein levels in the PFC or DH, which does not offer support for the hypothesis that NMDAR hypofunction would induce neural disinhibition in these regions. In the I-VH of scPCP treated female rats, we found a significant reduction in GAD67 protein levels, which was present across both cohorts. In contrast, no changes in GAD67 protein levels were found in the I-VH of male rats, suggesting that scPCP treatment may have sex-specific neuropathological effects. The influence of sex on scPCP induced physiological changes was also apparent in chapter 2, where body weight reductions were more pronounced in male rats. Therefore, although behavioural effects of scPCP were consistent across males and females in the present studies, scPCP treatment may have different physiological effects in males and females, highlighting the importance of using both sexes in research. Importantly, however, PV levels were found to be increased in the I-VH of both male and female scPCP treated rats in cohort 1. Although this finding contrasts with the many studies reporting PV-immunoreactive cell reductions using immunohistochemistry,

studies investigating PV protein and mRNA levels have been less univocal in support for PV reductions, with a complex pattern of different findings reported across studies (as discussed in chapter 3). We propose that this apparent PV increase found in our study may, perhaps, rather reflect an experience-related decrease of PV in control rats (Donato et al., 2013). This finding may, therefore, warrant further histological investigations in a cohort of rats which have not undergone behavioural testing. In the context of the behavioural results reported in chapter 2, findings from cohort 1 rats of increased PV, and decreased GAD67 in female scPCP treated rats, suggest that such GABAergic alterations do not lead to impaired watermaze DMP task performance or sustained NOR deficits. In addition, in cohort 2 rats, the reduced GAD67 in the female scPCP treated rats is unlikely to entirely account for the sustained NOR impairment, given that male scPCP treated rats also showed NOR deficits but no changes in I-VH GAD67 levels. Therefore, overall, chapter 3 demonstrated that NMDAR hypofunction, caused by scPCP treatment, leads to limited alterations in GABAergic markers, which are unlikely to entirely account for the NOR deficits reported in chapter 2. Importantly, we also do not rule out the possibility that these findings, and the relatively varied findings in previous studies, may represent sampling errors due to inherent variability of the histological measures within the scPCP model and small sample sizes. One gap in our knowledge of the scPCP model is how long following treatment GABAergic changes may occur. In this thesis, we collected brains at 6 weeks post scPCP treatment, as PV-immunoreactive cell deficits have been suggested to be most pronounced at this point (Jenkins et al., 2008; Cadinu et al., 2018). However, this observation alone makes attributing an NOR deficit to PV changes problematic, since NOR impairments may be observed from only 1 week post scPCP treatment. It would, therefore, be useful to determine whether any differences in PV and GAD67 protein expression are found with different lengths of washout.

In chapter 4, we examined the impact of scPCP treatment in female rats on the synaptic excitability of hippocampal circuits. Using evoked in vivo recordings under urethane anaesthesia, we applied low frequency train stimulation to the subiculum or CA3 region, with the hope of replicating findings of reverberatory responses (or re-entrance) in the hippocampal formation, as reported in Kloosterman et al. (2004) and Davis et al (2014). Such re-entrance may be considered a measure of overall excitability within the hippocampal formation, and we hypothesised that re-entrance would be increased in scPCP treated rats, due to a reduction in local GABAergic inhibition. We found that a subset of rats in both treatment groups exhibited hippocampal response reverberation, consistent with re-entrance via the deep to superficial connections in the entorhinal cortex, followed by activation of the

perforant path (Deadwyler et al., 1975; Kloosterman et al., 2003, 2004). A comparison across treatment groups revealed limited evidence of increased instances of re-entrance (and perhaps hyperexcitability) following subiculum stimulation, but decreased instances of re-entrance following Schaffer collateral stimulation. In addition, scPCP treated rats showed an increase in the frequency of dentate gyrus population spikes observed during the train stimuli, which may suggest weaker inhibitory control. However, both conclusions are limited by the small sample size. Nevertheless, current source density analysis revealed a laminar profile of synaptic currents that was similar across both treatment groups, and consistent with previous reports of Schaffer collateral and perforant path activation, indicating intact fibre pathways in scPCP treated rats. Overall, to our knowledge, this is the first study to confirm that hippocampal re-entrance, which has been suggested to be important for the temporal storage of information (Iijima et al., 1996; Kloosterman et al., 2003; Ohara et al., 2018), is intact in scPCP treated rats. Furthermore, we suggest that investigating re-entrance phenomena is a useful tool for probing overall hippocampal network activity. Future studies using a larger sample size would be useful to complement this work.

Finally, in chapter 5, we aimed to examine the impact of prefrontal and hippocampal neural disinhibition on NOR. The NOR task has been used widely to study cognitive deficits in rodent models of relevance to schizophrenia, with GABAergic changes in these models suggested to contribute to the NOR deficits (e.g., Cadinu et al., 2018). Using local microinfusions of the GABA-A receptor antagonist picrotoxin, and agonist muscimol, we found that mPFC disinhibition and functional inhibition did not impair NOR. Therefore, the prefrontal GABAergic deficits previously reported in NMDAR hypofunction models (but not found in this thesis), are unlikely to contribute to scPCP-induced NOR deficits. In the hippocampus, however, we found that both functional inhibition and neural disinhibition affected NOR performance. This may suggest that reduced hippocampal GABAergic inhibition contributes to the scPCP-induced NOR impairments, as we have demonstrated a role for hippocampal GABAergic inhibition in intact NOR. However, given that functional inhibition also affected NOR performance (although this was only present at the higher dose in the ventral hippocampus), it may also be the case that an increase in hippocampal GABAergic inhibition is implicated in scPCP-induced NOR deficits. Thus, overall, the study suggested that alterations in hippocampal, but not prefrontal, GABAergic activity has the potential to disrupt NOR performance, and, therefore, hippocampal GABA changes may contribute to scPCP-induced NOR impairments. However, this hypothesis is not supported by the findings in chapter 2, which indicated no pronounced hippocampal dysfunction in scPCP treated rats. Furthermore, the NOR deficits found in this

chapter appeared to be weaker than scPCP-induced NOR deficits, and mainly affected novel object exploration. It is therefore likely that scPCP-induced NOR deficits are also driven by impairments in other brain regions. The perirhinal cortex presents as the most likely candidate for this, given its prominent role in NOR (Warburton & Brown, 2015). Indeed, a study examining regional brain volume reductions in scPCP treated rats found that perirhinal cortex volume reductions in scPCP treated rats was correlated with reduced novel object exploration (Doostdar et al., 2019).

6.2 Discussion of thesis findings in the context of schizophrenia

Although the scope of this thesis was to examine the link between NMDAR hypofunction and neural disinhibition, reference has been made throughout to how these processes are affected in schizophrenia. Therefore, it is perhaps pertinent to discuss some of the findings of this thesis in the context of findings in schizophrenia. Indeed, if we were explicitly examining the link between NMDAR hypofunction and neural disinhibition, the use of a NMDAR subunit knockout model may have been more appropriate. The scPCP model, on the other hand, was chosen for its relevance to the cognitive symptom domain of schizophrenia, as well as for the GABAergic changes reported in the model which appear to mirror findings in post-mortem schizophrenia studies. The first finding of this thesis, that scPCP treatment does not impair watermaze DMP performance, indicates that the scPCP model does not show one key cognitive deficit associated with schizophrenia, as patients with schizophrenia have shown impairments on hippocampus-dependent tasks in general (Bast, 2011; Cirillo & Seidman, 2003; Piskulic et al., 2007; Saykin et al., 1991; Tamminga et al., 2010) and specifically on virtual analogues of place learning tasks in the watermaze (Fajnerová et al., 2014; Folley et al., 2010; Hanlon et al., 2006). A cognitive deficit following scPCP treatment was confirmed in this thesis using the NOR task, and findings from chapter 5 suggest that this deficit may be, in part, mediated by changes in hippocampal GABAergic inhibition. Such NOR deficits have been suggested to be relevant to recognition memory impairments in schizophrenia (Grayson et al., 2015; Lyon et al., 2012; Meltzer et al., 2013). We also found that the NOR deficit in scPCP treated rats was sensitive to disruption, which we hypothesised may be due to increased handling or aerobic exercise. Interestingly, aerobic exercise has also been reported to improve cognitive function in patients with schizophrenia (Falkai et al., 2017; Firth et al., 2017). However, it should be noted that, whereas the watermaze task has a virtual analogue for testing in humans, the translatability of the NOR task to human visual memory tests has been questioned, making direct comparisons challenging (Lyon et al., 2012; Mumby, 2001).

One of the most consistent post-mortem findings in schizophrenia is a reduction in GABAergic markers. Although many of these studies were based on interneuron density changes, GABAergic deficits in schizophrenia are generally considered to reflect a reduction in protein and/or mRNA expression per neuron, rather than cell death (Dienel et al., 2023; Enwright et al., 2016; Hashimoto et al., 2003). Studies in NMDAR hypofunction models have also mainly demonstrated interneuron density changes using immunohistochemistry, whereas protein and mRNA analyses have produced a more complex pattern of results (see chapter 3). Importantly, although our finding of decreased GAD67 in female scPCP treated rats is consistent with findings in schizophrenia, the increased relative PV protein levels found in cohort 1 scPCP treated rats is difficult to reconcile with findings in schizophrenia. In addition, the present study is not the only study to have reported an increase in PV protein following scPCP treatment (Fletcher et al., 2023). Therefore, it is important that NMDAR hypofunction studies not only examine interneuron cell density but also protein and/or mRNA levels in order to validate findings of altered GABAergic markers with the findings in schizophrenia. Furthermore, although much attention has been given to parvalbumin and GAD67 deficits in schizophrenia, other GABAergic markers have also been reported to be reduced, with somatostatin, in particular, showing reductions in schizophrenia (Alherz et al., 2017; Dienel et al., 2023; Fung et al., 2010, 2014; Konradi et al., 2011; Morris et al., 2008). It is therefore important that somatostatin protein levels and interneuron density are characterised in NMDAR hypofunction models, in order to determine the extent to which scPCP treatment may recapitulate GABAergic deficits of relevance to schizophrenia. Nevertheless, while direct comparisons of findings in the scPCP model to schizophrenia may be limited, the scPCP model still offers the opportunity to examine the impact of NMDAR hypofunction, which has been implicated in many disorders (Ibi et al., 2017; Kumar & Foster, 2013; Newcomer et al., 2000; Zhou & Sheng, 2013; Zorumski & Izumi, 2012), and thus presents a useful tool to enhance our understanding of how NMDAR hypofunction may lead to pathology and symptoms in these disorders.

6.3 Conclusions

Overall, we have demonstrated that scPCP treatment does not result in a behavioural profile which matches the key behavioural deficits found following acute pharmacological ventral hippocampal disinhibition, suggesting that scPCP treatment does not result in pronounced hippocampal disinhibition. In addition, ex vivo histological studies revealed only limited evidence for reduced GABA markers in scPCP treated rats, with GAD67 protein reductions found only in females and only in the intermediate to ventral hippocampus, with no changes

found in the dorsal hippocampus or PFC. Importantly, we also found an increase in PV in cohort 1 male and female scPCP treated rats, which does not support the overarching thesis hypothesis. Investigations into the excitability of the hippocampal neural network following scPCP treatment, by monitoring instances of re-entrance following low frequency train stimulation, revealed limited evidence for increased excitability in the perforant path, but decreased excitability of the Schaffer collaterals. This may suggest that hippocampal pathways are differentially affected by scPCP treatment. However, conclusions from this study are limited by the small sample size. Finally, we have demonstrated a role for hippocampal, but not prefrontal, GABAergic inhibition in intact NOR over a short 1 min retention delay. This finding suggests that hippocampal GABAergic deficits may contribute, in part, to NOR deficits found in NMDAR hypofunction models. Thus, overall, we have found limited evidence for a link between NMDAR hypofunction and neural disinhibition in PFC and hippocampus in the modulation of cognition. Crucially, the lack of a watermaze DMP task impairment in scPCP treated rats, combined with weak post-mortem evidence for reduced GABAergic markers, suggests that scPCP treatment does not lead to pronounced hippocampal disinhibition and, thus, is unlikely to underlie the cognitive deficits in the model.

References

Abdul-Monim, Z., Neill, J. C., & Reynolds, G. P. (2007). Sub-chronic PCP induces a deficit in reversal learning and in parvalbumin-immunoreactive GABAergic neurons in the rat. *Journal of Psychopharmacology*, *21*, 198–205.

Ahnaou, A., Huysmans, H., Biermans, R., Manyakov, N. V, & Drinkenburg, W. (2017). Ketamine: differential neurophysiological dynamics in functional networks in the rat brain. *Translational Psychiatry*, *7*(9), e1237–e1237.

Ainge, J. A., Heron-Maxwell, C., Theofilas, P., Wright, P., de Hoz, L., & Wood, E. R. (2006). The role of the hippocampus in object recognition in rats: examination of the influence of task parameters and lesion size. *Behavioural Brain Research*, *167*(1), 183–195.

Akbarian, S., Kim, J. J., Potkin, S. G., Hagman, J. O., Tafazzoli, A., Bunney Jr, W. E., & Jones, E. G. (1995). Gene Expression for Glutamic Acid Decarboxylase Is Reduced Without Loss of Neurons in Prefrontal Cortex of Schizophrenics. *Archives of General Psychiatry*, *52*(4), 258–266. https://doi.org/10.1001/archpsyc.1995.03950160008002

Akirav, I., & Maroun, M. (2006). Ventromedial prefrontal cortex is obligatory for consolidation and reconsolidation of object recognition memory. *Cerebral Cortex*, *16*(12), 1759–1765.

Aksoy-Aksel, A., & Manahan-Vaughan, D. (2013). The temporoammonic input to the hippocampal CA1 region displays distinctly different synaptic plasticity compared to the Schaffer collateral input in vivo: significance for synaptic information processing. *Frontiers in Synaptic Neuroscience*, *5*, 5.

Albasser, M. M., Amin, E., Lin, T.-C. E., Iordanova, M. D., & Aggleton, J. P. (2012). Evidence that the rat hippocampus has contrasting roles in object recognition memory and object recency memory. *Behavioral Neuroscience*, *126*(5), 659.

Albasser, M. M., Chapman, R. J., Amin, E., Iordanova, M. D., Vann, S. D., & Aggleton, J. P. (2010). New behavioral protocols to extend our knowledge of rodent object recognition memory. *Learning & Memory*, *17*(8), 407–419.

Alger, B. E., & Teyler, T. J. (1976). Long-term and short-term plasticity in the CA1, CA3, and dentate regions of the rat hippocampal slice. *Brain Research*, *110*(3), 463–480. https://doi.org/https://doi.org/10.1016/0006-8993(76)90858-1

Alherz, F., Alherz, M., & Almusawi, H. (2017). NMDAR hypofunction and somatostatin-expressing GABAergic interneurons and receptors: A newly identified correlation and its effects in schizophrenia. *Schizophrenia Research: Cognition*, *8*, 1–6.

Alstott, J., & Timberlake, W. (2009). Effects of rat sex differences and lighting on locomotor exploration of a circular open field with free-standing central corners and without peripheral walls. *Behavioural Brain Research*, *196*(2), 214–219. https://doi.org/https://doi.org/10.1016/j.bbr.2008.09.001

Amaral, D. G., & Witter, M. P. (1989). The three-dimensional organization of the hippocampal formation: a review of anatomical data. *Neuroscience*, *31*(3), 571–591.

Amat-Foraster, M., Celada, P., Richter, U., Jensen, A. A., Plath, N., Artigas, F., & Herrik, K. F. (2019). Modulation of thalamo-cortical activity by the NMDA receptor antagonists ketamine and phencyclidine in the awake freely-moving rat. *Neuropharmacology*, *158*, 107745.

Amitai, N., Kuczenski, R., Behrens, M. M., & Markou, A. (2012). Repeated phencyclidine administration alters glutamate release and decreases GABA markers in the prefrontal cortex of rats. *Neuropharmacology*, *62*(3), 1422–1431.

Anastasio, N. C., & Johnson, K. M. (2008). Atypical anti-schizophrenic drugs prevent changes in cortical N-methyl-D-aspartate receptors and behavior following sub-chronic phencyclidine administration in developing rat pups. *Pharmacology Biochemistry and Behavior*, *90*(4), 569–577.

Andersen, J. D., & Pouzet, B. (2004). Spatial memory deficits induced by perinatal treatment of rats with PCP and reversal effect of D-serine. *Neuropsychopharmacology*, *29*(6), 1080–1090. https://doi.org/10.1038/sj.npp.1300394

Andersen, P., Bliss, T. V. P., & Skrede, K. K. (1971). Lamellar organization of hippocampal excitatory pathways. *Experimental Brain Research*, *13*, 222–238.

Andrews-Zwilling, Y., Gillespie, A. K., Kravitz, A. V, Nelson, A. B., Devidze, N., Lo, I., Yoon, S. Y., Bien-Ly, N., Ring, K., Zwilling, D., Potter, G. B., Rubenstein, J. L. R., Kreitzer, A. C., & Huang, Y. D. (2012). Hilar GABAergic Interneuron Activity Controls Spatial Learning and Memory Retrieval. *Plos One*, *7*(7), 12. https://doi.org/10.1371/journal.pone.0040555

Anticevic, A., Corlett, P. R., Cole, M. W., Savic, A., Gancsos, M., Tang, Y. Q., Repovs, G., Murray, J. D., Driesen, N. R., Morgan, P. T., Xu, K., Wang, F., & Krystal, J. H. (2015). N-Methyl-D-Aspartate Receptor Antagonist Effects on Prefrontal Cortical Connectivity Better Model Early Than Chronic Schizophrenia. *Biological Psychiatry*, *77*(6), 569–580. https://doi.org/10.1016/j.biopsych.2014.07.022

Antonucci, F., Alpár, A., Kacza, J., Caleo, M., Verderio, C., Giani, A., Martens, H., Chaudhry, F. A., Allegra, M., & Grosche, J. (2012). Cracking down on inhibition: selective removal of GABAergic interneurons from hippocampal networks. *Journal of Neuroscience*, *32*(6), 1989–2001.

Arnt, J., Bang-Andersen, B., Grayson, B., Bymaster, F. P., Cohen, M. P., DeLapp, N. W., Giethlen, B., Kreilgaard, M., McKinzie, D. L., & Neill, J. C. (2010). Lu AE58054, a 5-HT6 antagonist, reverses cognitive impairment induced by subchronic phencyclidine in a novel object recognition test in rats. *International Journal of Neuropsychopharmacology*, *13*(8), 1021–1033.

Arvanov, V. L., & Wang, R. Y. (1999). Clozapine, but not haloperidol, prevents the functional hyperactivity of N-methyl-D-aspartate receptors in rat cortical neurons induced by subchronic administration of phencyclidine. *Journal of Pharmacology and Experimental Therapeutics*, *289*(2), 1000–1006.

Ásgeirsdóttir, H. N., Cohen, S. J., & Stackman Jr, R. W. (2020). Object and place information processing by CA1 hippocampal neurons of C57BL/6J mice. *Journal of Neurophysiology*, *123*(3), 1247–1264.

Ashby, D. M., Habib, D., Dringenberg, H. C., Reynolds, J. N., & Beninger, R. J. (2010). Subchronic MK-801 treatment and post-weaning social isolation in rats: differential effects on locomotor activity and hippocampal long-term potentiation. *Behavioural Brain Research*, *212*(1), 64–70.

Asif-Malik, A., Dautan, D., Young, A. M. J., & Gerdjikov, T. V. (2017). Altered cortico-striatal crosstalk underlies object recognition memory deficits in the sub-chronic phencyclidine model of schizophrenia. *Brain Structure and Function*, *222*(7), 3179–3190.

Baker, K. B., & Kim, J. J. (2002). Effects of stress and hippocampal NMDA receptor antagonism on recognition memory in rats. *Learning & Memory*, *9*(2), 58–65.

Bannerman, D. M., Sprengel, R., Sanderson, D. J., McHugh, S. B., Rawlins, J. N., Monyer, H., & Seeburg, P. H. (2014). Hippocampal synaptic plasticity, spatial memory and anxiety. *Nature reviews. Neuroscience*, *15*(3), 181–192. https://doi.org/10.1038/nrn3677

Barker, G. R. I., Bird, F., Alexander, V., & Warburton, E. C. (2007). Recognition memory for objects, place, and temporal order: a disconnection analysis of the role of the medial prefrontal cortex and perirhinal cortex. *Journal of Neuroscience*, *27*(11), 2948–2957.

Barker, G. R. I., & Warburton, E. C. (2011). When is the hippocampus involved in recognition memory? *Journal of Neuroscience*, *31*(29), 10721–10731.

Barnes, S. A., Sawiak, S. J., Caprioli, D., Jupp, B., Buonincontri, G., Mar, A. C., Harte, M. K., Fletcher, P. C., Robbins, T. W., & Neill, J. C. (2015). Impaired limbic cortico-striatal structure and sustained visual attention in a rodent model of schizophrenia. *International Journal of Neuropsychopharmacology*, *18*(2), pyu010. https://doi.org/10.1093/ijnp/pyu010

Bast, T. (2011). The hippocampal learning-behavior translation and the functional significance of hippocampal dysfunction in schizophrenia. *Current Opinion in Neurobiology*, *21*(3), 492–501. https://doi.org/https://doi.org/10.1016/j.conb.2011.01.003

Bast, T., da Silva, B. M., & Morris, R. G. M. (2005). Distinct Contributions of Hippocampal NMDA and AMPA Receptors to Encoding and Retrieval of One-Trial Place Memory. *The Journal of Neuroscience*, *25*(25), 5845–5856. https://doi.org/10.1523/jneurosci.0698-05.2005

Bast, T., & Feldon, J. (2003). Hippocampal modulation of sensorimotor processes. *Progress in Neurobiology*, *70*(4), 319–345.

Bast, T., Pezze, M., & McGarrity, S. (2017). Cognitive deficits caused by prefrontal cortical and hippocampal neural disinhibition. *British Journal of Pharmacology*, *174*(19), 3211–3225.

Bast, T., Wilson, I. A., Witter, M. P., & Morris, R. G. M. (2009). From rapid place learning to behavioral performance: a key role for the intermediate hippocampus. *PLoS Biology*.

Bast, T., Zhang, W. N., & Feldon, J. (2001a). Hyperactivity, decreased startle reactivity, and disrupted prepulse inhibition following disinhibition of the rat ventral hippocampus by the GABAA receptor antagonist picrotoxin. *Psychopharmacology*, *156*(2), 225–233.

Bast, T., Zhang, W. N., & Feldon, J. (2001b). The ventral hippocampus and fear conditioning in rats. *Experimental Brain Research*, *139*(1), 39–52.

Batiuk, M. Y., Tyler, T., Dragicevic, K., Mei, S., Rydbirk, R., Petukhov, V., Deviatiiarov, R., Sedmak, D., Frank, E., & Feher, V. (2022). Upper cortical layer–driven network impairment in schizophrenia. *Science Advances*, *8*(41), eabn8367.

Bauer, M., Buckley, M. G., & Bast, T. (2021). Individual differences in theta-band oscillations in a spatial memory network revealed by electroencephalography predict rapid place learning. *Brain and Neuroscience Advances*, *5*, 23982128211002724.

Beasley, C. L., & Reynolds, G. P. (1997). Parvalbumin-immunoreactive neurons are reduced in the prefrontal cortex of schizophrenics. *Schizophrenia Research*, *24*(3), 349–355.

Beasley, C. L., Zhang, Z. J., Patten, I., & Reynolds, G. P. (2002). Selective deficits in prefrontal cortical GABAergic neurons in schizophrenia defined by the presence of calcium-binding proteins. *Biological Psychiatry*, *52*(7), 708–715.

Beer, Z., Chwiesko, C., Kitsukawa, T., & Sauvage, M. M. (2013). Spatial and stimulus-type tuning in the LEC, MEC, POR, PrC, CA1, and CA3 during spontaneous item recognition memory. *Hippocampus*, *23*(12), 1425–1438.

Behrens, M. M., Ali, S. S., Dao, D. N., Lucero, J., Shekhtman, G., Quick, K. L., & Dugan, L. L. (2007). Ketamine-induced loss of phenotype of fast-spiking interneurons is mediated by NADPH-oxidase. *Science*, *318*(5856), 1645–1647.

Behrens, M. M., Ali, S. S., & Dugan, L. L. (2008). Interleukin-6 mediates the increase in NADPH-oxidase in the ketamine model of schizophrenia. *Journal of Neuroscience*, *28*(51), 13957–13966.

Beiko, J., Lander, R., Hampson, E., Boon, F., & Cain, D. P. (2004). Contribution of sex differences in the acute stress response to sex differences in water maze performance in the rat. *Behavioural Brain Research*, *151*(1–2), 239–253.

Benes, F. M., & Berretta, S. (2001). GABAergic interneurons: implications for understanding schizophrenia and bipolar disorder. *Neuropsychopharmacology*, *25*(1), 1–27.

Benes, F. M., Lim, B., Matzilevich, D., Walsh, J. P., Subburaju, S., & Minns, M. (2007). Regulation of the GABA cell phenotype in hippocampus of schizophrenics and bipolars. *Proceedings of the National Academy of Sciences*, *104*(24), 10164–10169.

Benes, F. M., McSparren, J., Bird, E. D., SanGiovanni, J. P., & Vincent, S. L. (1991). Deficits in small interneurons in prefrontal and cingulate cortices of schizophrenic and schizoaffective patients. *Archives of General Psychiatry*, *48*(11), 996–1001.

Beninger, R. J., Beuk, J., Banasikowski, T. J., van Adel, M., Boivin, G. A., & Reynolds, J. N. (2010). Subchronic phencyclidine in rats: alterations in locomotor activity, maze performance, and GABAA receptor binding. *Behavioural Pharmacology*, *21*(1), 1–10.

Benn, A., Barker, G. R. I., Stuart, S. A., Roloff, E. v L., Teschemacher, A. G., Warburton, E. C., & Robinson, E. S. J. (2016). Optogenetic stimulation of prefrontal glutamatergic neurons enhances recognition memory. *Journal of Neuroscience*, *36*(18), 4930–4939.

Benneyworth, M. A., Roseman, A. S., Basu, A. C., & Coyle, J. T. (2011). Failure of NMDA receptor hypofunction to induce a pathological reduction in PV-positive GABAergic cell markers. *Neuroscience Letters*, *488*(3), 267–271.

Beraki, S., Diaz-Heijtz, R., Tai, F., & Ogren, S. O. (2009). Effects of repeated treatment of phencyclidine on cognition and gene expression in C57BL/6 mice. *International Journal of Neuropsychopharmacology*, *12*(2), 243–255. https://doi.org/10.1017/s1461145708009152

Bitanihirwe, B. K. Y., & Woo, T. U. W. (2014). Transcriptional dysregulation of γ-aminobutyric acid transporter in parvalbumin-containing inhibitory neurons in the prefrontal cortex in schizophrenia. *Psychiatry Research*, *220*(3), 1155–1159.

Blaszczyk, J., & Tajchert, K. (1996). Sex and strain differences of acoustic startle reaction development in adolescent albino Wistar and hooded rats. *Acta Neurobiologiae Experimentalis*, *56*, 919–926.

Braun, I., Genius, J., Grunze, H., Bender, A., Möller, H. J., & Rujescu, D. (2007). Alterations of hippocampal and prefrontal GABAergic interneurons in an animal model of psychosis induced by NMDA receptor antagonism. *Schizophrenia Research*, *97*(1–3), 254–263.

Braun, U., Schäfer, A., Bassett, D. S., Rausch, F., Schweiger, J. I., Bilek, E., Erk, S., Romanczuk-Seiferth, N., Grimm, O., & Geiger, L. S. (2016). Dynamic brain network reconfiguration as a potential schizophrenia genetic risk mechanism modulated by NMDA receptor function. *Proceedings of the National Academy of Sciences*, *113*(44), 12568–12573.

Breier, A., Malhotra, A. K., Pinals, D. A., Weisenfeld, N. I., & Pickar, D. (1997). Association of ketamine-induced psychosis with focal activation of the prefrontal cortex in healthy volunteers. *The American Journal of Psychiatry*.

Broadbent, N. J., Gaskin, S., Squire, L. R., & Clark, R. E. (2010). Object recognition memory and the rodent hippocampus. *Learning & Memory*, *17*(1), 5–11.

Buckley, M. G., & Bast, T. (2018). A new human delayed-matching-to-place test in a virtual environment reverse-translated from the rodent watermaze paradigm: Characterization of performance measures and sex differences. *Hippocampus*, *28*(11), 796–812. https://doi.org/10.1002/hipo.22992

Buzsáki, G. (1984). Feed-forward inhibition in the hippocampal formation. *Progress in Neurobiology*, *22*(2), 131–153. https://doi.org/https://doi.org/10.1016/0301-0082(84)90023-6

Buzsáki, G. (1996). The hippocampo-neocortical dialogue. *Cerebral Cortex*, *6*(2), 81–92.

Buzsáki, G., & Czeh, G. (1981). Commissural and perforant path interactions in the rat hippocampus: field potentials and unitary activity. *Experimental Brain Research*, *43*, 429–438.

Buzsáki, G., & Wang, X. J. (2012). Mechanisms of gamma oscillations. *Annual Review of Neuroscience*, *35*, 203–225.

Bygrave, A. M., Kilonzo, K., Kullmann, D. M., Bannerman, D. M., & Kätzel, D. (2019). Can N-Methyl-D-Aspartate Receptor Hypofunction in Schizophrenia Be Localized to an Individual Cell Type? In *Frontiers in Psychiatry* (Vol. 10). Frontiers Media S.A. https://doi.org/10.3389/fpsyt.2019.00835

Cabungcal, J. H., Steullet, P., Morishita, H., Kraftsik, R., Cuenod, M., Hensch, T. K., & Do, K. Q. (2013). Perineuronal nets protect fast-spiking interneurons against oxidative stress. *Proceedings of the National Academy of Sciences*, *110*(22), 9130–9135.

Cadinu, D., Grayson, B., Podda, G., Harte, M. K., Doostdar, N., & Neill, J. C. (2018). NMDA receptor antagonist rodent models for cognition in schizophrenia and identification of novel drug treatments, an update. *Neuropharmacology*, *142*, 41–62. https://doi.org/https://doi.org/10.1016/j.neuropharm.2017.11.045

Canning, K. J., Wu, K., Peloquin, P., Kloosterman, F., & Leung, L. S. (2000). Physiology of the entorhinal and perirhinal projections to the hippocampus studied by current source density analysis. *Annals of the New York Academy of Sciences*, *911*, 55–72. https://doi.org/10.1111/j.1749-6632.2000.tb06719.x

Carlen, M., Meletis, K., Siegle, J. H., Cardin, J. A., Futai, K., Vierling-Claassen, D., Ruehlmann, C., Jones, S. R., Deisseroth, K., & Sheng, M. (2012). A critical role for NMDA receptors in parvalbumin interneurons for gamma rhythm induction and behavior. *Molecular Psychiatry*, *17*(5), 537–548.

Catts, V. S., Lai, Y. L., Weickert, C. S., Weickert, T. W., & Catts, S. V. (2016). A quantitative review of the postmortem evidence for decreased cortical N-methyl-D-aspartate receptor expression levels in schizophrenia: How can we link molecular abnormalities to mismatch negativity deficits? *Biological Psychology*, *116*, 57–67.

Chao, O. Y., Nikolaus, S., Yang, Y.-M., & Huston, J. P. (2022). Neuronal circuitry for recognition memory of object and place in rodent models. *Neuroscience & Biobehavioral Reviews*, 104855.

Cinalli Jr, D. A., Cohen, S. J., Guthrie, K., & Stackman Jr, R. W. (2020). Object recognition memory: Distinct yet complementary roles of the mouse CA1 and perirhinal cortex. *Frontiers in Molecular Neuroscience*, *13*, 527543.

Cirillo, M. A., & Seidman, L. J. (2003). Verbal declarative memory dysfunction in schizophrenia: from clinical assessment to genetics and brain mechanisms. *Neuropsychology Review*, *13*, 43–77.

Clarke, J. R., Cammarota, M., Gruart, A., Izquierdo, I., & Delgado-García, J. M. (2010). Plastic modifications induced by object recognition memory processing. *Proceedings of the National Academy of Sciences*, *107*(6), 2652–2657.

Clark, R. E., Zola, S. M., & Squire, L. R. (2000). Impaired recognition memory in rats after damage to the hippocampus. *Journal of Neuroscience*, *20*(23), 8853–8860.

Cochran, S. M., Kennedy, M., McKerchar, C. E., Steward, L. J., Pratt, J. A., & Morris, B. J. (2003). Induction of metabolic hypofunction and neurochemical deficits after chronic intermittent exposure to phencyclidine: differential modulation by antipsychotic drugs. *Neuropsychopharmacology*, *28*(2), 265–275.

Cohen, S. J., Munchow, A. H., Rios, L. M., Zhang, G., Ásgeirsdóttir, H. N., & Stackman Jr, R. W. (2013). The rodent hippocampus is essential for nonspatial object memory. *Current Biology*, *23*(17), 1685–1690.

Cohen, S. J., & Stackman Jr, R. W. (2015). Assessing rodent hippocampal involvement in the novel object recognition task. A review. *Behavioural Brain Research*, *285*, 105–117. https://doi.org/https://doi.org/10.1016/j.bbr.2014.08.002

Cohen, S. M., Tsien, R. W., Goff, D. C., & Halassa, M. M. (2015). The impact of NMDA receptor hypofunction on GABAergic neurons in the pathophysiology of schizophrenia. *Schizophrenia Research*, *167*(1–3), 98–107.

Cole, E., Ziadé, J., Simundic, A., & Mumby, D. G. (2020). Effects of perirhinal cortex and hippocampal lesions on rats' performance on two object-recognition tasks. *Behavioural Brain Research*, *381*, 112450.

Curley, A. A., Arion, D., Volk, D. W., Asafu-Adjei, J. K., Sampson, A. R., Fish, K. N., & Lewis, D. A. (2011). Cortical deficits of glutamic acid decarboxylase 67 expression in schizophrenia: clinical, protein, and cell type-specific features. *American Journal of Psychiatry*, *168*(9), 921–929.

Curran, H. V., & Monaghan, L. (2001). In and out of the K-hole: a comparison of the acute and residual effects of ketamine in frequent and infrequent ketamine users. *Addiction*, *96*(5), 749–760.

Damgaard, T., Larsen, D. B., Hansen, S. L., Grayson, B., Neill, J. C., & Plath, N. (2010). Positive modulation of alpha-amino-3-hydroxy-5-methyl-4-isoxazolepropionic acid (AMPA) receptors reverses sub-chronic PCP-induced deficits in the novel object recognition task in rats. *Behavioural Brain Research*, *207*(1), 144–150.

Damgaard, T., Plath, N., Neill, J. C., & Hansen, S. L. (2011). Extrasynaptic GABA A receptor activation reverses recognition memory deficits in an animal model of schizophrenia. *Psychopharmacology*, *214*(2), 403–413.

da Silva, B. M., Bast, T., & Morris, R. G. M. (2014). Spatial memory: behavioral determinants of persistence in the watermaze delayed matching-to-place task. *Learning & Memory*, *21*(1), 28–36. https://doi.org/10.1101/lm.032169.113

Davis, K. E., Fox, S., & Gigg, J. (2014). Increased hippocampal excitability in the 3xTgAD mouse model for Alzheimer's disease in vivo. *PLoS One*, *9*(3), e91203.

Deacon, T. W., Eichenbaum, H., Rosenberg, P., & Eckmann, K. W. (1983). Afferent connections of the perirhinal cortex in the rat. *Journal of Comparative Neurology*, *220*(2), 168–190.

Deadwyler, S. A., West, J. R., Cotman, C. W., & Lynch, G. (1975). Physiological studies of the reciprocal connections between the hippocampus and entorhinal cortex. *Experimental Neurology*, *49*(1), 35–57. https://doi.org/https://doi.org/10.1016/0014-4886(75)90194-6

de Jonge, J. C., Vinkers, C. H., Hulshoff Pol, H. E., & Marsman, A. (2017). GABAergic Mechanisms in Schizophrenia: Linking Postmortem and In Vivo Studies. *Frontiers in Psychiatry*, *8*. https://www.frontiersin.org/articles/10.3389/fpsyt.2017.00118

de Landeta, A. B., Pereyra, M., Medina, J. H., & Katche, C. (2020). Anterior retrosplenial cortex is required for long-term object recognition memory. *Scientific Reports*, *10*(1), 4002.

de Lima, M. N., Luft, T., Roesler, R., & Schröder, N. (2006). Temporary inactivation reveals an essential role of the dorsal hippocampus in consolidation of object recognition memory. *Neuroscience Letters*, *405*(1–2), 142–146.

Dere, E., Huston, J. P., & Silva, M. A. D. S. (2007). The pharmacology, neuroanatomy and neurogenetics of one-trial object recognition in rodents. *Neuroscience & Biobehavioral Reviews*, *31*(5), 673–704.

Devan, B. D., Tobin, E. L., Dunn, E. N., & Magalis, C. (2016). Sex differences on the competitive place task in the water maze: The influence of peripheral pool time on spatial navigation performance in rats. *Behavioural Processes*, *132*, 34–41.

Didriksen, M., Skarsfeldt, T., & Arnt, J. (2007). Reversal of PCP-induced learning and memory deficits in the Morris' water maze by sertindole and other antipsychotics. *Psychopharmacology*, *193*(2), 225–233. https://doi.org/10.1007/s00213-007-0774-3

Dienel, S. J., Fish, K. N., & Lewis, D. A. (2023). The Nature of Prefrontal Cortical GABA Neuron Alterations in Schizophrenia: Markedly Lower Somatostatin and Parvalbumin Gene Expression Without Missing Neurons. *American Journal of Psychiatry*, appi-ajp.

Dienel, S. J., & Lewis, D. A. (2019). Alterations in cortical interneurons and cognitive function in schizophrenia. *Neurobiology of Disease*, *131*, 104208.

Dix, S., Gilmour, G., Potts, S., Smith, J. W., & Tricklebank, M. (2010). A within-subject cognitive battery in the rat: differential effects of NMDA receptor antagonists. *Psychopharmacology*, *212*(2), 227–242. https://doi.org/10.1007/s00213-010-1945-1

Dolorfo, C. L., & Amaral, D. G. (1998a). Entorhinal cortex of the rat: organization of intrinsic connections. *Journal of Comparative Neurology*, *398*(1), 49–82.

Dolorfo, C. L., & Amaral, D. G. (1998b). Entorhinal cortex of the rat: topographic organization of the cells of origin of the perforant path projection to the dentate gyrus. *Journal of Comparative Neurology*, *398*(1), 25–48.

Donato, F., Rompani, S. B., & Caroni, P. (2013). Parvalbumin-expressing basket-cell network plasticity induced by experience regulates adult learning. *Nature*, *504*(7479), 272–276.

Doostdar, N., Kim, E., Grayson, B., Harte, M. K., Neill, J. C., & Vernon, A. C. (2019). Global brain volume reductions in a sub-chronic phencyclidine animal model for schizophrenia and their relationship to recognition memory. *Journal of Psychopharmacology*, *33*(10), 1274–1287.

Douglas, R. M., & Goddard, G. V. (1975). Long-term potentiation of the perforant path-granule cell synapse in the rat hippocampus. *Brain Research*, *86*(2), 205–215. https://doi.org/https://doi.org/10.1016/0006-8993(75)90697-6

Douglas, R. M., McNaughton, B. L., & Goddard, G. V. (1983). Commissural inhibition and facilitation of granule cell discharge in fascia dentata. *Journal of Comparative Neurology*, *219*(3), 285–294.

Egerton, A., Reid, L., McGregor, S., Cochran, S. M., Morris, B. J., & Pratt, J. A. (2008). Subchronic and chronic PCP treatment produces temporally distinct deficits in attentional set shifting and prepulse inhibition in rats. *Psychopharmacology*, *198*(1), 37–49.

Egerton, A., Reid, L., McKerchar, C. E., Morris, B. J., & Pratt, J. A. (2005). Impairment in perceptual attentional set-shifting following PCP administration: a rodent model of set-shifting deficits in schizophrenia. *Psychopharmacology*, *179*(1), 77–84.

Ellis, S. N., & Honeycutt, J. A. (2021). Sex Differences in Affective Dysfunction and Alterations in Parvalbumin in Rodent Models of Early Life Adversity. *Frontiers in Behavioral Neuroscience*, *15*. https://www.frontiersin.org/articles/10.3389/fnbeh.2021.741454

Ennaceur, A., & Delacour, J. (1988). A new one-trial test for neurobiological studies of memory in rats. 1: Behavioral data. *Behavioural Brain Research*, *31*(1), 47–59.

Ennaceur, A., Neave, N., & Aggleton, J. P. (1997). Spontaneous object recognition and object location memory in rats: the effects of lesions in the cingulate cortices, the medial prefrontal cortex, the cingulum bundle and the fornix. *Experimental Brain Research*, *113*(3), 509–519.

Enomoto, T., Ishibashi, T., Tokuda, K., Ishiyama, T., Toma, S., & Ito, A. (2008). Lurasidone reverses MK-801-induced impairment of learning and memory in the Morris water maze and radial-arm maze tests in rats. *Behavioural Brain Research*, *186*(2), 197–207. https://doi.org/10.1016/j.bbr.2007.08.012

Enomoto, T., Maric, T. T., & Floresco, S. B. (2011). Reducing prefrontal gamma-aminobutyric acid activity induces cognitive, behavioral, and dopaminergic abnormalities that resemble schizophrenia. *Biological Psychiatry*, *69*(5), 432–441.

Enwright, J. F., Sanapala, S., Foglio, A., Berry, R., Fish, K. N., & Lewis, D. A. (2016). Reduced labeling of parvalbumin neurons and perineuronal nets in the dorsolateral prefrontal cortex of subjects with schizophrenia. *Neuropsychopharmacology*, *41*(9), 2206–2214.

Etherington, L.-A., Mihalik, B., Pálvölgyi, A., Ling, I., Pallagi, K., Kertész, S., Varga, P., Gunn, B., & Brown, A. (2017). *Selective inhibition of extra-synaptic 5-GABAA receptors by S44819, a new therapeutic agent*.

Fajnerová, I., Rodriguez, M., Levčík, D., Konrádová, L., Mikoláš, P., Brom, C., Stuchlík, A., Vlček, K., & Horáček, J. (2014). A virtual reality task based on animal research–spatial learning and memory in patients after the first episode of schizophrenia. *Frontiers in Behavioral Neuroscience*, *8*, 157.

Falkai, P., Malchow, B., & Schmitt, A. (2017). Aerobic exercise and its effects on cognition in schizophrenia. *Current Opinion in Psychiatry*, *30*(3), 171–175.

Farrant, M., & Nusser, Z. (2005). Variations on an inhibitory theme: phasic and tonic activation of GABAA receptors. *Nature Reviews Neuroscience*, *6*(3), 215–229.

Faul, F., Erdfelder, E., Lang, A.-G., & Buchner, A. (2007). G*Power 3: A flexible statistical power analysis program for the social, behavioral, and biomedical sciences. *Behavior Research Methods*, *39*(2), 175–191. https://doi.org/10.3758/BF03193146

Fawcett, J. W., Oohashi, T., & Pizzorusso, T. (2019). The roles of perineuronal nets and the perinodal extracellular matrix in neuronal function. *Nature Reviews Neuroscience*, *20*(8), 451–465.

Featherstone, R. E., Liang, Y., Saunders, J. A., Tatard-Leitman, V. M., Ehrlichman, R. S., & Siegel, S. J. (2012). Subchronic ketamine treatment leads to permanent changes in EEG, cognition and the astrocytic glutamate transporter EAAT2 in mice. *Neurobiology of Disease*, *47*(3), 338–346.

Fell, J., & Axmacher, N. (2011). The role of phase synchronization in memory processes. *Nature Reviews Neuroscience*, *12*(2), 105–118.

Ferguson, B. R., & Gao, W. J. (2018). PV interneurons: critical regulators of E/I balance for prefrontal cortex-dependent behavior and psychiatric disorders. *Frontiers in Neural Circuits*, *12*, 37.

Firth, J., Stubbs, B., Rosenbaum, S., Vancampfort, D., Malchow, B., Schuch, F., Elliott, R., Nuechterlein, K. H., & Yung, A. R. (2017). Aerobic exercise improves cognitive functioning in people with schizophrenia: a systematic review and meta-analysis. *Schizophrenia Bulletin*, *43*(3), 546–556.

Fletcher, J., Gigg, J., & Harte, M. (2022). Investigating the mechanisms underlying the beneficial effects of exercise on cognitive impairment associated with schizophrenia - focus on parvalbumin interneurons and perineuronal nets. *FENS Forum Abstract*, S04-007, 3025.

Fletcher, J., Jimenez Pulido, I., Grayson, B., Gigg, J., & Harte, M. (2023). Characterisation of prefrontal hypofunction in the subchronic phencyclidine model. *BNA Festival of Neuroscience Abstract*, T_PZ2_034 (TP), 100.

Flores-Barrera, E., Thomases, D. R., & Tseng, K. Y. (2020). MK-801 exposure during adolescence elicits enduring disruption of prefrontal E–I balance and its control of fear extinction behavior. *Journal of Neuroscience*, *40*(25), 4881–4887.

Folley, B. S., Astur, R., Jagannathan, K., Calhoun, V. D., & Pearlson, G. D. (2010). Anomalous neural circuit function in schizophrenia during a virtual Morris water task. *NeuroImage*, *49*(4), 3373–3384. https://doi.org/https://doi.org/10.1016/j.neuroimage.2009.11.034

Forwood, S. E., Winters, B. D., & Bussey, T. J. (2005). Hippocampal lesions that abolish spatial maze performance spare object recognition memory at delays of up to 48 hours. *Hippocampus*, *15*(3), 347–355.

Freeman, J. A., & Nicholson, C. (1975). Experimental optimization of current source-density technique for anuran cerebellum. *Journal of Neurophysiology*, *38*(2), 369–382. https://doi.org/10.1152/jn.1975.38.2.369

Fuchs, E. C., Zivkovic, A. R., Cunningham, M. O., Middleton, S., LeBeau, F. E. N., Bannerman, D. M., Rozov, A., Whittington, M. A., Traub, R. D., & Rawlins, J. N. P. (2007). Recruitment of parvalbumin-positive interneurons determines hippocampal function and associated behavior. *Neuron*, *53*(4), 591–604.

Fung, S. J., Fillman, S. G., Webster, M. J., & Weickert, C. S. (2014). Schizophrenia and bipolar disorder show both common and distinct changes in cortical interneuron markers. *Schizophrenia Research*, *155*(1–3), 26–30.

Fung, S. J., Webster, M. J., Sivagnanasundaram, S., Duncan, C., Elashoff, M., & Weickert, C. S. (2010). Expression of interneuron markers in the dorsolateral prefrontal cortex of the developing human and in schizophrenia. *American Journal of Psychiatry*, *167*(12), 1479–1488.

Gabbott, P. L. A., Dickie, B. G. M., Vaid, R. R., Headlam, A. J. N., & Bacon, S. J. (1997). Local-circuit neurones in the medial prefrontal cortex (areas 25, 32 and 24b) in the rat: morphology and quantitative distribution. *Journal of Comparative Neurology*, *377*(4), 465–499.

Gábriel, R., Lesauter, J., Bánvölgyi, T., Petrovics, G., Silver, R., & Witkovsky, P. (2004). AII amacrine neurons of the rat retina show diurnal and circadian rhythms of parvalbumin immunoreactivity. *Cell and Tissue Research*, *315*(2), 181–186. https://doi.org/10.1007/s00441-003-0785-2

Gacsályi, I., Móricz, K., Gigler, G., Wellmann, J., Nagy, K., Ling, I., Barkóczy, J., Haller, J., Lambert, J. J., & Szénási, G. (2017). Behavioural pharmacology of the α5-GABAA receptor antagonist S44819: Enhancement and remediation of cognitive performance in preclinical models. *Neuropharmacology*, *125*, 30–38.

Gandal, M. J., Edgar, J. C., Klook, K., & Siegel, S. J. (2012). Gamma synchrony: towards a translational biomarker for the treatment-resistant symptoms of schizophrenia. *Neuropharmacology*, *62*(3), 1504–1518.

Gaskin, S., Tardif, M., Cole, E., Piterkin, P., Kayello, L., & Mumby, D. G. (2010). Object familiarization and novel-object preference in rats. *Behavioural Processes*, *83*(1), 61–71.

Geyer, M. A., Krebs-Thomson, K., Braff, D. L., & Swerdlow, N. R. (2001). Pharmacological studies of prepulse inhibition models of sensorimotor gating deficits in schizophrenia: a decade in review. *Psychopharmacology*, *156*(2), 117–154.

Gigg, J., McEwan, F., Smausz, R., Neill, J., & Harte, M. K. (2020). Synaptic biomarker reduction and impaired cognition in the sub-chronic PCP mouse model for schizophrenia. *Journal of Psychopharmacology*, 0269881119874446.

Gilmour, G., Dix, S., Fellini, L., Gastambide, F., Plath, N., Steckler, T., Talpos, J., & Tricklebank, M. (2012). NMDA receptors, cognition and schizophrenia–testing the validity of the NMDA receptor hypofunction hypothesis. *Neuropharmacology*, *62*(3), 1401–1412.

Gilmour, G., Pioli, E. Y., Dix, S. L., Smith, J. W., Conway, M. W., Jones, W. T., Loomis, S., Mason, R., Shahabi, S., & Tricklebank, M. D. (2009). Diverse and often opposite behavioural effects of NMDA receptor antagonists in rats: implications for “NMDA antagonist modelling” of schizophrenia. *Psychopharmacology*, *205*(2), 203–216. https://doi.org/10.1007/s00213-009-1530-7

Gomes da Silva, S., Doná, F., da Silva Fernandes, M. J., Scorza, F. A., Cavalheiro, E. A., & Arida, R. M. (2010). Physical exercise during the adolescent period of life increases hippocampal parvalbumin expression. *Brain and Development*, *32*(2), 137–142. https://doi.org/https://doi.org/10.1016/j.braindev.2008.12.012

Gonçalves, S., Hathway, G. J., Woodhams, S. G., Chapman, V., & Bast, T. (2023). No Evidence for Cognitive Impairment in an Experimental Rat Model of Knee Osteoarthritis and Associated Chronic Pain. *The Journal of Pain*. https://doi.org/10.1016/J.JPAIN.2023.04.002

Gonzalez-Burgos, G., Hashimoto, T., & Lewis, D. A. (2010). Alterations of cortical GABA neurons and network oscillations in schizophrenia. *Current Psychiatry Reports*, *12*(4), 335–344.

Gonzalez-Burgos, G., & Lewis, D. A. (2008). GABA neurons and the mechanisms of network oscillations: implications for understanding cortical dysfunction in schizophrenia. *Schizophrenia Bulletin*, *34*(5), 944–961.

Gonzalez-Burgos, G., & Lewis, D. A. (2012). NMDA receptor hypofunction, parvalbumin-positive neurons, and cortical gamma oscillations in schizophrenia. *Schizophrenia Bulletin*, *38*(5), 950–957.

Good, M. A., Barnes, P., Staal, V., McGregor, A., & Honey, R. C. (2007). Context-but not familiarity-dependent forms of object recognition are impaired following excitotoxic hippocampal lesions in rats. *Behavioral Neuroscience*, *121*(1), 218.

Grayson, B., Adamson, L., Harte, M., Leger, M., Marsh, S., Piercy, C., & Neill, J. C. (2014). The involvement of distraction in memory deficits induced by NMDAR antagonism: Relevance to cognitive deficits in schizophrenia. *Behavioural Brain Research*, *266*, 188–192.

Grayson, B., Idris, N. F., & Neill, J. C. (2007). Atypical antipsychotics attenuate a sub-chronic PCP-induced cognitive deficit in the novel object recognition task in the rat. *Behavioural Brain Research*, *184*(1), 31–38.

Grayson, B., Leger, M., Piercy, C., Adamson, L., Harte, M., & Neill, J. C. (2015). Assessment of disease-related cognitive impairments using the novel object recognition (NOR) task in rodents. *Behavioural Brain Research*, *285*, 176–193.

Grayson, B., & Neill, J. C. (2004). The effect of PCP on novel object recognition in the rat. *Journal of Psychopharmacology*, *18*(3), A72–A72.

Gruart, A., Sánchez-Campusano, R., Fernández-Guizán, A., & Delgado-García, J. M. (2015). A differential and timed contribution of identified hippocampal synapses to associative learning in mice. *Cerebral Cortex*, *25*(9), 2542–2555.

Grunze, H. C., Rainnie, D. G., Hasselmo, M. E., Barkai, E., Hearn, E. F., McCarley, R. W., & Greene, R. W. (1996). NMDA-dependent modulation of CA1 local circuit inhibition. *Journal of Neuroscience*, *16*(6), 2034–2043.

Guidotti, A., Auta, J., Davis, J. M., Gerevini, V. D., Dwivedi, Y., Grayson, D. R., Impagnatiello, F., Pandey, G., Pesold, C., Sharma, R., Uzunov, D., & Costa, E. (2000). Decrease in Reelin and Glutamic Acid Decarboxylase 67 (GAD67) Expression in Schizophrenia and Bipolar Disorder: A Postmortem Brain Study. *Archives of General Psychiatry*, *57*(11), 1061–1069. https://doi.org/10.1001/archpsyc.57.11.1061

Gwilt, M., Bauer, M., & Bast, T. (2020). Frequency-and state-dependent effects of hippocampal neural disinhibition on hippocampal local field potential oscillations in anesthetized rats. *Hippocampus*, *30*(10), 1021–1043.

Haettig, J., Stefanko, D. P., Multani, M. L., Figueroa, D. X., McQuown, S. C., & Wood, M. A. (2011). HDAC inhibition modulates hippocampus-dependent long-term memory for object location in a CBP-dependent manner. *Learning & Memory*, *18*(2), 71–79.

Hammond, R. S., Tull, L. E., & Stackman, R. W. (2004). On the delay-dependent involvement of the hippocampus in object recognition memory. *Neurobiology of Learning and Memory*, *82*(1), 26–34.

Hanlon, F. M., Weisend, M. P., Hamilton, D. A., Jones, A. P., Thoma, R. J., Huang, M., Martin, K., Yeo, R. A., Miller, G. A., & Cañive, J. M. (2006). Impairment on the hippocampal-dependent virtual Morris water task in schizophrenia. *Schizophrenia Research*, *87*(1–3), 67–80.

Hardingham, G. E., & Do, K. Q. (2016). Linking early-life NMDAR hypofunction and oxidative stress in schizophrenia pathogenesis. *Nature Reviews Neuroscience*, *17*(2), 125.

Harkness, J. H., Bushana, P. N., Todd, R. P., Clegern, W. C., Sorg, B. A., & Wisor, J. P. (2019). Sleep disruption elevates oxidative stress in parvalbumin-positive cells of the rat cerebral cortex. *Sleep*, *42*(1), zsy201.

Harris, V. M. (2015). Protein Detection by Simple Western™ Analysis. In B. T. Kurien & R. H. Scofield (Eds.), *Western Blotting: Methods and Protocols* (pp. 465–468). Springer New York. https://doi.org/10.1007/978-1-4939-2694-7_47

Hashimoto, T., Volk, D. W., Eggan, S. M., Mirnics, K., Pierri, J. N., Sun, Z., Sampson, A. R., & Lewis, D. A. (2003). Gene expression deficits in a subclass of GABA neurons in the prefrontal cortex of subjects with schizophrenia. *Journal of Neuroscience*, *23*(15), 6315–6326.

Hauser, M. J., Isbrandt, D., & Roeper, J. (2017). Disturbances of novel object exploration and recognition in a chronic ketamine mouse model of schizophrenia. *Behavioural Brain Research*, *332*, 316–326.

Heckers, S., & Konradi, C. (2015). GABAergic mechanisms of hippocampal hyperactivity in schizophrenia. *Schizophrenia Research*, *167*(1–3), 4–11.

He, J., Liu, F., Zu, Q., Xu, Z., Zheng, H., Li, X., & Wang, W. (2018). Chronic administration of quetiapine attenuates the phencyclidine-induced recognition memory impairment and hippocampal oxidative stress in rats. *NeuroReport*, *29*(13), 1099–1103.

Hernandez, A. R., Truckenbrod, L. M., Campos, K. T., Williams, S. A., & Burke, S. N. (2020). Sex differences in age-related impairments vary across cognitive and physical assessments in rats. *Behavioral Neuroscience*, *134*(2), 69.

Hertel, P., Mathé, J. M., Nomikos, G. G., Iurlo, M., Mathé, A. A., & Svensson, T. H. (1995). Effects of D-amphetamine and phencyclidine on behavior and extracellular concentrations of neurotensin and dopamine in the ventral striatum and the medial prefrontal cortex of the rat. *Behavioural Brain Research*, *72*(1–2), 103–114.

Hevers, W., Hadley, S. H., Lüddens, H., & Amin, J. (2008). Ketamine, but not phencyclidine, selectively modulates cerebellar GABAA receptors containing α6 and δ subunits. *Journal of Neuroscience*, *28*(20), 5383–5393.

Holcomb, H. H., Lahti, A. C., Medoff, D. R., Cullen, T., & Tamminga, C. A. (2005). Effects of noncompetitive NMDA receptor blockade on anterior cingulate cerebral blood flow in volunteers with schizophrenia. *Neuropsychopharmacology*, *30*(12), 2275–2282.

Homayoun, H., & Moghaddam, B. (2007). NMDA receptor hypofunction produces opposite effects on prefrontal cortex interneurons and pyramidal neurons. *Journal of Neuroscience*, *27*(43), 11496–11500.

Honeycutt, J. A., & Chrobak, J. J. (2018). Parvalbumin Loss Following Chronic Sub-Anesthetic NMDA Antagonist Treatment is Age-Dependent in the Hippocampus: Implications for Modeling NMDA Hypofunction. *Neuroscience*, *393*, 73–82. https://doi.org/https://doi.org/10.1016/j.neuroscience.2018.09.031

Horiguchi, M., Hannaway, K. E., Adelekun, A. E., Huang, M., Jayathilake, K., & Meltzer, H. Y. (2013). D1 receptor agonists reverse the subchronic phencyclidine (PCP)-induced novel object recognition (NOR) deficit in female rats. *Behavioural Brain Research*, *238*, 36–43.

Horiguchi, M., Hannaway, K. E., Adelekun, A. E., Jayathilake, K., & Meltzer, H. Y. (2012). Prevention of the phencyclidine-induced impairment in novel object recognition in female rats by co-administration of lurasidone or tandospirone, a 5-HT 1A partial agonist. *Neuropsychopharmacology*, *37*(10), 2175–2183.

Horiguchi, M., Huang, M., & Meltzer, H. Y. (2011a). Interaction of mGlu 2/3 agonism with clozapine and lurasidone to restore novel object recognition in subchronic phencyclidine-treated rats. *Psychopharmacology*, *217*(1), 13.

Horiguchi, M., Huang, M., & Meltzer, H. Y. (2011b). The role of 5-hydroxytryptamine 7 receptors in the phencyclidine-induced novel object recognition deficit in rats. *Journal of Pharmacology and Experimental Therapeutics*, *338*(2), 605–614.

Horiguchi, M., & Meltzer, H. Y. (2013). Blonanserin reverses the phencyclidine (PCP)-induced impairment in novel object recognition (NOR) in rats: role of indirect 5-HT1A partial agonism. *Behavioural Brain Research*, *247*, 158–164.

Huang, H., Zheng, S., Chen, M., Xie, L., Li, Z., Guo, M., Wang, J., Lu, M., & Zhu, X. (2021). The potential of the P2X7 receptor as a therapeutic target in a sub-chronic PCP-induced rodent model of schizophrenia. *Journal of Chemical Neuroanatomy*, *116*, 101993.

Hu, J. H., Ma, Y. H., Jiang, J., Yang, N., Duan, S., Jiang, Z. H., Mei, Z. T., Fei, J., & Guo, L.-H. (2004). Cognitive impairment in mice over-expressing γ-aminobutyric acid transporter I (GAT1). *NeuroReport*, *15*(1), 9–12.

Ibi, M., Liu, J., Arakawa, N., Kitaoka, S., Kawaji, A., Matsuda, K., Iwata, K., Matsumoto, M., Katsuyama, M., & Zhu, K. (2017). Depressive-like behaviors are regulated by NOX1/NADPH oxidase by redox modification of NMDA receptor 1. *Journal of Neuroscience*, *37*(15), 4200–4212.

Idris, N. F., Grayson, B., & Neill, J. C. (2006). The emerging role of NMDA receptor hypofunction in mediation of reversal learning deficits in the rat. *J Psychopharmacol*, *20*(Suppl (5), A68.

Idris, N., Neill, J., Grayson, B., Bang-Andersen, B., Witten, L. M., Brennum, L. T., & Arnt, J. (2010). Sertindole improves sub-chronic PCP-induced reversal learning and episodic memory deficits in rodents: involvement of 5-HT 6 and 5-HT 2A receptor mechanisms. *Psychopharmacology*, *208*(1), 23.

Ihalainen, J., Savolainen, K., Tanila, H., & Forsberg, M. M. (2016). Comparison of phencyclidine-induced spatial learning and memory deficits and reversal by sertindole and risperidone between Lister Hooded and Wistar rats. *Behavioural Brain Research*, *305*, 140–147. https://doi.org/10.1016/j.bbr.2016.02.032

Iijima, T., Witter, M. P., Ichikawa, M., Tominaga, T., Kajiwara, R., & Matsumoto, G. (1996). Entorhinal-hippocampal interactions revealed by real-time imaging. *Science*, *272*(5265), 1176–1179.

Isaacson, J. S., & Scanziani, M. (2011). How inhibition shapes cortical activity. *Neuron*, *72*(2), 231–243.

Izhikevich, E. M., Desai, N. S., Walcott, E. C., & Hoppensteadt, F. C. (2003). Bursts as a unit of neural information: selective communication via resonance. *Trends in Neurosciences*, *26*(3), 161–167.

Jackson, M. E., Homayoun, H., & Moghaddam, B. (2004). NMDA receptor hypofunction produces concomitant firing rate potentiation and burst activity reduction in the prefrontal cortex. *Proceedings of the National Academy of Sciences*, *101*(22), 8467–8472.

Jackson, S. J., Hussey, R., Jansen, M. A., Merrifield, G. D., Marshall, I., MacLullich, A., Yau, J. L. W., & Bast, T. (2011). Manganese-enhanced magnetic resonance imaging (MEMRI) of rat brain after systemic administration of MnCl2: Hippocampal signal enhancement without disruption of hippocampus-dependent behavior. *Behavioural Brain Research*, *216*(1), 293–300.

Jacobs, N. S., Allen, T. A., Nguyen, N., & Fortin, N. J. (2013). Critical role of the hippocampus in memory for elapsed time. *Journal of Neuroscience*, *33*(34), 13888–13893.

Janhunen, S. K., Svard, H., Talpos, J., Kumar, G., Steckler, T., Plath, N., Lerdrup, L., Ruby, T., Haman, M., Wyler, R., & Ballard, T. M. (2015). The subchronic phencyclidine rat model: relevance for the assessment of novel therapeutics for cognitive impairment associated with schizophrenia. *Psychopharmacology*, *232*(21–22), 4059–4083. https://doi.org/10.1007/s00213-015-3954-6

Javitt, D. C., & Zukin, S. R. (1991). Recent advances in the phencyclidine model of schizophrenia. *The American Journal of Psychiatry*.

Jeevakumar, V., Driskill, C., Paine, A., Sobhanian, M., Vakil, H., Morris, B., Ramos, J., & Kroener, S. (2015). Ketamine administration during the second postnatal week induces enduring schizophrenia-like behavioral symptoms and reduces parvalbumin expression in the medial prefrontal cortex of adult mice. *Behavioural Brain Research*, *282*, 165–175. https://doi.org/10.1016/j.bbr.2015.01.010

Jeevakumar, V., & Kroener, S. (2016). Ketamine administration during the second postnatal week alters synaptic properties of fast-spiking interneurons in the medial prefrontal cortex of adult mice. *Cerebral Cortex*, *26*(3), 1117–1129.

Jenkins, T. A., Harte, M. K., McKibben, C. E., Elliott, J. J., & Reynolds, G. P. (2008). Disturbances in social interaction occur along with pathophysiological deficits following sub-chronic phencyclidine administration in the rat. *Behavioural Brain Research*, *194*(2), 230–235.

Jenkins, T. A., Harte, M. K., & Reynolds, G. P. (2010). Effect of subchronic phencyclidine administration on sucrose preference and hippocampal parvalbumin immunoreactivity in the rat. *Neuroscience Letters*, *471*(3), 144–147.

Jentsch, J. D., Elsworth, J. D., Redmond Jr, D. E., & Roth, R. H. (1997a). Phencyclidine increases forebrain monoamine metabolism in rats and monkeys: modulation by the isomers of HA966. *Journal of Neuroscience*, *17*(5), 1769–1775.

Jentsch, J. D., & Roth, R. H. (1999). The neuropsychopharmacology of phencyclidine: from NMDA receptor hypofunction to the dopamine hypothesis of schizophrenia. *Neuropsychopharmacology*, *20*(3), 201–225.

Jentsch, J. D., Tran, A., Le, D., Youngren, K. D., & Roth, R. H. (1997b). Subchronic phencyclidine administration reduces mesoprefrontal dopamine utilization and impairs prefrontal cortical-dependent cognition in the rat. *Neuropsychopharmacology*, *17*(2), 92–99.

Jodo, E., Suzuki, Y., Katayama, T., Hoshino, K.-Y., Takeuchi, S., Niwa, S.-I., & Kayama, Y. (2005). Activation of medial prefrontal cortex by phencyclidine is mediated via a hippocampo-prefrontal pathway. *Cerebral Cortex*, *15*(5), 663–669.

Jonasson, Z. (2005). Meta-analysis of sex differences in rodent models of learning and memory: a review of behavioral and biological data. *Neuroscience & Biobehavioral Reviews*, *28*(8), 811–825.

Kaalund, S. S., Riise, J., Broberg, B. V, Fabricius, K., Karlsen, A. S., Secher, T., Plath, N., & Pakkenberg, B. (2013). Differential expression of parvalbumin in neonatal phencyclidine-treated rats and socially isolated rats. *Journal of Neurochemistry*, *124*(4), 548–557.

Kaar, S. J., Angelescu, I., Marques, T. R., & Howes, O. D. (2019). Pre-frontal parvalbumin interneurons in schizophrenia: a meta-analysis of post-mortem studies. *Journal of Neural Transmission*, *126*, 1637–1651.

Kafkas, A., & Montaldi, D. (2018). How do memory systems detect and respond to novelty? *Neuroscience Letters*, *680*, 60–68.

Kargieman, L., Santana, N., Mengod, G., Celada, P., & Artigas, F. (2007). Antipsychotic drugs reverse the disruption in prefrontal cortex function produced by NMDA receptor blockade with phencyclidine. *Proceedings of the National Academy of Sciences*, *104*(37), 14843–14848.

Kätzel, D., Wolff, A. R., Bygrave, A. M., & Bannerman, D. M. (2020). Hippocampal hyperactivity as a druggable circuit-level origin of aberrant salience in schizophrenia. *Frontiers in Pharmacology*, *11*, 486811.

Keilhoff, G., Becker, A., Grecksch, G., Wolf, G., & Bernstein, H.-G. (2004). Repeated application of ketamine to rats induces changes in the hippocampal expression of parvalbumin, neuronal nitric oxide synthase and cFOS similar to those found in human schizophrenia. *Neuroscience*, *126*(3), 591–598.

Kim, J. M., Kim, D. H., Lee, Y., Park, S. J., & Ryu, J. H. (2014). Distinct roles of the hippocampus and perirhinal cortex in GABAA receptor blockade-induced enhancement of object recognition memory. *Brain Research*, *1552*, 17–25.

King, M. V, Sleight, A. J., Woolley, M. L., Topham, I. A., Marsden, C. A., & Fone, K. C. F. (2004). 5-HT6 receptor antagonists reverse delay-dependent deficits in novel object discrimination by enhancing consolidation—an effect sensitive to NMDA receptor antagonism. *Neuropharmacology*, *47*(2), 195–204.

Kinney, J. W., Davis, C. N., Tabarean, I., Conti, B., Bartfai, T., & Behrens, M. M. (2006). A specific role for NR2A-containing NMDA receptors in the maintenance of parvalbumin and GAD67 immunoreactivity in cultured interneurons. *Journal of Neuroscience*, *26*(5), 1604–1615.

Kittelberger, K., Hur, E. E., Sazegar, S., Keshavan, V., & Kocsis, B. (2012). Comparison of the effects of acute and chronic administration of ketamine on hippocampal oscillations: relevance for the NMDA receptor hypofunction model of schizophrenia. *Brain Structure and Function*, *217*(2), 395–409.

Kjaerby, C., Broberg, B. V, Kristiansen, U., & Dalby, N. O. (2014). Impaired GABAergic inhibition in the prefrontal cortex of early postnatal phencyclidine (PCP)-treated rats. *Cerebral Cortex*, *24*(9), 2522–2532.

Kleinknecht, K. R., Bedenk, B. T., Kaltwasser, S. F., Grünecker, B., Yen, Y.-C., Czisch, M., & Wotjak, C. T. (2012). Hippocampus-dependent place learning enables spatial flexibility in C57BL6/N mice. *Frontiers in Behavioral Neuroscience*, *6*, 87.

Klimczak, P., Rizzo, A., Castillo-Gómez, E., Perez-Rando, M., Gramuntell, Y., Beltran, M., & Nacher, J. (2021). Parvalbumin Interneurons and Perineuronal Nets in the Hippocampus and Retrosplenial Cortex of Adult Male Mice After Early Social Isolation Stress and Perinatal NMDA Receptor Antagonist Treatment. *Frontiers in Synaptic Neuroscience*, *13*. https://www.frontiersin.org/articles/10.3389/fnsyn.2021.733989

Kloosterman, F., van Haeften, T., & Lopes da Silva, F. H. (2004). Two reentrant pathways in the hippocampal-entorhinal system. *Hippocampus*, *14*(8), 1026–1039. https://doi.org/https://doi.org/10.1002/hipo.20022

Kloosterman, F., Van Haeften, T., Witter, M. P., & Lopes da Silva, F. H. (2003). Electrophysiological characterization of interlaminar entorhinal connections: an essential link for re-entrance in the hippocampal–entorhinal system. *European Journal of Neuroscience*, *18*(11), 3037–3052.

Koh, M. T., Shao, Y., Sherwood, A., & Smith, D. R. (2016). Impaired hippocampal-dependent memory and reduced parvalbumin-positive interneurons in a ketamine mouse model of schizophrenia. *Schizophrenia Research*, *171*(1–3), 187–194.

Konradi, C., Yang, C. K., Zimmerman, E. I., Lohmann, K. M., Gresch, P., Pantazopoulos, H., Berretta, S., & Heckers, S. (2011). Hippocampal interneurons are abnormal in schizophrenia. *Schizophrenia Research*, *131*(1–3), 165–173.

Korotkova, T., Fuchs, E. C., Ponomarenko, A., von Engelhardt, J., & Monyer, H. (2010). NMDA receptor ablation on parvalbumin-positive interneurons impairs hippocampal synchrony, spatial representations, and working memory. *Neuron*, *68*(3), 557–569.

Krystal, J. H., Karper, L. P., Seibyl, J. P., Freeman, G. K., Delaney, R., Bremner, J. D., Heninger, G. R., Bowers, M. B., & Charney, D. S. (1994). Subanesthetic effects of the noncompetitive NMDA antagonist, ketamine, in humans: psychotomimetic, perceptual, cognitive, and neuroendocrine responses. *Archives of General Psychiatry*, *51*(3), 199–214.

Kumar, A., & Foster, T. C. (2013). Linking redox regulation of NMDAR synaptic function to cognitive decline during aging. *Journal of Neuroscience*, *33*(40), 15710–15715.

Kumaran, D., & Maguire, E. A. (2007). Match–mismatch processes underlie human hippocampal responses to associative novelty. *Journal of Neuroscience*, *27*(32), 8517–8524.

Landreth, K., Burgess, M., Watson, L., Lorusso, J. M., Grayson, B., Harte, M. K., & Neill, J. C. (2023). Handling prevents and reverses cognitive deficits induced by sub-chronic phencyclidine in a model for schizophrenia in rats. *Physiology & Behavior*, *263*, 114117. https://doi.org/https://doi.org/10.1016/j.physbeh.2023.114117

Landreth, K., Simanaviciute, U., Fletcher, J., Grayson, B., Grant, R. A., Harte, M. H., & Gigg, J. (2021). Dissociating the effects of distraction and proactive interference on object memory through tests of novelty preference. *Brain and Neuroscience Advances*, *5*, 23982128211003200.

Le Cozannet, R., Fone, K. C. F., & Moran, P. M. (2010). Phencyclidine withdrawal disrupts episodic-like memory in rats: reversal by donepezil but not clozapine. *International Journal of Neuropsychopharmacology*, *13*(8), 1011–1020. https://doi.org/10.1017/s1461145710000234

Ledda, F., & Paratcha, G. (2017). Mechanisms regulating dendritic arbor patterning. *Cellular and Molecular Life Sciences*, *74*(24), 4511–4537. https://doi.org/10.1007/s00018-017-2588-8

Lee, G. S., & Zhou, Y. (2019). NMDAR hypofunction animal models of schizophrenia. *Frontiers in Molecular Neuroscience*, *12*, 185.

Leger, M., Alvaro, G., Large, C., Harte, M., & Neill, J. (2015). P.3.c.003 AUT6, a novel Kv3 channel modulator, reverses cognitive and neurobiological dysfunction in a rat model of relevance to schizophrenia symptomatology. *European Neuropsychopharmacology*, *25*, S480. https://doi.org/10.1016/S0924-977X(15)30653-2

Lehmann, J., Pryce, C. R., & Feldon, J. (1999). Sex differences in the acoustic startle response and prepulse inhibition in Wistar rats. *Behavioural Brain Research*, *104*(1–2), 113–117.

Leppä, E., Linden, A.-M., Vekovischeva, O. Y., Swinny, J. D., Rantanen, V., Toppila, E., Höger, H., Sieghart, W., Wulff, P., & Wisden, W. (2011). Removal of GABAA receptor γ2 subunits from parvalbumin neurons causes wide-ranging behavioral alterations. *Plos One*, *6*(9), e24159.

Letzkus, J. J., Wolff, S. B. E., & Lüthi, A. (2015). Disinhibition, a circuit mechanism for associative learning and memory. *Neuron*, *88*(2), 264–276.

Leung, L. S., Peloquin, P., & Canning, K. (2008). Paired-Pulse Depression of Excitatory Postsynaptic Current Sinks in Hippocampal CA1 In Vivo. *Hippocampus*, *18*, 1008–1020. https://doi.org/10.1002/hipo.20458

Leung, L. S., Roth, L., & Canning, K. J. (1995). Entorhinal inputs to hippocampal CA1 and dentate gyrus in the rat: A current-source-density study. *Journal of Neurophysiology*, *73*(6), 2392–2403. https://doi.org/10.1152/jn.1995.73.6.2392

Lewis, D. A. (2014). Inhibitory neurons in human cortical circuits: substrate for cognitive dysfunction in schizophrenia. *Current Opinion in Neurobiology*, *26*, 22–26.

Lewis, D. A., Curley, A. A., Glausier, J. R., & Volk, D. W. (2012). Cortical parvalbumin interneurons and cognitive dysfunction in schizophrenia. *Trends in Neurosciences*, *35*(1), 57–67.

Lewis, D. A., Hashimoto, T., & Volk, D. W. (2005). Cortical inhibitory neurons and schizophrenia. *Nature Reviews Neuroscience*, *6*(4), 312–324.

Li, J. T., Su, Y. A., Wang, H. L., Zhao, Y. Y., Liao, X. M., Wang, X. D., & Si, T. M. (2016). Repeated blockade of NMDA receptors during adolescence impairs reversal learning and disrupts GABAergic interneurons in rat medial prefrontal cortex. *Frontiers in Molecular Neuroscience*, *9*, 17.

Lin, X., Amalraj, M., Blanton, C., Avila, B., Holmes, T. C., Nitz, D. A., & Xu, X. (2021). Noncanonical projections to the hippocampal CA3 regulate spatial learning and memory by modulating the feedforward hippocampal trisynaptic pathway. *PLoS Biology*, *19*(12), e3001127.

Li, Q., Clark, S., Lewis, D. V, & Wilson, W. A. (2002). NMDA receptor antagonists disinhibit rat posterior cingulate and retrosplenial cortices: a potential mechanism of neurotoxicity. *Journal of Neuroscience*, *22*(8), 3070–3080.

Lisman, J. E., Coyle, J. T., Green, R. W., Javitt, D. C., Benes, F. M., Heckers, S., & Grace, A. A. (2008). Circuit-based framework for understanding neurotransmitter and risk gene interactions in schizophrenia. *Trends in Neurosciences*, *31*(5), 234–242.

Logue, S. F., Paylor, R., & Wehner, J. M. (1997). Hippocampal lesions cause learning deficits in inbred mice in the Morris water maze and conditioned-fear task. *Behavioral Neuroscience*, *111*(1), 104.

López, A. J., Kramár, E., Matheos, D. P., White, A. O., Kwapis, J., Vogel-Ciernia, A., Sakata, K., Espinoza, M., & Wood, M. A. (2016). Promoter-specific effects of DREADD modulation on hippocampal synaptic plasticity and memory formation. *Journal of Neuroscience*, *36*(12), 3588–3599.

Lőrincz, A., Szatmáry, B., & Szirtes, G. (2002). The mystery of structure and function of sensory processing areas of the neocortex: a resolution. *Journal of Computational Neuroscience*, *13*, 187–205.

Luby, E. D., Cohen, B. D., Rosenbaum, G., Gottlieb, J. S., & Kelley, R. (1959). Study of a new schizophrenomimetic drug—Sernyl. *AMA Archives of Neurology & Psychiatry*, *81*(3), 363–369.

Lück, C., Haitjema, C., & Heger, C. (2021). Simple Western: Bringing the Western Blot into the Twenty-First Century. *Methods in molecular biology (Clifton, N.J.)*, *2261*, 481–488. https://doi.org/10.1007/978-1-0716-1186-9_30

Lüttjohann, A., Fabene, P. F., & van Luijtelaar, G. (2009). A revised Racine's scale for PTZ-induced seizures in rats. *Physiology & Behavior*, *98*(5), 579–586.

Lyon, L., Saksida, L. M., & Bussey, T. J. (2012). Spontaneous object recognition and its relevance to schizophrenia: a review of findings from pharmacological, genetic, lesion and developmental rodent models. *Psychopharmacology*, *220*(4), 647–672.

Maeda, K., Lerdrup, L., Sugino, H., Akazawa, H., Amada, N., McQuade, R. D., Stensbøl, T. B., Bundgaard, C., Arnt, J., & Kikuchi, T. (2014). Brexpiprazole II: antipsychotic-like and procognitive effects of a novel serotonin-dopamine activity modulator. *Journal of Pharmacology and Experimental Therapeutics*, *350*(3), 605–614.

Malhotra, A. K., Pinals, D. A., Weingartner, H., Sirocco, K., Missar, C. D., Pickar, D., & Breier, A. (1996). NMDA receptor function and human cognition: the effects of ketamine in healthy volunteers. *Neuropsychopharmacology*, *14*(5), 301–307.

Martínez-Pinteño, A., García-Cerro, S., Mas, S., Torres, T., Boloc, D., Rodríguez, N., Lafuente, A., Gassó, P., Arnaiz, J. A., & Parellada, E. (2020). The positive allosteric modulator of the mGlu2 receptor JNJ-46356479 partially improves neuropathological deficits and schizophrenia-like behaviors in a postnatal ketamine mice model. *Journal of Psychiatric Research*, *126*, 8–18. https://doi.org/https://doi.org/10.1016/j.jpsychires.2020.04.005

Martinez, Z. A., Ellison, G. D., Geyer, M. A., & Swerdlow, N. R. (1999). Effects of sustained phencyclidine exposure on sensorimotor gating of startle in rats. *Neuropsychopharmacology*, *21*(1), 28–39.

Masur, J., Schutz, M. T., & Boerngen, R. (1980). Gender differences in open-field behavior as a function of age. *Developmental Psychobiology: The Journal of the International Society for Developmental Psychobiology*, *13*(2), 107–110.

Mauney, S. A., Athanas, K. M., Pantazopoulos, H., Shaskan, N., Passeri, E., Berretta, S., & Woo, T.-U. W. (2013). Developmental pattern of perineuronal nets in the human prefrontal cortex and their deficit in schizophrenia. *Biological Psychiatry*, *74*(6), 427–435.

Ma, Y. H., Zhou, X. G., Duan, S. H., Hu, J. H., Lu, B. F., Yu, Y., Mei, Z. T., Fei, J., & Guo, L. H. (2001). Overexpression of gamma-aminobutyric acid transporter subtype I leads to cognitive deterioration in transgenic mice. *Acta Pharmacologica Sinica*, *22*(4), 340–348.

Ma, Y. N., Sun, Y. X., Wang, T., Wang, H., Zhang, Y., Su, Y. A., Li, J. T., & Si, T. M. (2020). Subchronic MK-801 treatment during adolescence induces long-term, not permanent, excitatory-inhibitory imbalance in the rat hippocampus. *European Journal of Pharmacology*, *867*, 8. https://doi.org/10.1016/j.ejphar.2019.172807

Ma, Y. N., Sun, Y. X., Wang, T., Wang, H., Zhang, Y., Su, Y. A., Li, J. T., & Si, T. M. (2020). Subchronic MK-801 treatment during adolescence induces long-term, not permanent, excitatory-inhibitory imbalance in the rat hippocampus. *European Journal of Pharmacology*, *867*, 172807. https://doi.org/https://doi.org/10.1016/j.ejphar.2019.172807

McDonald, R. J., Yim, T. T., Lehmann, H., Sparks, F. T., Zelinski, E. L., Sutherland, R. J., & Hong, N. S. (2010). Expression of a conditioned place preference or spatial navigation task following muscimol-induced inactivations of the amygdala or dorsal hippocampus: A double dissociation in the retrograde direction. *Brain Research Bulletin*, *83*(1–2), 29–37.

McGarrity, S., Mason, R., Fone, K. C., Pezze, M., & Bast, T. (2017). Hippocampal neural disinhibition causes attentional and memory deficits. *Cerebral Cortex*, *27*(9), 4447–4462.

McKibben, C. E., Jenkins, T. A., Adams, H. N., Harte, M. K., & Reynolds, G. P. (2010). Effect of pretreatment with risperidone on phencyclidine-induced disruptions in object recognition memory and prefrontal cortex parvalbumin immunoreactivity in the rat. *Behavioural Brain Research*, *208*(1), 132–136. https://doi.org/https://doi.org/10.1016/j.bbr.2009.11.018

McLean, S. L., Grayson, B., Idris, N. F., Lesage, A. S., Pemberton, D. J., Mackie, C., & Neill, J. C. (2011). Activation of α7 nicotinic receptors improves phencyclidine-induced deficits in cognitive tasks in rats: implications for therapy of cognitive dysfunction in schizophrenia. *European Neuropsychopharmacology*, *21*(4), 333–343.

McLean, S. L., Harte, M. K., Neill, J. C., & Young, A. M. J. (2017). Dopamine dysregulation in the prefrontal cortex relates to cognitive deficits in the sub-chronic PCP-model for schizophrenia: A preliminary investigation. *Journal of Psychopharmacology*, *31*(6), 660–666.

McLean, S. L., Idris, N. F., Woolley, M. L., & Neill, J. C. (2009). D1-like receptor activation improves PCP-induced cognitive deficits in animal models: Implications for mechanisms of improved cognitive function in schizophrenia. *European Neuropsychopharmacology*, *19*(6), 440–450.

McNaughton, B. L., & Barnes, C. A. (1977). Physiological identification and analysis of dentate granule cell responses to stimulation of the medial and lateral perforant pathways in the rat. *Journal of Comparative Neurology*, *175*(4), 439–453. https://doi.org/https://doi.org/10.1002/cne.901750404

Meltzer, H. Y., Rajagopal, L., Huang, M., Oyamada, Y., Kwon, S., & Horiguchi, M. (2013). Translating the N-methyl-D-aspartate receptor antagonist model of schizophrenia to treatments for cognitive impairment in schizophrenia. *International Journal of Neuropsychopharmacology*, *16*(10), 2181–2194.

Miller, L. R., Marks, C., Becker, J. B., Hurn, P. D., Chen, W., Woodruff, T., McCarthy, M. M., Sohrabji, F., Schiebinger, L., & Wetherington, C. L. (2017). Considering sex as a biological variable in preclinical research. *The FASEB Journal*, *31*(1), 29–34.

Mitsadali, I., Grayson, B., Idris, N. F., Watson, L., Burgess, M., & Neill, J. (2020). Aerobic exercise improves memory and prevents cognitive deficits of relevance to schizophrenia in an animal model. *Journal of Psychopharmacology*, *34*(7), 695–708.

Molina, L. A., Skelin, I., & Gruber, A. J. (2014). Acute NMDA receptor antagonism disrupts synchronization of action potential firing in rat prefrontal cortex. *Plos One*, *9*(1), e85842.

Morgan, C. J. A., Dodds, C. M., Furby, H., Pepper, F., Fam, J., Freeman, T. P., Hughes, E., Doeller, C., King, J., Howes, O., & Stone, J. M. (2014). Long-term heavy ketamine use is associated with spatial memory impairment and altered hippocampal activation. *Frontiers in Psychiatry*, *5*, 11. https://doi.org/10.3389/fpsyt.2014.00149

Morici, J. F., Bekinschtein, P., & Weisstaub, N. V. (2015). Medial prefrontal cortex role in recognition memory in rodents. *Behavioural Brain Research*, *292*, 241–251.

Morris, H. M., Hashimoto, T., & Lewis, D. A. (2008). Alterations in somatostatin mRNA expression in the dorsolateral prefrontal cortex of subjects with schizophrenia or schizoaffective disorder. *Cerebral Cortex*, *18*(7), 1575–1587.

Morris, R. G. M. (1981). Spatial localization does not require the presence of local cues. *Learning and Motivation*, *12*(2), 239–260.

Morris, R. G. M. (2008). Morris water maze. *Scholarpedia*, *3*, 6315.

Morris, R. G. M., Anderson, E., Lynch, G. S. a, & Baudry, M. (1986). Selective impairment of learning and blockade of long-term potentiation by an N-methyl-D-aspartate receptor antagonist, AP5. *Nature*, *319*(6056), 774–776.

Morris, R. G. M., Davis, S., & Butcher, S. P. (1990a). Hippocampal synaptic plasticity and NMDA receptors: a role in information storage? *Philosophical Transactions of the Royal Society of London. Series B: Biological Sciences*, *329*(1253), 187–204.

Morris, R. G. M., Garrud, P., Rawlins, J. N. P. al, & O'Keefe, J. (1982). Place navigation impaired in rats with hippocampal lesions. *Nature*, *297*(5868), 681–683.

Morris, R. G. M., Schenk, F., Tweedie, F., & Jarrard, L. E. (1990b). Ibotenate lesions of hippocampus and/or subiculum: dissociating components of allocentric spatial learning. *European Journal of Neuroscience*, *2*(12), 1016–1028.

Morris, R. G., Steele, R. J., Bell, J. E., & Martin, S. J. (2013). N-methyl-d-aspartate receptors, learning and memory: chronic intraventricular infusion of the NMDA receptor antagonist d-AP5 interacts directly with the neural mechanisms of spatial learning. *The European journal of neuroscience*, *37*(5), 700–717. https://doi.org/10.1111/ejn.12086

Mumby, D. G. (2001). Perspectives on object-recognition memory following hippocampal damage: lessons from studies in rats. *Behavioural Brain Research*, *127*(1–2), 159–181.

Mumby, D. G., Tremblay, A., Lecluse, V., & Lehmann, H. (2005). Hippocampal damage and anterograde object-recognition in rats after long retention intervals. *Hippocampus*, *15*(8), 1050–1056.

Murray, A. J., Sauer, J. F., Riedel, G., McClure, C., Ansel, L., Cheyne, L., Bartos, M., Wisden, W., & Wulff, P. (2011). Parvalbumin-positive CA1 interneurons are required for spatial working but not for reference memory. *Nature Neuroscience*, *14*(3), 297–299. https://doi.org/10.1038/nn.2751

Myers, C. E., & Scharfman, H. E. (2011). Pattern separation in the dentate gyrus: A role for the CA3 backprojection. *Hippocampus*, *21*(11), 1190–1215. https://doi.org/https://doi.org/10.1002/hipo.20828

Nagelhus, A., Andersson, S. O., Cogno, S. G., Moser, E. I., & Moser, M.-B. (2023). Object-centered population coding in CA1 of the hippocampus. *Neuron*. https://doi.org/10.1016/J.NEURON.2023.04.008

Nakatani-Pawlak, A., Yamaguchi, K., Tatsumi, Y., Mizoguchi, H., & Yoneda, Y. (2009). Neonatal Phencyclidine Treatment in Mice Induces Behavioral, Histological and Neurochemical Abnormalities in Adulthood. *Biological and Pharmaceutical Bulletin*, *32*(9), 1576–1583. https://doi.org/10.1248/bpb.32.1576

Nakazawa, K., McHugh, T. J., Wilson, M. A., & Tonegawa, S. (2004). NMDA receptors, place cells and hippocampal spatial memory. *Nature Reviews Neuroscience*, *5*(5), 361–372.

Nakazawa, K., Zsiros, V., Jiang, Z., Nakao, K., Kolata, S., Zhang, S., & Belforte, J. E. (2012). GABAergic interneuron origin of schizophrenia pathophysiology. *Neuropharmacology*, *62*(3), 1574–1583.

Neill, J. C., Barnes, S., Cook, S., Grayson, B., Idris, N. F., McLean, S. L., Snigdha, S., Rajagopal, L., & Harte, M. K. (2010). Animal models of cognitive dysfunction and negative symptoms of schizophrenia: focus on NMDA receptor antagonism. *Pharmacology & Therapeutics*, *128*(3), 419–432.

Neill, J. C., Grayson, B., Kiss, B., Gyertyán, I., Ferguson, P., & Adham, N. (2016). Effects of cariprazine, a novel antipsychotic, on cognitive deficit and negative symptoms in a rodent model of schizophrenia symptomatology. *European Neuropsychopharmacology*, *26*(1), 3–14. https://doi.org/https://doi.org/10.1016/j.euroneuro.2015.11.016

Nelson, A. J. D., Cooper, M. T., Thur, K. E., Marsden, C. A., & Cassaday, H. J. (2011). The effect of catecholaminergic depletion within the prelimbic and infralimbic medial prefrontal cortex on recognition memory for recency, location, and objects. *Behavioral Neuroscience*, *125*(3), 396.

Neugebauer, N. M., Miyauchi, M., Sato, T., Tadano, J., Akal, H., Ardehali, H., & Meltzer, H. Y. (2018). Hippocampal GABAA antagonism reverses the novel object recognition deficit in sub-chronic phencyclidine-treated rats. *Behavioural Brain Research*, *342*, 11–18. https://doi.org/https://doi.org/10.1016/j.bbr.2017.12.033

Newcomer, J. W., Farber, N. B., & Olney, J. W. (2000). NMDA receptor function, memory, and brain aging. *Dialogues in Clinical Neuroscience*, *2*(3), 219–232. https://doi.org/10.31887/DCNS.2000.2.3/jnewcomer

Ninan, I., Jardemark, K. E., & Wang, R. Y. (2003). Olanzapine and clozapine but not haloperidol reverse subchronic phencyclidine-induced functional hyperactivity of N-methyl-D-aspartate receptors in pyramidal cells of the rat medial prefrontal cortex. *Neuropharmacology*, *44*(4), 462–472.

Nomura, T., Oyamada, Y., Fernandes, H. B., Remmers, C. L., Xu, J., Meltzer, H. Y., & Contractor, A. (2016). Subchronic phencyclidine treatment in adult mice increases GABAergic transmission and LTP threshold in the hippocampus. *Neuropharmacology*, *100*, 90–97.

Nuechterlein, K. H., Barch, D. M., Gold, J. M., Goldberg, T. E., Green, M. F., & Heaton, R. K. (2004). Identification of separable cognitive factors in schizophrenia. *Schizophrenia Research*, *72*(1), 29–39.

Numan, R. (2015). A prefrontal-hippocampal comparator for goal-directed behavior: The intentional self and episodic memory. *Frontiers in Behavioral Neuroscience*, *9*, 323.

Ohara, S., Onodera, M., Simonsen, Ø. W., Yoshino, R., Hioki, H., Iijima, T., Tsutsui, K. I., & Witter, M. P. (2018). Intrinsic projections of layer Vb neurons to layers Va, III, and II in the lateral and medial entorhinal cortex of the rat. *Cell Reports*, *24*(1), 107–116.

Okamoto, M., Katayama, T., Suzuki, Y., Hoshino, K.-Y., Yamada, H., Matsuoka, N., & Jodo, E. (2012). Neonatal administration of phencyclidine decreases the number of putative inhibitory interneurons and increases neural excitability to auditory paired clicks in the hippocampal CA3 region of freely moving adult mice. *Neuroscience*, *224*, 268–281.

Oliveira, A. M. M., Hawk, J. D., Abel, T., & Havekes, R. (2010). Post-training reversible inactivation of the hippocampus enhances novel object recognition memory. *Learning & Memory*, *17*(3), 155–160.

Olsen, R. K., Moses, S. N., Riggs, L., & Ryan, J. D. (2012). The hippocampus supports multiple cognitive processes through relational binding and comparison. *Frontiers in Human Neuroscience*, *6*, 146.

Pafundo, D. E., Miyamae, T., Lewis, D. A., & Gonzalez-Burgos, G. (2018). Presynaptic Effects of N-Methyl-D-Aspartate Receptors enhance parvalbumin cell–mediated inhibition of pyramidal cells in mouse prefrontal cortex. *Biological Psychiatry*, *84*(6), 460–470.

Paine, T. A., Slipp, L. E., & Carlezon, W. A. (2011). Schizophrenia- Like Attentional Deficits Following Blockade of Prefrontal Cortex GABA(A) Receptors. *Neuropsychopharmacology*, *36*(8), 1703–1713. https://doi.org/10.1038/npp.2011.51

Pantazopoulos, H., Woo, T. U. W., Lim, M. P., Lange, N., & Berretta, S. (2010). Extracellular matrix-glial abnormalities in the amygdala and entorhinal cortex of subjects diagnosed with schizophrenia. *Archives of General Psychiatry*, *67*(2), 155–166.

Paxinos, G., & Watson, C. (1998). *The rat brain in stereotaxic coordinates. New York. Acad*.

Paxinos, G., & Watson, C. (2006). *The rat brain in stereotaxic coordinates: hard cover edition*. Elsevier.

Paxinos, G., & Watson, C. (2013). *The rat brain in stereotaxic coordinates* (7th ed.). Academic press.

Payne, K., Wilson, C. J., Young, S., Fifkova, E., & Groves', P. M. (1982). Evoked Potentials and Long-Term Potentiation in the Mouse Dentate Gyrus after Stimulation of the Entorhinal Cortex. In *EXPERIMENTAL NEUROLOGY* (Vol. 75).

Penttonen, M., Kamondi, A., Sik, A., Acsády, L., & Buzsáki, G. (1997). Feed-forward and feed-back activation of the dentate gyrus in vivo during dentate spikes and sharp wave bursts. *Hippocampus*, *7*(4), 437–450. https://doi.org/https://doi.org/10.1002/(SICI)1098-1063(1997)7:4<437::AID-HIPO9>3.0.CO;2-F

Pérez, M. Á., Morales, C., Santander, O. C., García, F., Gómez, I., Peñaloza-Sancho, V., Fuentealba, P., Dagnino-Subiabre, A., Moya, P. R., & Fuenzalida, M. (2019). Ketamine-treatment during late adolescence impairs inhibitory synaptic transmission in the prefrontal cortex and working memory in adult rats. *Frontiers in Cellular Neuroscience*, *13*, 372.

Pettersen, K. H., Devor, A., Ulbert, I., Dale, A. M., & Einevoll, G. T. (2006). Current-source density estimation based on inversion of electrostatic forward solution: Effects of finite extent of neuronal activity and conductivity discontinuities. *Journal of Neuroscience Methods*, *154*(1–2), 116–133. https://doi.org/10.1016/J.JNEUMETH.2005.12.005

Pezze, M., & Bast, T. (2012). Dopaminergic modulation of hippocampus-dependent learning: Blockade of hippocampal D1-class receptors during learning impairs 1-trial place memory at a 30-min retention delay. *Neuropharmacology*, *63*(4), 710–718. https://doi.org/10.1016/j.neuropharm.2012.05.036

Pezze, M., Marshall, H. J., Fone, K. C. F., & Cassaday, H. J. (2015). Dopamine D1 receptor stimulation modulates the formation and retrieval of novel object recognition memory: role of the prelimbic cortex. *European Neuropsychopharmacology*, *25*(11), 2145–2156.

Pezze, M., Marshall, H. J., Fone, K. C. F., & Cassaday, H. J. (2017). Role of the anterior cingulate cortex in the retrieval of novel object recognition memory after a long delay. *Learning & Memory*, *24*(7), 310–317.

Pezze, M., McGarrity, S., Mason, R., Fone, K. C., & Bast, T. (2014). Too Little and Too Much: Hypoactivation and Disinhibition of Medial Prefrontal Cortex Cause Attentional Deficits. *Journal of Neuroscience*, *34*(23), 7931–7946. https://doi.org/10.1523/jneurosci.3450-13.2014

Phensy, A., Lindquist, K. L., Lindquist, K. A., Bairuty, D., Gauba, E., Guo, L., Tian, J., Du, H., & Kroener, S. (2020). Deletion of the Mitochondrial Matrix Protein CyclophilinD Prevents Parvalbumin Interneuron Dysfunctionand Cognitive Deficits in a Mouse Model of NMDA Hypofunction. *Journal of Neuroscience*, *40*(32), 6121–6132.

Piskulic, D., Olver, J. S., Norman, T. R., & Maruff, P. (2007). Behavioural studies of spatial working memory dysfunction in schizophrenia: A quantitative literature review. *Psychiatry Research*, *150*(2), 111–121. https://doi.org/https://doi.org/10.1016/j.psychres.2006.03.018

Pitkanen, M., Sirvio, J., MacDonald, E., Niemi, S., Ekonsalo, T., & Riekkinen, P. (1995). The effects of D-cycloserine and MK-801 on the performance of rats in two spatial learning and memory tasks. *European Neuropsychopharmacology*, *5*(4), 457–463.

Pitsikas, N., Boultadakis, A., & Sakellaridis, N. (2008). Effects of sub-anesthetic doses of ketamine on rats' spatial and non-spatial recognition memory. *Neuroscience*, *154*(2), 454–460.

Pollard, M., Varin, C., Hrupka, B., Pemberton, D. J., Steckler, T., & Shaban, H. (2012). Synaptic transmission changes in fear memory circuits underlie key features of an animal model of schizophrenia. *Behavioural Brain Research*, *227*(1), 184–193.

Povysheva, N. V, Gonzalez-Burgos, G., Zaitsev, A. V, Kröner, S., Barrionuevo, G., Lewis, D. A., & Krimer, L. S. (2006). Properties of excitatory synaptic responses in fast-spiking interneurons and pyramidal cells from monkey and rat prefrontal cortex. *Cerebral Cortex*, *16*(4), 541–552.

Powell, S. B., Sejnowski, T. J., & Behrens, M. M. (2012). Behavioral and neurochemical consequences of cortical oxidative stress on parvalbumin-interneuron maturation in rodent models of schizophrenia. *Neuropharmacology*, *62*(3), 1322–1331. https://doi.org/10.1016/J.NEUROPHARM.2011.01.049

Preston, A. R., & Eichenbaum, H. (2013). Interplay of hippocampus and prefrontal cortex in memory. *Current Biology*, *23*(17), R764–R773.

Prior, M. J. W., Bast, T., McGarrity, S., Goldschmidt, J., Vincenz, D., Seaton, A., Hall, G., & Pitiot, A. (2021). Ratlas-LH: An MRI template of the Lister hooded rat brain with stereotaxic coordinates for neurosurgical implantations. *Brain and Neuroscience Advances*, *5*, 23982128211036332. https://doi.org/10.1177/23982128211036332

Pyndt Jørgensen, B., Krych, L., Pedersen, T. B., Plath, N., Redrobe, J. P., Hansen, A. K., Nielsen, D. S., Pedersen, C. S., Larsen, C., & Sørensen, D. B. (2015). Investigating the long-term effect of subchronic phencyclidine-treatment on novel object recognition and the association between the gut microbiota and behavior in the animal model of schizophrenia. *Physiology & Behavior*, *141*, 32–39.

Raam, T., McAvoy, K. M., Besnard, A., Veenema, A. H., & Sahay, A. (2017). Hippocampal oxytocin receptors are necessary for discrimination of social stimuli. *Nature Communications*, *8*(1), 2001.

Racine, R. J. (1972). Modification of seizure activity by electrical stimulation: II. Motor seizure. *Electroencephalography and Clinical Neurophysiology*, *32*(3), 281–294.

Rajagopal, L., Huang, M., Michael, E., Kwon, S., & Meltzer, H. Y. (2018). TPA-023 attenuates subchronic phencyclidine-induced declarative and reversal learning deficits via GABA A receptor agonist mechanism: possible therapeutic target for cognitive deficit in schizophrenia. *Neuropsychopharmacology*, *43*(12), 2468–2477.

Rajagopal, L., W Massey, B., Huang, M., Oyamada, Y., & Y Meltzer, H. (2014). The novel object recognition test in rodents in relation to cognitive impairment in schizophrenia. *Current Pharmaceutical Design*, *20*(31), 5104–5114.

Redrobe, J. P., Bull, S., & Plath, N. (2010). Translational aspects of the novel object recognition task in rats abstinent following sub-chronic treatment with phencyclidine (PCP): effects of modafinil and relevance to cognitive deficits in schizophrenia. *Frontiers in Psychiatry*, *1*, 146.

Redrobe, J. P., Elster, L., Frederiksen, K., Bundgaard, C., de Jong, I. E. M., Smith, G. P., Bruun, A. T., Larsen, P. H., & Didriksen, M. (2012). Negative modulation of GABA A α5 receptors by RO4938581 attenuates discrete sub-chronic and early postnatal phencyclidine (PCP)-induced cognitive deficits in rats. *Psychopharmacology*, *221*(3), 451–468.

Regan, M. C., Romero-Hernandez, A., & Furukawa, H. (2015). A structural biology perspective on NMDA receptor pharmacology and function. *Current Opinion in Structural Biology*, *33*, 68–75. https://doi.org/https://doi.org/10.1016/j.sbi.2015.07.012

Reichel, J. M., Nissel, S., Rogel-Salazar, G., Mederer, A., Käfer, K., Bedenk, B. T., Martens, H., Anders, R., Grosche, J., & Michalski, D. (2015). Distinct behavioral consequences of short-term and prolonged GABAergic depletion in prefrontal cortex and dorsal hippocampus. *Frontiers in Behavioral Neuroscience*, *8*, 452.

Reilly, W., Koirala, B., & Devaud, L. L. (2009). Sex differences in acoustic startle responses and seizure thresholds between ethanol-withdrawn male and female rats. *Alcohol & Alcoholism*, *44*(6), 561–566.

Reynolds, G. P. (2022). The neurochemical pathology of schizophrenia: post-mortem studies from dopamine to parvalbumin. *Journal of Neural Transmission*, *129*(5), 643–647. https://doi.org/10.1007/s00702-021-02453-6

Reynolds, G. P., & Neill, J. C. (2016). *Modelling the cognitive and neuropathological features of schizophrenia with phencyclidine*. SAGE Publications Sage UK: London, England.

Reynolds, G. P., Zhang, Z. J., & Beasley, C. L. (2001). Neurochemical correlates of cortical GABAergic deficits in schizophrenia: selective losses of calcium binding protein immunoreactivity. *Brain Research Bulletin*, *55*(5), 579–584.

Riordan, A. J., Schaler, A. W., Fried, J., Paine, T. A., & Thornton, J. E. (2018). Estradiol and luteinizing hormone regulate recognition memory following subchronic phencyclidine: Evidence for hippocampal GABA action. *Psychoneuroendocrinology*, *91*, 86–94.

Rocco, B. R., Lewis, D. A., & Fish, K. N. (2016). Markedly lower glutamic acid decarboxylase 67 protein levels in a subset of boutons in schizophrenia. *Biological Psychiatry*, *79*(12), 1006–1015.

Rossato, J. I., Bevilaqua, L. R. M., Myskiw, J. C., Medina, J. H., Izquierdo, I., & Cammarota, M. (2007). On the role of hippocampal protein synthesis in the consolidation and reconsolidation of object recognition memory. *Learning & Memory*, *14*(1–2), 36–46.

Rotaru, D. C., Lewis, D. A., & Gonzalez-Burgos, G. (2012). *The role of glutamatergic inputs onto parvalbumin-positive interneurons: relevance for schizophrenia*.

Rotaru, D. C., Yoshino, H., Lewis, D. A., Ermentrout, G. B., & Gonzalez-Burgos, G. (2011). Glutamate receptor subtypes mediating synaptic activation of prefrontal cortex neurons: relevance for schizophrenia. *Journal of Neuroscience*, *31*(1), 142–156.

Rowland, L. M., Astur, R. S., Jung, R. E., Bustillo, J. R., Lauriello, J., & Yeo, R. A. (2005a). Selective cognitive impairments associated with NMDA receptor blockade in humans. *Neuropsychopharmacology*, *30*(3), 633–639. https://doi.org/10.1038/sj.npp.1300642

Rowland, L. M., Beason-Held, L., Tamminga, C. A., & Holcomb, H. H. (2010). The interactive effects of ketamine and nicotine on human cerebral blood flow. *Psychopharmacology*, *208*(4), 575–584. https://doi.org/10.1007/s00213-009-1758-2

Rowland, L. M., Bustillo, J. R., Mullins, P. G., Jung, R. E., Lenroot, R., Landgraf, E., Barrow, R., Yeo, R., Lauriello, J., & Brooks, W. M. (2005b). Effects of ketamine on anterior cingulate glutamate metabolism in healthy humans: a 4-T proton MRS study. *American Journal of Psychiatry*, *162*(2), 394–396.

Rujescu, D., Bender, A., Keck, M., Hartmann, A. M., Ohl, F., Raeder, H., Giegling, I., Genius, J., McCarley, R. W., Moller, H. J., & Grunze, H. (2006). A pharmacological model for psychosis based on N-methyl-D-aspartate receptor hypofunction: Molecular, cellular, functional and Behavioral abnormalities. *Biological Psychiatry*, *59*(8), 721–729. https://doi.org/10.1016/j.biopsych.2005.08.029

Sabbagh, J. J., Murtishaw, A. S., Bolton, M. M., Heaney, C. F., Langhardt, M., & Kinney, J. W. (2013). Chronic ketamine produces altered distribution of parvalbumin-positive cells in the hippocampus of adult rats. *Neuroscience Letters*, *550*, 69–74. https://doi.org/10.1016/j.neulet.2013.06.040

Sakai, T., Oshima, A., Nozaki, Y., Ida, I., Haga, C., Akiyama, H., Nakazato, Y., & Mikuni, M. (2008). Changes in density of calcium-binding-protein-immunoreactive GABAergic neurons in prefrontal cortex in schizophrenia and bipolar disorder. *Neuropathology*, *28*(2), 143–150.

Sampedro-Piquero, P., Castilla-Ortega, E., Zancada-Menendez, C., Santín, L. J., & Begega, A. (2016). Environmental enrichment as a therapeutic avenue for anxiety in aged Wistar rats: Effect on cat odor exposition and GABAergic interneurons. *Neuroscience*, *330*, 17–25. https://doi.org/https://doi.org/10.1016/j.neuroscience.2016.05.032

Santana, N., Troyano-Rodriguez, E., Mengod, G., Celada, P., & Artigas, F. (2011). Activation of thalamocortical networks by the N-methyl-D-aspartate receptor antagonist phencyclidine: reversal by clozapine. *Biological Psychiatry*, *69*(10), 918–927.

Sawangjit, A., Oyanedel, C. N., Niethard, N., Salazar, C., Born, J., & Inostroza, M. (2018). The hippocampus is crucial for forming non-hippocampal long-term memory during sleep. *Nature*, *564*(7734), 109–113.

Saykin, A. J., Gur, R. C., Gur, R. E., Mozley, P. D., Mozley, L. H., Resnick, S. M., Kester, D. B., & Stafiniak, P. (1991). Neuropsychological function in schizophrenia: selective impairment in memory and learning. *Archives of General Psychiatry*, *48*(7), 618–624.

Scharfman, H. E. (2007). The CA3 "backprojection" to the dentate gyrus. In H. E. Scharfman (Ed.), *Progress in Brain Research* (Vol. 163, pp. 627–637). Elsevier. https://doi.org/https://doi.org/10.1016/S0079-6123(07)63034-9

Schobel, S. A., Chaudhury, N. H., Khan, U. A., Paniagua, B., Styner, M. A., Asllani, I., Inbar, B. P., Corcoran, C. M., Lieberman, J. A., & Moore, H. (2013). Imaging patients with psychosis and a mouse model establishes a spreading pattern of hippocampal dysfunction and implicates glutamate as a driver. *Neuron*, *78*(1), 81–93.

Schroeder, U., Schroeder, H., Schwegler, H., & Sabel, B. A. (2000). Neuroleptics ameliorate phencyclidine-induced impairments of short-term memory. *British Journal of Pharmacology*, *130*(1), 33–40.

Schwabe, K., Brosda, J., Wegener, N., & Koch, M. (2005). Clozapine enhances disruption of prepulse inhibition after sub-chronic dizocilpine-or phencyclidine-treatment in Wistar rats. *Pharmacology Biochemistry and Behavior*, *80*(2), 213–219.

Secher, T., Berezin, V., Bock, E., & Glenthoj, B. (2009). Effect of an NCAM mimetic peptide FGL on impairment in spatial learning and memory after neonatal phencyclidine treatment in rats. *Behavioural Brain Research*, *199*(2), 288–297. https://doi.org/10.1016/j.bbr.2008.12.012

Seillier, A., & Giuffrida, A. (2009). Evaluation of NMDA receptor models of schizophrenia: divergences in the behavioral effects of sub-chronic PCP and MK-801. *Behavioural Brain Research*, *204*(2), 410–415.

Selakovic, D., Joksimovic, J., Zaletel, I., Puskas, N., Matovic, M., & Rosic, G. (2017). The opposite effects of nandrolone decanoate and exercise on anxiety levels in rats may involve alterations in hippocampal parvalbumin–positive interneurons. *PLoS One*, *12*(12), e0189595.

Shelnutt, S. R., Gunnell, M., & Owens, S. M. (1999). Sexual Dimorphism in Phencyclidine In Vitro Metabolism and Pharmacokinetics in Rats. *Journal of Pharmacology and Experimental Therapeutics*, *290*(3), 1292–1298. http://jpet.aspetjournals.org/content/jpet/290/3/1292.full.pdf

Shojaei, A., Anaraki, A. K., Mirnajafi-Zadeh, J., & Atapour, N. (2017). Modifications of inhibitory transmission onto pyramidal neurons by postnatal exposure to MK-801: Effects of enriched environment. *International Journal of Developmental Neuroscience*, *57*, 56–61.

Sik, A., Ylinen, A., Penttonen, M., & Buzsáki, G. (1994). Inhibitory CA1-CA3-hilar region feedback in the hippocampus. *Science*, *265*(5179), 1722–1724.

Sircar, R. (2003). Postnatal phencyclidine-induced deficit in adult water maze performance is associated with N-methyl-D-aspartate receptor upregulation. *International Journal of Developmental Neuroscience*, *21*(3), 159–167. https://doi.org/10.1016/s0736-5748(03)00026-1

Sloviter, R. S. (1991). Feedforward and feedback inhibition of hippocampal principal cell activity evoked by perforant path stimulation: GABA-mediated mechanisms that regulate excitability in vivo. *Hippocampus*, *1*(1), 31–40.

Smith, J. W., Gastambide, F., Gilmour, G., Dix, S., Foss, J., Lloyd, K., Malik, N., & Tricklebank, M. (2011). A comparison of the effects of ketamine and phencyclidine with other antagonists of the NMDA receptor in rodent assays of attention and working memory. *Psychopharmacology*, *217*(2), 255–269.

Snigdha, S., Idris, N., Grayson, B., Shahid, M., & Neill, J. C. (2011a). Asenapine improves phencyclidine-induced object recognition deficits in the rat: evidence for engagement of a dopamine D 1 receptor mechanism. *Psychopharmacology*, *214*(4), 843–853.

Snigdha, S., Neill, J. C., McLean, S. L., Shemar, G. K., Cruise, L., Shahid, M., & Henry, B. (2011b). Phencyclidine (PCP)-Induced Disruption in Cognitive Performance is Gender-Specific and Associated with a Reduction in Brain-Derived Neurotrophic Factor (BDNF) in Specific Regions of the Female Rat Brain. *Journal of Molecular Neuroscience*, *43*(3), 337–345. https://doi.org/10.1007/s12031-010-9447-5

Sohal, V. S., Zhang, F., Yizhar, O., & Deisseroth, K. (2009). Parvalbumin neurons and gamma rhythms enhance cortical circuit performance. *Nature*, *459*(7247), 698–702.

Solbach, S., & Celio, M. R. (1991). Ontogeny of the calcium binding protein parvalbumin in the rat nervous system. *Anatomy and Embryology*, *184*(2), 103–124.

Sood, P., Idris, N. F., Cole, S., Grayson, B., Neill, J. C., & Young, A. M. J. (2011). PD168077, a D4 receptor agonist, reverses object recognition deficits in rats: potential role for D4 receptor mechanisms in improving cognitive dysfunction in schizophrenia. *Journal of Psychopharmacology*, *25*(6), 792–800.

Sorrenti, V., Cecchetto, C., Maschietto, M., Fortinguerra, S., Buriani, A., & Vassanelli, S. (2021). Understanding the effects of anesthesia on cortical electrophysiological recordings: a scoping review. *International Journal of Molecular Sciences*, *22*(3), 1286.

Sosa, M., Gillespie, A. K., & Frank, L. M. (2018). Neural activity patterns underlying spatial coding in the hippocampus. In *Current Topics in Behavioral Neurosciences* (Vol. 37, pp. 43–100). https://doi.org/10.1007/7854_2016_462

Speers, L. J., & Bilkey, D. K. (2021). Disorganization of Oscillatory Activity in Animal Models of Schizophrenia. *Frontiers in Neural Circuits*, 108.

Squire, L. R., & Zola-Morgan, S. (1991). The medial temporal lobe memory system. *Science*, *253*(5026), 1380–1386.

Stackman Jr, R. W., Cohen, S. J., Lora, J. C., & Rios, L. M. (2016). Temporary inactivation reveals that the CA1 region of the mouse dorsal hippocampus plays an equivalent role in the retrieval of long-term object memory and spatial memory. *Neurobiology of Learning and Memory*, *133*, 118–128.

Steele, R. J., & Morris, R. G. M. (1999). Delay-dependent impairment of a matching-to-place task with chronic and intrahippocampal infusion of the NMDA-Antagonist D-AP5. *Hippocampus*, *9*(2), 118–136. https://doi.org/10.1002/(sici)1098-1063(1999)9:2<118::aid-hipo4>3.0.co;2-8

Stefanko, D. P., Barrett, R. M., Ly, A. R., Reolon, G. K., & Wood, M. A. (2009). Modulation of long-term memory for object recognition via HDAC inhibition. *Proceedings of the National Academy of Sciences*, *106*(23), 9447–9452.

Stepan, J., Dine, J., & Eder, M. (2015). Functional optical probing of the hippocampal trisynaptic circuit in vitro: network dynamics, filter properties, and polysynaptic induction of CA1 LTP. *Frontiers in Neuroscience*, *9*, 160.

Steullet, P., Cabungcal, J. H., Coyle, J., Didriksen, M., Gill, K., Grace, A. A., Hensch, T. K., LaMantia, A. S., Lindemann, L., & Maynard, T. M. (2017). Oxidative stress-driven parvalbumin interneuron impairment as a common mechanism in models of schizophrenia. *Molecular Psychiatry*, *22*(7), 936–943.

Steullet, P., Cabungcal, J. H., Monin, A., Dwir, D., O'Donnell, P., Cuenod, M., & Do, K. Q. (2016). Redox dysregulation, neuroinflammation, and NMDA receptor hypofunction: A "central hub" in schizophrenia pathophysiology? *Schizophrenia Research*, *176*(1), 41–51. https://doi.org/https://doi.org/10.1016/j.schres.2014.06.021

Sun, N., Harte, M., & Gigg, J. (2022). Investigating hippocampal synaptic deficits in the sub-chronic phencyclidine rat model for schizophrenia. *FENS Forum Abstract*, S03-025, 2333.

Sun, N., Harte, M., & Gigg, J. (2023). Aerobic exercise improves dorsal hippocampal CA1 synaptic plasticity and novel object memory in the sub-chronic phencyclidine rat model for schizophrenia. *BNA Festival of Neuroscience Abstract*, M_PZ4_096 (TP), 285.

Sun, Q., Li, X., Li, A., Zhang, J., Ding, Z., Gong, H., & Luo, Q. (2020). Ventral hippocampal-prefrontal interaction affects social behavior via parvalbumin positive neurons in the medial prefrontal cortex. *Iscience*, *23*(3), 100894.

Sun, Y., Nguyen, A. Q., Nguyen, J. P., Le, L., Saur, D., Choi, J., Callaway, E. M., & Xu, X. (2014). Cell-type-specific circuit connectivity of hippocampal CA1 revealed through Cre-dependent rabies tracing. *Cell Reports*, *7*(1), 269–280.

Sutcliffe, J. S., Marshall, K. M., & Neill, J. C. (2007). Influence of gender on working and spatial memory in the novel object recognition task in the rat. *Behavioural Brain Research*, *177*(1), 117–125. https://doi.org/https://doi.org/10.1016/j.bbr.2006.10.029

Sutherland, R. J., Whishaw, I. Q., & Kolb, B. (1983). A behavioural analysis of spatial localization following electrolytic, kainate-or colchicine-induced damage to the hippocampal formation in the rat. *Behavioural Brain Research*, *7*(2), 133–153.

Suzuki, Y., Jodo, E., Takeuchi, S., Niwa, S., & Kayama, Y. (2002). Acute administration of phencyclidine induces tonic activation of medial prefrontal cortex neurons in freely moving rats. *Neuroscience*, *114*(3), 769–779.

Tamminga, C. A., Stan, A. D., & Wagner, A. D. (2010). The hippocampal formation in schizophrenia. *American Journal of Psychiatry*, *167*(10), 1178–1193.

Tanimizu, T., Kono, K., & Kida, S. (2018). Brain networks activated to form object recognition memory. *Brain Research Bulletin*, *141*, 27–34.

Tanqueiro, S. R., Mouro, F. M., Ferreira, C. B., Freitas, C. F., Fonseca-Gomes, J., Simões do Couto, F., Sebastião, A. M., Dawson, N., & Diógenes, M. J. (2021). Sustained NMDA receptor hypofunction impairs brain-derived neurotropic factor signalling in the PFC, but not in the hippocampus, and disturbs PFC-dependent cognition in mice. *Journal of Psychopharmacology*, *35*(6), 730–743.

Tao, R., Davis, K. N., Li, C., Shin, J. H., Gao, Y., Jaffe, A. E., Gondre-Lewis, M. C., Weinberger, D. R., Kleinman, J. E., & Hyde, T. M. (2018). GAD1 alternative transcripts and DNA methylation in human prefrontal cortex and hippocampus in brain development, schizophrenia. *Molecular Psychiatry*, *23*(6), 1496–1505.

Thomases, D. R., Cass, D. K., & Tseng, K. Y. (2013). Periadolescent exposure to the NMDA receptor antagonist MK-801 impairs the functional maturation of local GABAergic circuits in the adult prefrontal cortex. *Journal of Neuroscience*, *33*(1), 26–34.

Thomsen, M. S., Christensen, D. Z., Hansen, H. H., Redrobe, J. P., & Mikkelsen, J. D. (2009). α7 Nicotinic acetylcholine receptor activation prevents behavioral and molecular changes induced by repeated phencyclidine treatment. *Neuropharmacology*, *56*(6–7), 1001–1009. https://doi.org/10.1016/J.NEUROPHARM.2009.02.003

Thomsen, M. S., Hansen, H. H., & Mikkelsen, J. D. (2010). Opposite effect of phencyclidine on activity-regulated cytoskeleton-associated protein (Arc) in juvenile and adult limbic rat brain regions. *Neurochemistry International*, *56*(2), 270–275.

Torrey, E. F., Barci, B. M., Webster, M. J., Bartko, J. J., Meador-Woodruff, J. H., & Knable, M. B. (2005). Neurochemical markers for schizophrenia, bipolar disorder, and major depression in postmortem brains. *Biological Psychiatry*, *57*(3), 252–260.

Traynelis, S. F., Wollmuth, L. P., McBain, C. J., Menniti, F. S., Vance, K. M., Ogden, K. K., Hansen, K. B., Yuan, H., Myers, S. J., & Dingledine, R. (2010). Glutamate receptor ion channels: structure, regulation, and function. *Pharmacological Reviews*, *62*(3), 405–496.

Tregellas, J. R., Smucny, J., Harris, J. G., Olincy, A., Maharajh, K., Kronberg, E., Eichman, L. C., Lyons, E., & Freedman, R. (2014). Intrinsic hippocampal activity as a biomarker for cognition and symptoms in schizophrenia. *American Journal of Psychiatry*, *171*(5), 549–556.

Troyano-Rodriguez, E., Lladó-Pelfort, L., Santana, N., Teruel-Martí, V., Celada, P., & Artigas, F. (2014). Phencyclidine inhibits the activity of thalamic reticular gamma-aminobutyric acidergic neurons in rat brain. *Biological Psychiatry*, *76*(12), 937–945.

Tsai, C. W., Tsai, S. J., Pan, Y. J., Lin, H. M., Pan, T. Y., & Yang, F. Y. (2022). Transcranial Ultrasound Stimulation Reverses Behavior Changes and the Expression of Calcium-Binding Protein in a Rodent Model of Schizophrenia. *Neurotherapeutics*, *19*(2), 649–659. https://doi.org/10.1007/s13311-022-01195-x

Tse, M. T., Piantadosi, P. T., & Floresco, S. B. (2015). Prefrontal cortical gamma-aminobutyric acid transmission and cognitive function: drawing links to schizophrenia from preclinical research. *Biological Psychiatry*, *77*(11), 929–939.

Tsien, J. Z., Huerta, P. T., & Tonegawa, S. (1996). The essential role of hippocampal CA1 NMDA receptor-dependent synaptic plasticity in spatial memory. *Cell*, *87*(7), 1327–1338. https://doi.org/10.1016/s0092-8674(00)81827-9

Tsivion-Visbord, H., Perets, N., Sofer, T., Bikovski, L., Goldshmit, Y., Ruban, A., & Offen, D. (2020). Mesenchymal stem cells derived extracellular vesicles improve behavioral and biochemical deficits in a phencyclidine model of schizophrenia. *Translational Psychiatry*, *10*(1), 305. https://doi.org/10.1038/s41398-020-00988-y

Tuscher, J. J., Taxier, L. R., Fortress, A. M., & Frick, K. M. (2018). Chemogenetic inactivation of the dorsal hippocampus and medial prefrontal cortex, individually and concurrently, impairs object recognition and spatial memory consolidation in female mice. *Neurobiology of Learning and Memory*, *156*, 103–116.

Umbricht, D., Schmid, L., Koller, R., Vollenweider, F. X., Hell, D., & Javitt, D. C. (2000). Ketamine-induced deficits in auditory and visual context-dependent processing in

healthy volunteers: implications for models of cognitive deficits in schizophrenia. *Archives of General Psychiatry*, *57*(12), 1139–1147.

Unal, G., Sirvanci, S., & Aricioglu, F. (2021). α7 nicotinic receptor agonist and positive allosteric modulators differently improved schizophrenia-like cognitive deficits in male rats. *Behavioural Brain Research*, *397*, 112946.

Urakawa, S., Takamoto, K., Hori, E., Sakai, N., Ono, T., & Nishijo, H. (2013). Rearing in enriched environment increases parvalbumin-positive small neurons in the amygdala and decreases anxiety-like behavior of male rats. *BMC Neuroscience*, *14*(1), 13. https://doi.org/10.1186/1471-2202-14-13

Valle, F. P. (1970). Effects of strain, sex, and illumination on open-field behavior of rats. *The American Journal of Psychology*, 103–111.

van Strien, N. M., Cappaert, N. L. M., & Witter, M. P. (2009). The anatomy of memory: an interactive overview of the parahippocampal–hippocampal network. *Nature Reviews Neuroscience*, *10*(4), 272–282. https://doi.org/10.1038/nrn2614

Vinogradova, O. S. (2001). Hippocampus as comparator: role of the two input and two output systems of the hippocampus in selection and registration of information. *Hippocampus*, *11*(5), 578–598.

Volk, D. W., Austin, M. C., Pierri, J. N., Sampson, A. R., & Lewis, D. A. (2000). Decreased glutamic acid decarboxylase67 messenger RNA expression in a subset of prefrontal cortical γ-aminobutyric acid neurons in subjects with schizophrenia. *Archives of General Psychiatry*, *57*(3), 237–245.

Vollenweider, F. X., Leenders, K. L., Scharfetter, C., Antonini, A., Maguire, P., Missimer, J., & Angst, J. (1997). Metabolic hyperfrontality and psychopathology in the ketamine model of psychosis using positron emission tomography (PET) and [18F] fluorodeoxyglucose (FDG). *European Neuropsychopharmacology*, *7*(1), 9–24.

Vreugdenhil, M., Jefferys, J. G. R., Celio, M. R., & Schwaller, B. (2003). Parvalbumin-deficiency facilitates repetitive IPSCs and gamma oscillations in the hippocampus. *Journal of Neurophysiology*, *89*(3), 1414–1422.

Wang, C. Z., Yang, S. F., Xia, Y., & Johnson, K. M. (2008). Postnatal phencyclidine administration selectively reduces adult cortical parvalbumin-containing interneurons. *Neuropsychopharmacology*, *33*(10), 2442–2455.

Wang, H. X., & Gao, W. J. (2009). Cell type-specific development of NMDA receptors in the interneurons of rat prefrontal cortex. *Neuropsychopharmacology*, *34*(8), 2028–2040.

Wang, J., Bast, T., Wang, Y., & Zhang, W. (2015). Hippocampus and two-way active avoidance conditioning: Contrasting effects of cytotoxic lesion and temporary inactivation. *Hippocampus*, *25*(12), 1517–1531.

Wang, X., Hu, Y., Liu, W., Ma, Y., Chen, X., Xue, T., & Cui, D. (2021). Molecular Basis of GABA Hypofunction in Adolescent Schizophrenia-Like Animals. *Neural Plasticity*, *2021*.

Warburton, E. C., & Brown, M. W. (2015). Neural circuitry for rat recognition memory. *Behavioural Brain Research*, *285*, 131–139.

Wass, C., Archer, T., Palsson, E., Fejgin, K., Alexandersson, A., Klamer, D., Engel, J. A., & Svensson, L. (2006). Phencyclidine affects memory in a nitric oxide-dependent manner: Working and reference memory. *Behavioural Brain Research*, *174*(1), 49–55. https://doi.org/10.1016/j.bbr.2006.07.003

Waters, S. J., Basile, B. M., & Murray, E. A. (2023). Reevaluating the role of the hippocampus in memory: A meta-analysis of neurotoxic lesion studies in nonhuman primates. *Hippocampus*, *33*(6), 787–807.

Wesseling, H., Want, E. J., Guest, P. C., Rahmoune, H., Holmes, E., & Bahn, S. (2015). Hippocampal proteomic and metabonomic abnormalities in neurotransmission, oxidative stress, and apoptotic pathways in a chronic phencyclidine rat model. *Journal of Proteome Research*, *14*(8), 3174–3187.

Whishaw, I. Q., & Jarrard, L. E. (1996). Evidence for extrahippocampal involvement in place learning and hippocampal involvement in path integration. *Hippocampus*, *6*(5), 513–524. https://doi.org/10.1002/(sici)1098-1063(1996)6:5<513::aid-hipo4>3.0.co;2-j

Wieschollеck, V., & Manahan-Vaughan, D. (2012). PDE4 inhibition enhances hippocampal synaptic plasticity in vivo and rescues MK801-induced impairment of long-term potentiation and object recognition memory in an animal model of psychosis. *Translational Psychiatry*, *2*(3), e89–e89.

Williams, S. A., Gwilt, M., Hock, R., Taylor, C., Loayza, J., Stevenson, C. W., Cassaday, H. J., & Bast, T. (2022). Hippocampal disinhibition reduces contextual and elemental fear conditioning while sparing the acquisition of latent inhibition. *Eneuro*, *9*(1).

Williams, S. A., Hock, R., Oelschlegel, A., Prior, M., Goldschmidt, J., & Bast, T. (2020). Brain-wide activation changes caused by hippocampal neural disinhibition: A translational imaging study using SPECT and MRS in a rat model. *FENS Abstract*.

Wingert, J. C., & Sorg, B. A. (2021). Impact of perineuronal nets on electrophysiology of parvalbumin interneurons, principal neurons, and brain oscillations: a review. *Frontiers in Synaptic Neuroscience*, 22.

Winters, B. D., Forwood, S. E., Cowell, R. A., Saksida, L. M., & Bussey, T. J. (2004). Double dissociation between the effects of peri-postrhinal cortex and hippocampal lesions on tests of object recognition and spatial memory: heterogeneity of function within the temporal lobe. *Journal of Neuroscience*, *24*(26), 5901–5908.

Winters, B. D., Saksida, L. M., & Bussey, T. J. (2008). Object recognition memory: neurobiological mechanisms of encoding, consolidation and retrieval. *Neuroscience & Biobehavioral Reviews*, *32*(5), 1055–1070.

Witter, M. P. (1993). Organization of the entorhinal-hippocampal system: a review of current anatomical data. *HIPPOCAMPUS-NEW YORK-CHURCHILL LIVINGSTONE-*, *3*, 33.

Woo, T. U. W., Walsh, J. P., & Benes, F. M. (2004). Density of glutamic acid decarboxylase 67 messenger RNA-containing neurons that express the N-methyl-D-aspartate receptor subunit NR2A in the anterior cingulate cortex in schizophrenia and bipolar disorder. *Archives of General Psychiatry*, *61*(7), 649–657.

Wu, K., Canning, K. J., & Leung, L. S. (1998). Functional interconnections between CA3 and the dentate gyrus revealed by current source density analysis. *Hippocampus*, *8*(3), 217–230. https://doi.org/https://doi.org/10.1002/(SICI)1098-1063(1998)8:3<217::AID-HIPO5>3.0.CO;2-G

Xi, D., Zhang, W., Wang, H. X., Stradtman III, G. G., & Gao, W. J. (2009). Dizocilpine (MK-801) induces distinct changes of N-methyl-D-aspartic acid receptor subunits in parvalbumin-containing interneurons in young adult rat prefrontal cortex. *International Journal of Neuropsychopharmacology*, *12*(10), 1395–1408.

Young, J. W., Powell, S. B., Risbrough, V., Marston, H. M., & Geyer, M. A. (2009). Using the MATRICS to guide development of a preclinical cognitive test battery for research in schizophrenia. *Pharmacology & Therapeutics*, *122*(2), 150–202.

Yu, B., Wang, C., Liu, J., Johnson, K. M., & Gallagher, J. P. (2002). Adaptation to chronic PCP results in hyperfunctional NMDA and hypofunctional GABAA synaptic receptors. *Neuroscience*, *113*(1), 1–10.

Yu, J. Y., Fang, P., Wang, C., Wang, X. X., Li, K., Gong, Q., Luo, B.-Y., & Wang, X. D. (2018). Dorsal CA1 interneurons contribute to acute stress-induced spatial memory deficits. *Neuropharmacology*, *135*, 474–486.

Yushkevich, P. A., Gao, Y., & Gerig, G. (2016). ITK-SNAP: An interactive tool for semi-automatic segmentation of multi-modality biomedical images. *2016 38th Annual International Conference of the IEEE Engineering in Medicine and Biology Society (EMBC)*, 3342–3345. https://doi.org/10.1109/EMBC.2016.7591443

Zain, M. A., Rouhollahi, E., Pandy, V., Mani, V., Majeed, A. A., Wong, W. F., & Mohamed, Z. (2018). Phencyclidine dose optimisation for induction of spatial learning and memory deficits related to schizophrenia in C57BL/6 mice. *Experimental Animals*, *67*(4), 421–429. https://doi.org/10.1538/expanim.18-0006

Zhang, H., Sun, X., Wang, J., Zhang, Z., Zhao, H., Li, H., Ji, M., Li, K., & Yang, J. (2016). Reactive oxygen species-mediated loss of phenotype of parvalbumin interneurons contributes to long-term cognitive impairments after repeated neonatal ketamine exposures. *Neurotoxicity Research*, *30*(4), 593–605.

Zhang, W. N., Bast, T., & Feldon, J. (2002a). Effects of hippocampal N-methyl-[D]-aspartate infusion on locomotor activity and prepulse inhibition: Differences between the dorsal and ventral hippocampus. *Behavioral Neuroscience*, *116*(1), 72–84. https://doi.org/10.1037/0735-7044.116.1.72

Zhang, W. N., Bast, T., & Feldon, J. (2002b). Prepulse inhibition in rats with temporary inhibition/inactivation of ventral or dorsal hippocampus. *Pharmacology Biochemistry and Behavior*, *73*(4), 929–940.

Zhang, W. N., Bast, T., Xu, Y., & Feldon, J. (2014). Temporary inhibition of dorsal or ventral hippocampus by muscimol: distinct effects on measures of innate anxiety on the elevated plus maze, but similar disruption of contextual fear conditioning. *Behavioural Brain Research*, *262*, 47–56.

Zhang, Y., Behrens, M. M., & Lisman, J. E. (2008). Prolonged exposure to NMDAR antagonist suppresses inhibitory synaptic transmission in prefrontal cortex. *Journal of Neurophysiology*, *100*(2), 959–965.

Zhang, Y., Yoshida, T., Katz, D. B., & Lisman, J. E. (2012). NMDAR antagonist action in thalamus imposes delta oscillations on the hippocampus. *Journal of Neurophysiology*, *107*(11), 3181–3189.

Zhang, Z. J., & Reynolds, G. P. (2002). A selective decrease in the relative density of parvalbumin-immunoreactive neurons in the hippocampus in schizophrenia. *Schizophrenia Research*, *55*(1–2), 1–10.

Zhou, Q., & Sheng, M. (2013). NMDA receptors in nervous system diseases. *Neuropharmacology*, *74*, 69–75. https://doi.org/https://doi.org/10.1016/j.neuropharm.2013.03.030

Zorumski, C. F., & Izumi, Y. (2012). NMDA receptors and metaplasticity: Mechanisms and possible roles in neuropsychiatric disorders. *Neuroscience & Biobehavioral Reviews*, *36*(3), 989–1000. https://doi.org/https://doi.org/10.1016/j.neubiorev.2011.12.011

Zucker, R. S., & Regehr, W. G. (2002). Short-term synaptic plasticity. *Annual Review of Physiology*, *64*(1), 355–405.

Appendix: Additional work

Can levetiracetam ameliorate neurocognitive effects of hippocampal disinhibition? In vivo electrophysiological and behavioural studies

Miriam Gwilt[1], Adam Seaton[1], Stuart Williams1, Marie Pezze[1], **Charlotte Taylor[1]**, Joanna Loayza[1], Boris Ferger[2] and Tobias Bast[1]

[1]School of Psychology and Neuroscience@Nottingham, University of Nottingham, [2]Boehringer Ingelheim Pharma GmbH & Co. KG, Biberach, Germany

Background: Hippocampal neural disinhibition (decreased GABA function) has been implicated in cognitive disorders, including schizophrenia and age-related cognitive decline (Bast et al., 2017, *BrJPharmacology*). We previously showed that hippocampal disinhibition in rats by local microinfusion of the GABA-A antagonist picrotoxin disrupts memory and attention, increases locomotor activity, and enhances hippocampal multi-unit burst firing under anaesthesia (McGarrity et al., 2017, *CerebCortex*). Low doses of levetiracetam, the second-generation antiepileptic, have been shown to decrease both age-related hippocampal neural hyperactivity and cognitive deficits in humans and rodent models (Haberman et al., 2017, *Neurotherapeutics*). Here, we tested if systemic levetiracetam would antagonize 1) the enhanced hippocampal burst firing and 2) the open-field locomotor hyperactivity caused by hippocampal disinhibition by picrotoxin.

Methods and Results: 1) Using multi-unit recordings under anaesthesia, we replicated that hippocampal picrotoxin (150 ng) enhances hippocampal burst firing. Levetiracetam selectively attenuated the increased burst duration, with this effect being significant at 10 mg/kg (i.p.), but not 50 mg/kg; 50 mg/kg slightly reduced the peak frequency in bursts under baseline conditions. Based on these findings, we used 10 mg/kg for the locomotor studies. 2) Levetiracetam (10 mg/kg) attenuated locomotor hyperactivity caused by hippocampal disinhibition; this was supported by a strong trend towards an interaction of systemic injection (levetiracetam vs. saline) and hippocampal infusion (picrotoxin vs. saline) in a 2X2 within-subjects study (p = 0.0523).

Conclusions: Low-dose levetiracetam attenuated some neural and behavioural effects of hippocampal disinhibition. Levetiracetam's impact on clinically relevant cognitive impairments caused by hippocampal disinhibition (McGarrity et al., 2017, *CerebCortex*) remains to be examined.

MIA-induced osteoarthritis-like chronic knee pain: impact on cognitive functions in Lister hooded rats?

Sara Gonçalves[1, 2], Stephen Woodhams[1, 2], **Charlotte Taylor**[3], Marie Pezze[3], Mohsen Shahtaheri[2], Gareth Hathway[1, 2], Tobias Bast[2, 3], Victoria Chapman[1, 2]

[1]School of Life Sciences, University of Nottingham, [2]Arthritis UK Pain Centre, University of Nottingham, [3]School of Psychology, University of Nottingham

Chronic pain has been associated with physiological changes in forebrain regions, including impairments in memory and cognitive flexibility. Here, we examine the impact of OA-like chronic pain on selected cognitive function in a well-characterised rodent model.

We adapted the monoiodoacetate (MIA) model of chronic OA-like joint pain for use in adult male Lister Hooded (LH) rats. We compared memory and behavioural flexibility in MIA-treated and control LH rats, using the Watermaze delayed-matching-to-place (DMP) test, novel object recognition (NOR) and an operant response-shifting task. Nociceptive behaviour and sensorimotor activity were also measured as well as joint pathology, which was confirmed histologically.

MIA injection caused robust pain behaviour, mainly in weight-bearing asymmetry ($F_{(1,13)} = 59.4$; $p < 0.0001$), accompanied by significant cartilage damage and synovitis. MIA-injected rats showed minor motor deficits with reduced rearing ($F_{(1,13)} = 4.86$; $P = 0.046$). However, there was no significant impairment in watermaze DMP performance, which is highly sensitive to hippocampal dysfunction, indicating that MIA-treated LH rats do not have substantially altered hippocampal function. In addition, MIA injection did not affect NOR memory or behavioural flexibility.

Our data are consistent with human neuroimaging studies indicating that OA pain may affect hippocampal function less than other chronic pain conditions, as chronic back pain and complex regional pain syndrome. There is evidence that chronic pain patients on long-term opioid treatment may have significantly reduced cognitive performance especially in chronic pain patients. In ongoing studies, we will examine the additive impact of long-term morphine treatment on cognitive performance in MIA-treated rats.

Hippocampal disinhibition reduces cue and contextual fear conditioning whilst sparing the formation of latent inhibition

Stuart Williams[1,3], Miriam Gwilt[1,3], Rebecca Hock[1,3], **Charlotte Taylor**[1,3], Joanna Loayza[1,3], Carl Stevenson[2,3], Helen Cassaday[1,3], Tobias Bast[1,3]

[1]School of Psychology, University of Nottingham, [2]School of Biosciences, University of Nottingham, [3]Neuroscience@Nottingham

Hippocampal neural disinhibition (i.e., reduced GABAergic inhibition) is a key feature of schizophrenia pathophysiology (Heckers & Konradi, 2015, *SchizophrRes*). The hippocampus is part of the fear circuit and can modulate prefrontal and striatal mechanisms, including dopamine signalling (Bast et al., 2011, *CurrOpinNeurobiol*), which plays a role in salience modulation (Lingawi et al., 2017, *CerebCortex*; Morres et al., 2020, *Neuron*). Therefore, hippocampal neural disinhibition may contribute to impairments in fear conditioning and salience modulation associated with schizophrenia (Jensen et al., 2008, *Neuropsychopharmacology*).

To test this hypothesis, we examined the effect of ventral hippocampal disinhibition by picrotoxin (GABA-A antagonist) infusion in rats (McGarrity et al., 2017, *CerebCortex*) on fear conditioning and salience modulation, as reflected by latent inhibition (LI), using a conditioned-emotional response paradigm with a light CS (Nelson et al., 2011, *JPsychopharm*). Reduced conditioning in rats pre-exposed (PE) to the CS, compared to non-pre-exposed (NPE) rats, was used to measure LI. Picrotoxin or saline were infused prior to both pre-exposure and conditioning (Experiment 1) or pre-exposure only (Experiment 2). Data was analysed by ANOVA with infusion and pre-exposure as between-subjects factors.

In Exp. 1, hippocampal disinhibition virtually abolished fear conditioning to the light CS, as reflected by a significantly increased suppression ratio in picrotoxin compared to saline rats; this resulted in similarly low conditioning in PE and NPE groups, whereas saline rats showed marked LI, as reflected by stronger conditioning (lower suppression ratios) in PE than NPE rats. Hippocampal picrotoxin prior to PE and conditioning also reduced contextual fear conditioning, indicated by reduced latency to lick compared to the saline group during re-exposure to the conditioning context. In Exp. 2, hippocampal picrotoxin at pre-exposure only did not affect conditioning or the formation of LI.

Overall, ventral hippocampal disinhibition markedly disrupted fear conditioning to a light CS, resembling reduced aversive cue conditioning in schizophrenia. However, we found no evidence that hippocampal disinhibition disrupts the formation of LI.

Prefrontal Disinhibition Disrupts Reversal Performance

Jacco Renstrom[1], **Charlotte Taylor**[1], Joanna Loayza[1], Silvia Maggi[1], Paula Moran[1], Carl Stevenson[2], Moritz von Heimendahl[3], Serena Deiana[3], Tobias Bast[1]

[1]School of Psychology, University of Nottingham, UK, [2]School of Biosciences, University of Nottingham, UK, [3]Boehringer Ingelheim Pharma GmbH & Co. KG, Biberach, Germany

A reduction in prefrontal GABAergic inhibition, so-called neural disinhibition, is a key feature of schizophrenia. Additionally, schizophrenia is characterised by marked reversal learning deficits (Leeson et al., 2009, *BiolPsychiatry*). Reversal learning has mainly been found to require the orbitofrontal, but not prefrontal, cortex (Boulougouris et al., 2007*, BehavBrainRes).* However, we hypothesised that prefrontal disinhibition may impair reversal performance, because such disinhibition causes aberrant prefrontal neuron firing and may, thus, also disrupt processing in projections sites (Bast et al., 2017, *BrJPharmacol*), including the orbitofrontal cortex (Sesack et al., 1989, *JCompNeurol*).

We manipulated prefrontal GABAergic activity in rats using local microinfusions of a GABA receptor agonist (muscimol), resulting in functional inhibition, and antagonist (picrotoxin), resulting in disinhibition (Pezze et al., 2014, *JNeurosci*). Reversal learning performance was assessed using an operant two-lever repeated reversal paradigm adapted from Brady & Floresco (2015, *JVisExp*), similar to Boulougouris et al. (2007*, BehavBrainRes*). Beyond classical performance measures, such as trials-to-criterion, we looked at trial-by-trial strategy probabilities to understand the role of prefrontal GABA in the implementation of successful strategies underlying reversal performance.

Prefrontal disinhibition, but not inhibition, markedly impaired repeated reversal performance. Although prefrontal disinhibition reduced expression of the old rule, rats with prefrontal disinhibition failed to show the expected reduction in adherence to the old rule and shift to the new rule following reversal. Trial-by-trial strategy analysis suggested that prefrontal disinhibition disrupted the pursuit of strategies supporting reversal performance, including a lose-shift strategy.

Overall, although reversal performance does not require prefrontal neural activity (i.e., is unaffected by muscimol inhibition), aberrant prefrontal activity due to disinhibition disrupts reversal performance.

Further characterisation of the rat model of Tourette-related striatal disinhibition: in vivo electrophysiological and behavioural studies

Joanna Loayza, **Charlotte Taylor**, Jacco Renstrom, Rachel Grasmeder Allen, Stephen Jackson, Tobias Bast

School of Psychology, University of Nottingham

Tourette's syndrome is characterised by loss of GABAergic inhibition, so called neural disinhibition, in the striatum. Dorsal-striatal microinjection of GABA-A antagonists, including picrotoxin, produces tic-like movements in rodents and primates that resemble motor tics in Tourette's.

Here, we unilaterally infused picrotoxin (300 ng/0.5 µl) or saline (0.5 µl) into the anterior dorsal striatum of young adult male Lister hooded rats and characterised further the neuro-behavioural impact of striatal disinhibition by electrophysiological and behavioural measurements.

Electrophysiological recordings in the striatum under isoflurane anaesthesia showed that picrotoxin disinhibition, apart from evoking large LFP spike-wave discharges, markedly enhanced multi-unit burst firing. In freely moving rats, striatal picrotoxin reliably induced tic-like movements, which involved lifting the contralateral forelimb, rotating the head and torso before returning to normal body posture. Some of these movements lasted for several seconds and led to the whole-body rotation around its long axis. Automated photobeam measurements revealed that striatal disinhibition increased locomotor activity and fine motor counts. The time course of the latter matched that of tic-like movements, suggesting a simple automated way to measure these. Striatal disinhibition did not affect prepulse-inhibition (PPI) of the acoustic startle response, but tended to reduce startle. Data was analysed using ANOVAs.

Our electrophysiological findings in anaesthetised rats show that striatal disinhibition caused marked spike-wave discharges in striatum, similar to previous findings in freely moving rats, and markedly enhanced burst firing of striatal neurons. In freely moving rats, striatal disinhibition reliably produced tic-like movements, and we characterised the time course and key features of these movements. Striatal disinhibition increased locomotor activity suggesting such disinhibition may contribute to hyperactivity, which is often comorbid with Tourette's. Contrasting with PPI disruption in Tourette's, striatal disinhibition in rats did not affect PPI, suggesting GABAergic inhibition is not required for intact PPI and deficits in PPI are not necessary for tic-like movements.

Too little and too much: prefrontal inhibition impairs early acquisition of operant reversal learning, whereas prefrontal disinhibition impairs later serial reversal performance in rats

Jacco Renstrom[1], **Charlotte Taylor**[1], Joanna Loayza[1], Luke O'Hara[1], Rachel Grasmeder Allen[1], Silvia Maggi[1], Paula Moran[1], Carl Stevenson[2], Moritz von Heimendahl[3], Serena Deiana[3], Tobias Bast[1]

[1]School of Psychology, University of Nottingham, UK, [2]School of Biosciences, University of Nottingham, UK, [3]Boehringer Ingelheim Pharma GmbH & Co. KG, Biberach, Germany

Schizophrenia has been associated with both hypofrontality (i.e., reduced prefrontal cortex activation) and prefrontal disinhibition (i.e., reduced GABAergic neural inhibition). Additionally, schizophrenia is characterised by marked reversal learning deficits. Reversal learning has mainly been found to require the orbitofrontal (OFC), but not prefrontal, cortex (PFC). However, the PFC may still be required for reversal learning if the reversal is particularly demanding. Additionally, even if the PFC is not required, local disinhibition may impair reversal performance, as such disinhibition causes aberrant prefrontal neuron firing and may, thus, also disrupt processing in projection sites, including the OFC.

Here, we examined the impact of medial PFC inhibition and disinhibition in rats, by infusion of the GABA-A receptor agonist muscimol or antagonist picrotoxin, respectively, on an operant two-lever reversal task. In two cohorts, we studied the impact on early reversals (task naïve rats with significant between-session performance improvements) and on later serial reversals (when rats showed relatively stable performance indicating reversal proficiency).

In addition to classical performance measures, including responses to criterion, we used a Bayesian trial-by-trial analysis to examine strategies underlying reversal performance and how these were affected by prefrontal manipulations. Data was analysed using ANOVAs with infusion, trials and task stages as variables.

PFC inhibition impaired early, but not late, reversal performance by increasing perseveration and impairing 'lose-shift' behaviour. In contrast, PFC disinhibition disrupted late reversal performance, characterised by impairments in both exploitatory and exploratory strategies, resulting in slower switching to the new response-reward associations.

Results indicate that PFC hypoactivity impairs exploration during early reversal stages, which disrupts early reversal acquisition. At later reversal stages, hypoactivity does not impair performance, indicating the PFC is not required when task proficiency is high. In contrast, PFC

disinhibition impaired later serial reversal performance by impairing both exploration and exploitation.

Contribution of medial prefrontal cortex D1 receptors to early and repeated reversal learning in rats

Luke O'Hara, Jacco Renstrom, Rachel Grasmeder Allen, **Charlotte Taylor**, Joanna Loayza, Tobias Bast, Silvia Maggi

School of Psychology, University of Nottingham

Cognitive flexibility allows individuals to adjust their behaviour in response to changes in their environment. A form of cognitive flexibility is reversal learning: the ability to switch between responses when the reward contingency of the responses is reversed. Impaired in Schizophrenia and other neuropsychiatric disorders, reversal learning depends on frontal cortex function. The prefrontal cortex receives midbrain dopamine projections, which convey information about reward feedback signals. Moreover, dopamine D1 receptors in the medial prefrontal cortex (mPFC) have been implicated in learning and attention. However, whether mPFC D1 receptors play a role in the acquisition of reversal learning or in flexibly switching between response rules after repeated exposure is not fully understood.

To address this, we examined the impact of mPFC infusion of the D1 receptor agonist SKF 81297 or the antagonist SCH 23390 on reversal performance on a two-lever task in male Lister hooded rats. In one cohort, we tested the impact on early reversals, when rats were naïve and showed significant between-session performance improvements. In another cohort, we tested the impact on later repeated reversals, when rats had 'learnt to reverse' and their performance was relatively stable across reversals.

In both experiments, mPFC SCH, but not SKF, increased response omissions and latencies compared to saline infusions. Furthermore, mPFC SCH impaired the expression of the previous rule and decreased perseverative errors during early reversals, but not later reversals. Moreover, a Bayesian trial-by-trial analysis revealed that mPFC SKF increased perseveration, whereas SCH decreased perseveration, during later reversals. These findings suggest that mPFC D1 receptors modulate the expression/exploitation of recently learnt rules and inhibit exploratory behaviour. Specifically, D1 antagonism reduces expression of a previously learned rule and promotes exploration, whereas D1 agonism promotes exploitation at the expense of exploration. Additional Bayesian trial-by-trial analyses are on the way to examine the emergence of exploratory versus exploitative behaviour across reversals.

Ventral hippocampal functional inhibition disrupts repeated reversal learning, whereas disinhibition disrupts expression of the previous response

Rachel Grasmeder Allen, **Charlotte Taylor**, Jacco Renstrom, Joanna Loayza, Luke O'Hara, Jacob Juty, Neave Smith, Silvia Maggi, Tobias Bast

School of Psychology, University of Nottingham, UK

Reversal learning is a form of cognitive flexibility and involves switching from one response to another when the reward contingencies of the responses are reversed. Recently, we found that medial prefrontal cortex (mPFC) disinhibition by the GABA-A receptor antagonist picrotoxin markedly impaired repeated reversal learning performance in rats. mPFC functional inhibition by the GABA-A receptor agonist muscimol did not impair repeated reversal learning performance, although it impaired acquisition of reversal learning. The ventral hippocampus (VH) strongly projects to the mPFC, and VH disinhibition may disrupt functions depending on appropriate mPFC activity (McGarrity et al., 2017, *CerebCortex*). However, little is known about how changes in hippocampal activity affect reversal learning.

Here, we examined how VH functional inhibition or disinhibition, by muscimol or picrotoxin infusion, affected repeated reversal performance on a two-lever reversal task in male Lister hooded rats. Rats were trained to acquire a spatial discrimination (right or left lever) and then completed four reversals, to achieve relatively stable reversal performance levels. Then, the impact of saline, muscimol and picrotoxin infusion into the VH on repeated reversals was compared within-subjects. Retraining days, without infusions, were interleaved between reversal days to reinforce the previous rule before the next reversal; on infusion days, 20 'reminder' trials to test expression of the previous rule preceded reversal trials. Data were analysed by repeated-measures ANOVA, using infusion as within-subjects factor.

Repeated reversal learning was impaired by VH functional inhibition (increased responses to criterion), but unaffected by disinhibition. This indicates that repeated reversal learning requires VH activity, but not balanced levels of VH activity. In contrast, VH disinhibition, but not inhibition, impaired expression of the previous response during reminder trials (reduced % of correct responses, increased omissions). This suggests that such expression does not require VH activity, but is disrupted by aberrant activation of VH projection sites. Bayesian trial-by-trial analysis will be used to examine how VH manipulations affected strategies underlying reversal performance.